Nano-Vectorisation de siRNA via des nanocapsules lipidiques : contournement de la résistance du mélanome aux chimiothérapies conventionnelles

Pauline Resnier

l'université nantes angers le mans
PÔLE DE RECHERCHE ET D'ENSEIGNEMENT SUPÉRIEUR

université angers

Thèse de Doctorat

Pauline RESNIER

Mémoire présenté en vue de l'obtention du
grade de Docteur de l'Université d'Angers
sous le label de L'Université Nantes Angers Le Mans

École doctorale : *Biologie - Santé*

Discipline : *Sciences pharmaceutiques*
Spécialité : *Pharmacologie expérimentale et clinique*
Unité de recherche : *Inserm UMR_S 1066*

Soutenue le *25 Novembre 2014*
Thèse N° : *1418*

Nano-vectorisation de siRNA via des nanocapsules lipidiques

Contournement de la résistance du mélanome aux chimiothérapies conventionnelles

JURY

Rapporteurs :	**Claude MALVY**, Professeur d'Université, Université Paris Sud **Benoit FRISCH**, Directeur de recherche CNRS, Université de Strasbourg
Examinateurs :	**Tristan MONTIER**, Professeur d'Université – Praticien hospitalier, Université de Brest **Marie MORILLE**, Maitre de conférences, Université de Montpellier
Directeur de Thèse :	**Catherine PASSIRANI**, Professeur d'Université, Université d'Angers
Co-directeur de Thèse :	**Jean-Pierre BENOIT**, Professeur d'Université – Praticien hospitalier, Université d'Angers

2013-2014

Thèse de Doctorat
Discipline : Sciences pharmaceutiques
Spécialité : Pharmacologie expérimentale et clinique

Nano-vectorisation de siRNA via des nanocapsules lipidiques

Contournement de la résistance du mélanome aux chimiothérapies conventionnelles

RESNIER Pauline

Sous la direction du Pr
PASSIRANI Catherine

Membres du jury
MALVY Claude | Rapporteur
FRISCH Benoit | Rapporteur
MONTIER Tristan | Examinateur
MORILLE Marie | Examinateur
PASSIRANI Catherine | Directeur de thèse
BENOIT Jean-Pierre | Co-Directeur de thèse

Soutenu publiquement le :
25 Novembre 2014

université angers

REMERCIEMENTS

Je tiens à remercier en premier lieu le Professeur Jean-Pierre BENOIT, Directeur de l'unité INSERM U1066, de m'avoir accueillie au sein de son laboratoire pour mon stage de Master 2 ainsi que ma thèse. Merci pour vos encouragements et vos conseils tout au long de mes travaux.

Je remercie chaleureusement et sincèrement le Professeur Catherine PASSIRANI, qui m'a accueillie dès ma formation de Master 2 pour poursuivre ensuite l'aventure en thèse. Je te remercie de la confiance que tu m'as accordée durant ces quatre années. J'ai apprécié cette autonomie, tout en appréciant ta disponibilité et tes conseils avisés dès que besoin, cela a été un savant mélange dosé à la perfection. Ces quatre ans avec toi ont été très formateurs et agréables, professionnellement et humainement parlant. Merci pour cette expérience unique, dont je me souviendrai longtemps.

Je remercie le Professeur Claude MALVY, Professeur de l'Université de Paris Sud ainsi que le Directeur de recherche Benoit FRISCH, de l'Université de Strasbourg, d'avoir accepté de consacrer du temps à l'évaluation de ce travail en qualité de rapporteurs.

Je tiens également à remercier le Professeur Tristan MONTIER, de l'Université de Brest, pour avoir participé à mon jury de thèse en tant qu'examinateur. Merci pour tes remarques constructives qui ont su faire avancer ce projet de thèse, ainsi que pour ta participation et le temps que tu as consacré à la revue. Je remercie aussi les membres de ton équipe avec qui j'ai pu collaborer de façon brève mais intense, dont Nathalie, Caroline et Yann. L'accueil des Bretons est toujours très agréable.

Je remercie également le Docteur Marie MORILLE, Maitre de conférences à l'Université de Montpellier pour avoir accepté d'être examinateur de ma thèse. Merci de t'être replongée, j'espère avec plaisir, dans la problématique des LNC après quelques années de recul.

Je remercie la municipalité d'Angers Loire Métropole qui a financé ma thèse durant les trois ans. Je tiens également à remercier les organismes tels que « l'Association de la Recherche sur le Cancer » ainsi que la fondation « Ligue contre le cancer » du comité du Maine-et-Loire et de l'Ille-et-Vilaine qui ont participé activement aux financements de ce projet de thèse. Je remercie par la même occasion le Cancéropôle Grand Ouest pour la bourse octroyée qui m'a permis de participer à un congrès international en dernière année de thèse.

Je tiens à remercier les diverses équipes qui ont participé à la réussite de ce projet. Tout d'abord, l'équipe du Docteur Véronique MATHIEU, de l'Université Libre de Bruxelles, qui m'a accueillie dans le « grand nord » afin de réaliser correctement les western blot et m'a aidée dans la réalisation de la revue.
Je remercie également le Docteur Cédric GAILLARD pour sa participation et sa collaboration aux expérimentations nécessitant la cryoTEM. Merci de m'avoir accueillie deux ou trois après-midi afin de découvrir le monde de l'infiniment petit.
Puis, Le Docteur Igor CHOURPA, de l'Université de Tours, pour le temps qu'il a consacré aux expérimentations, pour l'analyse pointue qu'il nous a fournie dans le domaine du FRET et mon initiation à la découverte des particules cosmiques... Merci également à toute son équipe pour son accueil chaleureux.
Enfin, je n'oublie pas les nombreux autres collaborateurs qui m'ont fourni des outils indispensables tels que les affitins avec Frédéric PECORARI de l'université de Nantes, les tétraéthers de PEG avec Thierry BENVEGNU de l'Ecole de chimie de Rennes, et les ferrocifènes avec Gérard JAOUEN et Anne VESSIERES de Ecole de chimie de Paris. J'espère que ces premiers travaux feront naître des collaborations solides et durables avec l'unité 1066 d'Angers.

J'ai une pensée pour nos deux animaliers préférés du SCAHU : j'ai nommé Mr Pierre LEGRAS et Mr Jérôme ROUX. Merci pour votre bonne humeur et votre aide pour la mise en place des expérimentations animales.
Merci à Jérôme CAYON et Catherine GUILLET, pour leur aide et leur participation active au projet me permettant ainsi de dompter le cytomètre et d'avoir de magnifiques histogrammes dans les publications.

J'ai également une pensée envers ceux qui ont débuté cette thématique de recherche sur les LNC siRNA. A toi, Stephanie, qui m'a appris le secret de cette formulation, et aussi emmenée à Brest, il y a déjà maintenant 4 ans. Je te remercie pour la patience et la pédagogie dont tu as fait preuve durant mon stage de Master 2. Cela été une très grande et agréable expérience. J'ai d'ailleurs été ravie de poursuivre notre collaboration avec ton équipe de Tours. Je te souhaite le meilleur pour la suite. A très vite j'espère.

Je n'oublie pas également les membres de l'unité qui ont participé à la réussite de ce travail de thèse, car on est loin d'être seul.
Merci à toi, Jérôme, je t'ai donné du fil à retordre avec mes innovations farfelues. Mais tu as toujours été de la partie et tu as réussi à résoudre ces problèmes et faire avancer ce projet. J'ai vraiment apprécié de travailler avec toi mais j'ai aussi beaucoup apprécié ta personne en dehors du laboratoire. Tu es une belle personne même si tu sais parfois te montrer un peu têtu ! Prends soin de toi et n'arrête pas la guitare. Que du bonheur pour votre vie à deux !

Et toi, Nolwenn, j'ai appris à te connaître en faisant les cartons de l'IBT et en vidant la salle de chromato. Cela m'a d'ailleurs valu le surnom de mini Nolwenn durant le début de mon stage de M2. Mais en fait, notre collaboration professionnelle a été assez brève. Vive la manip du complément !!! On s'est bien rattrapées sur les footings à l'étang St Nicolas, ou sur la Zumba et autres activités sportives. Ne te tue pas à la tache quand même. Plein de bisous à Orégane. On se donne rendez-vous pour de futurs footings... ;-).
Merci à toi, Anne, notre référence en biologie qui est plus qu'indispensable au milieu de tous ces pharmaciens. Tu m'as souvent débloqué de nombreuses situations tortueuses et tu as toujours de bons conseils. Merci pour le temps que tu m'as consacré, le chapitre de livre, la publication de Master 2, la relecture des travaux et l'œil d'expert sur les résultats. Bon courage avec ton nouvel étudiant.

La thèse, ce sont aussi des collègues de bureau qui vous supportent à chaque moment; dans vos moments de réussite (assez brefs) mais surtout dans les moments de démotivation ! Merci à vous tous, vous avez été formidables. Après mon installation à l'IBS, bureau 4299, j'ai été accueillie au laboratoire par un trio mémorable, les mousquetaires.

Merci à mon premier Mousquetaire, Audrey, je me rappelle encore le premier jour où nous nous sommes rencontrées, la tornade Audrey ! Mon opinion n'a pas évolué en trois ans, une femme peut vraiment être multitâche ! Tu es une vraie fureur de vie et tu as mis une bonne humeur et une bonne ambiance dans ce bureau. Je te remercie pour ton aide, ton soutien, et les astuces que nous avons partagées. Tu es partie poursuivre à Lyon. Ca a laissé un petit vide mais on le comble en repensant à tous ces moments comme le GTRV et à ces mots magnifiques tels que la « cultivation ». Je te l'ai déjà dit à ton départ, mais que du bonheur pour l'avenir, Audrey, et de l'amour...

A mon deuxième Mousquetaire, Anne-Claire, ma voisine de bureau. On a appris à se connaître à Nantes en attendant avec notre cochon tout juste mort et encore chaud…. On a partagé, ce jour-là, une expérience que je ne suis pas prête de revivre. Je me rappellerai toujours la tête des douaniers en regardant ces falcons jaunes dans le coffre de ta Clio et nous laissant continuer notre route, perplexes. Je pense qu'ils se demandent encore ce que cela pouvait être. En tout cas, ça a commencé sur les chapeaux de roue. Ah ce mucus ! Je suis également persuadée après ces quatre ans en ta compagnie que certaines personnes peuvent avoir de réelles mauvaises ondes pour l'outil informatique. LOL. ;-). Je te souhaite le meilleur pour la suite. Bon courage avec Patrick.

Enfin, le troisième Mousquetaire, Anne-Laure, ma co-équipière avec Catherine. J'ai appris à te connaitre pendant mon M2, où nous avons dansé (chorégraphie des poules), fait des chapeaux de Catherinette, beaucoup rit au JJ et tout cela avec une petite dose sport, tout de même. Et j'aurai toujours une douceur amère que tu aies quitté le bureau plus tôt que prévu. La vie est ainsi, la thèse est ainsi. Je reste admirative de ta force et de ton courage pendant ta thèse. Je pense que Catherine a été bien servie avec un binôme comme le nôtre. Nous avons poursuivi notre chemin avec quelques activités sportives en commun! Je suis vraiment heureuse d'avoir fait ces trois ans en ta compagnie. J'espère que tout se passe pour le mieux de l'autre côté de la manche et que Nieto travaille son français. Je n'en doute pas. Carpe Diem.

Il fallait bien un homme dans ce bureau. A toi, Khaled ! Bravo pour ton courage dans cet environnement exclusivement féminin, fait de bavardages et de lectures de Public ou Closer ! Tu as d'ailleurs souvent fui afin d'avoir la tranquillité nécessaire pour travailler… Je te comprends. Voici que ces trois ans de thèse se terminent pour toi aussi. Bonne chance pour la dernière ligne droite avec Fred et pour l'épreuve du grand froid qui t'attend à Clermont.

De nouvelles têtes ont fait leur apparition avec le départ des uns. A toi, Angélique, ma « parigo » préférée, tu auras su apporter de nombreux fous rires et surtout de nombreuses questions au quotidien, plus ou moins scientifiques d'ailleurs ;-). Un grand merci pour ton dynamisme qui nous pousse à aller toujours plus loin, à ton enthousiasme communicatif, à des mots incongrus qui peuvent voler dans la pièce contre ton ordinateur ou tes bactéries, et qui nous font tant sourire (sans doute « menthe verveine »). Lisbonne se souvient sûrement encore de toi et les voitures klaxonnent en ton honneur. Tu tiens le bon bout. Je garde un œil sur toi, je ne pars pas loin. Rendez-vous dans un an pour te revoir avec ta petite famille (qui sait ?).

Enfin, dernière arrivée au sein du bureau, Claire. La vie commune dans notre bureau aura été brève. Mais elle nous a permis de partager de bons moments. Merci pour ton aide concernant les WB, le dépannage pour les cellules. Avec tout ça, je te dois au moins dix paquets de bonbons pour ta réserve d'écureuil !! Bon courage pour la suite, ne perds pas ta motivation et ta détermination, je suis sûre que tu es sur la bonne voie ! Bonjour à Pipou et bon courage pour la suite à Saint Germain. Ancenis n'est pas loin !

Enfin, je n'oublie pas les autres membres de l'unité. Je vous remercie tous sans exception pour votre sympathie, et pour votre accueil au sein de l'unité dans laquelle je me suis sentie très vite intégrée. Je remercie plus particulièrement les quelques directeurs de thèse qui sont passés régulièrement dans notre bureau : Emmanuel, Patrick, et Frédéric qui ont su apporter une touche d'humour quotidienne. Je remercie Edith pour son aide au quotidien sur les questions administratives, merci pour ta réactivité sans faille. Je pense également à Laurence pour le microscope, à Sylvie pour les Western blot et merci à Guillaume pour les statistiques, tu m'as enlevé une grosse épine du pied ! J'en oublie certainement.... et je m'excuse par avance.

J'ai une pensée pour la vieille génération des doctorants : Sandy, JP, Gaétan. Merci à toi Gaétan pour ton aide au tout début de mon stage de M2 pour la Q-PCR, le design des siRNA. J'espère qu'il fait beau et chaud à Miami, peut-être nous reverrons-nous un jour dans un congrès ;-)! Merci à Sandy, non seulement pour le bureau que tu m'as légué, j'en ai été honorée, mais aussi pour les trajets et les footings partagés ensemble. Que de bons moments, bonne continuation à la pharmacie de l'hôpital et beaucoup de bonheur à ta famille. Puis, J-P, merci pour les pauses thés froids ! Et puis plus récemment pour ton aide dans la réalisation dans mon futur projet, j'espère pourvoir suivre tes pas ! A très vite.

Puis, je pense à vous, doctorantes et doctorants de ma promotion au sein de l'Unité U1066 : Amin, Anabelle, Delphine, Fabien et Gaël. Bon courage à vous pour la dernière ligne droite !
La thèse, c'est aussi une vie en dehors du labo. Merci à toi, Thomas, pour les discussions dans le train qui ont fait que les trajets ont paru moins longs et bien plus agréables ! Le mois de Novembre n'est jamais le plus ponctuel.... En tout cas, tu es le bienvenu à Ancenis si tu t'y arrêtes un jour.... Merci à toi Hélène pour les trajets en vélo et le badminton en deuxième année, ça été un très bon défouloir ! Evite tout de même de te casser les jambes à l'avenir ! Prends soin de toi et n'abandonne pas. Le bout du chemin est à portée de main.

La thèse est aussi un partage d'expériences avec d'autres doctorants, personnels. Je ne vous oublie pas : Elodie, Leila, Emilie (A), Emilie (R), Florian (merci pour tes jeux de mots si drôles, ils nous manquent tous), et à tous les prochains qui vont suivre....

Par ailleurs, cette thèse n'aurait été la même sans l'aide des différents stagiaires qui ont travaillé dans le cadre de leur formation à la réalisation et à la progression des expérimentations : merci à Yann, Pierre, Nesrin, Alessandro, Anthea et Natacha. Merci à vous tous et plus particulièrement aux trois derniers qui sont arrivés à la toute fin de ma thèse et qui ont certainement subi ma possible pression de fin de thèse. Je tiens à m'excuser si cela été le cas. Bon courage à vous tous pour la suite. Je prends d'ailleurs rendez-vous pour l'Italie le plus vite possible pour venir vous voir, Anthea et Alessandro (prépare la pizza).

Enfin, un petit mot pour Céline et Patricia, nos secrétaires, qui savent gérer les urgences qu'on donne aux derniers moments. Merci à vous deux.

J'ai une pensée pour mes collègues de M2 STIS d'Angers qui ont partagé avec moi les années de Master et qui eux aussi arrivent à la fin de leur thèse. J'espère que tout se passe bien pour vous. Bon courage à toi, Gégé, nous aurons fait la totalité de notre cursus ensemble côte à côte. Merci pour les pauses café qui ont fait du bien au moral. Nos chemins se séparent maintenant, mais tiens moi au courant des péripéties de ta vie. Bon courage à toi, Barbara, plein de bonheur avec Arnold. A toi Mick, à toi Greg, à toi Anne-Claire (que du bonheur avec ton petit loulou), à toi Mathilde, à toi Eloïse. On se reverra peut-être dans 10 ans.

La thèse, c'est aussi l'occasion d'aller chercher d'autres expériences que la recherche. J'ai eu la chance et l'opportunité de pouvoir faire des vacations ainsi que du monitorat durant ces trois années.
Je remercie les enseignants de l'Université Catholique de l'Ouest qui m'ont permis de me lancer dans ce projet. Merci à Isabelle METAIS, à Hanane PERREIN, à Amélie CHATEL, Pablo SIMO et Catherine MOUNEYRAC ainsi que les étudiants UCO. Je tiens également à remercier la section biochimie de l'IUT d'Angers : Sophie FAGOT, les techniciennes (Laëtitia et Blandine) ainsi que les autres enseignants. Cela été une expérience professionnelle très enrichissante dans une ambiance sympathique. Bonne reprise à vous.

La vie personnelle et la vie professionnelle sont souvent liées et je me rappelle que mon premier jour dans ce laboratoire a été le jour de la naissance de Dorian, premier enfant dans ma bande d'amis, le 6 septembre 2010. Même si ce choix de poursuivre en thèse n'a pas toujours été évident, vous avez toujours été là pour me soutenir. A vous les amies, Elise, Carole, Claire et vos « moitiés ». A vous qui avez passé

plus de la moitié de votre vie à me connaître et à me soutenir. Merci de m'avoir changé les idées durant les weekends avec des sorties, des restaurants, ou du sport. Merci, pour votre soutien sans faille. Je vous embrasse les filles.

Enfin, je pense à mon entourage le plus proche qu'est la famille. Je remercie bien sûr toute la famille de Ronan au grand complet, ses parents, la famille Jadeau : Jérôme, Aude, Lucile et Adèle ; et la famille Ronco : Nicolas, Solène, Zélie et Gaspard. J'ai été accueillie à bras ouvert dans cette famille qui a souvent pris des nouvelles du bon déroulement de ma thèse. J'ai commencé ma thèse par un séjour mémorable avec vous à la Maison Orré, et j'aurai le plaisir de poursuivre l'après-thèse au châlet l'Oréade pour de magnifiques moments. Merci à vous tous pour ces moments de pause entre le boulot. Et merci à Aude pour le temps que tu as consacré à la relecture de ces quelques pages.

Merci à toute ma famille, oncle, tante, cousin, cousine, parrain qui ont toujours eu des mots réconfortants. Et, je tiens à remercier avec beaucoup d'émotion mes parents, ma sœur Marie, mon beau-frère José, sans oublier mon neveu, Malcolm, pour votre soutien inconditionnel durant toutes ces années d'études. Merci à vous, papa et maman, de m'avoir donné la chance et l'opportunité de faire les études que je souhaitais dans les meilleures conditions, même si cela ne semble plus en finir. Merci pour tout, merci de m'avoir suivie pas à pas et d'être là à chaque instant important de ma vie. Je suis ici grâce à vous. Je vous embrasse.

Je clos mes remerciements en exprimant tout mon amour et toute ma gratitude à toi, Ronan. Merci de m'avoir accompagnée, supportée et aidée pendant ces années de durs labeurs que sont les années de thèse. Merci pour ton soutien quotidien et tes attentions de chaque jour qui m'ont permis de vivre ma thèse plus sereinement. Ma thèse n'aurait pas été la même sans toi. L'aventure se poursuit pour nous deux vers de nouveaux horizons..../m/

« Là où se trouve une volonté,

Il existe un chemin »

Winston Churchill

*« A toi, **Simone** »*

SOMMAIRE

INTRODUCTION GENERALE 1

1. LE MELANOME 2
2. LA CHIMIO-SENSIBILISATION VIA LA SOUS-UNITE ALPHA 1 15
3. LES NANOMEDECINES 28
4. LES OBJECTIFS DE LA THESE 34

REVUE BIBLIOGRAPHIQUE 46

CHAPITRE I : DEVELOPPEMENT ET CARACTERISATION DES NANOCAPSULES LIPIDIQUES CHARGEES EN SIRNA 64

1. PUBLICATION N° 1: SIRNA LNCS – A NOVEL PLATFORM OF LIPID NANOCAPSULES FOR SYSTEMIC SIRNA ADMINISTRATION 66
2. PUBLICATION N° 2: EFFICIENT *IN VITRO* GENE THERAPY WITH PEG SIRNA LIPID NANOCAPSULES FOR PASSIVE TARGETING STRATEGY FOR MELANOMA 72
3. BREVET : NANOCAPSULES LIPIDIQUES CHARGEES EN SIRNA 95

CHAPITRE II : NANOCAPSULES LIPIDIQUES DE SIRNA ET CIBLAGE TUMORAL 97

1. Publication n° 3: innovative Affitin and PEG modifications onto siRNA lipid nanocapsules influence cell uptake, *in vivo* biodistribution and tumor targeting 99

Chapitre III : Evaluation du potentiel therapeutique des nanocapsules lipidiques de siRNA 126

1. Publication n° 4: Efficient ferrocifen anticancer drug and Bcl-2 gene therapy using lipid nanocapsules for in vivo melanoma treatment 128

Discussion generale 150

1. Genese des travaux 151
2. Formulation et optimisation du procede 152
3. Preuve de concept 155
4. Application en oncologie 159
5. Un avenir en clinique ? 164

Conclusion & perspectives 170

Annexes 173

1. Chapitre de livre 175
2. Publication annexe 194
3. Curriculum vitae 203

ABREVIATIONS

ADN	Acide désoxyribonucléiques
AJCC	American joint committee on cancer
ALAT	Alanine Amino transférase
ARNm	ARN messager
ASAT	Aspartate amino transférase
Bcl-2	B-cell lymphoma 2
BCNU	Carmustine ou bis-chloroethylnitrosourea
BFI	Biofluorescence
BRCA1	Breast cancer 1
CD	Cluster de différenciation
CDK	Cyclin-dependent kinase
CR	Charge ratio
Cryo-TEM	Microscopie électronique à transmission cryogénique
CTLA-4	Cytotoxic T-lymphocyte antigen 4 ou CD152
DiD	1,1'-dioctadecyl-3,3,3',3'-tetramethylindodicarbocyanine perchlorate
DiI	1,1'-dioctadecyl-3,3,3',3'-tetramethylindocarbocyanine perchlorate
DLS	Dynamic light scattering
DR	Death receptor
DOPE	1,2-dioleoyl-sn-glycero-3-phosphoethanolamine
DOTAP	1,2-dioleoyl-3-trimethylammonium-propane
DSPE-PEG	1,2-distearoyl-sn-glycero-3-phosphoethanolamine-N-[methoxy (polyethylene glycol)-2000]
malDSPE-PEG	1,2-distearoyl-sn-glycero-3-phosphoethanolamine-N-[maleimide (polyethylene glycol)-2000]

DTIC	Dacarbazine ou 5-(3,3-dimethyl-1-triazenyl)imidazole-4-carboxamide
DTT	Dithiothréitol
EE	Efficacité d'encapsulation
EGFR	Epidermal growth factor receptor
EPR	Enhanced permeability and retention
EtB	Bromure d'éthidium
FAMM	Familial atypical mole melanoma
FcDiOH	Ferrociphenol
FDA	Food and drug administration
FRET	Förster resonance energy transfer
HS-PEG	Hydroxystéarate de polyéthylène glycol
IAP	Inhibiteurs de l'apoptose
IF	Interférons
IL	Interleukine
INCa	Institut national du cancer
i.p	Injection intrapéritonéale
i.v	Injection intraveineuse
LDH	Lactate déshydrogénase
LNC	Nanocapsules lipidiques
MAP-Kinase	Mitogen-activated protein kinase
MC1R	Melanocortin 1 receptor
MITF	Microphthalmia-associated transcription factor
mTOR	Mammalian target of rapamycin
MTS	3-(4,5-dimethylthiazol-2-yl)-5-(3-carboxymethoxyphenyl)-2-(4-sulfophenyl)-2H tetrazolium
Na/K ATPase	Pompe à sodium/potassium
NHS	Sérum humain normal

OD	Densité optique
OMS	Organisation mondiale de la santé
PDI	Index de polydispersité
PEG	Polyethylène glycol
PI3K	Phosphoinositol 3 kinase
ROS	Dérivés réactifs de l'oxygène
siRNA	ARN interférents
SLN	Solid lipid nanoparticles
SND	Syndrome des Naevus Dysplasiques
TE-PEG	Tetraether-polyethylène glycol
TNF	Tumor necrosis factor
TRAIL	TNF- related apoptosis inducing ligand
UICC	Union Internationale Contre le Cancer
UV	Ultraviolet
ZIP	Zone d'inversion de phase

LISTE DES FIGURES & TABLES

Figures

Figure 1 : Incidence mondiale du mélanome en fonction du sexe des patients 2

Figure 2 : Message publicitaire représentant les cinq précautions avant et pendant une exposition solaire, extrait du site de l'INCa 4

Figure 3 : ABCDE du mélanome permettant d'évaluer la malignité d'un grain de beauté 6

Figure 4 : Développement du mélanome avec les différentes phases de progression 7

Figure 5 : Mécanisme de cancérogénèse du mélanome 15

Figure 6 : Voie de signalisation et dérégulations des deux principales voies de l'apoptose dans le cas de mélanome 17

Figure 7 : Voie de signalisation des MAP kinase, de la PI3K et de NF-κB, et leurs dérégulations dans le cas de mélanome 19

Figure 8 : Caractérisation structurale des membres de la famille Bcl-2 21

Figure 9 : Structure de la pompe à sodium avec ses différentes sous-unités 22

Figure 10 : Schéma d'activation des voies impliquées par le recrutement de la pompe à sodium au niveau du signalosome 24

Figure 11 : Voie de signalisation des ARN interférents 27

Figure 12 : Les différents types de vecteurs synthétiques 28

Figure 13 : Schématisation du procédé de formulation des nanocapsules lipidiques 31

Figure 14 : Structure chimique de deux dérivés organométalliques possédant un groupement ferrocènes 33

Figure 15 : Comparaison de la stabilité des LNC siRNA avant et après optimisation 96

Figure 16 : Représentation schématique des LNC siRNA 153

Figure 17 : Suivi du signal de bioluminescence issu de cellules de mélanome sous-cutané au cours du temps 159

Figure 18 : Expérience d'extinction de la luciférase exprimée par des cellules de mélanome humain transformées. 160

Figure 19 : Impact de l'association des nanocapsules lipidiques chargées en siRNA et de différentes chimiothérapies sur des cellules issues de mélanome humain 159

Figure 20 : Impact du ciblage de la sous-unité alpha 1 de la pompe à sodium via des LNC siRNA sur un modèle de mélanome sous-cutané 161

Figure 21 : Représentation schématique bilan des travaux de thèse 161

Tableaux

Tableau 1 : Description des critères permettant de classer les différents stades de mélanome 10

Tableau 2 : Inhibiteurs chimiques ciblant la molécule Bcl-2 en essai clinique 25

Tableau 3 : Récapitulatif des essais cliniques utilisant des nanomédecines pour l'encapsulation de chimiothérapie ou siRNA dans le cadre d'un traitement contre le mélanome 30

INTRODUCTION GENERALE

INTRODUCTION GENERALE

1. Le mélanome

1.1. En quelques chiffres

Le cancer est une cause majeure de décès dans le monde, à l'origine de 8,2 millions de décès en 2012, soit environ 13 % de la mortalité mondiale (site de l'OMS, *www.who.int*). Avec environ 8 250 nouveaux cas estimés et 1 570 décès en France en 2010, le mélanome, cancer de la peau le plus fréquent, se situe au neuvième rang des cancers tous sexes confondus, et se place au onzième rang des cancers masculins et au neuvième rang des cancers féminins (site de l'INCA, *http://www.e-cancer.fr)*.

Parmi l'ensemble des cancers, le mélanome est celui qui montre la plus forte augmentation d'incidence depuis ces trente dernières années [1]. Une incidence mondiale qui a doublé en 15 ans et qui est estimée en 2011 à 10,5 cas pour 100 000 hommes et 9,7 cas pour 100 000 femmes (Figure 1). En 2010, une étude statistique américaine a montré que les cancers cutanés tels que le mélanome touchaient majoritairement le type caucasien avec une incidence de 29 cas pour 100 000 caucasiens contre 1 cas pour 100 000 non-caucasiens (Etude du National Cancer Institute). Cette étude a également démontré que, malgré un âge médian des patients de 61 ans, le mélanome touche de façon non négligeable une population plus jeune (25-30 ans), voire adolescente.

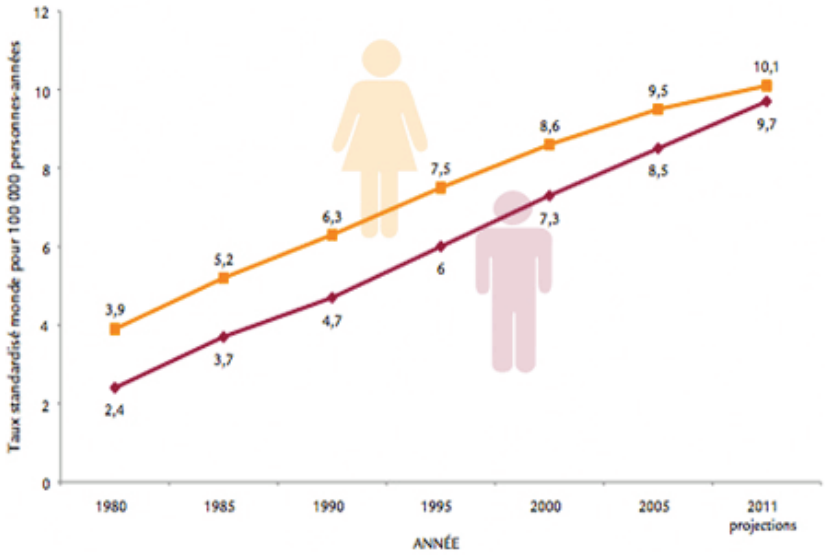

Figure 1 : Incidence mondiale du mélanome en fonction du sexe des patients (issu du site www.mélanome-patients.fr)

1.2. Les facteurs de risque

Plusieurs facteurs de risque pour le mélanome sont aujourd'hui reconnus grâce aux données statistiques. On sait aujourd'hui que les personnes de type caucasien ont bien plus de risque que les personnes avec une hyperpigmentation, car celle-ci leur offre un effet protecteur [2]. L'âge et le genre sont aussi des facteurs de risque de développement d'un mélanome. Si les femmes sont préférentiellement touchées lorsqu'elles sont jeunes, les hommes ont, eux, 1,6 fois plus de risques d'être atteint de cette pathologie au cours de leur vie. Cependant, les deux facteurs principaux décrits à l'heure actuelle sont les antécédents familiaux et les expositions aux ultra-violets (UV).

1.2.1. Les antécédents familiaux

De nombreuses pathologies cancéreuses ont vu un lien de transmission entre les générations, comme le cancer du sein avec la mutation du gène BRCA1 [3]. Pour le mélanome, une histoire familiale avec une multiplication de cas de mélanome augmente le risque individuel de développer cette maladie jusqu'à un facteur 3 à 6 [4]. Le risque est d'autant plus grand que le nombre de membres affectés est important [5].

Le premier cas d'historique familial pour le mélanome fait l'objet d'un rapport écrit au début du XIXème siècle par un chirurgien britannique, William Norris [6]. Il faudra attendre le milieu du XXème siècle, pour que soir réalisée la description du Syndrome « Familial Multiple Mole and Melanoma » (FAMM) par Clark et Lynch [7, 8]. Ce syndrome familial est annoncé lorsque plusieurs membres familiaux (au moins deux) de parenté proche (frère, soeur, oncle, tante) déclarent des mélanomes ou des naevi dysplasiques (grain de beauté atypique).

Il existe aussi le Syndrome de *Naevus* Dysplasique (SND) caractérisé par la présence d'un nombre important de grains de beauté (50-100 nevi) avec au moins l'un d'entre ayant un diamètre supérieur à 8 mm ou une forme atypique [9].

Récemment, les analyses génomiques ont mis en évidence les gènes impliqués dans le développement du mélanome familial. Dans 20 à 40% de ces mélanomes, des mutations du gène CDKN2A codant pour la protéine Cyclin-dependent Kinase 2a (CDK) ou p16 ont été démontrées [10]. De plus, le gène CDK4 [11], le gène du xeroderma pigmentosum [12], le gène du récepteur de la melanocortin-1 (MC1R) [13] et le gène codant pour la protéine kinase B-Raf [14] ont tous montré une relation avec les formes de mélanome familial (cf. Introduction, § 1.4.5).

1.2.2. L'exposition solaire

Si les mécanismes de transformation des nevi en mélanomes malins sont aujourd'hui encore mal définis, il apparait clairement que l'exposition aux radiations UV est le facteur environnemental contribuant majoritairement à la formation de mélanome [15].

Les radiations UV sont classées en deux catégories, les UVA et les UVB, selon leur longueur d'onde. Les UVA ont une longueur d'onde comprise entre 320-400 nm, alors que les UVB se situent entre 280-320 nm [16]. Alors que les UVA sont normalement superficiels avec une atteinte de l'épiderme, les UVB, eux, peuvent atteindre une profondeur plus importante dans le derme de la peau. Naturellement, les rayons solaires sont filtrés au niveau de l'atmosphère avec la couche d'ozone. Cependant, les UV peuvent passer au travers ce filtre et sont alors responsables des coups de soleil. Les expositions répétées à ces rayonnements et l'accumulation de brûlures lors des coups de soleil ont toutes deux une corrélation directe avec l'apparition de mélanome malin [17].

Pourquoi l'exposition aux UV favorise-elle l'apparition de mélanome ? L'exposition importante de la peau au soleil, conduisant à une exposition aux UVA et les UVB, s'accompagne d'altérations de la structure de l'ADN, même pour des doses inférieures à celles déclenchant des coups de soleil. Les systèmes cellulaires de réparation des dommages de l'ADN (cascade de signalisation induisant Check1/2), qui ont en charge l'intégrité de l'ensemble des gènes, peuvent être saturés lors d'expositions intenses et/ou répétées, ce qui a pour conséquence l'apparition de mutations génétiques, voire le développement tumoral (*Fiche prévention, Rayonnements ultraviolets et risques de cancers*, INCA) [18].

Si l'environnement naturel nous expose aux UVB, les UVA sont principalement utilisés pour les cabines de bronzage dans les établissements esthétiques. Les UVA sont en effet connus pour pénétrer plus profondément dans les tissus, contrairement aux UVB qui restent plus superficiels. Les rayonnements UVA, donc, ont été historiquement perçus comme moins susceptibles de causer des coups de soleil nuisibles au niveau superficiel. Cependant, de récentes études ont désormais prouvé une corrélation significative entre l'utilisation des cabines UV et le risque de formation de mélanome [19, 20]. Ce risque apparait d'autant plus important si l'utilisation des cabines est régulière ; mais il diminue avec l'âge. Depuis 2009, l'exposition aux installations de bronzage artificiel est reconnue comme cancérigène [21]. Avec une incidence record du mélanome, l'Australie devrait être cette année le premier pays à réglementer l'utilisation des cabines de bronzage [2].

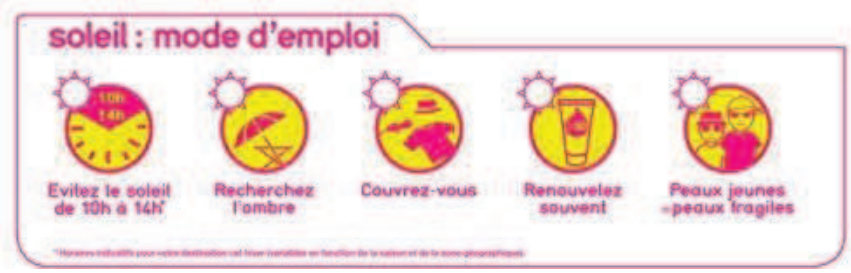

Figure 2 : Message publicitaire représentant les cinq précautions avant et pendant une exposition au soleil, extrait du site de l'INCa

1.2.3. La prévention et le dépistage

La façon la plus efficace d'atténuer le risque de développer un mélanome est de réduire l'exposition aux UV. Une prévention accrue a été menée depuis la dernière décennie en collaboration avec l'Institut National du Cancer (INCa). La prévention passe par la médiatisation de cinq précautions indispensables à prendre en cas d'exposition : éviter l'exposition entre 10h et 14h, rechercher l'ombre, se protéger avec des vêtements, des lunettes adaptées et un chapeau, renouveler régulièrement la crème solaire avec un indice adapté et prendre plus de précautions envers les enfants et les adolescents (Figure 2).

D'ailleurs, comment fonctionne une crème solaire ? Leur mode d'action se base sur la capacité de certaines molécules à arrêter les UV. On distingue deux catégories de molécules : les filtres minéraux ou les filtres chimiques. Les filtres minéraux vont agir comme des miroirs, se sont, entre autres, les crèmes à base d'oxyde de titane, de talc, ou encore d'oxyde de zinc. Les filtres chimiques, quant à eux, fonctionnent comme la mélanine. Ils absorbent les UV en passant par un état d'excitation, puis retourne à un état stable, pouvant ainsi recommencer un cycle. Les filtres chimiques sont les molécules telles que les esters cinnamiques, les salicylates, les dérivés du camphre, ou encore les benzophénones. Leurs propriétés leur permettent alors de stopper les UVA, ou les UVB. Une meilleure protection sera donc apportée par un mélange de principes actifs.

L'un des challenges du traitement du mélanome consiste également à mettre en place des moyens de dépistage précoce de la pathologie. Un mélanome localisé sera de très bon pronostic, après une simple ablation du grain de beauté, contrairement aux formes métastasées (cf. Introduction, § 1.3). Pour cela, cinq critères simples et facilement identifiables sont utilisés et communiqués au grand public au sein des cabinets médicaux et à travers les spécialistes dermatologues, afin de différencier et suspecter la présence d'un mélanome.

Ces signes sont résumés par le sigle ABCDE (Figure 3). Un mélanome présentera préférentiellement :

- une **A**symétrie : les lésions du mélanome ne sont ni rondes, ni régulièrement ovales
- des **B**ords irréguliers : les contours des mélanomes sont festonnés, dentelés ou mal définis
- une **C**ouleur inhomogène : le mélanome comporte des dégradés marron, brun clair, roux, blanc et/ou des zones bleu-noir
- un **D**iamètre supérieur à 6 mm : au-dessus de ce diamètre, les lésions sont hautement suspectées d'être des mélanomes
- une **E**volution : se traduisant par une augmentation de taille, de volume, ou un changement de couleur, ou de forme.

Figure 3 : ABCDE du mélanome permettant d'évaluer la malignité d'un grain de beauté

La mise en évidence d'un ou plusieurs de ces signes doit alerter le patient à effectuer un examen plus approfondi par un professionnel de santé. Si la suspicion persiste après examen visuel, une biopsie sera réalisée afin de vérifier s'il s'agit d'un mélanome malin.

1.3. Le développement et le pronostic des mélanomes

1.3.1. Développement et description pathologique

- *Le développement tumoral*

Le mélanome est un cancer dérivant des mélanocytes, les cellules pigmentaires de notre peau, situées entre le derme et l'épiderme. Paradoxalement, les mélanocytes permettent normalement la protection contre les UV grâce à la production de la mélanine, pigment à l'origine de la couleur de la peau et des cheveux. Dans le cas du mélanome, certaines de ces cellules pigmentaires dérivent d'un *neavus* et prolifèrent jusqu'à la formation d'un mélanome *in situ* (Figure 4).

Le mélanome *in situ* est caractérisé par une phase d'extension horizontale toujours au niveau superficiel du derme. Par définition, le mélanome *in situ* n'a pas atteint la membrane basale. Par conséquent, il n'a pas accès aux vaisseaux sanguins, ni lymphatiques et n'a pas de risque de former des métastases. Suite à cette première phase de prolifération, la croissance s'étend à la verticale et progresse en profondeur dans le derme et l'hypoderme. Cette phase d'extension verticale donne lieu à des lésions palpables. Plus la masse tumorale s'enfonce, plus il y a de risque qu'elle soit en contact avec des vaisseaux lymphatiques ou sanguins et qu'elle provoque une dissémination des cellules tumorales (Figure 4.). On distingue alors deux stades : les mélanomes loco-régionaux et les mélanomes métastasés. Les ganglions lymphatiques proches du mélanome sont les premiers touchés et forment les métastases en transit, caractéristiques des mélanomes loco-régionaux. Puis, les cellules cancéreuses vont se propager vers d'autres tissus ou organes plus éloignés et ainsi former des métastases à distance, caractéristiques des mélanomes de haut grade. Ces métastases à distance sont fréquemment localisées sur la peau et dans les ganglions lymphatiques, mais on les retrouve

également au niveau des poumons, du foie et du cerveau. Aujourd'hui, le pronostic des patients diagnostiqués pour un mélanome métastatique est dramatique, avec une médiane de survie comprise entre 2 et 10 mois et une survie à 5 ans de 5 à 10% [22, 23].

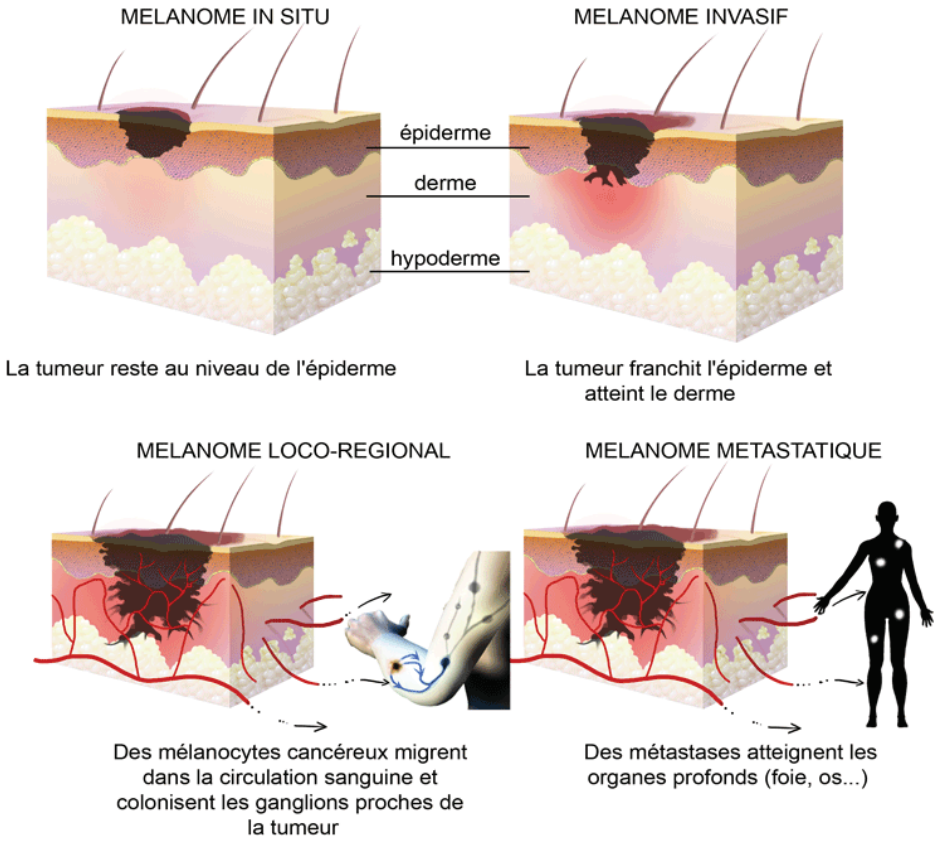

Figure 4 : Développement du mélanome avec les différentes phases de progression (issu du site www.melanome-patients.fr)

- *Catégories histologiques*

On classe les mélanomes selon cinq catégories histologiques basées sur la localisation et la croissance : le mélanome superficiel extensif, le mélanome nodulaire, le lentigo malin, le mélanome acral lentigineux et le mélanome desmoplastique. Cependant, la catégorie histologique du mélanome n'influence pas majoritairement le pronostic du patient. Cela étant dit, certains types histologiques sont plus susceptibles d'être détectés à un stade avancé, ce qui affecte indirectement le pronostic associé [2].

Le mélanome superficiel extensif correspond au type de mélanome le plus fréquent (60-70 % des mélanomes). Il n'est pas nécessairement associé à l'exposition au soleil, et peut toucher tout tissu dermique. Comme son nom l'indique, le mélanome superficiel extensif commence par une lésion pigmentée qui va s'étendre de plus en plus, en restant superficielle. Avec le temps, ces mélanomes peuvent envahir plus profondément le derme.

Le mélanome nodulaire représente 15 à 30% de tous les mélanomes. Cette catégorie de mélanome reste une exception par rapport au modèle de croissance habituel : la phase de croissance verticale est présente précocement dans le développement de la tumeur, augmentant le risque d'atteinte des vaisseaux et donc du potentiel métastatique. Les mélanomes nodulaires sont bourgeonnants tels des lésions papuleuses voir hémorragiques qui sont souvent de mauvais pronostic en raison de l'épaisseur de la tumeur (supérieure à la moyenne) et d'une ulcération fréquente.

Le lentigo malin ou mélanome de Dubreuilh (5-10 %) siège sur les zones photo-exposées (surtout le visage avec une peau endommagée par le soleil), et touche particulièrement les sujets de plus de 60 ans. Ce sous-type se présente comme une tache, sombre, avec une pigmentation variable, des bords irréguliers et une lente évolution. Il n'est pas rare d'observer des lentigos malins devenir très grands avant le diagnostic car la lente progression de la lésion peut passer inaperçue par le patient. Dans l'ensemble, le pronostic des lentigos malins est meilleur que celui des autres sous-types histologiques parce que la lésion est souvent superficielle, mais un retard dans la prise en charge peut contrecarrer ce diagnostic favorable.

Le mélanome acral lentigineux siège, comme son nom l'indique, sur les extrémités. Cette catégorie de mélanome se développe dans des endroits discrets tels que la paume de la main, la plante des pieds, ou dans les zones sous-unguéales (sous les ongles des doigts et des orteils). Il ne représente que 2 à 10% des mélanomes mais il reste le mélanome majoritaire chez les populations asiatiques (45%) et les populations noires (70%) considérées comme les populations présumées à faible risque. Le diagnostic est souvent tardif, avec des tumeurs de stade avancé, contribuant à un mauvais pronostic. Le retard dans le diagnostic s'explique par une confusion de ces lésions avec de simples hématomes sous-unguéaux.

Le mélanome desmoplastique est une catégorie rare de mélanome cutané. Décrit pour la première fois par Conley en 1971, il ne représente que 1,7 à 4% des mélanomes [24]. Cliniquement, il se présente comme une lésion amélanotique, le plus souvent dans la région de la tête et du cou. Ce type de mélanome est associé aux fortes expositions solaires, et reste plus fréquent chez l'homme. Le mélanome desmoplastique n'a pas le même comportement que les autres types de mélanome. Ces lésions présentent un neurotropisme naturel, ce qui entraine des récidives locales dans la plupart des cas, avec une diminution du risque de métastases ganglionnaires. Les analyses réalisées sur des groupes de patients montrent que le taux de récidives locales est estimé à 50% et celui des métastases ganglionnaires est inférieur à 10% [25]. Même si le risque d'expansion du mélanome est plus faible, la biopsie des chaines ganglionnaires reste une nécessité [26].

1.3.2. Les différents stades évolutifs du mélanome

Si le type histologique n'influence pas spécifiquement le pronostic du patient, les examens médicaux effectués lors du diagnostic permettent de déterminer le stade du mélanome, c'est-à-dire, d'évaluer l'étendue de la pathologie au moment des examens. Pour l'évaluation, trois critères sont pris en compte : épaisseur et ulcération de la tumeur, atteinte ou non des ganglions lymphatiques, et la présence ou non de métastases, permettant de définir le stade du cancer selon la classification TNM. TNM signifie « tumeur, ganglions (node), métastases » selon la classification de l'Union Internationale contre le Cancer (UICC) et de « American Joint Committee on Cancer » (AJCC).

- *Le paramètre T*

Il s'agit d'évaluer les caractéristiques de la tumeur primaire en prenant en compte l'épaisseur et l'ulcération. L'insertion en profondeur dans le derme et l'hypoderme est associée à un risque de propension. L'épaisseur de la tumeur donne donc une indication sur le degré d'extension de la maladie au moment du diagnostic. De plus, l'ulcération en surface du mélanome est également un important facteur de pronostic. Il s'agit de la destruction de l'épiderme en regard du mélanome, cette ulcération étant visible au microscope, ou parfois à l'œil nu. Les tumeurs de petites tailles et sans ulcération sont notées en tumeur de classe I, ce sont les moins dangereuses (Tableau 1). Les tumeurs de stade II désignent les mélanomes localisés de plus grande épaisseur ou avec ulcération mais pour lesquels les ganglions lymphatiques ne sont pas atteints.

- *Le paramètre N*

Il s'agit d'évaluer l'atteinte des ganglions lymphatiques, en détectant la présence ou non de métastases dites « en transit ». Les cellules cancéreuses qui circulent entre le mélanome primitif et les ganglions lymphatiques les plus proches peuvent y former de nouvelles tumeurs cutanées ou sous cutanées appelées métastases en transit. Elles démontrent une dissémination locale des cellules tumorales et donc un danger plus important de développer des métastases. Ce developpement correspond au stade III désignant les mélanomes qui, quelle que soit leur épaisseur, présentent un envahissement locorégional avec une atteinte des ganglions lymphatiques ou la présence de métastases « en transit » (Tableau 1).

- *Le paramètre M*

Le paramètre M s'intéresse à la présence ou non de métastases à distance. Les cellules cancéreuses peuvent envahir d'autres organes que les ganglions lymphatiques et y développer des métastases à distance. Les organes les plus souvent touchés par des métastases lors d'un mélanome sont le poumon, le foie et le cerveau. Ces mélanomes sont classés en stade IV quelles que soient leur

épaisseur et l'atteinte ganglionnaire. On parle aussi de mélanome métastatique (Tableau 1). La connaissance du stade du mélanome au moment du diagnostic est déterminante pour adapter le traitement.

Classe	Catégorie T	Epaisseur de la tumeur	Ulcération et indice mitotique
Stade I	T1	≤ 1,00 mm	a : sans ulcération et mitose < 1/mm^3 b : avec ulcération et mitose ≥ 1/mm^3
	T2	1,01 – 2,00	a : sans ulcération b : avec ulcération
Stade II	T3	2,01 – 4,00	a : sans ulcération b : avec ulcération
	T4	> 4,00 mm	a : sans ulcération b : avec ulcération
	Catégorie N	**Nombre de ganglions sentinelles**	**Taille des nodules**
Stade III	N1	1	a : micrométastases b : macrométastases
	N2	2-3	a : micrométastases b : macrométastases
	N3	> 4	a : micrométastases b : macrométastases
	Catégorie M	**Site des métastases**	**Dosage LDH (sanguin)**
Stade IV	M1a	Métastases cutanées, sous-cutanées et chaines ganglionnaires	Normal
	M1b	Métastases pulmonaires	Normal
	M1c	Métastases intestinales Autres métastases à distance	Normal à Elevé

Tableau 1 : **Description des critères permettant de classer les différents stades du mélanome** (issu de Dunki-Jacobs *et al.*,[2]). LDH : lactate deshydrogénase

1.3.3. Les indicateurs pronostiques

Afin d'évaluer le degré de malignité du mélanome, plusieurs facteurs pronostiques sont observés, en ordre d'importance : l'épaisseur de la tumeur avec l'indice de Breslow, la présence d'ulcération, l'indice mitotique (nombre de mitose/mm²), l'âge du patient, la localisation de la tumeur primaire et enfin le sexe du patient.

Développé dans les années 70 par Alexander Breslow, l'indice de Breslow est l'indicateur le plus fiable aujourd'hui [27]. Cet indice permet une corrélation entre l'épaisseur de la tumeur et la survie des patients. Il consiste à mesurer verticalement, au micromètre oculaire, l'épaisseur depuis la granuleuse de l'épiderme jusqu'à la cellule tumorale la plus profonde. Le risque de métastase peut être estimé de manière reproductible à partir de la profondeur de l'invasion :

- Faible épaisseur : épaisseur du mélanome inférieure à 0,76 mm = 0% de métastase
- Epaisseur intermédiaire : 0,76 à 1,5 mm = 30%
  1,51 à 2,25 mm = 33%
  2,26 à 3 mm = 69%
- Epaisseur importante : supérieure à 3 mm = 84%

La présence d'ulcération représente également un facteur pronostic robuste [28, 29]. L'ulcération est définie cliniquement comme l'absence d'épithélium intact autour du mélanome. La présence d'un mélanome ulcéré est de mauvais pronostic comparativement aux mélanomes non-ulcérés, même si le patient a des métastases loco-régionales. L'agressivité tumorale associée à l'ulcération est aujourd'hui encore mal comprise [28]. Mais il semble que celle-ci soit en lien avec la capacité des cellules tumorales à métastaser.

L'indice mitotique est un des facteurs les plus récemment décrits et joue un rôle capital dans le pronostic des tumeurs ayant une faible épaisseur (indice de Breslow <1mm) [30]. Il est le seul indicateur pour évaluer l'atteinte possible des ganglions lymphatiques après biopsie sur les tumeurs de bas grade. Un indice mitotique faible (inférieur à 1 division/mm^3) sera associé à un meilleur pronostique.

Les autres indicateurs ont une importance moindre. On sait aujourd'hui que les patients âgés ont un risque accru de mortalité comparativement aux jeunes patients [31]. De plus, les tumeurs primaires situées au niveau du tronc (tête, cou, torse, dos) sont de moins bon pronostic que les tumeurs situées sur les membres [32]. Enfin, les femmes ont un meilleur pronostic que les hommes pour des raisons encore inconnues à l'heure actuelle [33]. Le rôle des hormones apparait comme l'un des facteurs pouvant expliquer ces disparités [34].

1.4. Les traitements actuels

1.4.1. La chirurgie

La chirurgie est la première option envisagée. Cependant, elle reste une alternative curative uniquement valable en cas de mélanomes *in situ* ou loco-régionaux. Systématiquement, lorsque cela est possible, une ablation de la tumeur primaire est effectuée avec une marge chirurgicale de 1 cm pour les tumeurs de plus de 2 mm d'épaisseur. On peut également effectuer une excision des chaines lymphatiques ou ganglions sentinelles pour lesquels on suspecte ou on a démontré la présence de métastases en transit.

1.4.2. La radiothérapie

La radiothérapie est un outil thérapeutique classiquement utilisé pour les patients atteints de pathologies cancéreuses. Cependant, cette technique est aujourd'hui peu utilisée dans le cadre des thérapies contre le mélanome. Une forte radiorésistance a été très rapidement observée, limitant son utilisation dans le cadre des thérapies pour le mélanome [35]. En effet, la nature radiorésistante des cellules de mélanome peut s'expliquer par les mécanismes altérés lors des expositions aux rayonnements UV, favorisant la survie [36].

Pourtant, elle reste préconisée chez les patients après excision de la tumeur primaire et des ganglions lymphatiques ayant un risque modéré ou élevé de rechute locale. Le protocole prescrit, dans ce cas, est un dosage de 6 à 9 Gy pour des sessions de 30 à 50 Gy au total. Cependant, si la littérature démontre que ce traitement retarde la rechute, il n'améliore pas la survie des patients [37]. Elle est également utilisée en traitement palliatif lors d'apparition de métastases osseuses.

1.4.3. La chimiothérapie

Les agents chimio-thérapeutiques restent, à l'heure actuelle, les agents les plus efficaces dans la lutte anti-tumorale. Les premières chimiothérapies ont été effectuées dans les années 1940 avec un dérivé azoté du gaz moutarde sur les leucémies, puis l'utilisation du méthotréxate a permis d'obtenir les premières rémissions. Fortes de ce succès, de nombreuses autres substances, parfois naturelles comme le paclitaxel provenant de l'écorce d'if, ou la vinblastine extraite de la pervenche, ont été recherchées pour leur propriété anti-cancéreuse au cours des décennies suivantes. Ces molécules présentent différentes voies d'action comme l'alkylation de l'ADN ou l'inhibition de la polymérisation des microtubules, indispensables à la division cellulaire, et induisant fatalement la mort cellulaire.

Le Melphalan, moutarde azotée, est encore utilisé en perfusion isolée dans le cadre de rechute du mélanome, quand la dissémination est confinée à un membre supérieur ou inférieur (jambes, bras). Ce concept permet de limiter la circulation de l'agent chimio-thérapeutique uniquement à la région d'intérêt. Le taux de réponse après perfusion isolée peut aller jusqu'à 80% des patients avec 40 à 60% de réponse complète [38, 39]. Cependant, la réponse peut être tardive et souvent non durable avec des rechutes dans les 9 à 21 mois suivant l'intervention. Lorsque la réponse est complète, la survie à 10 ans est de 49% alors que la survie à 5 ans pour les patients non répondeurs est seulement de 7% [40].

Lorsque la présence de métastases est généralisée (intestin, poumon, foie, cerveau), la chimiothérapie de référence aujourd'hui utilisée en clinique est la dacarbazine (DTIC, Déticène™), seule ou en association selon le protocole DBDT (Dacarbazine, Cisplatine, BCNU, Tamoxifène). Bien que le mécanisme d'action exact de la dacarbazine ne soit pas connu, celle-ci agit possiblement

en tant qu'agent alkylant. Inactive par elle-même, elle est décomposée par N-déméthylation par les microsomes hépatiques, et donne naissance à un ion méthyldiazonium, le diazométhane (l'agent alkylant), et à un métabolite principal inactif [41]. D'autres hypothèses sur son mécanisme d'action ont également été soulevées, incluant l'inhibition de la synthèse de l'ADN, par son action en tant qu'analogue de l'antipurine et par son interaction avec les groupes sulfhydriles. La dacarbazine est injectée par voie intraveineuse de 2,4 à 4,5 mg/kg/j pendant 4 à 5 jours en monothérapie, ou à raison de 250 mg/m^2/j en perfusion pendant 5 jours, toutes les 3 à 4 semaines, en polychimiothérapie. Malheureusement, le taux maximal de réponse aux traitements chimio-thérapeutiques chez les patients est de l'ordre de 15% avec moins de 5% de réponse complète [41-43]. Les traitements proposés par les chimiothérapies sont donc aujourd'hui largement insuffisantes.

1.4.4. Les immunostimulants

Historiquement, l'utilisation d'immunostimulants tels que l'interféron (IF) α 2b, a été initiée dans les années 80 pour les patients présentant un fort risque de rechute après chirurgie d'un mélanome loco-régional. Ils sont administrés en perfusion intraveineuse à raison de 20 MIU/m², 5 jours par semaine pendant un mois, suivie d'un traitement sous-cutané de 10 MIU/m² à raison de 3 fois par semaine pendant 11 mois. L'essai clinique de Kirkwood et de ses collaborateurs démontre une différence faible mais significative de la survie lorsque les patients atteints de mélanome de grade IIB/III sont traités avec de fortes doses d'IFα2b [44]. Ce traitement est aujourd'hui approuvé par la FDA pour les grades IIB/III. Cependant, ces fortes doses induisent de nombreux effets secondaires : symptômes grippaux, fatigue, malaise, anorexie, et potentiellement une atteinte hépatique.

Un deuxième immunostimulant est également approuvé par la FDA. De hautes doses d'interleukine-2 (IL-2) sont préconisées en cas de mélanome métastasé (grade IV). Cependant, seulement 6% des patients répondent à ce traitement et aucun bénéfice sur la survie n'est aujourd'hui admis avec, tout comme pour l'IFα2b, de nombreux problèmes de tolérance [45].

1.4.5. Les thérapies ciblées

Durant la dernière décennie, de nombreux progrès ont été faits dans la prise en charge des mélanomes de haut grade (III/IV) avec le développement des thérapies ciblées. Dans ce cas, le traitement s'attarde sur une anomalie des cellules cancéreuses ou du microenvironnement tumoral afin de bloquer spécifiquement la prolifération cancéreuse.

On a longtemps supposé que l'absence de réponse immunitaire de l'hôte jouait un rôle majeur dans le développement du mélanome et la formation des métastases. La compréhension des mécanismes induisant cette non-réponse ont permis de mettre à jour une nouvelle piste thérapeutique. Le CTLA-4 (Cytotoxic T-Lymphocyte-associated antigen 4) est décrit comme le

régulateur de l'inhibition des lymphocytes T [46]. Le développement de l'ipilimumab (Yervoy®), anticorps monoclonal ciblant et bloquant le CTLA-4, a permis de promouvoir la réponse immunitaire anti-tumorale [47, 48]. Un essai clinique de phase III a mis en évidence une augmentation de la survie globale passant de 6,4 mois à 10,1 mois [49].

D'autres voies moléculaires sont connues pour jouer un rôle dans la progression tumorale telle que la voie des MAP-Kinase (Mitogen-Activated Protein) avec la protéine B-Raf, associée au syndrome familial comme vu précédemment (cf. Introduction, § 1.2.1). Des mutations de B-Raf sont retrouvées dans 40 à 60 % des mélanomes cutanés, induisant une activation permanente de la voie des MAP-Kinase [50]. Dans 90 % des cas, cette mutation correspond à une substitution d'une valine en acide glutamique à la position 600 (V600E). Cette protéine B-Raf V600E est spécifiquement inhibée par l'anticorps monoclonal vémurafenib (Zelboraf®) [51]. La survie après 6 mois de traitement est de 84% pour les patients recevant le vémurafenib contre 64% pour la dacarbazine, avec un taux de réponse bien plus élevé (48% vs 5% pour la dacarbazine) [52]. En 2012, la FDA a approuvé l'ipilimumab et le vémurafenib pour le traitement de mélanomes de stade IV. Bien que ces deux médicaments aient apporté l'espoir de traiter une maladie historiquement réfractaire à une thérapie systémique, il reste cependant encore beaucoup de chemin à parcourir. Même si l'ipilimumab a montré une amélioration significative de la survie globale, on observe un taux de réponse de seulement 11%, similaire à celui obtenu avec la Dacarbazine. Inversement, le vémurafenib présente un taux de réponse impressionnant, mais la durabilité de la réponse clinique reste faible, avec une résistance acquise à ce médicament quasi-systématique chez les patients [53].

L'identification de nouvelles cibles moléculaires doit donc se poursuivre, ainsi que le développement de nouveaux essais cliniques, afin d'évaluer la combinaison qui permettra de faire progresser le traitement du mélanome de haut grade.

2. L'amélioration des chimiothérapies

2.1. Le phénomène de résistance

A l'heure actuelle, les traitements chimiothérapeutiques échouent pour les hauts grades de mélanome, ou mélanomes métastasés, avec un taux de réponse maximal évalué à 16% avec la dacarbazine. Une multitude d'agents chimiothérapeutiques ont été testés tels que la carmustine, la vinblastine, seules ou en association, mais aucun bénéfice sur la survie n'a pu être observé [54]. Dès les années 1980, les expérimentations *in vivo* sur différents modèles tumoraux de mélanome confirment la forte résistance du mélanome vis-à-vis des agents chimiothérapeutiques [55].

Cette résistance peut s'expliquer par le processus de cancérogénèse du mélanome (Figure 5). Comme décrit précedemment, les rayonnements ou autres facteurs environnementaux induisent la mutation de cetains gènes. Dans un premier temps, des mutations fréquentes sont observées au niveau du gène B-Raf impliqué dans la prolifération (cf. Introduction, § 2.1.2), au niveau du gène $p16^{INK4A}$ impliqué dans la régulation des dommages à l'ADN et au niveau des gènes impliqués dans la régulation de l'apoptose (protéine p53), MITF (Microphthalmia-associated transcription factor), N-Ras, ou encore Bcl-2. La littérature montre que durant cette première progression, la tendance va vers une augmentation des signaux anti-apoptotiques (Bcl-2, Mcl-1 et $Bcl\text{-}_{XL}$). Par la suite, des mutations supplémentaires viennent s'ajouter avec le temps, touchant plus particulièrement les voies de signalisation de la prolifération et de la survie, ainsi qu'une diminution des signaux pro-apoptotiques (Bad, Bax).

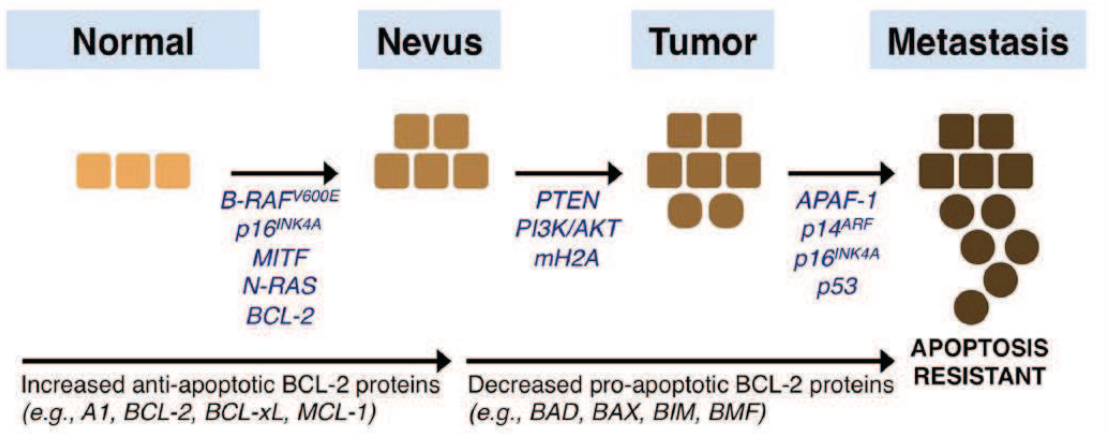

Figure 5 : Mécanisme de cancérogénèse du mélanome (issu de Anvekar *et al.,* 2011, Frontiers in oncology)

Cette résistance observée aux agents chimiothérapeutiques est donc principalement liée à un dysfonctionnement du processus de mort cellulaire, qu'est l'apoptose, au sein des cellules de mélanome [56, 57]. Ce dysfonctionnement s'explique par le déséquilibre de la balance entre les acteurs favorisant ou inhibant l'apoptose, avec une diminution des pro-apoptotiques et une

augmentation des anti-apoptotiques. Par ailleurs, on observe également la présence de signaux intenses de survie et de prolifération comme le montrent les mutations induites de B-Raf ou MITF. Dans ce cas, les voies de signalisation des MAPkinases, de la PI3K (phosphoinositol 3 kinase) et du facteur NF-kB sont généralement toutes impliquées. Ce sont les dérégulations de ces deux processus majeurs, l'apoptose et la survie cellulaire, qui expliquent la forte chimiorésistance observée dans le cadre du mélanome [58].

2.1.1. L'apoptose et la chimiorésistance

Le processus d'apoptose est un processus complexe de régulation entre les acteurs pro et anti-apoptotiques. Si la cancérogénèse démontre l'action irrémédiable de certains de ces effecteurs comme Bcl-2, de nombreuses autres perturbations de ce phénomène sont liées à la chimiorésistance. On différencie deux voies d'action possibles de l'apoptose. La voie extrinsèque est initiée par des stimuli externes avec les récepteurs de mort tel que TRAIL (TNF-related apoptosis-induced ligand) (Figure 6) [59]. La fixation du ligand, tel que le TNF-α (Tumor necrosis factor) ou le Fas ligand, sur le récepteur induit l'activation de la caspase 8 ou 10. Il peut également conduire à l'activation des protéines Bid et Bad (pro-apoptotiques à domaine BH3) reliant ainsi la seconde voie possible de l'apoptose.

Cette seconde voie dite voie intrinsèque de l'apoptose, est, quant à elle, induite par le régulateur p53, après des dommages de l'ADN ou un stress oxydatif important présent lors des rayonnements UV, comme cité précédemment (Figure 6). En effet, par défaut, la protéine Bcl-2 ou ses homologues (Mcl-1, Bcl-$_{XL}$) bloque l'action des protéines Bax ou Bak par la formation d'un complexe avec celles-ci. Dans le cas d'un stress cellulaire, la protéine p53 favorise l'action des protéines pro-apoptotiques à domaine BH3 (Bim, Bad…) permettant de libérer Bax et/ou Bak. Ces molécules vont alors se positionner à la membrane mitochondriale afin d'engendrer la libération du cytochrome C. Une fois dans le cytoplasme, une cascade d'activation de protéine induit la formation de l'apoptosome (complexe formé de molécules APAF-1 et de cytochrome C) menant à l'activation des caspases. En effet, les deux voies, intrinsèques et extrinsèques, se rejoignent alors par l'activation commune de la voie des caspases avec la caspase 3 et 7, finalisant l'apoptose (Figure 5). De nombreux effecteurs moléculaires entrent en jeu dans ces deux voies d'action, pouvant entraîner, à chaque niveau de la cascade moléculaire, des dérégulations en faveur de l'inhibition du processus de « suicide cellulaire » et de la chimiorésistance.

- *Les récepteurs de mort*

Les mélanomes sont très immunoréactifs et résistent à l'attaque pro-apoptotique des cellules immunes médiées par le granzyme et les ligands de mort par la voie extrinsèque [60]. Les

lymphocytes infiltrant les mélanomes ont montré une sécrétion importante de TNF-α, CD95L et TRAIL afin de favoriser la mort de cellules tumorales par voie extrinsèque [61-63], entraînant alors une pression de sélection élevée pour les mélanomes à acquérir une résistance aux stimuli de mort par ligands. Alors que la résistance par la voie du CD95 est principalement liée à sa propre répression ou mutation, les phénomènes de résistance avec les TRAIL sont dus à la perte du récepteur DR4 (Death receptor 4), à l'inactivation du récepteur DR5, ou encore à la diminution de l'O-glycolysation des récepteurs TRAIL [58, 64].

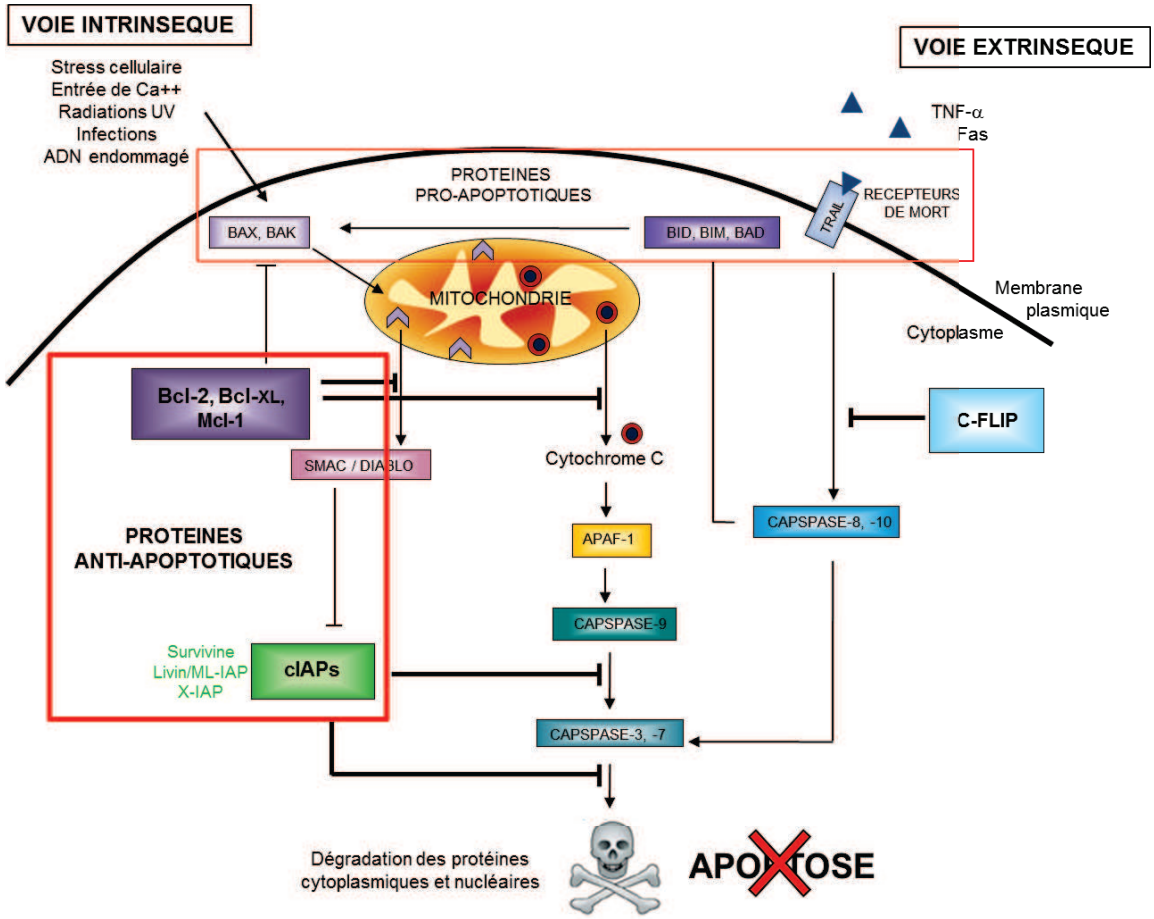

Figure 6 : **Voie de signalisation et dérégulations des deux principales voies de l'apoptose dans le cas du mélanome** (inspiré de Riedl *et al.,* 2004)

➢ *Les protéines de la famille Bcl-2*

La voie intrinsèque ou mitochondriale est fortement régie par la famille des protéines Bcl-2. Cette voie est activée dans les cellules de mélanome en réponse à divers stimuli, y compris les signaux extrinsèques [65-67]. La famille de protéines Bcl-2 se compose de membres de la famille anti-et pro-

apoptotique comprenant des protéines à multi-domaine (BH1 à BH4) (Bak, Bax, Bcl-2, Mcl-1) et les protéines à domaine BH3 uniquement (Bad, Bim, Bid) [68]. Plusieurs protéines anti-apoptotiques, en particulier, la protéine Bcl-2, Bcl-$_{XL}$ et Mcl-1 sont fortement exprimées dans les mélanomes et dans des lignées cellulaires de mélanome [69-71]. Un rapport élevé Bcl-2/Bax a été mis en corrélation avec la résistance à l'apoptose via CD95 et celle induite par les céramides (médiateur lipidique) [65]. Si le rôle de Bcl-2 dans la survie cellulaire est aujourd'hui évident, son implication dans le phénomène de résistance reste incertain avec une surexpression controversée dans les métastases alors que celles de Bcl-$_{XL}$ et Mcl-1 augmentent [72]. Cependant, l'analyse de métastases exposées aux traitements chimiothérapeutiques combinés a révélé un taux élevé de Bcl-2, comparativement aux régions en régression après le traitement [73]. Cette observation fait donc le lien entre l'expression de Bcl-2 et le phénomène de chimiorésistance observé dans le mélanome. Cette protéine Bcl-2 sera décrite ultérieurement dans le cadre de ces travaux (cf. Introduction, § 2.2.1).

- *Les caspases*

Les caspases 8 et 10 ont un rôle essentiel dans la transduction du signal des récepteurs de mort [58]. Ces deux caspases sont majoritairement surexprimées dans les mélanomes. Cependant, en cas de résistance à la voie d'apoptose extrinsèque, leur expression est inhibée [74]. De plus, les régulateurs des caspases peuvent également être bloqués par les protéines inhibitrices, comme cFLIP, fréquemment exprimées dans les mélanomes et leurs métastases [75]. Cette surexpression dans les mélanomes a été corrélée avec la résistance au processus d'apoptose extrinsèque alors que leur inhibition provoque une sensibilisation à ce processus [76, 77].

Les deux voies apoptotiques se confondent alors au niveau des caspases effectrices, qui peuvent être régulées par des inhibiteurs de caspases (les cIAPs) [78]. Dans le mélanome, l'expression de la survivine et des protéines livin/ML-IAP et X-IAP (X-linked IAP) a été mise en relation avec la résistance aux chimiothérapies, ainsi que la progression tumorale et une baisse de la survie des patients [79]. Une chimiosensibilité envers le carboplatine a pu être obtenue après l'inhibition de X-IAP lors d'expérimentations sur des modèles *in vitro* de mélanome [77, 80, 81].

2.1.2. Survie, prolifération cellulaire et chimiorésistance

Le phénomène de résistance aux chimiothérapies est également étroitement lié aux grandes voies de signalisation induites par l'activation des facteurs de croissance qui, invariablement, interagissent avec le processus de survie cellulaire et de prolifération et donc défavorisent le processus d'apoptose. Ces voies de signalisation sont la voie des MAPK (Mitogen activated protein kinase), la voie de la PI3K-Akt et enfin celle du NF-κB (Figure 7).

➢ *La voie des MAPK*

Cette voie de signalisation est activée par les récepteurs aux facteurs de croissance tels que l'EGFR (Epidermal Growth Factor Receptor) avec une transduction du signal par les protéines GTP-Ras. Ensuite, les protéines kinases Raf, MEK et ERK1/2 sont phosphorylées successivement, amenant à l'activation de multiples facteurs de transcription [82, 83]. Dans les mélanomes, l'activation constitutive de ERK1/2 est fréquemment observée, mais elle résulte de la mutation activatrice de B-Raf (60% des cas) et de N-Ras (30% des cas) [50, 84]. Des connexions évidentes ont été mises en évidence entre les MAPK et le processus de survie cellulaire, entrainant une chimiorésistance pour laquelle les membres de la famille Bcl-2 jouent un rôle essentiel comme effecteur [85]. Les MAPK engendrent également une inhibition des protéines pro-apoptotiques telles que Bim et Bad par phosphorylation, ou PUMA par régulation négative [86, 87] ainsi qu'une stimulation des molécules anti-apoptotiques telles que Mcl-1 [88]. De plus, l'un des facteurs de transcription initiés par les MAPK est MITF. Ce dernier possède un rôle primordial dans la résistance à l'apoptose avec une sur-activation de Bcl-2 (anti-apoptotique) [89].

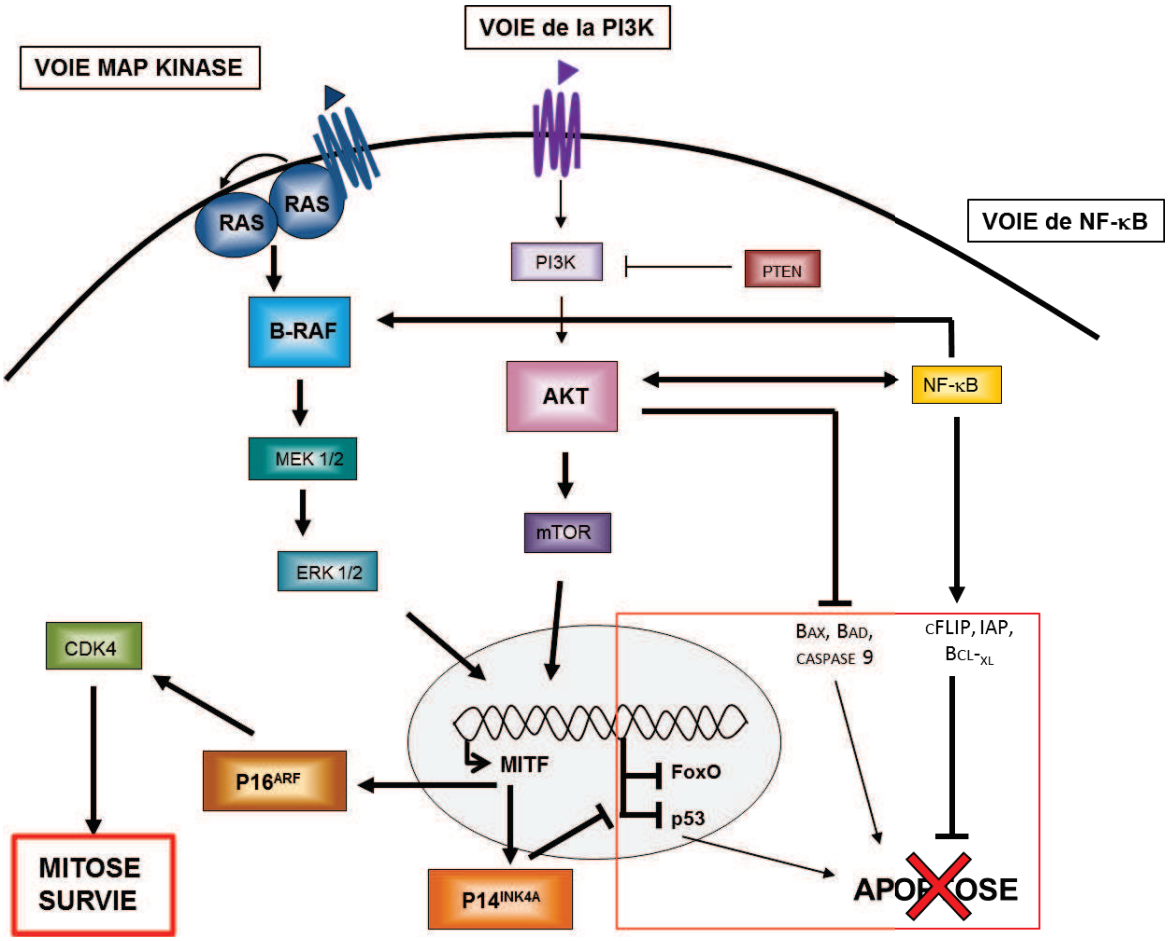

Figure 7 : Voies de signalisation des MAP kinase, de la PI3K et de NF-κB impliquées dans la prolifération et la survie cellulaire

➢ *La voie de la PI3K*

La survie cellulaire est permise par l'activation de la PI3K entrainant la phosphorylation de la protéine kinase B/Akt, puis l'activation de la protéine mTOR (mammalian Target of Rapamycin) [90]. Cette voie a été reliée à la chimiorésistance dans de multiples cancers [91]. La protéine Akt est connue pour avoir des fonctions anti-apoptotiques par la phosphorylation de Bax, Bad et la caspase 9 [92-94], ainsi que des fonctions pro-apoptotiques par l'inhibition des facteurs de transcription FoxO et p53 [90]. La protéine mTOR joue également un rôle dans l'inhibition de l'autophagie et de l'apoptose, favorisant la croissance tumorale ainsi que le phénomène de chimiorésistance [95-97]. L'activité anti-apoptotique présente dans les cellules de mélanome a pu être reliée à l'inactivation de Bad par Akt [98] ou au lien avec la voie de NF-κB et Akt [99].

➢ *La voie de NF-κB*

Les facteurs de transcription de la famille de NF-κB sont des hétéro ou homodimères formés par 5 sous-unités : NF-κB1 (p50/p105), NF-κB2 (p52/p100), RelA (p65), RelB et RecC [100]. Ces différents dimères sont retenus dans le cytoplasme par des interactions avec les inhibiteurs des NF-κBs (I-κBs). L'activation et la translocation des dimères NF-κB vers le noyau s'effectue par la voie canonique via les cytokines ou via l'activation induite par les lipopolysaccharides (LPS), démontrant leur rôle dans l'immunité. La stimulation de la voie de signalisation induit une dégradation par les voies de protéasome des I-κBs par le complexe de kinase I-κB (IKK), entrainant alors la translocation nucléaire de NF-κB [101]. En parallèle à l'implication dans la réponse immunitaire, les protéines NF-κB ont montré leur importance dans la progression tumorale, la formation de métastases et la chimiorésistance [102, 103]. Leur action anti-apoptotique est associée à l'activation des effecteurs anti-apoptotiques tels que les protéines IAP, c-FLIP et Bcl-$_{XL}$ [104]. Un taux élevé des IKK et des NF-κB a été démontré dans les mélanomes impliquant une voie de signalisation secondaire par une boucle de rétrocontrôle entre les MAPK et les kinases induites par les NF-κB [99, 105]. L'activité anormalement forte de NF-κB dans le mélanome a été corrélée au phénomène de chimio et radiorésistance [106-108].

2.2. Une thérapie ciblée pour chimio-sensibiliser

De plus en plus de thérapies sont aujourd'hui orientées sur le ciblage spécifique de ces molécules impliquées dans le processus de cancérogénèse et plus particulièrement celles liées aux phénomènes de chimiorésistance. Deux protéines semblent aujourd'hui avoir un potentiel intéressant pour aider les chimiothérapies à être efficaces contre le mélanome : un effecteur direct de l'apoptose

(la protéine Bcl-2), et un effecteur indirect de la prolifération et la survie (la sous-unité alpha1 de la pompe à sodium).

2.2.1. La protéine Bcl-2

La protéine Bcl-2 (B-cell lymphoma 2), découverte dans les années 1980, est une protéine de 26 kDA soit 239 acides aminés dont le gène est situé, chez l'homme, sur le chromosome 18 au locus q21.33. Elle est le premier membre décrit d'une famille de protéines qui portera son nom, toutes constituées de quatre domaines d'homologie, nommés BH1, BH2, BH3, BH4, ainsi que d'un domaine transmembranaire (Figure 8) [109]. Grâce à la présence de ces différents domaines d'homologie, la protéine Bcl-2 a un rôle primordial dans l'inhibition de l'apoptose via sa forte affinité avec certaines protéines pro-apoptotiques. Localisée dans la membrane mitochondriale, Bcl-2 empêche l'homodimérisation de Bax, ou de Bak et de certaines autres protéines pro-apoptotiques de la même famille (Figure 8) [109].

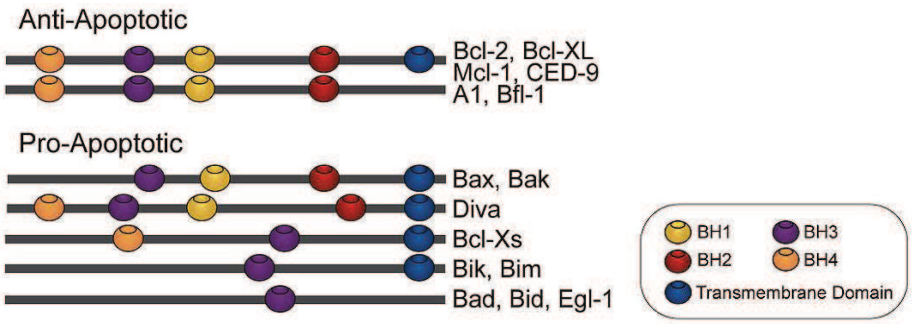

Figure 8 : **Caractérisation structurale des membres de la famille Bcl-2**

La protéine Bcl-2 a été premièrement reliée au processus de cancérogénèse dans le lymphome à cellules B, puis dans de nombreuses autres formes de cancer. Cette protéine primordiale dans le phénomène d'apoptose est généralement surexprimée dans les métastases issues de mélanome par rapport aux sites primaires de développement tumoral [110]. Cependant, certaines études parallèles prouvent le contraire, avec une diminution de l'expression de Bcl-2 au sein des métastases [72]. En effet, plusieurs études montrent qu'une baisse de Bcl-2 est corrélée avec deux facteurs de pronostic : l'augmentation de l'épaisseur de la tumeur et la présence de lactate déshydrogénase [72, 111]. Cependant, même si le niveau de Bcl-2 seul ne suffit pas à être un facteur pronostic fiable [112], son taux sanguin élevé permet tout de même de discriminer les patients atteints de mélanome et le groupe contrôle [113].

De façon intéressante, la surexpression de Bcl-2 a été mise en évidence après un traitement chimiothérapeutique, démontrant ainsi son lien direct avec la chimiorésistance acquise des cellules

de mélanome [73]. Dans ce cas, elle entraine une impossibilité du processus de mort cellulaire par apoptose et ainsi une survie augmentée des cellules cancéreuses. Bcl-2 a également montré une implication dans l'angiogénèse en condition hypoxique avec l'activation d'un certain nombre de métalloprotéases (MMP-2, MMP-7) ou avec l'augmentation de VEGF (Vascular Endothelial Growth Factor) et de HIF-1 (Hypoxia-inducible factor 1) [114, 115].

2.2.2. La sous-unité alpha 1 de la pompe à sodium Na/K ATPase

La pompe à sodium/potassium (Na^+/K^+ ATPase, i.e. NaK) est une protéine transmembranaire découverte dans les années 50 par un Danois, Jens Christian Skou, qui recevra le prix Nobel de chimie en 1997 pour cette découverte majeure [116]. En effet, l'activité enzymatique de cette protéine utilise l'énergie issue de la dégradation de l'ATP (Adénosine TriPhosphate) en ADP (Adénosine DiPhosphate) et phosphate inorganique, pour transporter des ions potassium (K^+) et sodium (Na^+) contre leur gradient de concentration, afin de rétablir l'équilibre. La protéine permet d'échanger les ions Na^+ issus du milieu intracellulaire avec les ions K^+ issus du milieu extracellulaire dans un rapport précis (3 Na^+/2 K^+). Cette pompe ionique joue un rôle essentiel dans le maintien du potentiel de repos et le rétablissement de l'équilibre initial après le potentiel d'action observé spécifiquement dans les cellules nerveuses, musculaires et cardiaques.

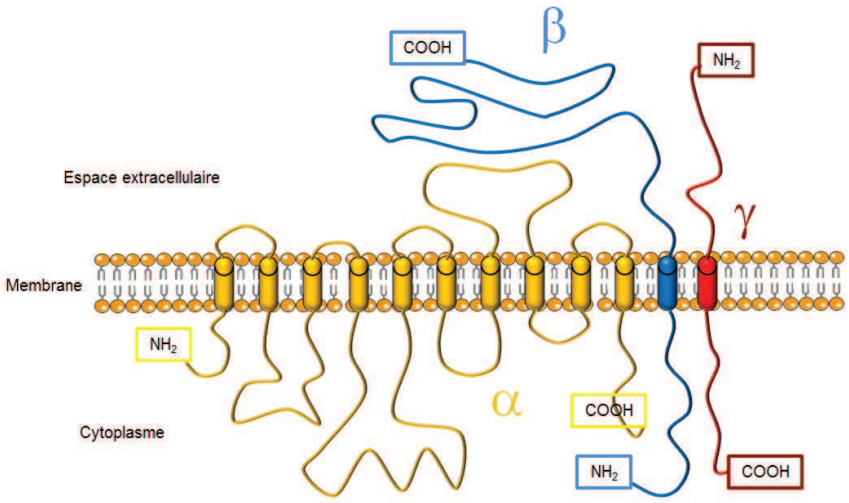

Figure 9 : Structure de la pompe à sodium avec ses différentes sous-unités

Cette protéine transmembranaire est composée de trois sous-unités : alpha, béta et FXYD (ou gamma) (Figure 9). La sous-unité béta, ou sous-unité chaperonne, est essentielle pour l'ancrage correct de la protéine au niveau de la membrane plasmique. Elle permet également le recrutement et l'interaction avec la sous-unité régulatrice FXYD (ou gamma). La sous-unité alpha est la sous-unité la plus importante en terme de taille et de fonction. Elle comprend dix domaines transmembranaires

formant un pore permettant la fonction de pompe ainsi que les sites de reconnaissance de l'ATP, des ions Na^+ et K^+. Pour chacune des sous-unités de cette protéine, différents isoformes tissu-dépendants (3 pour la sous-unité alpha, 3 pour la béta et 7 pour la FXYD) ont été découverts et peuvent s'associer indépendamment. Cette protéine est présente sur toutes les cellules de l'organisme mais on la retrouve plus exprimée dans certains tissus tels que le cœur (potentialisation de la membrane), les reins (échange d'ions), le cerveau ou encore la thyroïde [117]. Les trois isoformes alpha ($\alpha1$, $\alpha2$, $\alpha3$) sont retrouvés au niveau cardiaque et au niveau cérébral [118, 119], alors que l'isoforme $\alpha2$ est exprimé dans les muscles et le couple d'isoformes $\alpha1/\beta1$ se trouve, lui, majoritairement dans les cellules endothéliales participant au maintien des jonctions serrées [120].

La sous-unité alpha 1 est, elle, exprimée seule dans les reins ou dans les poumons [119] et, en association avec les autres isoformes, dans le cerveau ou dans le cœur. La localisation du gène se situe au niveau du chromosome 1 (1p21) non loin de l'isoforme alpha 2, contrairement à l'isoforme 3 présent sur le chromosome 13 (19p13) [121]. Cette protéine présente un intérêt inattendu en thérapeutique anti-cancéreuse. En effet, des études épidémiologiques ont démontré que des patients atteints de cancer du sein ou de la prostate survivaient plus longtemps s'ils étaient en parallèle sous digoxine (cardiotonique stéroïdien constituant un inhibiteur chimique de la pompe à sodium), un médicament qui est à l'heure actuelle prescrit pour les insuffisants cardiaques [122, 123]. De plus, plusieurs travaux montrent une fonction ou une expression dérégulée de cette protéine dans diverses pathologies cancéreuses, incluant les mélanomes métastatiques [124]. Des immuno-marquages ont révélé la surexpression plus spécifique de la sous-unité alpha 1 au niveau des mélanomes, en comparaison à des nevus bénins. La protéine est retrouvée surexprimée dans la moitié des métastases issues de mélanome, un résultat qui atteint même plus de 70% pour les métastases cérébrales [124]. De plus, cette surexpression est également corrélée à l'index de Breslow décrit précédemment (cf. Introduction, § 1.3.3).

Comment cette protéine impliquée dans l'osmorégulation intervient-elle dans le processus de cancérogénèse du mélanome ? Dans le cas des cellules cancéreuses, une partie du pool de la pompe à sodium est en fait associée à un tout autre rôle. Cette protéine se retrouve recrutée au niveau des cavéoles dans un signalosome permettant l'activation des voies moléculaires telles que Scr ou Ras, impliquées classiquement dans la cancérogénèse [125]. Les cellules cancéreuses profitent de la sous-unité FXYD associée à la sous-unité alpha 1 pour activer les signaux d'autres récepteurs tels que le récepteur à l'EGF (Epidermal Growth Factor), favorisant ainsi la prolifération, la survie et le processus de métastase.

En effet, ce signalosome permet l'activation des MAPKinases, via le récepteur à l'EGF, amenant finalement à l'activation de c-myc par la voie des MAPK (Figure 7). Ce facteur de transcription, c-myc, est largement décrit pour ses rôles pro-cancérigènes induisant la prolifération (avec par

exemple l'activation de CDK4), supprimant le processus de sénescence, et favorisant ainsi la résistance aux chimiothérapies [126, 127]. L'activation du récepteur de l'EGF (Epidermal growth factor) et la variation du taux de calcium intracellulaire vont également agir sur la voie NF-kB favorisant d'autant plus la prolifération et le blocage de l'apoptose [128] (Figure 10).

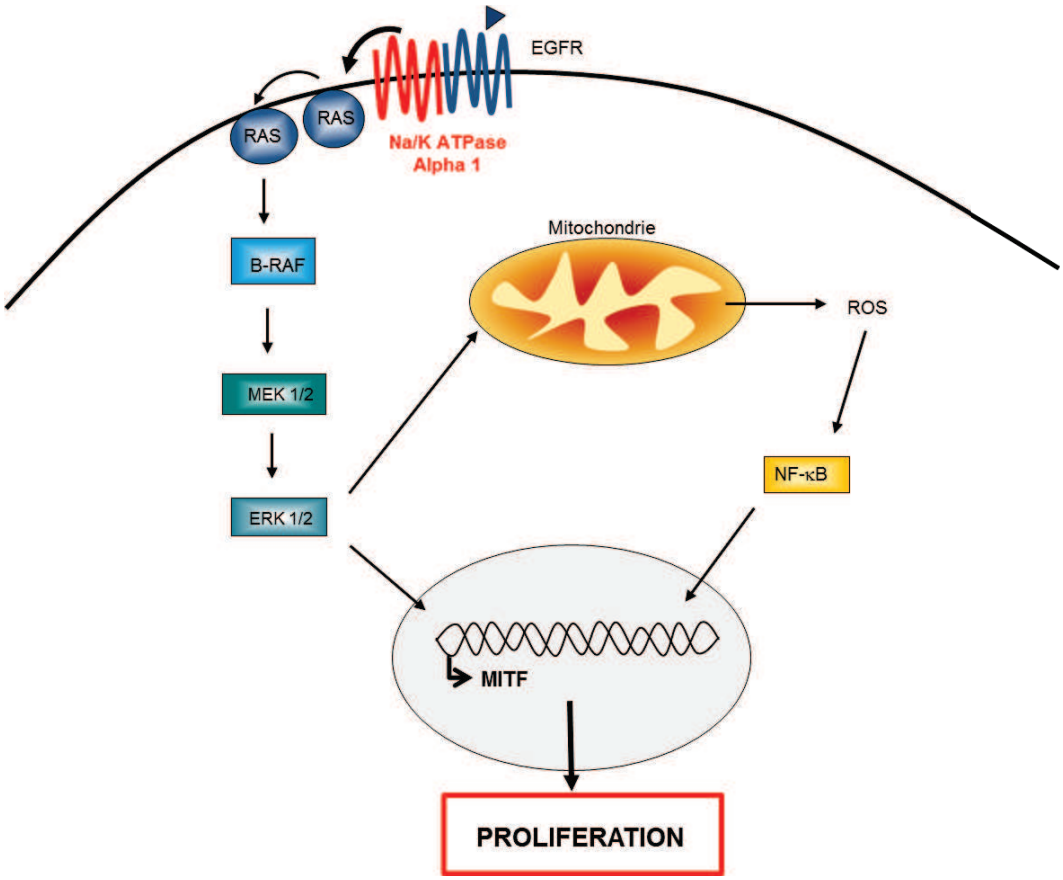

Figure 10 : **Schéma d'activation des voies impliquées par le recrutement de la pompe à sodium au niveau du signalosome** (à partir d'une figure issue de Prassas *et al.,* Nature Reviews Drug Discovery, 2008).

2.3. Les voies d'action

L'inhibition de protéines peut être réalisée selon différentes stratégies grâce aux développements de la chimie et de la biologie moléculaire. Si les anticorps ne s'appliquent qu'aux protéines accessibles à la surface des cellules tumorales telles que le CTLA-4 (cf. Introduction, § 1.4.5), les inhibiteurs chimiques spécifiques aux protéines d'intérêt fleurissent et sont utilisés depuis quelques années en cancérologie. Par ailleurs, la récente découverte des ARN interférents offre de nouvelles possibilités d'influer sur l'expression d'une protéine cible.

2.3.1. Les inhibiteurs chimiques

➢ *La protéine Bcl-2*

Le ciblage de la protéine Bcl-2 a été envisagé par des inhibiteurs chimiques dits « BH3-mimetics ». Ces molécules chimiques, par leur affinité avec Bcl-2, ont démontré un potentiel intéressant en préclinique, avec une synergie observée en association avec les inhibiteurs du protéasome (bortezomib) [129]. On dénombre actuellement 3 molécules en essais cliniques : AT-101 (Gossypol), GX15-070 (Obatoclax) et ABT-263.

Nom	Cancer	Phase essai clinique	Nom générique	Référence
AT-101	Leucémie, Poumon	I, II	Gossypol	[130]
GX15-070	Leucémie, Poumon	I/II	Obatoclax	[129]
ABT-263	Tumeur solide, lymphome	I	Navitoclax	[131]

Tableau 2 : Inhibiteurs chimiques ciblant la molécule Bcl-2 en essai clinique

La totalité des inhibiteurs de Bcl-2 a également la faculté de se lier avec d'autres protéines de la même famille que Bcl-2 telle que Mcl-1, Bcl-$_{XL}$. L'AT-101 est inhibiteur de Bcl-2 et de Mcl-1. ABT-263 se lie avec une forte affinité aux protéines Bcl-2, Bcl-$_{XL}$, et Bcl-$_{W}$, et interagit plus faiblement avec Mcl-1. Enfin, le GX15-070 est quant à lui capable de se lier au Bcl-2, Bcl-$_{XL}$, Bcl-$_{W}$ et Mcl-1 [130]. En effet, les inhibiteurs chimiques de Bcl-2 n'offrent pas de spécificité exclusive envers Bcl-2, entrainant des effets contradictoires comme avec l'ABT-263. En effet, ce dernier permet l'inhibition efficace de Bcl-2 et Bcl-$_{XL}$. Cependant, une boucle de rétro-contrôle semble entraîner l'activation de Mcl-1, limitant l'effet anti-cancéreux souhaité. La concomitance avec un inhibiteur de la voie PI3K permet de retrouver une efficacité significative [132].

Par ailleurs, si la phase I des essais cliniques concernant l'AT-101 a démontré une tolérance, même en concomitance avec l'étoposide ou le cisplatine [133], l'essai clinique de phase I/II concernant le GX15-070 associé au bortezomib chez des patients atteints de lymphome a montré une tolérance mitigée [129]. Des effets indésirables ont été constatés comprenant somnolence (87%), fatigue (61%), euphorie (57%) à des grades I/II. Des effets de sévérité III/IV ont été observés incluant des thrombopénies (21%), des anémies (13%) et des fatigues (13%). Pour le moment, aucun inhibiteur de Bcl-2 n'a obtenu d'autorisation de mise sur le marché.

➢ *La sous-unité alpha 1*

L'inhibition de la sous-unité alpha 1 est également rendue possible par des inhibiteurs chimiques tels que les stéroïdes cardiotoniques (ouabain, digoxin), aujourd'hui commercialisés dans le cadre

d'une autorisation de mise sur le marché pour les patients atteints d'insuffisance cardiaque. Des études menées avec des stéroïdes cardiotoniques ont montré que l'inhibition de la pompe à sodium dans les cellules cancéreuses conduit à i) une désorganisation du cytosquelette via l'actine, ii) une perte du partenariat avec le signalosome compromettant ainsi sa signalisation et iii) l'induction de la mort cellulaire par apoptose ou non-apoptotique telle que l'autophagie ou par perméabilisation de la membrane, même dans des lignées dites multi-résistantes [134, 135].

Cependant, tout comme pour la protéine Bcl-2, les inhibiteurs chimiques aujourd'hui disponibles ne permettent pas une spécificité limitée à une sous-unité. Ce manque de spécificité rend difficile le développement de ces composés à des fins anti-tumorales en raison d'une cardiotoxicité potentielle par le ciblage à la fois des sous-unités $\alpha 1$, $\alpha 2$ et $\alpha 3$.

Malgré un nombre grandissant de molécules chimiques, seuls quelques essais cliniques ont été menés en oncologie avec des résultats mitigés à ce jour et des toxicités non négligeables. Des essais complémentaires sont encore actuellement en cours (*www.clinicaltrials.gov*). Par conséquent, une autre alternative de ciblage de la pompe à sodium et de la protéine Bcl-2 doit être envisagée pour une application anti-cancéreuse.

2.3.2. Les ARN interférents

La thérapie génique est une nouvelle alternative récemment étudiée permettant de contrôler ou de modifier l'expression des gènes et donc des protéines. Cette stratégie thérapeutique a été initiée dans les années 80 avec le transfert de gène via l'utilisation de plasmide d'ADN. L'objectif était alors d'insérer une nouvelle copie fonctionnelle du gène au niveau du génome natif des patients pour ainsi corriger et produire la protéine qui se trouvait manquante ou défaillante. Dans ce cadre, la thérapie génique est premièrement pensée pour des maladies monogéniques telles que la β-thalassémie [136].

L'application de la thérapie génique pour la pathologie cancéreuse va émerger avec la découverte des petits ARN interférents (siRNA) à la fin des années 90. Fire met en évidence ce phénomène dans des plantes, puis chez le nématode *C.Elegans*. Ces petits ARN, dits interférents, ont la capacité d'interagir avec un ARN messager (ARNm) et d'inhiber ainsi leur traduction en protéine [137]. Ces siRNA sont pris en charge dans le cytoplasme par l'endonucléase Dicer (Figure 11). La protéine Ago2 s'ajoute pour former le complexe RISC (RNA induced silencing complex) et interagir avec l'ARNm cible, entraînant son clivage et/ou sa dégradation [138]. Cette action inhibitrice s'avère alors comme une alternative intéressante pour inhiber spécifiquement l'expression d'oncogènes intervenants dans le développement de pathologies cancéreuses.

Les siRNA offrent une stratégie de ciblage très spécifique avec la sélection d'une séquence personnalisée permettant de cibler une seule protéine telle que la sous-unité alpha 1 de la pompe à

sodium ou la protéine Bcl-2. Un oligonucléotide antisens de 18 bases, l'Oblimersen®, ciblant la protéine Bcl-2 a été développé à la fin des années 90. Son utilisation a démontré un effet de sensibilisation du mélanome à la dacarbazine [139]. Un essai clinique a prouvé le bénéfice de la combinaison de l'Oblimersen® avec la dacarbazine, entrainant une augmentation du taux de réponse à 13,5 contre 7,5% avec la dacarbazine seule [140]. Dernièrement, un essai clinique de phase I a conduit à des résultats prometteurs concernant l'utilisation de l'Oblimersen® en association avec le témozolomide, pour le traitement des mélanomes métastasés [141].

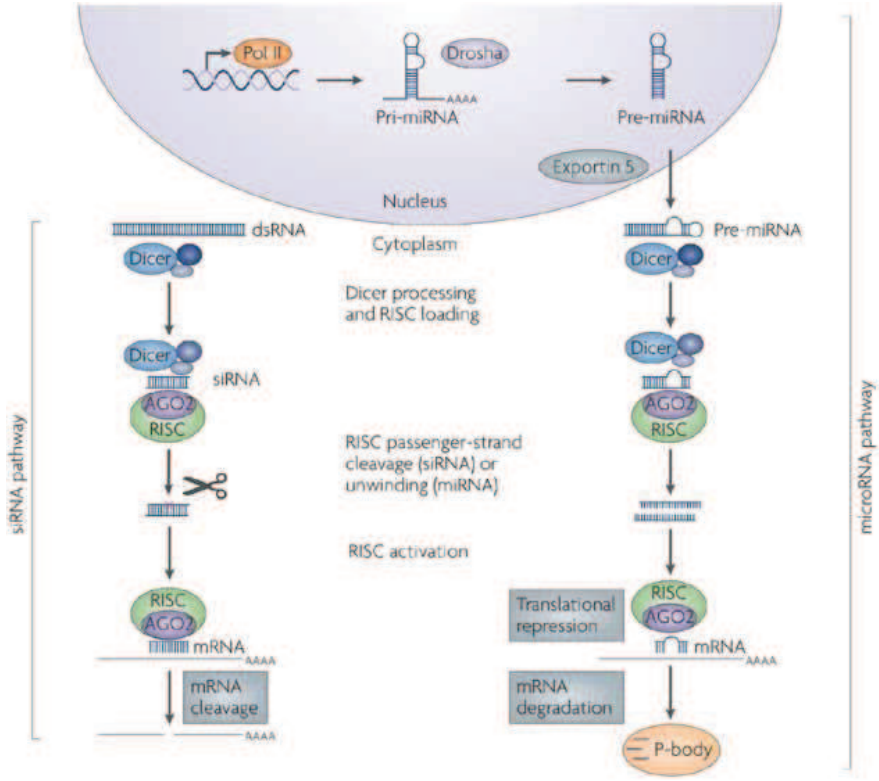

Figure 11 : Voie de signalisation des ARN interférents (issu de De Fougerolles *et al.,* Nature Reviews Drug Discovery, 2007)

Le ciblage par siRNA de la sous-unité alpha 1 a, quant à lui, été initié récemment sur un modèle cellulaire de mélanome [124]. Les premiers résultats démontrent une efficacité du siRNA véhiculé par des agents de transfection commerciaux à éteindre correctement la protéine cible.

Cependant, si ces molécules hydrophiles apparaissent comme un outil prometteur, elles ne peuvent pas passer les barrières biologiques telles que les membranes plasmiques. De plus, une injection intraveineuse est impossible du fait de la présence de nucléases dans le compartiment sanguin, entrainant une dégradation rapide de ces composés. Il devient donc indispensable de véhiculer les siRNA avec des systèmes novateurs permettant leur protection, le ciblage des cellules tumorales, ainsi que le passage des membranes plasmiques.

3. Les nanomédecines

3.1. Les objectifs des nanotechnologies et leurs applications

3.1.1. Les différents types de nanomédecines

Les nanomédecines concernent l'application de la nanotechnologie à la recherche médicale et notamment l'administration de médicaments sous forme de nanoparticules, objets à l'échelle nanométrique (10^{-9} mètres).

L'utilisation des nanotechnologies en pharmacologie a pour objectif, premièrement, de protéger un principe actif contre une dégradation potentielle, et deuxièmement de modifier la distribution naturelle de ce principe actif dans l'organisme. Il est alors théoriquement possible de diriger et d'accumuler le principe actif sur le site d'action souhaité et de l'éloigner des sites indésirables afin de limiter les effets secondaires. Les domaines d'application des nanomédecines en santé sont très variés. La cancérologie est un des domaines où l'on trouve le plus d'applications du fait des possibilités de vectorisation tumorale offertes par les nanoparticules.

Ces objets thérapeutiques de taille nanométrique sont divers et comprennent, entre autres, les dendrimères (A), les micelles (B), les liposomes (C), les nanoparticules (D, E), ou encore les nanocapsules (F) (Figure 12).

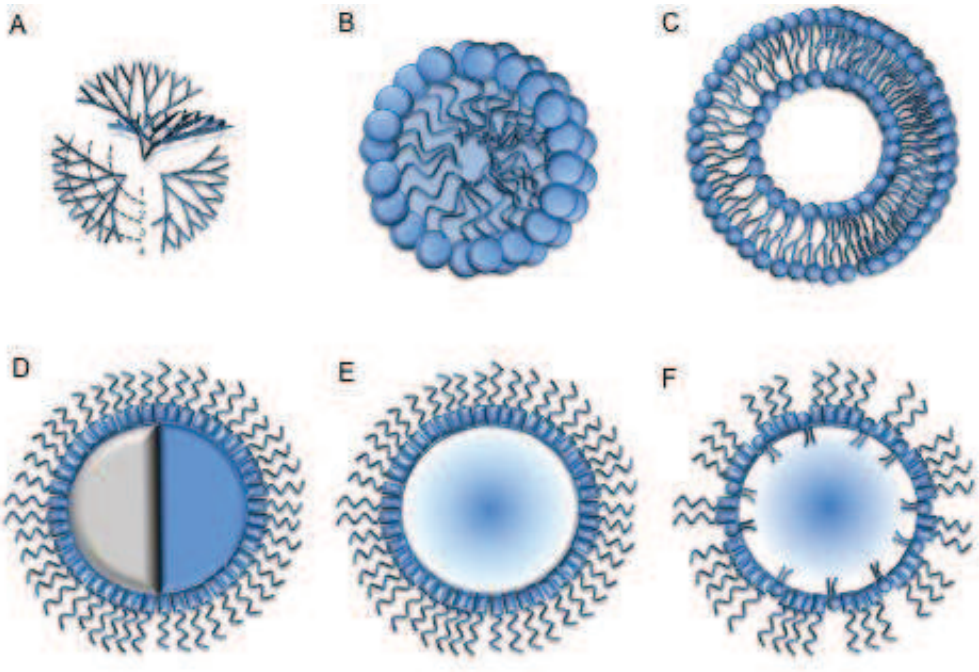

Figure 12 : Les différents types de vecteurs synthétiques. A : Dendrimères, B : Micelles, C : Liposomes, D : Nanoparticules polymériques, E : SLN (Nanoparticules lipidiques solides), F : LNC (Nanocapsules Lipidiques)

3.1.2. Les applications des nanomédecines en cancérologie

- *L'encapsulation des agents chimiothérapeutiques*

Certaines molécules anticancéreuses sont extrêmement lipophiles et leur administration chez le patient nécessite l'élaboration d'une forme galénique adaptée à leur injection dans la circulation sanguine. Les nanomédecines font partie des formes galéniques qui permettent de modifier les propriétés pharmaco-cinétiques de la molécule. Dans ce cas, ses propriétés de biodistribution et d'élimination dépendent alors des propriétés de la nanoparticule.

Dans la gamme des nanoparticules approuvées par la FDA figurent, entre autres, les formes liposomales de la doxorubicine avec Myocet® [142] et Caelyx®/Doxil® [143], les nanoparticules d'albumine pour le paclitaxel (Abraxane®) ainsi que la solution micellaire de paclitaxel (Genexol-PM). Un certain nombre de revues dans la littérature détaillent les propriétés et les applications diverses de ces nanomédecines en chimiothérapie [144].

- *L'encapsulation des ARN interférents*

L'encapsulation de molécules hydrophiles telles que les acides nucléiques (ADN, siRNA) est possible dans de nombreuses formes nanométriques par des procédés via des stratégies d'encapsulation différentes, comparativement aux molécules lipophiles. La plupart des études, aujourd'hui, développe des complexes basés sur les interactions de charges entre les acides nucléiques chargés négativement et des polymères ou lipides cationiques.

Un travail bibliographique est présenté à la suite de cette introduction et décrit les systèmes permettant de véhiculer et de protéger les siRNA (cf. Revue bibliographique). Par ailleurs, les diverses modifications de surface ont été répertoriées selon les stratégies de ciblage des tumeurs envisagées. Dans la seconde partie de cette revue, les différentes cibles moléculaires visées via des siRNA en cancérologie et les résultats obtenus, sur des modèles pré-cliniques, sont exposés et discutés.

3.2. Les nanomédecines et le mélanome

Certaines nanomédecines ont été développées et testées sur des modèles cellulaires ou précliniques de mélanome [145]. La dacarbazine, notamment, a été encapsulée avec succès dans des nanoparticules montrant des résultats prometteurs *in vitro* [146]. Cependant, l'un des exemples les plus frappants concernant l'amélioration des chimiothérapies reste le cas des molécules de la famille des taxanes telles que le paclitaxel ou le docétaxel, encapsulés au sein de différents types de nanomédecines. La conjugaison du paclitaxel avec l'albumine est commercialisée pour le cancer du sein depuis 2005 sous le nom d'Abraxane® [147]. Depuis, des essais cliniques sont menés sur des patients atteints de mélanome avec l'Abraxane® seul ou en association avec d'autres actifs tels que

le carboplatine ou des anti-angiogéniques. Cependant, très peu de bénéfices ont été observés en association avec le carboplatine avec une médiane à 11,1 mois contre 10,9 mois pour l'abraxane® seul [148]. Le docétaxel a également fait l'objet d'étude sur une possible nanoformulation à l'aide de polymères de carbométhylcellulose modifiés démontrant d'ores et déjà des résultats prometteurs sur les rongeurs avec des effets secondaires diminués. La doxorubicine avec des nanoparticules de fullerène a également montré de premiers résultats satisfaisants en pré-clinique [149, 150]. A l'heure actuelle, plusieurs formes de nanomédecines encapsulant des agents chimiothérapeutiques sont actuellement en essais cliniques sur le mélanome (Tableau 3).

A ce jour, un seul essai clinique basé sur l'utilisation d'ARN interférents est en cours dans le cadre de traitements de tumeurs solides telles que le mélanome (Tableau 3). Les siRNA, visant une sous-unité M2 de la ribonucléotide réductase, sont encapsulés dans des nanoparticules de cyclodextrines portant des ligands de ciblage de transferrine [50]. Cet essai de phase I a démontré la bonne tolérance de ce type de nanomédecines, avec une extinction de la protéine cible au niveau tumoral, après injection chez plusieurs patients.

Code	Molécule	Formulation	Phase Essai clinique	Réf.
ABI-007 Abraxane ®	Paclitaxel	Albumine	Phase II En association avec le Carboplatine et Temozolomide ou Bevacuzimab	[148]
			Phase II En association avec le Carboplatine	
			Phase I Seul	
			Phase II En association avec le Bevacuzimab	
BIND-014	Docétaxel	Nanoparticules PLGA PEG	Phase I	En cours
CALAA-01	siRNA RRM2	Nanoparticules de cyclodextrine	Phase I seul	[151]

Tableau 3 : Récapitulatifs des essais cliniques utilisant des nanomédecines pour l'encapsulation de chimiothérapie ou de siRNA dans le cadre d'un traitement contre le mélanome

3.3. Les nanocapsules lipidiques

Les nanocapsules lipidiques (LNC) sont des nanomédecines mises au point et brevetées par notre unité au début des années 2000 [152]. Ces nanocapsules au cœur huileux et à la coque constituée d'agents surfactants sont obtenues par un procédé d'inversion de phase dépendant de la température. Ce procédé sans solvant demande peu d'énergie et permet une transposition d'échelle aisément

envisageable par comparaison avec d'autres systèmes. La structure de la nanocapsule est constituée d'un cœur de triglycérides à chaines moyennes (Labrafac®) autour duquel s'organisent un surfactant hydrophile majoritaire à base de hydroxystéarate de polyéthylène glycol (HS-PEG) (Kolliphor® HS15) responsable de l'inversion de phase, et un surfactant lipophile composé principalement de phosphatidylcholine (lécithine, Lipoid®) qui participe à la rigidité de la coque. La taille de ces objets est contrôlée par la proportion entre les différents constituants permettant l'obtention d'une gamme variant de 20 à 100 nm [153] (Figure 13).

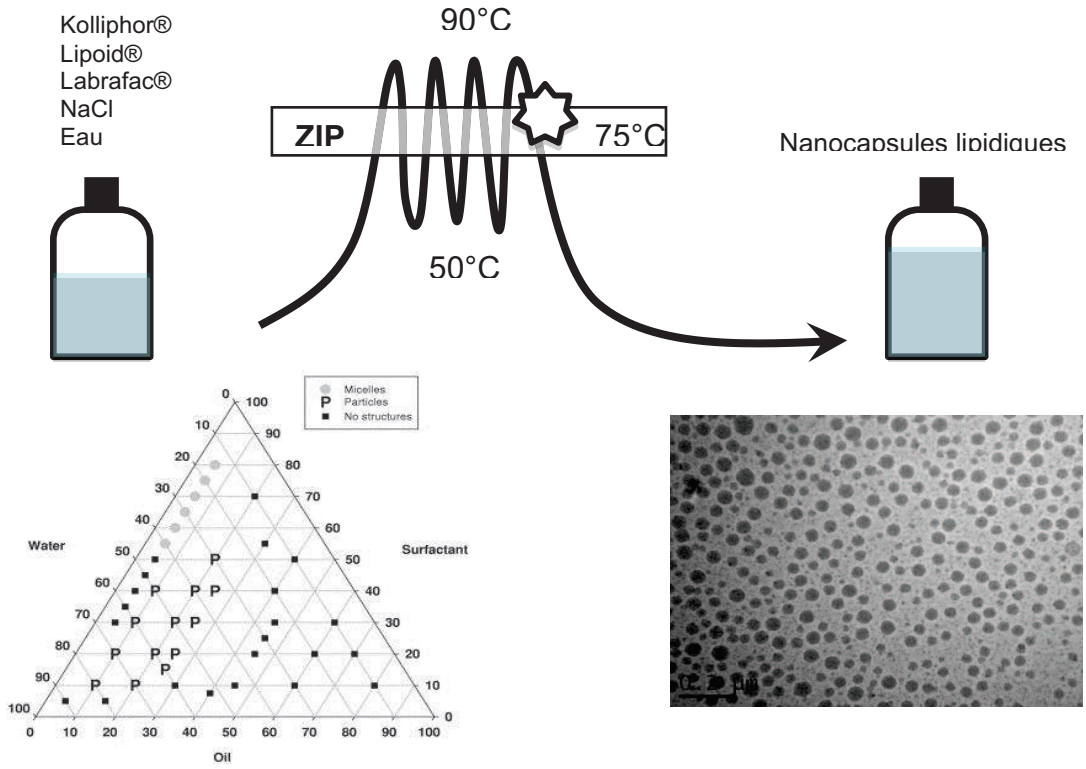

Figure 13 : A : Schématisation du procédé de formulation des nanocapsules lipidiques (LNC) avec une trempe (✡) au niveau de la zone d'inversion de phase (ZIP), B : diagramme de phase permettant d'obtenir les LNC (issu de Heurtault *et al.,* Pharm Res, 2002), C : Image des LNC par cryo-microscopie électronique.

La formulation est basée sur un procédé, dit d'inversion de phase d'émulsion, développé et breveté en 2002 [152]. Il s'agit de réaliser, dans un premier temps, une émulsion huile dans eau (H/E) à l'aide des différents constituants décrits précédemment. Cette émulsion est soumise à une augmentation de température. Celle-ci induit alors un changement de la balance hydrophilie/lipophilie (HLB) du HS-PEG. A ce moment, l'émulsion H/E devient alors émulsion E/H en passant par une microémulsion peut se former dans la zone d'inversion de phase (ZIP) (Figure 13). Cette inversion de phase est mise en évidence par une chute de la conductivité à haute

température. Plusieurs cycles de température sont ainsi réalisés entre 50 et 90°C. La dernière étape comprend une trempe, c'est-à-dire une addition à l'aide d'un volume d'eau à 4°C, au niveau de la zone d'inversion de phase afin de stabiliser et figer les nanocapsules lipidiques (LNC).

L'organisation des LNC offre la possibilité de modifier leur surface, afin d'adapter le comportement pharmacologique en fonction de la cible souhaitée. La modification de surface la plus couramment utilisée dans le domaine des nanomédicines consiste à recouvrir les particules avec de longues chaines de polyéthylène glycol (PEG) par une méthode de post-insertion de phospholipides pegylés dans la coque des LNC [154]. Cette couronne de PEG forme alors une barrière stérique hydrophile limitant les phénomènes d'adsorption des protéines sériques du système immunitaire. Les LNC dites pegylées ont alors un temps de circulation plasmatique prolongé et des études pré-cliniques ont démontré leur capacité à délivrer des principes actifs au niveau d'une tumeur solide [155]. Cette capacité d'accumulation dite de ciblage passif peut être expliquée par le phénomène de perméabilité accrue présent au niveau des endothéliums tumoraux, nommé effet EPR (Enhanced Permeability and Retention effect) [156]. Un ciblage actif par l'intermédiaire de ligands spécifiques reconnaissant des antigènes peut également être réalisé à la surface des LNC [157]. Dans ce cas, le greffage peut se faire, par exemple, à l'extrémité des phospholipides pegylés possédant des groupements fonctionnels.

3.3.1. L'encapsulation de chimiothérapies

Les LNC ont permis, depuis leur création, l'encapsulation avec succès de différents principes actifs anticancéreux tels que le paclitaxel [158], ou encore des ferrocifènes [159]. En effet, le cœur huileux des LNC permet aisément l'encapsulation de ces molécules lipophiles.

Les ferrocifènes sont des molécules basées sur la synthèse de molécules bio-organométalliques dérivées du ferrocène (Figure 14) [160]. Cette approche consiste à développer des dérivés ferrocéniques de l'hydroxytamoxifène, métabolite actif du tamoxifène, en substituant un groupement phényl par le ferrocène. Les molécules résultantes sont appelées ferrocifènes. Un certain nombre de composés dérivés ont été synthétisés et ont démontré de faibles IC_{50} sur différentes lignées de cancers du sein [161]. L'intérêt de ces nouvelles molécules est leur effet cytotoxique inattendu sur des modèles cellulaires résistants de cancer du sein (triple négatif par exemple). En effet, de récents travaux ont montré la formation de dérivés réactifs de l'oxygène (ROS) après incubation de dérivés ferrocèniques [162]. La présence du groupement ferrocène jouerait le rôle de catalyseur d'oxydation intramoléculaire associé à une production de dérivés réactifs de l'oxygène induisant un effet antiprolifératif et l'entrée en sénescence [163].

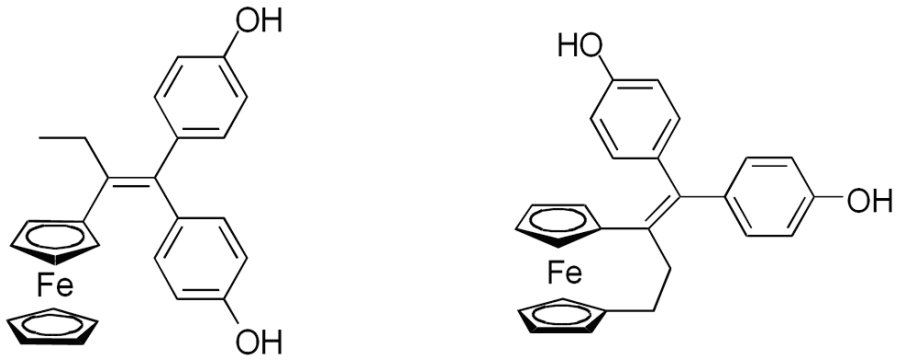

Figure 14 : Structure chimique de deux dérivés organométalliques possédant un groupement ferrocène : le ferrociphenol (FcDiOH, gauche) et l'ansa-ferrociphenol (ansa-FcDiOH)

L'utilisation des dérivés organométalliques encapsulés au sein des LNC a fait l'objet de plusieurs travaux de thèse au sein de notre laboratoire [159, 164, 165]. Leur encapsulation est aujourd'hui maitrisée et des essais sur les LNC chargées en ferrocifène ont montré des résultats satisfaisants dans plusieurs modèles tumoraux et plus particulièrement le glioblastome et le cancer du sein triple négatif [166]. Ces différentes considérations laissent présager une activité potentiellement prometteuse pour ce type de complexe dans le cadre de cellules dites « chimiorésistantes », telles que les cellules issues de mélanome métastatique.

3.3.2. L'encapsulation d'acides nucléiques

Les premiers travaux basés sur les acides nucléiques avec les LNC ont permis l'encapsulation possible de plasmide d'ADN afin de développer une stratégie de thérapie génique [167]. Pour cela, l'ADN est complexé à des lipides cationiques par des interactions électrostatiques menant à la formation de complexes nommés lipoplexes qui sont ajoutés aux autres composants des LNC. Par ailleurs, la température d'inversion de phase classiquement observée à 75°C est abaissée à 25°C par l'utilisation de Plurol afin d'éviter la dégradation du plasmide [167].

Les travaux réalisés par le Dr. Marie Morille montrent le potentiel des LNC ADN pour permettre une accumulation au niveau tumoral dans un modèle sous-cutané de gliome, mais il montre également la possibilité de transfecter efficacement *in vivo* [168, 169]. D'autres travaux de thèse ont permis d'étudier le potentiel thérapeutique de ce type de nanomédecines dans une stratégie de gène suicide sur un modèle de gliome sous-cutané [170, 171]. Aux vues de ces résultats prometteurs, l'utilisation du procédé d'encapsulation de l'ADN est potentiellement applicable à l'encapsulation d'autres formes d'acides nucléiques tels que les siRNA comme nous allons le voir dans le premier chapitre.

4. Les objectifs de la thèse

L'utilisation d'acides nucléiques tels que les siRNA représente aujourd'hui une alternative innovante pour cibler et éteindre spécifiquement une protéine impliquée dans le processus tumoral ainsi que dans les processus de chimiorésistance. Cependant, leur encapsulation au sein de nanoparticules est indispensable pour envisager leur utilisation en pré-clinique et clinique. Mes travaux de thèse s'inscrivent donc premièrement dans une optique de développement galénique de nanocapsules lipidiques encapsulant les siRNA ciblant la protéine Bcl-2 et la sous-unité alpha 1. Leur efficacité sur un modèle cellulaire de mélanome humain SK-Mel28, ainsi que sur un modèle préclinique après implantation sous-cutanée de ces mêmes cellules tumorales a été évaluée.

Les objectifs principaux de ces travaux sont :

- le développement, la compréhension et l'optimisation de la formulation des LNC siRNA,
- l'évaluation de leur efficacité à délivrer ce principe actif dans un modèle de mélanome,
- l'initiation de stratégies de ciblage intelligent des mélanomes dans le but d'une administration systémique,
- la co-encapsulation de siRNA et de molécules à fort potentiel anti-cancéreux telles que les ferrocifènes au sein des LNC,
- l'évaluation cellulaire et pré-clinique d'une stratégie de chimio-sensibilisation du mélanome.

Ce manuscrit rapporte les résultats obtenus lors de ces travaux et s'organise en trois chapitres.

Le premier chapitre s'intitule « Développement et caractérisation des LNC chargées en siRNA ». Ce chapitre concerne les premiers travaux de formulation, l'optimisation du procédé pour encapsuler les siRNA et les résultats de caractérisation de ces nanomédicaments. La première publication décrit le procédé de formulation ainsi que la méthode d'évaluation d'efficacité d'encapsulation des siRNA (Publication n°1). Le second article présente les expériences menées pour optimiser la formulation initiale grâce à une caractérisation plus poussée du nanosystème (Publication n°2). Suite à cela, une demande de brevet a été déposée en septembre 2014.

Puis, le second chapitre « LNC de siRNA et ciblage tumoral », s'articule autour des travaux qui ont porté sur le développement de plusieurs stratégies de ciblage tumoral. L'étude présente les différentes modifications de surface testées ainsi que leur impact sur l'internalisation dans les cellules tumorales, le comportement des LNC modifiées après injection intraveineuse ainsi que leur potentiel de ciblage tumoral (Publication n°3).

Dans le dernier chapitre nommé « Evaluation du potentiel thérapeutique des LNC de siRNA», les travaux menés à visée thérapeutique grâce à l'utilisation concomitante de la thérapie génique via les LNC et de chimiothérapies innovantes (ferrocifènes) sont présentés.

Bibliographie

[1] A.J. Miller, M.C. Mihm, Jr., Melanoma, N Engl J Med, 355 (2006) 51-65.

[2] E.M. Dunki-Jacobs, G.G. Callender, K.M. McMasters, Current management of melanoma, Curr Probl Surg, 50 (2013) 351-382.

[3] S.E. Filippini, A. Vega, Breast cancer genes: beyond BRCA1 and BRCA2, Front Biosci (Landmark Ed), 18 (2013) 1358-1372.

[4] A.A. Larson, S.A. Leachman, M.J. Eliason, L.A. Cannon-Albright, Population-based assessment of non-melanoma cancer risk in relatives of cutaneous melanoma probands, J Invest Dermatol, 127 (2007) 183-188.

[5] S.R. Florell, K.M. Boucher, G. Garibotti, J. Astle, R. Kerber, G. Mineau, C. Wiggins, R.D. Noyes, A. Tsodikov, L.A. Cannon-Albright, J.J. Zone, W.E. Samlowski, S.A. Leachman, Population-based analysis of prognostic factors and survival in familial melanoma, J Clin Oncol, 23 (2005) 7168-7177.

[6] W. Norris, Case of fungoid disease, Edinb Med Surg J, 16 (1820) 562-565.

[7] H.T. Lynch, A.J. Krush, Heredity and malignant melanoma: implications for early cancer detection, Can Med Assoc J, 99 (1968) 17-21.

[8] W.H. Clark, Jr., R.R. Reimer, M. Greene, A.M. Ainsworth, M.J. Mastrangelo, Origin of familial malignant melanomas from heritable melanocytic lesions. 'The B-K mole syndrome', Arch Dermatol, 114 (1978) 732-738.

[9] J.M. Naeyaert, L. Brochez, Clinical practice. Dysplastic nevi, N Engl J Med, 349 (2003) 2233-2240.

[10] E.A. Holland, H. Schmid, R.F. Kefford, G.J. Mann, CDKN2A (P16(INK4a)) and CDK4 mutation analysis in 131 Australian melanoma probands: effect of family history and multiple primary melanomas, Genes Chromosomes Cancer, 25 (1999) 339-348.

[11] H.E. Puntervoll, X.R. Yang, H.H. Vetti, I.M. Bachmann, M.F. Avril, M. Benfodda, C. Catricala, S. Dalle, A.B. Duval-Modeste, P. Ghiorzo, P. Grammatico, M. Harland, N.K. Hayward, H.H. Hu, T. Jouary, T. Martin-Denavit, A. Ozola, J.M. Palmer, L. Pastorino, D. Pjanova, N. Soufir, S.J. Steine, A.J. Stratigos, L. Thomas, J. Tinat, H. Tsao, R. Veinalde, M.A. Tucker, B. Bressac-de Paillerets, J.A. Newton-Bishop, A.M. Goldstein, L.A. Akslen, A. Molven, Melanoma prone families with CDK4 germline mutation: phenotypic profile and associations with MC1R variants, J Med Genet, 50 (2013) 264-270.

[12] K. Paszkowska-Szczur, R.J. Scott, P. Serrano-Fernandez, A. Mirecka, P. Gapska, B. Gorski, C. Cybulski, R. Maleszka, M. Sulikowski, L. Nagay, J. Lubinski, T. Debniak, Xeroderma pigmentosum genes and melanoma risk, Int J Cancer, 133 (2013) 1094-1100.

[13] M.B. Steck, The Role of Melanocortin 1 Receptor in Cutaneous Malignant Melanoma: Along the Mitogen-Activated Protein Kinase Pathway, Biol Res Nurs, (2014).

[14] F.G. Haluska, H. Tsao, H. Wu, F.S. Haluska, A. Lazar, V. Goel, Genetic alterations in signaling pathways in melanoma, Clin Cancer Res, 12 (2006) 2301s-2307s.

[15] H.E. Kanavy, M.R. Gerstenblith, Ultraviolet radiation and melanoma, Semin Cutan Med Surg, 30 (2011) 222-228.

[16] D.L. Narayanan, R.N. Saladi, J.L. Fox, Ultraviolet radiation and skin cancer, Int J Dermatol, 49 (2010) 978-986.

[17] J.E. Russak, D.S. Rigel, Risk factors for the development of primary cutaneous melanoma, Dermatol Clin, 30 (2012) 363-368.

[18] G.P. Pfeifer, A. Besaratinia, UV wavelength-dependent DNA damage and human non-melanoma and melanoma skin cancer, Photochem Photobiol Sci, 11 (2012) 90-97.

[19] J.A. Levine, M. Sorace, J. Spencer, D.M. Siegel, The indoor UV tanning industry: a review of skin cancer risk, health benefit claims, and regulation, J Am Acad Dermatol, 53 (2005) 1038-1044.

[20] W. Ting, K. Schultz, N.N. Cac, M. Peterson, H.W. Walling, Tanning bed exposure increases the risk of malignant melanoma, Int J Dermatol, 46 (2007) 1253-1257.

[21] F. El Ghissassi, R. Baan, K. Straif, Y. Grosse, B. Secretan, V. Bouvard, L. Benbrahim-Tallaa, N. Guha, C. Freeman, L. Galichet, V. Cogliano, A review of human carcinogens--part D: radiation, Lancet Oncol, 10 (2009) 751-752.

[22] M. Rastrelli, M. Alaibac, R. Stramare, V. Chiarion Sileni, M.C. Montesco, A. Vecchiato, L.G. Campana, C.R. Rossi, Melanoma m (zero): diagnosis and therapy, ISRN Dermatol, 2013 (2013) 616170.

[23] A.M. Matos, A.P. Francisco, Targets, Structures, and Recent Approaches in Malignant Melanoma Chemotherapy, ChemMedChem, (2013).

[24] J. Conley, R. Lattes, W. Orr, Desmoplastic malignant melanoma (a rare variant of spindle cell melanoma), Cancer, 28 (1971) 914-936.

[25] M.B. Lens, J.A. Newton-Bishop, A.P. Boon, Desmoplastic malignant melanoma: a systematic review, Br J Dermatol, 152 (2005) 673-678.

[26] M.E. Egger, K.M. Huber, E.M. Dunki-Jacobs, A.R. Quillo, C.R. Scoggins, R.C. Martin, 2nd, A.J. Stromberg, K.M. McMasters, G.G. Callender, Incidence of sentinel lymph node involvement in a modern, large series of desmoplastic melanoma, J Am Coll Surg, 217 (2013) 37-44; discussion 44-35.

[27] A. Breslow, Thickness, cross-sectional areas and depth of invasion in the prognosis of cutaneous melanoma, Ann Surg, 172 (1970) 902-908.

[28] V.N. Tompkins, Cutaneous melanoma: ulceration as a prognostic sign, Cancer, 6 (1953) 1215-1218.

[29] H. Grande Sarpa, K. Reinke, L. Shaikh, S.P. Leong, J.R. Miller, 3rd, R.W. Sagebiel, M. Kashani-Sabet, Prognostic significance of extent of ulceration in primary cutaneous melanoma, Am J Surg Pathol, 30 (2006) 1396-1400.

[30] B.A. Roach, A.L. Burton, M.P. Mays, B.A. Ginter, R.C. Martin, A.J. Stromberg, L. Hagendoorn, K.M. McMasters, C.R. Scoggins, Does mitotic rate predict sentinel lymph node metastasis or survival in patients with intermediate and thick melanoma?, Am J Surg, 200 (2010) 759-763; discussion 763-754.

[31] A.J. Page, A. Li, A. Hestley, D. Murray, G.W. Carlson, K.A. Delman, Increasing Age Is Associated with Worse Prognostic Factors and Increased Distant Recurrences despite Fewer Sentinel Lymph Node Positives in Melanoma, Int J Surg Oncol, 2012 (2012) 456987.

[32] G.G. Callender, M.E. Egger, A.L. Burton, C.R. Scoggins, M.I. Ross, A.J. Stromberg, L. Hagendoorn, R.C. Martin, 2nd, K.M. McMasters, Prognostic implications of anatomic location of primary cutaneous melanoma of 1 mm or thicker, Am J Surg, 202 (2011) 659-664; discussion 664-655.

[33] C.M. Balch, S.J. Soong, J.E. Gershenwald, J.F. Thompson, D.S. Reintgen, N. Cascinelli, M. Urist, K.M. McMasters, M.I. Ross, J.M. Kirkwood, M.B. Atkins, J.A. Thompson, D.G. Coit, D. Byrd, R. Desmond, Y. Zhang, P.Y. Liu, G.H. Lyman, A. Morabito, Prognostic factors analysis of 17,600 melanoma patients: validation of the American Joint Committee on Cancer melanoma staging system, J Clin Oncol, 19 (2001) 3622-3634.

[34] A. Nosrati, M.L. Wei, Sex disparities in melanoma outcomes: The role of biology, Arch Biochem Biophys, (2014).

[35] Coley WB., Leucutia T., The treatment of metastatic tumors of the skin: pigmented moles and melanomas, AJR Am J Roentgenol, (1924) 335-336.

[36] M.K. Khan, N. Khan, A. Almasan, R. Macklis, Future of radiation therapy for malignant melanoma in an era of newer, more effective biological agents, Onco Targets Ther, 4 (2011) 137-148.

[37] A. Hong, G. Fogarty, Role of radiation therapy in cutaneous melanoma, Cancer J, 18 (2012) 203-207.

[38] B.B. Kroon, E.M. Noorda, B.C. Vrouenraets, G.W. van Slooten, O.E. Nieweg, Isolated limb perfusion for melanoma, Surg Oncol Clin N Am, 17 (2008) 785-794, viii-ix.

[39] A. Testori, C. Verhoef, H.M. Kroon, E. Pennacchioli, M.B. Faries, A.M. Eggermont, J.F. Thompson, Treatment of melanoma metastases in a limb by isolated limb perfusion and isolated limb infusion, J Surg Oncol, 104 (2011) 397-404.

[40] A. Sanki, P.C. Kam, J.F. Thompson, Long-term results of hyperthermic, isolated limb perfusion for melanoma: a reflection of tumor biology, Ann Surg, 245 (2007) 591-596.

[41] L. Tentori, P.M. Lacal, G. Graziani, Challenging resistance mechanisms to therapies for metastatic melanoma, Trends Pharmacol Sci, 34 (2013) 656-666.

[42] P.B. Chapman, L.H. Einhorn, M.L. Meyers, S. Saxman, A.N. Destro, K.S. Panageas, C.B. Begg, S.S. Agarwala, L.M. Schuchter, M.S. Ernstoff, A.N. Houghton, J.M. Kirkwood, Phase III multicenter randomized trial of the Dartmouth regimen versus dacarbazine in patients with metastatic melanoma, J Clin Oncol, 17 (1999) 2745-2751.

[43] M.F. Avril, S. Aamdal, J.J. Grob, A. Hauschild, P. Mohr, J.J. Bonerandi, M. Weichenthal, K. Neuber, T. Bieber, K. Gilde, V. Guillem Porta, J. Fra, J. Bonneterre, P. Saiag, D. Kamanabrou, H. Pehamberger, J. Sufliarsky, J.L. Gonzalez Larriba, A. Scherrer, Y. Menu, Fotemustine compared with dacarbazine in patients with disseminated malignant melanoma: a phase III study, J Clin Oncol, 22 (2004) 1118-1125.

[44] J.M. Kirkwood, M.H. Strawderman, M.S. Ernstoff, T.J. Smith, E.C. Borden, R.H. Blum, Interferon alfa-2b adjuvant therapy of high-risk resected cutaneous melanoma: the Eastern Cooperative Oncology Group Trial EST 1684, J Clin Oncol, 14 (1996) 7-17.

[45] M.B. Atkins, J. Hsu, S. Lee, G.I. Cohen, L.E. Flaherty, J.A. Sosman, V.K. Sondak, J.M. Kirkwood, Phase III trial comparing concurrent biochemotherapy with cisplatin, vinblastine, dacarbazine, interleukin-2, and interferon alfa-2b with cisplatin, vinblastine, and dacarbazine alone in patients with metastatic malignant melanoma (E3695): a trial coordinated by the Eastern Cooperative Oncology Group, J Clin Oncol, 26 (2008) 5748-5754.

[46] S.J. O'Day, O. Hamid, W.J. Urba, Targeting cytotoxic T-lymphocyte antigen-4 (CTLA-4): a novel strategy for the treatment of melanoma and other malignancies, Cancer, 110 (2007) 2614-2627.

[47] L. Fong, E.J. Small, Anti-cytotoxic T-lymphocyte antigen-4 antibody: the first in an emerging class of immunomodulatory antibodies for cancer treatment, J Clin Oncol, 26 (2008) 5275-5283.

[48] G. Tosti, E. Cocorocchio, E. Pennacchioli, Anti-cytotoxic T lymphocyte antigen-4 antibodies in melanoma, Clin Cosmet Investig Dermatol, 6 (2013) 245-256.

[49] F.S. Hodi, S.J. O'Day, D.F. McDermott, R.W. Weber, J.A. Sosman, J.B. Haanen, R. Gonzalez, C. Robert, D. Schadendorf, J.C. Hassel, W. Akerley, A.J. van den Eertwegh, J. Lutzky, P. Lorigan, J.M. Vaubel, G.P. Linette, D. Hogg, C.H. Ottensmeier, C. Lebbe, C. Peschel, I. Quirt, J.I. Clark, J.D. Wolchok, J.S. Weber, J. Tian, M.J. Yellin, G.M. Nichol, A. Hoos, W.J. Urba, Improved survival with ipilimumab in patients with metastatic melanoma, N Engl J Med, 363 (2010) 711-723.

[50] H. Davies, G.R. Bignell, C. Cox, P. Stephens, S. Edkins, S. Clegg, J. Teague, H. Woffendin, M.J. Garnett, W. Bottomley, N. Davis, E. Dicks, R. Ewing, Y. Floyd, K. Gray, S. Hall, R. Hawes, J. Hughes, V. Kosmidou, A. Menzies, C. Mould, A. Parker, C. Stevens, S. Watt, S. Hooper, R. Wilson, H. Jayatilake, B.A. Gusterson, C. Cooper, J. Shipley, D. Hargrave, K. Pritchard-Jones, N. Maitland, G. Chenevix-Trench, G.J. Riggins, D.D. Bigner, G. Palmieri, A. Cossu, A. Flanagan, A. Nicholson, J.W. Ho, S.Y. Leung, S.T. Yuen, B.L. Weber, H.F. Seigler, T.L. Darrow, H. Paterson, R. Marais, C.J. Marshall, R. Wooster, M.R. Stratton, P.A. Futreal, Mutations of the BRAF gene in human cancer, Nature, 417 (2002) 949-954.

[51] G. Bollag, P. Hirth, J. Tsai, J. Zhang, P.N. Ibrahim, H. Cho, W. Spevak, C. Zhang, Y. Zhang, G. Habets, E.A. Burton, B. Wong, G. Tsang, B.L. West, B. Powell, R. Shellooe, A. Marimuthu, H. Nguyen, K.Y. Zhang, D.R. Artis, J. Schlessinger, F. Su, B. Higgins, R. Iyer, K. D'Andrea, A. Koehler, M. Stumm, P.S. Lin, R.J. Lee, J. Grippo, I. Puzanov, K.B. Kim, A. Ribas, G.A. McArthur, J.A. Sosman, P.B. Chapman, K.T. Flaherty, X. Xu, K.L. Nathanson, K. Nolop, Clinical efficacy of a RAF inhibitor needs broad target blockade in BRAF-mutant melanoma, Nature, 467 (2010) 596-599.

[52] P.B. Chapman, A. Hauschild, C. Robert, J.B. Haanen, P. Ascierto, J. Larkin, R. Dummer, C. Garbe, A. Testori, M. Maio, D. Hogg, P. Lorigan, C. Lebbe, T. Jouary, D. Schadendorf, A. Ribas, S.J. O'Day, J.A. Sosman, J.M. Kirkwood, A.M. Eggermont, B. Dreno, K. Nolop, J. Li, B. Nelson, J. Hou, R.J. Lee, K.T. Flaherty, G.A. McArthur, Improved survival with vemurafenib in melanoma with BRAF V600E mutation, N Engl J Med, 364 (2011) 2507-2516.

[53] I.V. Fedorenko, K.H. Paraiso, K.S. Smalley, Acquired and intrinsic BRAF inhibitor resistance in BRAF V600E mutant melanoma, Biochem Pharmacol, 82 (2011) 201-209.

[54] S. Lakhani, P. Selby, J.M. Bliss, T.J. Perren, M.E. Gore, T.J. McElwain, Chemotherapy for malignant melanoma: combinations and high doses produce more responses without survival benefit, Br J Cancer, 61 (1990) 330-334.

[55] R. Osieka, Studies on drug resistance in a human melanoma xenograft system, Cancer Treat Rev, 11 Suppl A (1984) 85-98.

[56] J.C. Reed, M. Pellecchia, Apoptosis-based therapies for hematologic malignancies, Blood, 106 (2005) 408-418.

[57] U. Fischer, K. Schulze-Osthoff, New approaches and therapeutics targeting apoptosis in disease, Pharmacol Rev, 57 (2005) 187-215.

[58] J. Eberle, B.M. Kurbanov, A.M. Hossini, U. Trefzer, L.F. Fecker, Overcoming apoptosis deficiency of melanoma-hope for new therapeutic approaches, Drug Resist Updat, 10 (2007) 218-234.

[59] S.J. Riedl, Y. Shi, Molecular mechanisms of caspase regulation during apoptosis, Nat Rev Mol Cell Biol, 5 (2004) 897-907.

[60] J.H. Russell, T.J. Ley, Lymphocyte-mediated cytotoxicity, Annu Rev Immunol, 20 (2002) 323-370.

[61] Y. Guilloux, C. Viret, N. Gervois, E. Le Drean, M.C. Pandolfino, E. Diez, F. Jotereau, Defective lymphokine production by most CD8+ and CD4+ tumor-specific T cell clones derived from human melanoma-infiltrating lymphocytes in response to autologous tumor cells in vitro, Eur J Immunol, 24 (1994) 1966-1973.

[62] W.D. Thomas, P. Hersey, TNF-related apoptosis-inducing ligand (TRAIL) induces apoptosis in Fas ligand-resistant melanoma cells and mediates CD4 T cell killing of target cells, J Immunol, 161 (1998) 2195-2200.

[63] P.J. Frost, L.H. Butterfield, V.B. Dissette, J.S. Economou, B. Bonavida, Immunosensitization of melanoma tumor cells to non-MHC Fas-mediated killing by MART-1-specific CTL cultures, J Immunol, 166 (2001) 3564-3573.

[64] K.W. Wagner, E.A. Punnoose, T. Januario, D.A. Lawrence, R.M. Pitti, K. Lancaster, D. Lee, M. von Goetz, S.F. Yee, K. Totpal, L. Huw, V. Katta, G. Cavet, S.G. Hymowitz, L. Amler, A. Ashkenazi, Death-receptor O-glycosylation controls tumor-cell sensitivity to the proapoptotic ligand Apo2L/TRAIL, Nat Med, 13 (2007) 1070-1077.

[65] M. Raisova, M. Bektas, T. Wieder, P. Daniel, J. Eberle, C.E. Orfanos, C.C. Geilen, Resistance to CD95/Fas-induced and ceramide-mediated apoptosis of human melanoma cells is caused by a defective mitochondrial cytochrome c release, FEBS Lett, 473 (2000) 27-32.

[66] W.D. Thomas, X.D. Zhang, A.V. Franco, T. Nguyen, P. Hersey, TNF-related apoptosis-inducing ligand-induced apoptosis of melanoma is associated with changes in mitochondrial membrane potential and perinuclear clustering of mitochondria, J Immunol, 165 (2000) 5612-5620.

[67] M.R. Hussein, A.K. Haemel, G.S. Wood, Apoptosis and melanoma: molecular mechanisms, J Pathol, 199 (2003) 275-288.

[68] P.T. Daniel, K. Schulze-Osthoff, C. Belka, D. Guner, Guardians of cell death: the Bcl-2 family proteins, Essays Biochem, 39 (2003) 73-88.

[69] E. Selzer, H. Schlagbauer-Wadl, I. Okamoto, H. Pehamberger, R. Potter, B. Jansen, Expression of Bcl-2 family members in human melanocytes, in melanoma metastases and in melanoma cell lines, Melanoma Res, 8 (1998) 197-203.

[70] A.M. Hossini, C.C. Geilen, L.F. Fecker, P.T. Daniel, J. Eberle, A novel Bcl-x splice product, Bcl-xAK, triggers apoptosis in human melanoma cells without BH3 domain, Oncogene, 25 (2006) 2160-2169.

[71] K.G. Wolter, M. Verhaegen, Y. Fernandez, Z. Nikolovska-Coleska, M. Riblett, C.M. de la Vega, S. Wang, M.S. Soengas, Therapeutic window for melanoma treatment provided by selective effects of the proteasome on Bcl-2 proteins, Cell Death Differ, 14 (2007) 1605-1616.

[72] L. Zhuang, C.S. Lee, R.A. Scolyer, S.W. McCarthy, X.D. Zhang, J.F. Thompson, P. Hersey, Mcl-1, Bcl-XL and Stat3 expression are associated with progression of melanoma whereas Bcl-2, AP-2 and MITF levels decrease during progression of melanoma, Mod Pathol, 20 (2007) 416-426.

[73] A. Hakansson, B. Gustafsson, A. Abdiu, L. Krysander, L. Hakansson, Bcl-2 expression in metastatic malignant melanoma. Importance for the therapeutic efficacy of biochemotherapy, Cancer Immunol Immunother, 52 (2003) 249-254.

[74] B.M. Kurbanov, C.C. Geilen, L.F. Fecker, C.E. Orfanos, J. Eberle, Efficient TRAIL-R1/DR4-mediated apoptosis in melanoma cells by tumor necrosis factor-related apoptosis-inducing ligand (TRAIL), J Invest Dermatol, 125 (2005) 1010-1019.

[75] M. Irmler, M. Thome, M. Hahne, P. Schneider, K. Hofmann, V. Steiner, J.L. Bodmer, M. Schroter, K. Burns, C. Mattmann, D. Rimoldi, L.E. French, J. Tschopp, Inhibition of death receptor signals by cellular FLIP, Nature, 388 (1997) 190-195.

[76] E. Zeise, M. Weichenthal, T. Schwarz, D. Kulms, Resistance of human melanoma cells against the death ligand TRAIL is reversed by ultraviolet-B radiation via downregulation of FLIP, J Invest Dermatol, 123 (2004) 746-754.

[77] M. Chawla-Sarkar, S.I. Bae, F.J. Reu, B.S. Jacobs, D.J. Lindner, E.C. Borden, Downregulation of Bcl-2, FLIP or IAPs (XIAP and survivin) by siRNAs sensitizes resistant melanoma cells to Apo2L/TRAIL-induced apoptosis, Cell Death Differ, 11 (2004) 915-923.

[78] B. Nachmias, Y. Ashhab, D. Ben-Yehuda, The inhibitor of apoptosis protein family (IAPs): an emerging therapeutic target in cancer, Semin Cancer Biol, 14 (2004) 231-243.

[79] G.M. Kasof, B.C. Gomes, Livin, a novel inhibitor of apoptosis protein family member, J Biol Chem, 276 (2001) 3238-3246.

[80] H. Yan, J. Thomas, T. Liu, D. Raj, N. London, T. Tandeski, S.A. Leachman, R.M. Lee, D. Grossman, Induction of melanoma cell apoptosis and inhibition of tumor growth using a cell-permeable Survivin antagonist, Oncogene, 25 (2006) 6968-6974.

[81] H.M. Kluger, M.M. McCarthy, A.B. Alvero, M. Sznol, S. Ariyan, R.L. Camp, D.L. Rimm, G. Mor, The X-linked inhibitor of apoptosis protein (XIAP) is up-regulated in metastatic melanoma, and XIAP cleavage by Phenoxodiol is associated with Carboplatin sensitization, J Transl Med, 5 (2007) 6.

[82] A.S. Dhillon, S. Hagan, O. Rath, W. Kolch, MAP kinase signalling pathways in cancer, Oncogene, 26 (2007) 3279-3290.

[83] G. Tortora, R. Bianco, G. Daniele, F. Ciardiello, J.A. McCubrey, M.R. Ricciardi, L. Ciuffreda, F. Cognetti, A. Tafuri, M. Milella, Overcoming resistance to molecularly targeted anticancer therapies: Rational drug combinations based on EGFR and MAPK inhibition for solid tumours and haematologic malignancies, Drug Resist Updat, 10 (2007) 81-100.

[84] E. Edlundh-Rose, S. Egyhazi, K. Omholt, E. Mansson-Brahme, A. Platz, J. Hansson, J. Lundeberg, NRAS and BRAF mutations in melanoma tumours in relation to clinical characteristics: a study based on mutation screening by pyrosequencing, Melanoma Res, 16 (2006) 471-478.

[85] K.S. Smalley, T.G. Eisen, Farnesyl transferase inhibitor SCH66336 is cytostatic, pro-apoptotic and enhances chemosensitivity to cisplatin in melanoma cells, Int J Cancer, 105 (2003) 165-175.

[86] K.M. Eisenmann, M.W. VanBrocklin, N.A. Staffend, S.M. Kitchen, H.M. Koo, Mitogen-activated protein kinase pathway-dependent tumor-specific survival signaling in melanoma cells through inactivation of the proapoptotic protein bad, Cancer Res, 63 (2003) 8330-8337.

[87] D.J. Panka, W. Wang, M.B. Atkins, J.W. Mier, The Raf inhibitor BAY 43-9006 (Sorafenib) induces caspase-independent apoptosis in melanoma cells, Cancer Res, 66 (2006) 1611-1619.

[88] Y.F. Wang, C.C. Jiang, K.A. Kiejda, S. Gillespie, X.D. Zhang, P. Hersey, Apoptosis induction in human melanoma cells by inhibition of MEK is caspase-independent and mediated by the Bcl-2 family members PUMA, Bim, and Mcl-1, Clin Cancer Res, 13 (2007) 4934-4942.

[89] G.G. McGill, M. Horstmann, H.R. Widlund, J. Du, G. Motyckova, E.K. Nishimura, Y.L. Lin, S. Ramaswamy, W. Avery, H.F. Ding, S.A. Jordan, I.J. Jackson, S.J. Korsmeyer, T.R. Golub, D.E. Fisher, Bcl2 regulation by the melanocyte master regulator Mitf modulates lineage survival and melanoma cell viability, Cell, 109 (2002) 707-718.

[90] B.D. Manning, L.C. Cantley, AKT/PKB signaling: navigating downstream, Cell, 129 (2007) 1261-1274.

[91] K.A. West, S.S. Castillo, P.A. Dennis, Activation of the PI3K/Akt pathway and chemotherapeutic resistance, Drug Resist Updat, 5 (2002) 234-248.

[92] S.R. Datta, H. Dudek, X. Tao, S. Masters, H. Fu, Y. Gotoh, M.E. Greenberg, Akt phosphorylation of BAD couples survival signals to the cell-intrinsic death machinery, Cell, 91 (1997) 231-241.

[93] M.H. Cardone, N. Roy, H.R. Stennicke, G.S. Salvesen, T.F. Franke, E. Stanbridge, S. Frisch, J.C. Reed, Regulation of cell death protease caspase-9 by phosphorylation, Science, 282 (1998) 1318-1321.

[94] S.J. Gardai, D.A. Hildeman, S.K. Frankel, B.B. Whitlock, S.C. Frasch, N. Borregaard, P. Marrack, D.L. Bratton, P.M. Henson, Phosphorylation of Bax Ser184 by Akt regulates its activity and apoptosis in neutrophils, J Biol Chem, 279 (2004) 21085-21095.

[95] J.B. Easton, P.J. Houghton, mTOR and cancer therapy, Oncogene, 25 (2006) 6436-6446.

[96] M. Hoyer-Hansen, M. Jaattela, AMP-activated protein kinase: a universal regulator of autophagy?, Autophagy, 3 (2007) 381-383.

[97] D.A. Guertin, D.M. Sabatini, Defining the role of mTOR in cancer, Cancer Cell, 12 (2007) 9-22.

[98] G. Li, J. Kalabis, X. Xu, F. Meier, M. Oka, T. Bogenrieder, M. Herlyn, Reciprocal regulation of MelCAM and AKT in human melanoma, Oncogene, 22 (2003) 6891-6899.

[99] P. Dhawan, A.B. Singh, D.L. Ellis, A. Richmond, Constitutive activation of Akt/protein kinase B in melanoma leads to up-regulation of nuclear factor-kappaB and tumor progression, Cancer Res, 62 (2002) 7335-7342.

[100] V. Baud, M. Karin, Is NF-kappaB a good target for cancer therapy? Hopes and pitfalls, Nat Rev Drug Discov, 8 (2009) 33-40.

[101] R. Ravi, A. Bedi, NF-kappaB in cancer--a friend turned foe, Drug Resist Updat, 7 (2004) 53-67.

[102] J.W. Antoon, M.D. White, E.M. Slaughter, J.L. Driver, H.S. Khalili, S. Elliott, C.D. Smith, M.E. Burow, B.S. Beckman, Targeting NFkB mediated breast cancer chemoresistance through selective inhibition of sphingosine kinase-2, Cancer Biol Ther, 11 (2011) 678-689.

[103] D. Santini, G. Schiavon, B. Vincenzi, L. Gaeta, F. Pantano, A. Russo, C. Ortega, C. Porta, S. Galluzzo, G. Armento, N. La Verde, C. Caroti, I. Treilleux, A. Ruggiero, G. Perrone, R. Addeo, P. Clezardin, A.O.

Muda, G. Tonini, Receptor activator of NF-kB (RANK) expression in primary tumors associates with bone metastasis occurrence in breast cancer patients, PLoS One, 6 (2011) e19234.

[104] F. Demarchi, C. Brancolini, Altering protein turnover in tumor cells: new opportunities for anti-cancer therapies, Drug Resist Updat, 8 (2005) 359-368.

[105] J. Yang, A. Richmond, Constitutive IkappaB kinase activity correlates with nuclear factor-kappaB activation in human melanoma cells, Cancer Res, 61 (2001) 4901-4909.

[106] A. Munshi, J.F. Kurland, T. Nishikawa, P.J. Chiao, M. Andreeff, R.E. Meyn, Inhibition of constitutively activated nuclear factor-kappaB radiosensitizes human melanoma cells, Mol Cancer Ther, 3 (2004) 985-992.

[107] M.F. Romano, R. Avellino, A. Petrella, R. Bisogni, S. Romano, S. Venuta, Rapamycin inhibits doxorubicin-induced NF-kappaB/Rel nuclear activity and enhances the apoptosis of melanoma cells, Eur J Cancer, 40 (2004) 2829-2836.

[108] K. Heon Seo, H.M. Ko, H.A. Kim, J.H. Choi, S. Jun Park, K.J. Kim, H.K. Lee, S.Y. Im, Platelet-activating factor induces up-regulation of antiapoptotic factors in a melanoma cell line through nuclear factor-kappaB activation, Cancer Res, 66 (2006) 4681-4686.

[109] M.L. Hartman, M. Czyz, Anti-apoptotic proteins on guard of melanoma cell survival, Cancer Lett, 331 (2013) 24-34.

[110] J. Utikal, U. Leiter, M. Udart, P. Kaskel, R.U. Peter, G.M. Krahn, Expression of c-myc and bcl-2 in primary and advanced cutaneous melanoma, Cancer Invest, 20 (2002) 914-921.

[111] L. Zhuang, R.A. Scolyer, R. Murali, S.W. McCarthy, X.D. Zhang, J.F. Thompson, P. Hersey, Lactate dehydrogenase 5 expression in melanoma increases with disease progression and is associated with expression of Bcl-XL and Mcl-1, but not Bcl-2 proteins, Mod Pathol, 23 (2010) 45-53.

[112] A. Gradilone, P. Gazzaniga, D. Ribuffo, S. Scarpa, E. Cigna, F. Vasaturo, U. Bottoni, D. Innocenzi, S. Calvieri, N. Scuderi, L. Frati, A.M. Agliano, Survivin, bcl-2, bax, and bcl-X gene expression in sentinel lymph nodes from melanoma patients, J Clin Oncol, 21 (2003) 306-312.

[113] F. Tas, D. Duranyildiz, H. Oguz, H. Camlica, V. Yasasever, E. Topuz, Circulating levels of vascular endothelial growth factor (VEGF), matrix metalloproteinase-3 (MMP-3), and BCL-2 in malignant melanoma, Med Oncol, 25 (2008) 431-436.

[114] D. Trisciuoglio, M. Desideri, L. Ciuffreda, M. Mottolese, D. Ribatti, A. Vacca, M. Del Rosso, L. Marcocci, G. Zupi, D. Del Bufalo, Bcl-2 overexpression in melanoma cells increases tumor progression-associated properties and in vivo tumor growth, J Cell Physiol, 205 (2005) 414-421.

[115] D. Trisciuoglio, A. Iervolino, G. Zupi, D. Del Bufalo, Involvement of PI3K and MAPK signaling in bcl-2-induced vascular endothelial growth factor expression in melanoma cells, Mol Biol Cell, 16 (2005) 4153-4162.

[116] J.C. Skou, M. Esmann, Preparation of membrane-bound and of solubilized (Na+ + K+)-ATPase from rectal glands of Squalus acanthias. The effect of preparative procedures on purity, specific and molar activity, Biochim Biophys Acta, 567 (1979) 436-444.

[117] E.D. Sverdlov, N.S. Akopyanz, K.E. Petrukhin, N.E. Broude, G.S. Monastyrskaya, N.N. Modyanov, Na+,K+-ATPase: tissue-specific expression of genes coding for alpha-subunit in diverse human tissues, FEBS Lett, 239 (1988) 65-68.

[118] O.I. Shamraj, D. Melvin, J.B. Lingrel, Expression of Na,K-ATPase isoforms in human heart, Biochem Biophys Res Commun, 179 (1991) 1434-1440.

[119] J.B. Lingrel, Na,K-ATPase: isoform structure, function, and expression, J Bioenerg Biomembr, 24 (1992) 263-270.

[120] O. Vagin, L.A. Dada, E. Tokhtaeva, G. Sachs, The Na-K-ATPase alpha(1)beta(1) heterodimer as a cell adhesion molecule in epithelia, Am J Physiol Cell Physiol, 302 (2012) C1271-1281.

[121] K.R. Vanmolkot, E.E. Kors, J.J. Hottenga, G.M. Terwindt, J. Haan, W.A. Hoefnagels, D.F. Black, L.A. Sandkuijl, R.R. Frants, M.D. Ferrari, A.M. van den Maagdenberg, Novel mutations in the Na+, K+-ATPase pump gene ATP1A2 associated with familial hemiplegic migraine and benign familial infantile convulsions, Ann Neurol, 54 (2003) 360-366.

[122] D.B. Seligson, S.A. Rajasekaran, H. Yu, X. Liu, M. Eeva, S. Tze, W. Ball, Jr., S. Horvath, J.B. deKernion, A.K. Rajasekaran, Na,K-adenosine triphosphatase alpha1-subunit predicts survival of renal clear cell carcinoma, J Urol, 179 (2008) 338-345.

[123] B. Stenkvist, Cardenolides and cancer, Anticancer Drugs, 12 (2001) 635-638.

[124] V. Mathieu, C. Pirker, E. Martin de Lassalle, M. Vernier, T. Mijatovic, N. DeNeve, J.F. Gaussin, M. Dehoux, F. Lefranc, W. Berger, R. Kiss, The sodium pump alpha1 sub-unit: a disease progression-related target for metastatic melanoma treatment, J Cell Mol Med, 13 (2009) 3960-3972.

[125] J. Liu, Z.J. Xie, The sodium pump and cardiotonic steroids-induced signal transduction protein kinases and calcium-signaling microdomain in regulation of transporter trafficking, Biochim Biophys Acta, 1802 (2010) 1237-1245.

[126] D. Zhuang, S. Mannava, V. Grachtchouk, W.H. Tang, S. Patil, J.A. Wawrzyniak, A.E. Berman, T.J. Giordano, E.V. Prochownik, M.S. Soengas, M.A. Nikiforov, C-MYC overexpression is required for continuous suppression of oncogene-induced senescence in melanoma cells, Oncogene, 27 (2008) 6623-6634.

[127] A. Porro, M. Haber, D. Diolaiti, N. Iraci, M. Henderson, S. Gherardi, E. Valli, M.A. Munoz, C. Xue, C. Flemming, M. Schwab, J.H. Wong, G.M. Marshall, G. Della Valle, M.D. Norris, G. Perini, Direct and coordinate regulation of ATP-binding cassette transporter genes by Myc factors generates specific transcription signatures that significantly affect the chemoresistance phenotype of cancer cells, J Biol Chem, 285 (2010) 19532-19543.

[128] I. Prassas, E.P. Diamandis, Novel therapeutic applications of cardiac glycosides, Nat Rev Drug Discov, 7 (2008) 926-935.

[129] A. Goy, F.J. Hernandez-Ilzaliturri, B. Kahl, P. Ford, E. Protomastro, M. Berger, A phase I/II study of the pan Bcl-2 inhibitor obatoclax mesylate plus bortezomib for relapsed or refractory mantle cell lymphoma, Leuk Lymphoma, (2014).

[130] M. Nguyen, R.C. Marcellus, A. Roulston, M. Watson, L. Serfass, S.R. Murthy Madiraju, D. Goulet, J. Viallet, L. Belec, X. Billot, S. Acoca, E. Purisima, A. Wiegmans, L. Cluse, R.W. Johnstone, P.

Beauparlant, G.C. Shore, Small molecule obatoclax (GX15-070) antagonizes MCL-1 and overcomes MCL-1-mediated resistance to apoptosis, Proc Natl Acad Sci U S A, 104 (2007) 19512-19517.

[131] M.J. Sale, S.J. Cook, The BH3 mimetic ABT-263 synergizes with the MEK1/2 inhibitor selumetinib/AZD6244 to promote BIM-dependent tumour cell death and inhibit acquired resistance, Biochem J, 450 (2013) 285-294.

[132] W. Wang, Y.Q. Wang, T. Meng, J.M. Yi, X.J. Huan, L.P. Ma, L.J. Tong, Y. Chen, J. Ding, J.K. Shen, Z.H. Miao, MCL-1 degradation mediated by JNK activation via MEKK1/TAK1-MKK4 contributes to anticancer activity of new tubulin inhibitor MT189, Mol Cancer Ther, 13 (2014) 1480-1491.

[133] W.R. Schelman, T.A. Mohammed, A.M. Traynor, J.M. Kolesar, R.M. Marnocha, J. Eickhoff, M. Keppen, D.B. Alberti, G. Wilding, N. Takebe, G. Liu, A phase I study of AT-101 with cisplatin and etoposide in patients with advanced solid tumors with an expanded cohort in extensive-stage small cell lung cancer, Invest New Drugs, 32 (2014) 295-302.

[134] F. Lefranc, R. Kiss, The sodium pump alpha1 subunit as a potential target to combat apoptosis-resistant glioblastomas, Neoplasia, 10 (2008) 198-206.

[135] T. Mijatovic, U. Jungwirth, P. Heffeter, M.A. Hoda, R. Dornetshuber, R. Kiss, W. Berger, The Na+/K+-ATPase is the Achilles heel of multi-drug-resistant cancer cells, Cancer Lett, 282 (2009) 30-34.

[136] M. Cavazzana-Calvo, S. Hacein-Bey-Abina, A. Fischer, [Ten years of gene therapy: thoughts and perspectives], Med Sci (Paris), 26 (2010) 115-118.

[137] A. Fire, S. Xu, M.K. Montgomery, S.A. Kostas, S.E. Driver, C.C. Mello, Potent and specific genetic interference by double-stranded RNA in Caenorhabditis elegans, Nature, 391 (1998) 806-811.

[138] A. de Fougerolles, H.P. Vornlocher, J. Maraganore, J. Lieberman, Interfering with disease: a progress report on siRNA-based therapeutics, Nat Rev Drug Discov, 6 (2007) 443-453.

[139] B. Jansen, H. Schlagbauer-Wadl, B.D. Brown, R.N. Bryan, A. van Elsas, M. Muller, K. Wolff, H.G. Eichler, H. Pehamberger, bcl-2 antisense therapy chemosensitizes human melanoma in SCID mice, Nat Med, 4 (1998) 232-234.

[140] B. Jansen, V. Wacheck, E. Heere-Ress, H. Schlagbauer-Wadl, C. Hoeller, T. Lucas, M. Hoermann, U. Hollenstein, K. Wolff, H. Pehamberger, Chemosensitisation of malignant melanoma by BCL2 antisense therapy, Lancet, 356 (2000) 1728-1733.

[141] P.A. Ott, J. Chang, K. Madden, R. Kannan, C. Muren, C. Escano, X. Cheng, Y. Shao, S. Mendoza, A. Gandhi, L. Liebes, A.C. Pavlick, Oblimersen in combination with temozolomide and albumin-bound paclitaxel in patients with advanced melanoma: a phase I trial, Cancer Chemother Pharmacol, 71 (2013) 183-191.

[142] G. Batist, J. Barton, P. Chaikin, C. Swenson, L. Welles, Myocet (liposome-encapsulated doxorubicin citrate): a new approach in breast cancer therapy, Expert Opin Pharmacother, 3 (2002) 1739-1751.

[143] J. Szebeni, P. Bedocs, R. Urbanics, R. Bunger, L. Rosivall, M. Toth, Y. Barenholz, Prevention of infusion reactions to PEGylated liposomal doxorubicin via tachyphylaxis induction by placebo vesicles: a porcine model, J Control Release, 160 (2012) 382-387.

[144] C.M. Dawidczyk, L.M. Russell, P.C. Searson, Nanomedicines for cancer therapy: state-of-the-art and limitations to pre-clinical studies that hinder future developments, Front Chem, 2 (2014) 69.

[145] F.B. Bombelli, C.A. Webster, M. Moncrieff, V. Sherwood, The scope of nanoparticle therapies for future metastatic melanoma treatment, Lancet Oncol, 15 (2014) e22-32.

[146] B. Ding, X. Wu, W. Fan, Z. Wu, J. Gao, W. Zhang, L. Ma, W. Xiang, Q. Zhu, J. Liu, X. Ding, S. Gao, Anti-DR5 monoclonal antibody-mediated DTIC-loaded nanoparticles combining chemotherapy and immunotherapy for malignant melanoma: target formulation development and in vitro anticancer activity, Int J Nanomedicine, 6 (2011) 1991-2005.

[147] E. Miele, G.P. Spinelli, E. Miele, F. Tomao, S. Tomao, Albumin-bound formulation of paclitaxel (Abraxane ABI-007) in the treatment of breast cancer, Int J Nanomedicine, 4 (2009) 99-105.

[148] L.A. Kottschade, V.J. Suman, T. Amatruda, 3rd, R.R. McWilliams, B.I. Mattar, D.A. Nikcevich, R. Behrens, T.R. Fitch, A.J. Jaslowski, S.N. Markovic, A phase II trial of nab-paclitaxel (ABI-007) and carboplatin in patients with unresectable stage IV melanoma : a North Central Cancer Treatment Group Study, N057E(1), Cancer, 117 (2011) 1704-1710.

[149] M.J. Ernsting, W.L. Tang, N.W. MacCallum, S.D. Li, Preclinical pharmacokinetic, biodistribution, and anti-cancer efficacy studies of a docetaxel-carboxymethylcellulose nanoparticle in mouse models, Biomaterials, 33 (2011) 1445-1454.

[150] P. Chaudhuri, A. Paraskar, S. Soni, R.A. Mashelkar, S. Sengupta, Fullerenol-cytotoxic conjugates for cancer chemotherapy, ACS Nano, 3 (2009) 2505-2514.

[151] M.E. Davis, J.E. Zuckerman, C.H. Choi, D. Seligson, A. Tolcher, C.A. Alabi, Y. Yen, J.D. Heidel, A. Ribas, Evidence of RNAi in humans from systemically administered siRNA via targeted nanoparticles, Nature, 464 (2010) 1067-1070.

[152] B. Heurtault, P. Saulnier, B. Pech, J.E. Proust, J.P. Benoit, A novel phase inversion-based process for the preparation of lipid nanocarriers, Pharm Res, 19 (2002) 875-880.

[153] B. Heurtault, P. Saulnier, B. Pech, M.C. Venier-Julienne, J.E. Proust, R. Phan-Tan-Luu, J.P. Benoit, The influence of lipid nanocapsule composition on their size distribution, Eur J Pharm Sci, 18 (2003) 55-61.

[154] T. Perrier, P. Saulnier, F. Fouchet, N. Lautram, J.P. Benoit, Post-insertion into Lipid NanoCapsules (LNCs): From experimental aspects to mechanisms, Int J Pharm, 396 (2010) 204-209.

[155] M. Morille, C. Passirani, E. Letrou-Bonneval, J.P. Benoit, B. Pitard, Galactosylated DNA lipid nanocapsules for efficient hepatocyte targeting, Int J Pharm, 379 (2009) 293-300.

[156] H. Maeda, J. Wu, T. Sawa, Y. Matsumura, K. Hori, Tumor vascular permeability and the EPR effect in macromolecular therapeutics: a review, J Control Release, 65 (2000) 271-284.

[157] A. Beduneau, P. Saulnier, F. Hindre, A. Clavreul, J.C. Leroux, J.P. Benoit, Design of targeted lipid nanocapsules by conjugation of whole antibodies and antibody Fab' fragments, Biomaterials, 28 (2007) 4978-4990.

[158] E. Roger, F. Lagarce, E. Garcion, J.P. Benoit, Lipid nanocarriers improve paclitaxel transport throughout human intestinal epithelial cells by using vesicle-mediated transcytosis, J Control Release, 140 (2009) 174-181.

[159] E. Allard, N.T. Huynh, A. Vessieres, P. Pigeon, G. Jaouen, J.P. Benoit, C. Passirani, Dose effect activity of ferrocifen-loaded lipid nanocapsules on a 9L-glioma model, Int J Pharm, 379 (2009) 317-323.

[160] Q. Michard, G. Jaouen, A. Vessieres, B.A. Bernard, Evaluation of cytotoxic properties of organometallic ferrocifens on melanocytes, primary and metastatic melanoma cell lines, J Inorg Biochem, 102 (2008) 1980-1985.

[161] A. Nguyen, V. Marsaud, C. Bouclier, S. Top, A. Vessieres, P. Pigeon, R. Gref, P. Legrand, G. Jaouen, J.M. Renoir, Nanoparticles loaded with ferrocenyl tamoxifen derivatives for breast cancer treatment, Int J Pharm, 347 (2008) 128-135.

[162] C. Lu, J.M. Heldt, M. Guille-Collignon, F. Lemaitre, G. Jaouen, A. Vessieres, C. Amatore, Quantitative analyses of ROS and RNS production in breast cancer cell lines incubated with ferrocifens, ChemMedChem, 9 (2014) 1286-1293.

[163] A. Vessieres, C. Corbet, J.M. Heldt, N. Lories, N. Jouy, I. Laios, G. Leclercq, G. Jaouen, R.A. Toillon, A ferrocenyl derivative of hydroxytamoxifen elicits an estrogen receptor-independent mechanism of action in breast cancer cell lines, J Inorg Biochem, 104 (2010) 503-511.

[164] N.T. Huynh, C. Passirani, E. Allard-Vannier, L. Lemaire, J. Roux, E. Garcion, A. Vessieres, J.P. Benoit, Administration-dependent efficacy of ferrociphenol lipid nanocapsules for the treatment of intracranial 9L rat gliosarcoma, Int J Pharm, 423 (2012) 55-62.

[165] A.L. Laine, A. Clavreul, A. Rousseau, C. Tetaud, A. Vessieres, E. Garcion, G. Jaouen, L. Aubert, M. Guilbert, J.P. Benoit, R.A. Toillon, C. Passirani, Inhibition of ectopic glioma tumor growth by a potent ferrocenyl drug loaded into stealth lipid nanocapsules, Nanomedicine, (2014).

[166] A.L. Laine, E. Adriaenssens, A. Vessieres, G. Jaouen, C. Corbet, E. Desruelles, P. Pigeon, R.A. Toillon, C. Passirani, The in vivo performance of ferrocenyl tamoxifen lipid nanocapsules in xenografted triple negative breast cancer, Biomaterials, 34 (2013) 6949-6956.

[167] A. Vonarbourg, C. Passirani, L. Desigaux, E. Allard, P. Saulnier, O. Lambert, J.P. Benoit, B. Pitard, The encapsulation of DNA molecules within biomimetic lipid nanocapsules, Biomaterials, 30 (2009) 3197-3204.

[168] M. Morille, C. Passirani, S. Dufort, G. Bastiat, B. Pitard, J.L. Coll, J.P. Benoit, Tumor transfection after systemic injection of DNA lipid nanocapsules, Biomaterials, 32 (2010) 2327-2333.

[169] M. Morille, T. Montier, P. Legras, N. Carmoy, P. Brodin, B. Pitard, J.P. Benoit, C. Passirani, Long-circulating DNA lipid nanocapsules as new vector for passive tumor targeting, Biomaterials, 31 (2010) 321-329.

[170] S. David, N. Carmoy, P. Resnier, C. Denis, L. Misery, B. Pitard, J.P. Benoit, C. Passirani, T. Montier, In vivo imaging of DNA lipid nanocapsules after systemic administration in a melanoma mouse model, Int J Pharm, 423 (2012) 108-115.

[171] S. David, T. Montier, N. Carmoy, P. Resnier, A. Clavreul, M. Mevel, B. Pitard, J.P. Benoit, C. Passirani, Treatment efficacy of DNA lipid nanocapsules and DNA multimodular systems after systemic administration in a human glioma model, J Gene Med, 14 (2012) 769-775.

REVUE BIBLIOGRAPHIQUE

REVUE BIBLIOGRAPHIQUE

Dans le but d'une administration systémique et intracellulaire, les acides nucléiques tels que les siRNA nécessitent d'être vectorisés afin de se voir protégés et de pouvoir traverser les membranes biologiques. Ainsi, les ARN interférents, utilisés pour les essais d'extinction de gène dans de nombreux modèles cellulaires, sont classiquement mélangés à des lipides cationiques. Cependant, leur injection *in vivo* est fortement compromise suite à la forte toxicité observée avec la plupart de ces lipoplexes.

Depuis cette découverte, de nombreuses formulations ont vu le jour afin de complexer avec succès les siRNA et rendre leur injection intraveineuse possible. Aujourd'hui, micelles, liposomes, dendrimères, et nanoparticules ont montré leur potentiel à encapsuler/adsorber les siRNA. Leur capacité à cibler le site tumoral a été évaluée dans de multiples stratégies incluant le ciblage passif et/ou actif. Leur potentiel en cancérologie a été étudié à l'aide de diverses expérimentations pharmacocinétiques et de biodistribution. Enfin, différentes protéines participant à différentes voies de signalisation ont été ciblées via des siRNA pour réduire la progression tumorale. Les mécanismes moléculaires généralement ciblés sont alors l'apoptose, le cycle cellulaire ou encore l'angiogenèse.

Un travail de recherche bibliographique a été entrepris, ici, afin de recenser les formulations actuellement à l'étude dans le cadre d'une délivrance de siRNA par voie systémique appliquée à la thérapie des pathologies cancéreuses. La première partie de ce travail s'est focalisée sur l'étude des caractéristiques des formulations comprenant leur composition, leurs paramètres physico-chimiques et leur capacité à encapsuler les siRNA. Une deuxième partie s'est consacrée aux stratégies de ciblage tumoral développées pour ce type de nanomédecines. Enfin, la dernière partie a permis de lister les différentes protéines ciblées à l'aide de siRNA sur des modèles animaux classiquement utilisés en cancérologie.

Depuis la parution de cette revue bibliographique, les essais cliniques sur le CALAA-01 se poursuivent. D'autres essais cliniques sur des formes nanoparticulaires pour la délivrance de siRNA par voie intraveineuse dans le cadre de pathologies cancéreuses sont en cours, incluant l'Atu027 qui correspond à des siRNA associés à une forme liposomale. De plus, cette année, un oligonucléotide antisens a été approuvé par la FDA pour une injection systémique, dans le cadre de l'hypercholestérolémie familiale.

Ce travail bibliographique a été publié en 2013 dans le journal Biomaterials.

Biomaterials 34 (2013) 6429–6443

Contents lists available at SciVerse ScienceDirect

Biomaterials

journal homepage: www.elsevier.com/locate/biomaterials

Review

A review of the current status of siRNA nanomedicines in the treatment of cancer

Pauline Resnier [a,b], Tristan Montier [c,d], Véronique Mathieu [e], Jean-Pierre Benoit [a,b], Catherine Passirani [a,b,*]

[a] LUNAM Université, F-49933 Angers, France
[b] INSERM U1066, Micro et Nanomédecines Biomimétiques, IBS – CHU, 4 Rue Larrey, F-49933 Angers, France
[c] INSERM Unité 1078, SFR 148 ScInBioS, Université de Bretagne Occidentale, Université Européenne de Bretagne, 46 Rue Félix Le Dantec, CS51819, 29218 Brest Cedex 02, France
[d] DUMG Université de Bretagne Occidentale, Université Européenne de Bretagne, 22 Avenue Camille Desmoulins, CHRU de Brest, 29200 Brest, France
[e] Laboratory of Toxicology, Faculty of Pharmacy, Université Libre de Bruxelles, Brussels 1050, Belgium

ARTICLE INFO

Article history:
Received 4 April 2013
Accepted 27 April 2013
Available online 30 May 2013

Keywords:
SiRNA
Delivery system
Cancerology
Systemic injection
Nanomedicine
Pathway targeting

ABSTRACT

RNA interference currently offers new opportunities for gene therapy by the specific extinction of targeted gene(s) in cancer diseases. However, the main challenge for nucleic acid delivery still remains its efficacy through intravenous administration. Over the last decade, many delivery systems have been developed and optimized to encapsulate siRNA and to specifically promote their delivery into tumor cells and improve their pharmacokinetics for anti-cancer purposes. This review aims to sum up the potential targets in numerous pathways and the properties of recently optimized siRNA synthetic nanomedicines with their preclinical applications and efficacy. Future perspectives in cancer treatment are discussed including promising concomitant treatment with chemotherapies or other siRNA. The outcomes in human clinical trials are also presented.

1. Introduction

The RNA interference (RNAi) mechanism was first discovered in plants [1] and demonstrated in the roundworm *Caenorhabditis elegans* after the microinjection of double-stranded RNA (dsRNA) leading to a transitory high extinction of gene expression [2]. The RNAi concept is based on the interaction of endogen micro-RNA (miRNA) with messenger RNA (mRNA) thanks to the perfect sequence homology observed between the strands [3]. Over the last few years, many kinds of approaches have been created based on the copy or use of this endogenous gene expression regulation system including small hairpin RNA (shRNA; a single strand RNA with a hairpin loop structure), DNA plasmid coding to shRNA, and small-interference RNA (siRNA; a double strand RNA). These structures are all integrated in the miRNA pathway and produce effective gene expression inhibition. This paper will only focus on the RNA form as siRNA (for more information on miRNA, shRNA, see review in the bibliography [4]). In the context of gene therapy applied to cancers, siRNA acts as a loss-of-function strategy that can inhibit virtually every single protein of interest expression regardless to its localization within the cells contrary to antibodies or tyrosine kinase inhibitors that respectively react only with surface antigens and tyrosine kinase protein. These small entities aim to modulate the expression of overexpressed or mutated genes identified as a key hurdle. Moreover, thanks to this non-integration in DNA, siRNA does not lead to genome modification, an important parameter for regulatory and safety considerations.

Major hindrance to their clinical development in oncology remains limited pharmacodynamic properties due notably to their physicochemical properties. For these reasons, the association of nucleic acid constructs with a multitude of delivery system [5]. These nanomedicines are necessary in order to protect and help them to cross these natural barriers (see our previous review [6]).

To date, numerous proteins have been targeted by siRNA embedded into non-viral delivery systems in cancer pathologies based on cell cycle, apoptosis, proliferation and angiogenesis pathway studies.

This review i) presents shortly the promising characteristics of nanocarriers to bypass the obstacles of intravenous injection and to

* Corresponding author. INSERM U1066, IBS – CHU, 4 Rue Larrey, 49933 Angers Cedex 9, France. Tel.: +33 244 688 534; fax: +33 244 688 546.
E-mail address: catherine.passirani@univ-angers.fr (C. Passirani).

0142-9612/$ – see front matter © 2013 Elsevier Ltd. All rights reserved.
http://dx.doi.org/10.1016/j.biomaterials.2013.04.060

target specifically cancer cells and ii) sums up the current status of preclinical and clinical studies conducted to date towards various molecular targets in this systemic context. The perspectives and opportunities to use siRNA delivery systems alone or in combination with other therapies are discussed.

2. SiRNA delivery systems

SiRNA interacts with cytoplasmic proteins, and in this way need to be taken up by the cell. This mechanism includes the first interaction with cell membrane, the penetration into classic endosomal vesicle or other mechanisms, and finally the escape of this vesicle to be delivered into the cytoplasm. Moreover, siRNA cannot be injected in systemic circulation. In fact, these nucleic acids are rapidly degraded by plasmatic nucleases. In consequence, the encapsulation of siRNA into a delivery system is expected to ameliorate their cell penetration, their delivery into cytoplasm after their protection in blood, their half-life time and finally their specific delivery on tumor site.

2.1. SiRNA encapsulation

The encapsulation of hydrophilic drugs such as nucleic acids and proteins has been already developed for numerous formulation processes (Table 1). From the classic liposomes to new triblock micelles, various encapsulation efficiencies have been obtained. High yields (80%–95%) have been observed with various types of liposomes based on cationic lipids as 1,2-DiOleoyl-3-Trimethyl-Ammonium-Propane (DOTAP) [7,8], O,O′-ditetradecanoyl-N-(α-trimethyl ammonio acetyl) diethanolamine chloride (DC-6–14) [9], or cholesterol and their derivates as 3β-[N-(N′,N′-dimethylamino-ethane) carbamoyl] cholesterol (DC–cholesterol) [10]. For nanoparticles, lower yield has been evaluated at 40% with calcium phosphate particle formulation developed by Li et al. [11], however, higher encapsulation efficiency has been observed for calcium phosphate nanoparticle process developed by Pittella and coworkers with 90% encapsulation yield [12]. For other nanoparticles, yields comprised between 65% to more than 95% are described with delivery system using natural lipids as lecithin [13,14], phosphatidylcholine [15], dextran [16], chitosan [17] or modified cholesterol [18] (Table 1). Contrary to liposomes and nanoparticles, complexes and micelles are usually formed with one kind of molecules and the encapsulation efficiency is depending in this case mainly on the lipid/siRNA charge ratio. Complete siRNA interaction was obtained with simple PEI complexes in association with polymer (glycol chitosan) [19] or protein (albumin) [20] and with copolymers as poly(2-(dimethylamino) ethyl methacrylate) (polyDMEAMA) [21], PEG-SS-poly(Pasp-DET) [22] or acetal-poly(ethylene oxide)-block-poly(ε-caprolactone) (acetal-PEO-b-PCL) [23].

However, if yields of encapsulation have been improved for each delivery system, important variations are observed on encapsulated doses of siRNA. While the majority of authors worked with around 200 μg by formulation, large scales have been observed from 50 μg [8,11,19] up to milligrams [15].

2.1.1. Cellular uptake

Nanocarrier proximity with cells can allow their passive penetration into cytoplasm by different mechanisms (Fig. 1). Multitude of

Table 1
Composition and encapsulation efficacy of siRNA delivery systems.

Type	Encapsulation	Composition	Encapsulation yield (%)	Refs.
Liposome 	Entrapment	DC–Chol, DOPE, DSPE–PEG, F′ab Her2	80	[10]
	Entrapment	DC-6–14, POPC, Chol, DOPE, DSPE–PEG	90	[9]
	Entrapment	DOTAP, DOPE, Chol, PEG–C16Ceramide	90	[7]
	Entrapment	DNA, protamine, DOTAP, Chol, DSPE–PEG	95	[8]
Nanoparticle 	Entrapment	PEG, lecithin, triglycerides, DOTAP, DOPE	65	[13]
	Entrapment/matrix	BHEM–Chol, mPEG–PLA	90	[18]
	Entrapment	Apolipoprotein A-I, Chol, CE, PC, Oligolysine	>90	[15]
	Entrapment	Dextran thiol, Dextran stearylamine, PEG-thiol	95	[16]
	Adsorption	Chitosan, Plurol, Ammonium nitrate, PIBCA	90	[17]
	Matrix	CaP, DOTAP, Chol and DSPE–PEG,	40	[11]
	Matrix	CaP, PEG–Pasp(DET–Aco)	90	[12]
	Matrix	PEI, Tripalmitin, DSPE–PEG–folate, Chol, Lecithin	85	[14]
Complex 	Matrix	PEI, Glycol chitosan polymer	100	[19]
	Matrix	PEI, HSA	100	[20]
Micelle 	Adsorption	poly(DMAEMA), mAB-SA	100	[21]
	Adsorption	PEG-SS-Pasp (DET)	100	[22]
	Adsorption	Acetal-PEO-b-PCCL	>90	[23]

Abbreviations, DC–Chol: 3β-[N-(N′,N′-dimethylaminoethane) carbamoyl] cholesterol; DOPE: dioleoylphosphatidylethanolamine; DSPE–PEG: 1,2-distearoyl-sn-glycero-3-phosphoethanolamine methoxy (polyethyleneglycol)-2000; F′ab Her2: antibody fragment of human endothelium growth factor receptor; DC-6–14: O,O′-ditetradecanoyl-N-(α-trimethyl ammonio acetyl) diethanolamine chloride; POPC: 1-palmitoyl-2-oleoyl-sn-glycero-3-phosphocholine; Chol: cholesterol; DOTAP: 1,2-DiOleoyl-3-TrimethylAmmonium-Propane; PEG–C16Ceramide: polyethylene glycol–C16–ceramide; PEG: polyethylene glycol; BHEM–Chol: N,N-bis(2-hydroxyethyl)-N-methyl-N-(2-cholesteryloxycarbonyl aminoethyl) ammonium bromide; mPEG–PLA: poly(ethylene-glycol)-b-poly(D,L-lactide); CE: cholesteryl oleate; PC: phosphatidylcholine; PEG-thiol: polyethylene glycol-thiol; PIBCA: poly(iso-butyl-cyanoacrylate); CaP: calcium phosphate; PEG–Pasp(DET): poly(ethylene glycol)-SS-poly{N-[N-(2-aminoethyl)-2-aminoethyl]aspartamide}; PEI: polyethyleneimine; HSA: human serum albumin; poly(DMAEMA): poly(2-(dimethylamino)ethyl methacrylate; mAB-SA: streptavidin-conjugated monoclonal antibody against CD22; acetal-PEO-b-PCCL: acetal-poly(ethylene oxide)-block-poly(ε-caprolactone).

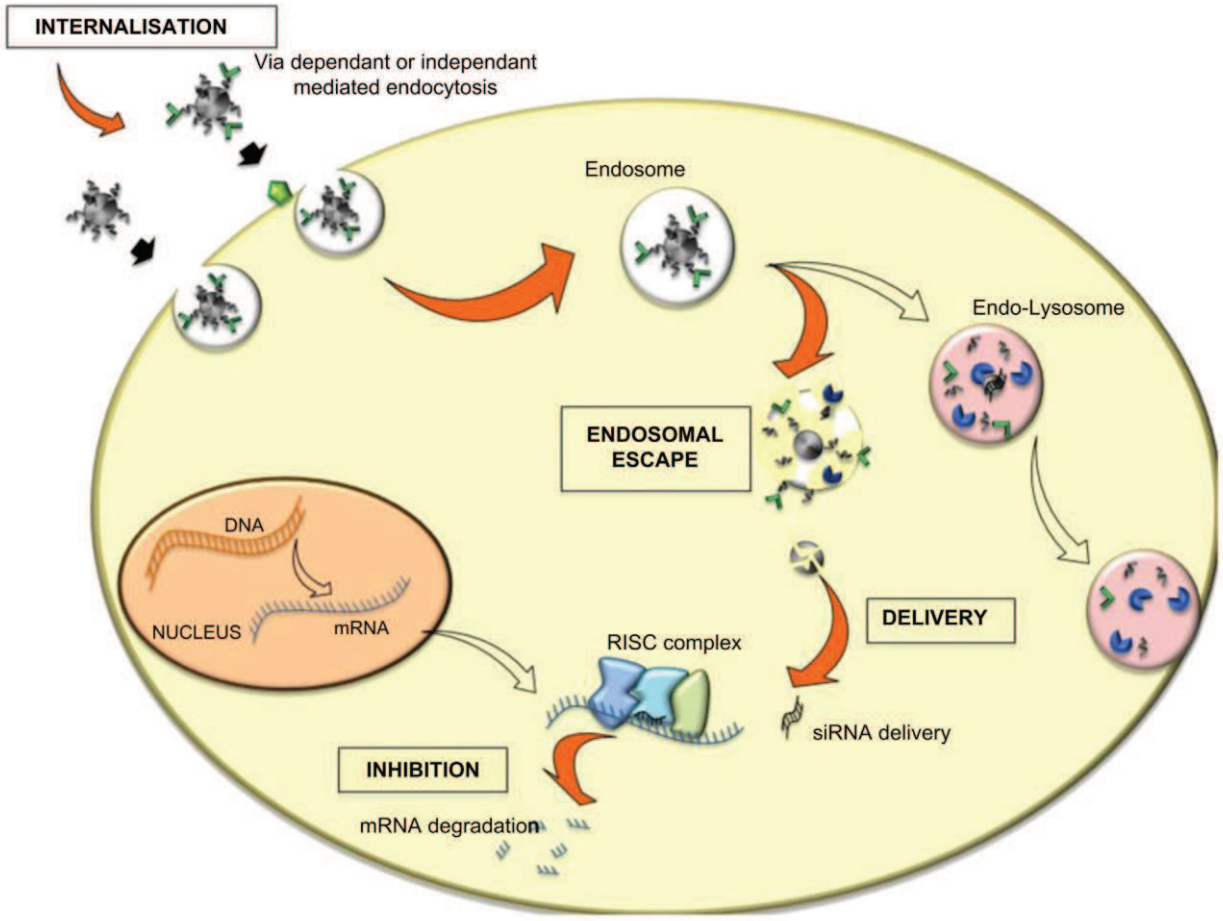

Fig. 1. Intracellular trafficking of siRNA delivery systems. Internalization of delivery systems can be realized by several mechanisms as clathrin, caveole pathways or lipid rafts. Two modalities are observed in this phenomenon, a receptor mediated endocytosis and a non-receptor mediated endocytosis. In all these cases, delivery systems are entrapped into endosomal vesicles. These vesicles fuse with lysosome and inevitably lead to siRNA degradation. To avoid this, delivery systems need to escape the endosomal vesicles. Finally, siRNA is delivered into the cytoplasm and produces their inhibitor effect.

endocytosis pathways is possible for delivery systems: clathrin-mediated endocytosis, lipid raft or caveolae, phagocytosis and macropinocytosis [24]. For example, high-density lipoprotein nanoparticles developed by Shahzad et al., showed efficient cellular uptake with 80% favored by major lipid compounds [15]. However, the global negative charge created by PEG and required for the stealth properties of delivery systems for passive targeting can prevent cellular uptake by charge repulsion of negative cell membrane. This surface modification can consequently interfere with efficient cellular siRNA delivery. Nonetheless, various pegylated delivery systems have demonstrated their efficiency to entry into cells even with PEG recovery. For example, two kinds of pegylated nanoparticles developed respectively Guo et al. [25] and Yang et al. [18] demonstrated a great cellular uptake with 60% and up to 95% of penetrated cells thanks to cholic acid moiety and a cholesterol derivates as N,N-bis(2-hydroxyethyl)-N-methyl-N-(2-cholesteryloxycarbonyl aminoethyl) ammonium bromide (BHEM–Chol) contained in shell structure. In addition, cationic lipid (DOTAP and oligolysinoyl lipid) constitution of liposomal forms led to a great cellular uptake with respectively more than 92% and 100% of siRNA labeled cells [26,27]. A complete cellular uptake was also obtained by poly(2-aminoethyl ethylene phosphate) (PPEEA) cationic block of micelleplex on breast cancer cells [28]. A high *in vitro* inhibition was obtained by these micelleplex with 75% of mRNA and protein extinction [10,28]. Then, lipid composition or positive charge is essential point to favor the cellular uptake of delivery system.

The most obvious mechanism for internalization occurs via receptors associated with the ligands used for the active targeting. In this case, receptors mediate endocytosis induced by ligand fixation and this leads to a facilitated internalization of siRNA delivery system in cytoplasmic vesicles through clathrin pathway. For example, *in vitro* transferrin and integrin targeting on respectively polyplexe and lipoplexe surface resulted in 100% of cellular uptake on mouse neuroblastoma and human glioblastoma cells [29,30]. Two micelle formulations modified with RGD peptide recognizing the $\alpha v\beta 3$ integrins showed a high cellular uptake in breast and ovarian cancer cells, respectively evaluated at 60% and 70% [23,31]. Finally, endogen molecules as folate can also be used to favor cellular uptake. Indeed, folate receptor expression was correlated with tumor localisation as described recently by Meier et al., in breast cancer [32]. Folate targeted siRNA nanoparticles penetrated at up to 90% in prostate cancer cells and produced a reduction of 80% mRNA and protein level *in vitro* [14].

2.1.2. Endosomal escape

After internalization, early endosomal vesicles are formed and mature in late endosomes characterized by an acidic pH and the presence of active enzymes to finally fuse with lysosome vesicles. In these endosomes, the degradation of nanocarriers can be initiated and nucleic acids destroyed by nucleases (Fig. 1). Accordingly, endosomal escape is a critical step for an efficient cytoplasmic siRNA delivery. Two principles have been already advanced to explain the mechanism of endosomal escape by delivery systems [33]. Firstly, proton sponge effect or pH buffering can be induced by the protonation of entrapped molecules in the acidic pH medium and produces an important inflow of water and ions as Cl^- and H^+, resulting in an osmotic swelling allowing the endosomal membrane rupture [34]. As PEG coating at the surface of delivery systems is known to limit the cellular uptake as well as the endosomal escape, new delivery systems have been developed with the view to break down the PEG linker in endosomal vesicle [34]. pH-sensitive linkers have been used in order to loss voluntary PEG chains and highlight the positive charges of polymers or lipids which can promote this proton sponge effect. Effective cytoplasmic localization was demonstrated by Wang et al., with nanoparticles containing N-(1-aminoethyl)iminobis [N-(oleicylcysteinylhistinyl-1-aminoethyl)propionamide] (EHCO) [30]. This polymerizable surfactant EHCO is a pH-sensitive amphiphilic molecule and its use induced a high endosomal membrane disruption [35]. Poly-L-lysine nanocarriers have also been modified to ameliorate their endosomal escape capacity thanks to PEG molecules coupled with cholic acid and a pH sensitive benzoic imine linker. In acidic conditions, cleavage of this linker was induced. In this way, toxic positive charges of poly-L-lysine became directly in contact with endosomal membrane and conducted to efficient disruption and the release of siRNA into the cytoplasm [25]. PEG-b-poly(propyl methacrylate-co-methacrylic acid) (PEG-b-P(PrMA-co-MAA)) polymers associated with PAMAM dendrimer also proved their capacity to avoid the lysosome destruction, 3 h after incubation [36]. The pH-responsive element was due to protonation of carboxylate groups of MAA and induced the proton sponge effect [37]. This protonation also caused the displacement of PEG-b-P(PrMA-co-MAA) from the dendrimer complex involving a second mechanism of membrane destabilization. Indeed, cationic lipids, polymers or peptides can fuse with endosomal membrane and perturb the bilayer organization thus causing pore and disruption [38]. The use of DOPE, a zwitterionic co-lipid, usually had led to this phenomenon. As an example, DOTAP/DOPE/cholesterol liposomes induced a cytoplasmic localization of siRNA confirmed by confocal microscopy analysis [39]. Association of DOPE with DC–cholesterol also conduced to an efficient endosomal escape [40]. Intracellular fluorescence was associated to siRNA internalization of DC–cholesterol/DOPE immunoliposomes, 2 h after incubation on breast cancer cells and resulted in 95% of mRNA extinction [10]. Otherwise, cholesterol derivate, BHEM–Chol, also induced perturbation into cell/organelle membranes [41] and its use in polymer nanoparticles led to cytoplasmic accumulation and no colocalization with lysosomes evidenced by microscopy analysis [18]. Polymers as PAsp(DET) provided an excellent ability of endosomal destabilization through the conformational change of flanking 1,2-diaminoethane pH-sensitive moiety [42]. Indeed, calcium phosphate nanoparticles surrounded by PAsp(DET) efficiently escaped the endosomal vesicles after 3 h and showed 80% of *in vitro* mRNA extinction [12]. Finally, Varkouhi and coworkers highlighted the potential of peptides in the endosomal escape mechanism. Fusiogenic peptides penetrated into phospholipid bilayers and created a pore provoking swelling choc [33]. Only 2 h after incubation, sh-GALA peptides combined to liposomes were localized in cytoplasm and confirmed their capacity to fuse with endosomal membrane and disrupt them [26]. *In vitro* mRNA extinction evaluated at 85% was induced after 24 h incubation with this sh-GALA liposomes [26]. Moreover, siRNA–peptide complexes developed by Canine et al., showed a perinuclear localization, demonstrating once again their efficient endosomal escape and *in vitro* protein extinction evaluated at 95% [43].

2.2. SiRNA protection

2.2.1. Enzymatic protection

To deliver intravenously an intact and efficient siRNA to the targeted cells *in vivo*, the protection of siRNA against plasmatic enzymes as nucleases is the first necessary step to overcome after systemic administration [44]. Naked siRNA is naturally completely degraded in 30 min into the bloodstream after recognition by plasmatic enzymes containing a double-stranded RNA binding domain [45]. To evaluate this degradation *in vitro*, incubations with serum or RNAse A at physiological temperature have been commonly realized as an indicator of the protection level of siRNA and *in vivo* evaluation of siRNA protection was realized by half-life study after intravenous injections into rodents (Table 2).

PEI complexes based on PEI alone or on PEI coated with human serum albumin (HSA) or atelocollagen resulted in *in vitro* and *in vivo* protection evaluated at less than 1 h [20,46–48]. The commercial form of PEI (JetPEI) provided the best protection with 2 h of siRNA detection *in vitro* [49]. In fact, *in vitro* protein inhibition evaluated at 85% and 50% was provided by lipid substituted PEI complexes and PEI–F25 LMW [28,50] and atelocollagen complex with more than 95% [14,48]. However, *in vivo* analysis highlighted the difficulty of PEI complex to protect and carry siRNA with low transfection efficacy estimated less than 50% and similar results were found with atelocollagen complex [14,48]. An *in vitro* longer protection, up to 6 h, could be obtained with PEI when it was associated with glycol chitosan and produced 80% of mRNA extinction [19]. Interestingly,

Table 2
Protection of siRNA by delivery systems.

Type	Delivery system	*In vitro* protection (h)	*In vivo* protection (h)	Refs.
Complexe	Atelocollagen	1	No data	[48]
	PEI	<1	No data	[46,47]
	PEI/HSA	<1	No data	[20]
	JetPEI®	2	No data	[49]
	Glycol chitosan/PEI nanoparticle	6	No data	[19]
	MPG-8 Peptide based delivery	No data	5	[51]
Micelle	Polyion complex micelle (PCIM)	4	No data	[36]
	PLL nanocarrier	48	No data	[25]
	Micelleplex	No data	12	[28]
	Multifunctional micellar nanocarriers	No data	24	[23]
Liposome	Her2-PEG-immunoliposome	9	No data	[10]
	Multifunctional nano-device (MEND)	24	No data	[26]
	Lipidic particle	No data	>2	[7,54]
	Pegylated cationic liposome	No data	>9	[55]
	Wrapped liposome	>3	>6	[52]
	Nanoparticle system	24	24	[53]
Nanoparticle	Cyclodextrin nanoparticle	4	No data	[56]
Dendrimer	PPI dendrimer	48	72	[58]

PEI: polyethyleneimine; HSA: Human serum albumin; PLL: Poly-L-Lysine; PPI: poly(propyleneimine).

peptide-based delivery with MPG-8 peptide was tested in mice and biofluorescence monitoring (BFI) of siRNA revealed a strong detection until 5 h after intravenous injection [51].

The micellar organization is in majority composed by hydrophobic block core and hydrophilic block extensions with positive charges siRNA can react with, being absorbed at this interface (Fig. 2). *In vitro* minimal time of protection induced by micellar systems estimated at 4 h, was obtained by polyion complex micelles (PCIM) and a maximal time, around 48 h, was reported by Guo et al., with PEG-SS-poly-L-lysine-cholic acid (PEG-SS-PLL-CA) nanocarriers [25,36]. Furthermore, *in vivo* validation was realized with two other micellar formulations. Micelleplex and multifunctional micellar nanocarriers demonstrated a long protection time of siRNA, respectively evaluated at 12 h and 24 h [23,28]. This long protection time allows an effective extinction *in vitro* and *in vivo*. In fact, dendrimers developed by Felber et al., inhibited 60% of the specific mRNA and 50% of protein *in vitro* [36,47] and analysis after intravenous injection into mice performed with siRNA poly-L-lysine micelles induced 60% of mRNA inhibition in tumor bearing mice [25].

Liposomes generally entrap siRNA into their aqueous core surrounded by a lipid bilayer shell (Fig. 2). In this case, degradation of siRNA depends on the delivery system stability into the bloodstream. Large variations have been observed between different liposome formulations. *In vitro* analyses showed a protection of 3 h and 9 h, respectively for wrapped liposomes [52], and multi-functional nano-devices (MEND) [26], and maximal time of 24 h have been obtained in some cases [10,53]. Moreover, with immunoliposomes, intravenous injections into mice were performed and blood analyses showed siRNA presence for at least 2 h and until 24 h. Lipidic particles [7,54], wrapped liposomes [52] and pegylated cationic liposomes [55] allowed an *in vivo* protection until 2 h, 6 h and 9 h respectively. Moreover, this protection is illustrated by extinction efficacy obtained with lipidic particle with extinction of mRNA at 70% *in vitro* and 60% *in vivo* [7]. As for *in vitro*, nanoparticle systems developed by Yagi et al., provided the longest protection time (24 h) [53]. Then, the first siRNA delivery system used in clinical test, i.e. cyclodextrin-containing polycations encapsulating siRNA, showed 4 h of protection after *in vitro* incubation with RNAse A [56]. Finally, poly(propyleneimine) [57] dendrimers of siRNA were developed by Taratula et al. [58]. This system presented the best protection times *in vitro* (48 h) with more than 70% of mRNA extinction and *in vivo* (72 h).

2.2.2. Protection from immunity and natural clearance

Innate immune system is naturally developed to detect and degrade extrinsic unknown objects as foreign delivery systems. Specific organs as liver, spleen and kidneys play a crucial role in their pharmacokinetic behavior as part of the reticulo-endothelial system (Fig. 3). In fact, the mononuclear phagocyte system (MPS) mainly situated in liver, represents a monocyte/macrophage rich zone that promotes filtration, capture and destruction of blood components as cellular fragments, bacteria, aggregates and also nano-objects [59]. Moreover, kidney by renal clearance mechanism controls the elimination of these delivery systems [59]. Important clearance appears when system diameter is less than 25 nm [60] (Fig. 3). Delivery systems whom size is comprised between 50 and 250 nm, can largely limit their degradation or elimination by these different mechanisms and increase their half-life in bloodstream. To illustrate this, a large majority of nanocarriers already developed for *in vivo* applications have their size comprised in this interval (Table 3).

Fig. 2. Methods of siRNA complexation with delivery systems. The siRNA localization into nanocarriers differs according to structure and organization of the delivery system. SiRNA can be incorporated into matrix structure and allows a global repartition in all volume of sphere (left). Second strategy consists to adsorb siRNA on surface of delivery systems in low depth (middle scheme). Last organization concerns shell/core structure observed for liposomes and some nanoparticles. In this case (right), siRNA is restrained in the core compartment of the delivery system.

The surface charge of the delivery systems is also a critical parameter to consider in order to obtain a suitable pharmacokinetic profile. Indeed, plasmatic proteins are negatively charged and can consequently form some aggregates with positive charges. These large complexes can be recognized by innate immune system (complement proteins or macrophages). The bricks of the complement are able to interact with plane surface and favor macrophage recruitment [60,61]. The endocytosis by macrophages can lead to the destruction of the delivery systems and thus siRNA. By presenting neutral or slightly negative charge at the surface, complement fixation and recognition by MPS can be avoided or largely limited (Fig. 3). To illustrate this, nanoparticles can present neutral or negative global charge, as mesoporous nanoparticles developed by Tanaka et al., or lipoprotein nanoparticles of Shahzad et al., (both with −3 mV) and LNCs with +7 mV of surface charge [13,15,57]. For other nanoparticles cited in Table 3, PEG has been added at the surface to create artificially a negative hydrophilic and flexible ring which can hide and limit the effect of positive charges of cationic lipids and/or polymers used for the complexation of siRNA. Indeed, PEG is able to modify zeta potential of nanoparticles thanks to dipole interactions with water [62]. In fact nanoparticles developed respectively by Yang et al., and Susa et al., exhibited negative or neutral global charge thanks to this PEG recovery [16,18]. PEI polymer provided the similar effect and led, for example, to a negative charge of −21 mV for solid hybrid PEI nanoparticles [14].

For micelles, copolymers like poly(DMAEMA) and PEO-b-PCL induce generally a neutral profile [21,23]. Furthermore, micelles can resort to pegylation in order to neutralize positive charge of block copolymers. For example, PCIM with PEG ring, were characterized by neutral zeta potential evaluated at +5 mV [36], and micelleplex developed by Mao et al., had largely negative global charge with a zeta potential of −21 mV [63].

Concerning peptide complexes, they present generally a slight positive charge as observed for peptide-based nanoparticles, and FDT nanocarriers with respectively +16 and +10 mV [43,51]. Same results were obtained with glycol chitosan/PEI complexes (+10 mV) [19] and other polymer complexes based on oligoethyleneimine derivates (OEI-HD) (−6 mV) [29].

In the case of liposomes, pegylation is a necessary step to hide the high level of positive charges due to cationic headgroups. Even with PEG recovery, zeta potentials can stay highly positive as it is the case for liposomes of polycation hyaluronic acid (LPH) [64], liposomes polycation DNA (LPD) [8,65], lipidic particles [7] and pegylated cationic liposomes [55] characterized by a zeta potential comprised between +11 and +48 mV (Table 3). Despite these positive charges, lipidic particles and pegylated cationic liposomes developed respectively by Wu et al., and Sonoke et al., allowed an *in vivo* long time circulation and protection of siRNA explained by an efficient steric repulsion due to the high flexibility and hydrophilicity of PEG [62].

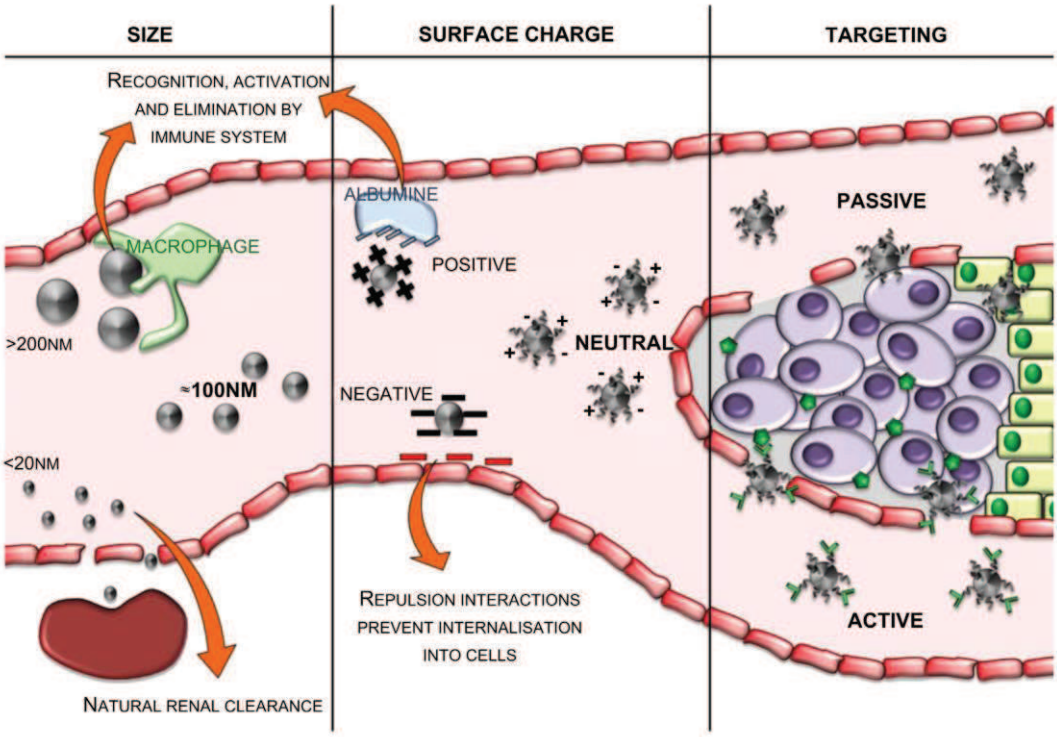

Fig. 3. Optimal physicochemical parameters to bypass the hurdle of intravenous administration and obtain a tumor targeting. Physico-chemical parameters and surface modifications are crucial to obtain a suitable profile into blood and an efficient tumor targeting. Particle of size inferior to 20 nm and superior to 200 nm is rapidly eliminated by respectively renal clearance and innate immune system (MPS). Intermediate size particles with positive charge surface are also rapidly recognized by the immune system and eliminated. Negative surface allows a long circulating profile but repulsion interactions between them and cell membrane prevents their internalization and the efficient delivery of siRNA into the cytoplasm. Nanocarriers with neutral surface are used to develop passive and active targeting. Enhanced permeability and retention (EPR) effect thanks to leaky vasculature allows a passive targeting of tumor site. Finally, active strategy with specific ligand induces the internalization of delivery systems into cancer cells.

2.3. Tumor targeting

2.3.1. Passive targeting

The advantage of delivery systems is to favor cellular uptake and target only tumor site and tumoral cells, in order to limit side effects and improve the therapeutic efficacy. Large fenestrations have been described on vessels situated around the tumor and they are associated with poor lymphatic drainage favoring the retention [66]. All of this provokes the Enhanced Permeability and Retention (EPR) effect demonstrated by Maeda et al., and leads to the development of passive targeting strategy consisting in natural accumulation in tumor site by long circulating or stealth delivery systems [66] (Fig. 3).

Numerous siRNA liposomes recently demonstrated this tumoral targeting. Neutral non-pegylated mesoporous silicon nanoparticles developed by Tanaka et al., and liposomes developed by Halder et al., have obtained a high tumor protein extinction superior at 80% after systemic injection into mice and consequently proved the accumulation of delivery system into tumor cells [57,67]. Passive accumulation was also achieved after single intravenous injection of fluorescent siRNA into pegylated LPD nanoparticles [68]. Cervical mouse cancer was successfully passively targeted by pegylated siRNA loaded lipid particles [7] and *in vivo* analysis highlighted an effective extinction estimated at more than 95% [65,69] Recently, novel pegylated cationic liposomes proved their efficacy to target pulmonary metastatic melanoma [9]. Moreover, synthetic polymers as PEI complex used by Grzelinski et al., allowed an efficient passive targeting of glioblastoma xenograft [46]. Then, new polymer, EHCO complexed with siRNA, was injected intravenously and demonstrated tumor site accumulation with 65% of protein extinction [29,30]. Micelleplex formed with triblock copolymer promoted breast cancer accumulation 4 h after intravenous injection [28]. Finally, Alexa555 siRNA lipoprotein nanoparticles were localized in ovarian tumor 48 h after a single intravenous administration 15].

Nonetheless, this strategy presents some limitations. EPR effect allows extravasation through inflammatory endothelium that possesses large fenestrations but does not lead to an exclusive cancerous cell targeting. Moreover, differential degree of vasculature, angiogenesis as well as tumor type, maturity and host environment, can play an important role in this EPR effect. Consequently, active targeting could be a way to enhance delivery system accumulation in desired tumor site and to help internalization into tumor cells.

2.3.2. Active targeting

In parallel to a passive clustering, an active targeting is more and more envisaged to enhance the preferential tumor accumulation and avoid side toxic effect. This can be obtained by grafting at the surface of the delivery system markers or ligands only expressed or at least overexpressed in tumors (tumoral environment or tumoral cells) (Fig. 3). For this purpose, chemical modifications on polymers have allowed the fixation of many families of molecules as peptides, antibodies and/or glucides (see Ref. [6]).

Table 3
Physico-chemical characteristics of siRNA delivery systems.

Type	Delivery system	Diameter [117]	Zeta potential (mV)	Refs.
Nanoparticle	Mesoporous silicon particle	26	−3	[57]
	Lipoprotein nanoparticle	10	−3	[15]
	Lipid nanocapsule (LNC)	60	−7	[13]
	Dextran nanoparticle	105	−0.2	[16]
	PEG–PLA nanoparticle	196	−17	[18]
	Lipid – PEI hybrid nanocarrier (LPN)	210	−21	[14]
Micelle	pH-responsive micelle	35	1	[21]
	Multifunctional micellar nanocarrier	103.4	4	[23]
	Polyion complex micelle (PCIM)	50–100	5	[36]
	Micelleplex	47.7	−21	[63]
Complexe	Peptide based nanoparticle	100–150	16	[51]
	FDT	78	10	[43]
	Glycol chitosan/PEI nanoparticle	350	10	[19]
	Polyplexes	155 ± 3	−6	[29]
Dendrimer	PPI dendrimer	101 ± 43	No data	[58]
Liposome	Liposome polycation hyaluronic acid (LPH)	170	11	[64]
	Liposome polycation DNA (LPD)	114	25	[8]
	Liposome polycation DNA (LPD) + NGR	197	31	[65]
	Lipidic particle	179	41	[7]
	Pegylated cationic liposome	100	48	[55]

PEG–PLA: poly(ethylene-glycol)-b-poly(D,L-lactide); PEI: polyethyleneimine; FDT: fusiogenic peptide – DNA condensing and endosomolytic motif – targeting motif; PPI: poly(propyleneimine).

Transferrin delivery system has demonstrated their efficacy to target tumor cell as transferring conjugated OEI-HD polyplexes with 85% of protein extinction in tumor cell after intravenous injection [29,30] and transferrin cyclodextrin-based nanoparticles with *in vivo* protein inhibition on murine model with a decrease estimated at 55% [70].

Tumor homing peptides are able to react with different receptors as, for example, integrin receptors with RGD peptide. In fact, Arg–Gly–Asp (RGD) motif is implicated in the fixation of alpha V integrin proteins on their receptor overexpressed on tumoral vessels [71]. Recently, two micelle formulations modified with RGD showed an efficient *in vivo* tumoral targeting in breast and ovarian cancer cells [23,31]. In fact, RDG chitosan nanoparticles showed *in vivo* mRNA and protein extinction respectively at 80% and 51% [31]. Moreover, *in vivo* experiments were also performed with RGD liposome delivery systems and conduced to a half-inhibition of protein expression in breast cancer cell bearing mice [39]. Another example has been prepared with the Asn–Gly–Arg (NGR) motif, discovered by phage display technology, that is able to interact with aminopeptidase N receptor (or CD13) [72]. The expression of this receptor was correlated with cancerous angiogenic property and cell mobility [73]. NGR liposomes were used by Chen et al., to target actively tumor vessels in sarcoma model and resulted in an efficient tumoral accumulation [65]. Ala–Pro–Arg–Pro–Gly (APRPG) peptide targets angiogenesis vessels as RGD and NGR [74,75] and was efficient on the surface of liposome formulation to induce an active *in vivo* tumor accumulation in colon tumor bearing mice [76]. Otherwise, peptide sequence isolated from releasing protein as hormone can be used to target specific cells or organs. For example, luteinizing hormono-releasing hormone (LHRH) plays an important role in multiple malignancies as cancer [77]. LHRH receptor has been described as a potential target for various cancers as hormone-dependent one [78]. A synthetic analog peptide was conjugated to siRNA dendrimers and provided an efficient and selective tumoral accumulation in ovarian cancer model [58].

In parallel, other molecules including for example polyunsaturated fatty acids, folic or, hyaluronic acids, can be used for active targeting [79]. Hyaluronic acid participates in cell growth, differentiation and migration [80] and is overexpressed in various cancers [81,82]. Chen et al., used a strategy based on hyaluronic acid grafted on pegylated liposomes and showed a preferential tumor localisation in melanoma bearing mice [64].

Antibodies have also been used to target specific cell receptors. Transferrin plays a major role in cell growth and its expression has been correlated with cancer progression. Antibodies of transferrin receptors have been largely used to target actively cancer cells [83,84]. For example, Pirollo et al., grafted an anti-transferrin antibody fragment on liposome to induce an active targeting of prostate and/or pancreatic model, observed as soon as 20 min after intravenous injection [85].

3. Current targets of siRNA in cancer therapy development

Good candidates for gene silencing in cancer therapy are legion when considering *in vitro* demonstration and/or use that are associated with anti-cancer effects. Few of them are nevertheless in the pipelines of pharmaceutical companies. General concerns about the targets to be considered for further drug development could be 1) differential expression level between cancer *vs* non-cancerous cells (generally overexpression in cancer cells; cancer type specificity should thus be considered as well as personalized medicine), 2) genetic concerns, e.g. highlighting the target to be associated with spontaneous cancer development in animal models and viability of the knock out models to decrease risk of toxicity (targeted delivery systems can be used to overcome, at least partly this problem), 3) characterized and crucial roles in cancer development, progression, resistance…, 4) multiple functionalities and/or localizations (in particular intracellular proteins) that cannot be inhibited by chemicals or reached by other therapeutic tools such as antibodies, 5) cellular half-life: protein with very rapid turn-over will increase the difficulty to develop a vector that can be administered in a practical point of view to obtain appropriate knock down timelines.

In this section we considered the different targets/pathways for which *in vivo* animal studies have been conducted successfully (Fig. 4). Table 4 summarizes these studies with detailed formulation, protocol and results.

3.1. Cell cycle

Cell cycle progression is strictly controlled as demonstrated in 1989 by Hartwell and Weinert by numerous effectors and checkpoints [86]. Main effectors of cell cycle progression are cyclins and cyclin-dependant kinases (cdk) such as cyclin B1–cdk1 complex which is the main effector implicated in G2/M transition [87]. Numerous studies have proven the overexpression of cyclin B1 in various cancers as oesophageal squamous cancer [88], non-small lung cancer [89], renal cancer [90] and prostate adenocarcinoma and was recently associated with a poor survival prognosis in breast cancer [91]. Cyclin B1 siRNA inhibition strategy was employed in prostate and lung cancer *in vivo* [51]. Eight intravenous injections of 10 μg siRNA complexed with peptide-based delivery systems to mice produced a reduction of about 92% of the prostate tumoral volume (Table 4). In a sub-cutaneous lung cancer model, tumor reduction reached 70% and half of the animals treated presented longer survival periods [51].

Polo-like-kinase 1 (Plk1) plays key roles during mitosis notably in the activation of cyclin B1–cdk1 complex and anaphase-

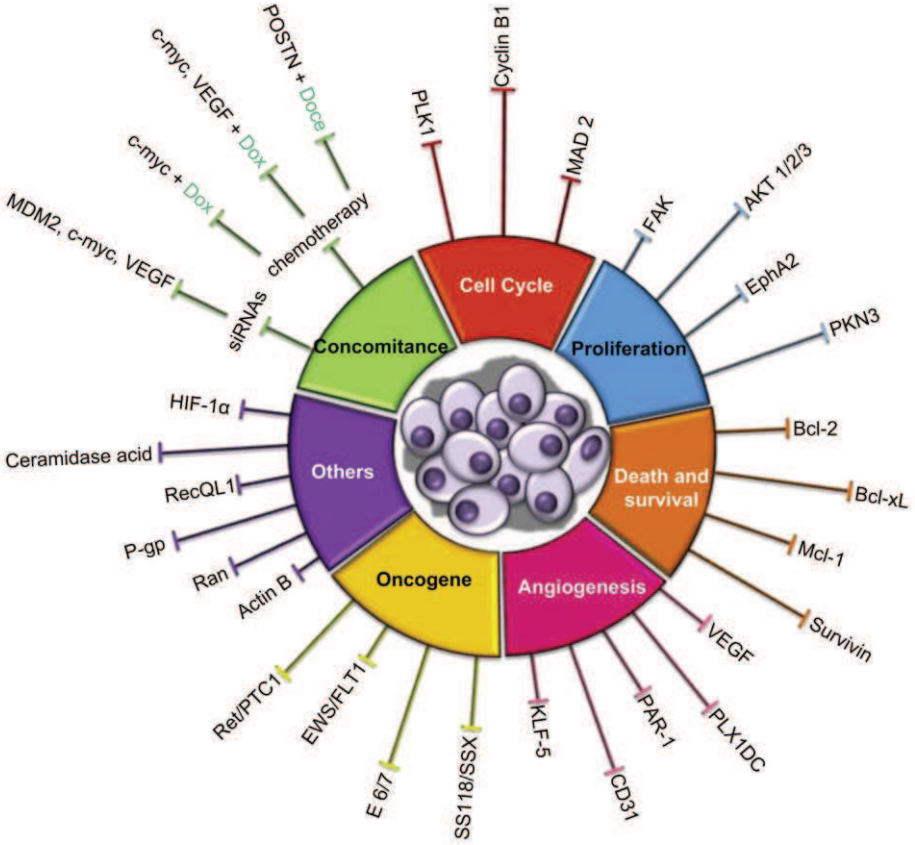

Fig. 4. Pathway targeting by siRNA delivery systems in cancer. Representation of siRNA targeted molecules used in preclinical studies to develop an anti-cancer treatment. Dox: doxorubicin; Doce: docetaxel. Plk1: polo-like kinase1; MAD2: mitotic-arrest deficient 2; EphA2: receptor of ephrins; AKT 1/2/3: KLFisoforme of serin–threonin kinase; PKN3: protein kinase N3; FAK: focal adhesion kinase; Bcl: B-cell lymphoma; Mcl-1: myeloid cell leukemia; VEGF: vascular endothelium growth factor; PAR-1: protease activated receptor 1; KLF-5: Kruppel-like factor 5; PLX1DC: plexin domain containing 1; HIF-1α: hypoxia inducible factor 1α; CA: ceramidase acid; MDM2: murine double minute 2; POSTN: periostin.

promoting complex/cyclosome (APC/C) for G2/M transition and spindle assembly checkpoint respectively [92]. Plk1 is overexpressed in multiple cancer types, including melanoma [93], non-small cell lung cancer [94], colorectal cancer [95], and breast cancer [96], with for some of them bad prognosis values. Inhibitions by siRNA or chemical agents validated Plk1 as an interesting target to combat cancer [97,98]. Two recent studies described Plk1 siRNA delivery systems. Sun et al., developed a micelleplex that was injected daily intravenously in sub-cutaneous breast tumor bearing mice from twelve days after tumor implantation to the end of the protocol at a siRNA concentration of 220 μg/kg. This treatment led to 70% of tumoral volume reduction compared to control group [28]. This protocol also demonstrated the recovery of effective apoptotic pathways with activation of caspase 3. A second study was realized on a breast organotypic tumor model. Treatment with Plk1 siRNA in PEG–PLA nanoparticles led to a 75% tumor growth inhibition after seven intravenous injections of 20 μg siRNA each [18].

Other checkpoint effectors' knock down could be useful to combat cancer, e.g. mitotic-arrest deficient 2 protein (MAD2) which is involved in the regulation of SAC [99]. MAD2, through sequestration of CDC20 into a complex, inhibits APC/C, maintains thereby the sisters' chromatids together till all chromosomes are bi-oriented to each spindle pole on metaphase plate, in order to prevent mis-segragation [100]. Liver cancer [101], lymphoma [102], lung [103], colon carcinoma [104], express high levels of MAD2. This up-regulation of this SAC regulator is associated with mitotic delay and chromosome instability that finally contributes to hallmarks of cancer as aneuploidy and genetic instability [10]. Knock down of MAD2 led to pro-apoptotic effects in osteasarcoma [105]. Kaestner et al., administered PEI/anti MAD2 siRNA complex intravenously MAD2 siRNA to sub-cutaneous colon carcinoma bearing mice. Injections of 10 μg of siRNA every two days during 14 days inhibited tumor growth of 35% [69].

3.2. Proliferation pathways

Cancer cells are characterized by sustained proliferation resulting from increased proliferative signals, decrease of negative feed-back signals and replicative immortality acquisition [10]. Cancer cells produce or force their environment to produce excessive growth factors as for example insulin growth factor (IGF), or epidermal growth factor (EGF) [106] but can become independent of these signals with mutations. Such external stimuli activate intracellular cascades like the MAPK pathways or the phosphoinositide-3-kinase (PI3K)/serin–threonin kinase AKT one, that promotes proliferation, division and survival and were clearly described in cancerogenesis mechanism [107]. EphA2 is a specific

Table 4
Protocol based on siRNA delivery in cancer therapy.

Pathway		SiRNA target	Cancer model	Tumoral cell injection	Total dose (μg)	Number of injections	Day of injection	Inhibition of tumor volume	Other effects	Refs.
Cell cycle		Cyclin B	Prostate	s.c	80	8	D0–21	70%–92%	50% long survival	[51]
		Plk1	Breast	s.c	141	32	D12–44	70%	Caspase 3 activation	[28]
				Orthotopic	140	7	D14–21	75%	/	[18]
		MAD2	Colon	s.c	70	7	D0–14	35%	Increased apoptosis	[69]
Proliferation		EphA2	Ovarian	i.p	5	1	D15	55%	/	[57]
		AKT1	Prostate	s.c	600	6	D0–15	66%	/	[114]
		AKT2	Prostate	s.c	600	7	D0–16	89%	/	[114]
		AKT3	Prostate	s.c	600	8	D0–17	57%	/	[114]
		PKN3	Prostate	Orthotopic	224	4	D1–4	60%	75% for metastasis	[117]
		FAK	Ovarian	i.p	24–30	8–10	D7–31 or 38	60%	/	[31]
Cell death and Survival		Bcl-2	Prostate	s.c	2000	10	D10–21	65%	/	[55]
		Bcl-xL	Prostate	s.c	1200	12	D1–24	40%	No inflammatory response	[48]
		Mcl-1	Breast	s.c	140	7	D9–19	75%	Maximal dose tested 53 mg/kg = no toxicity	[27]
		Survivin	Prostate	s.c	14	2	D2 and D7	30%	/	[14]
Angiogenesis		VEGF	Prostate[a]	s.c	7000	7	50 mm – D0–18	53%	No inflammatory response	[25]
			Prostate	s.c	560	5	D0–28	87%	No inflammatory response	[144]
		PAR-1	Melanoma	s.c	80	8	3–5 mm – D0–D28	77%	/	[168]
			Melanoma meta	i.v	100	10	D0–35	/	Decreased metastase number (81%)	[168]
		CD31	Prostate	Orthotopic	350	8	D35–49	65%	/	[117]
		KLF-5	Lung carcinoma[a]	s.c	350	7	D2–8	60%	/	[53]
			Prostate	s.c	1500	10	D7–16	48%	Prolonged survival median	[53]
		PLX1DC	Ovarian	i.p	24–30	8–10	D7–31 or 38	87%	Increased apoptose (35%),	[31]
Oncogene protein		E6/7	Renal[a]	s.c	120	3	D3–10	55%	No synergic effect with cisplatin	[7]
			Renal[a]	i.v	320	4	D1–11	/	Prolonged median survival 31D *vs* 21D	[7]
		ret/PTC1	Fibroblast	s.c	100	5	D0–9	90%	/	[17]
		EWS-FLI1	Ewing sarcoma	i.v	400	8	D1–24	80%	No inflammatory response	[70]
		SS18–SSX	Synovial sarcoma	s.c	1000	10	D3–28	83%	/	[52]
Other pathways	Hypoxy	HIF-1a	Glioblastoma	s.c	300	6	D21–36	50%	/	[30]
	Metabolism	CA	BT474	s.c	240	12	D10–22	75%	Increased apoptosis, non-immunogenic	[63]
	DNA repair	RecQL1	Colorectal meta	Spleen	500	10	D4–25	43%	/	[154]
			Pancreatic meta	Spleen	250	10	D4–15	31%	/	[154]
			Lung	s.c	400	8	D8–32	46%	/	[154]
	Nuclear transport	Ran	Neuroblastoma[a]	s.c	150	3	D7–13	49%	Increased apoptotic cell (12%), no hepatic toxicity	[29]
	Resistance	P-gp	Breast[a]	s.c	160	4	D11–17	60%	/	[39]
	Migration	Actine B	HT-1080	s.c	320	4	D11–D14	65%	No inflammatory response	[26]
SiRNA concomitance		MDM2, c-myc, VEGF	Melanoma[a]	i.v	18	2	D8 and 9	30%	No inflammatory response	[64]
		MDM2, c-myc, VEGF	Melanoma[a]	i.v	36	4	D10–18	/	Increased survival median + 6D, no inflammatory response	[8]
Chemotherapy Concomitance	Doxorubicin	c-myc	Colon	s.c	72	3	D1–3	60%	Increased apoptosis	[65]
	Doxorubicin	c-myc, VEGF	Ovarian	s.c	72	3	D1–3	57–60%	Increased apoptosis, no inflammatory response	[68]
	Docetaxel	POSTN	Ovarian	i.p	24–30	8–10	D7–31 or 38	90%	Increased apoptose (45%), decreased proliferation (60%)	[31]

Plk1: Polo-like kinase1; MAD2: mitotic-arrest deficient 2; EphA2: receptor of ephrins; AKT 1/2/3: KLFisoforme of serin–threonin kinase; PKN3: protein kinase N3; FAK: focal adhesion kinase; Bcl: B-cell lymphoma; Mcl-1: myeloid cell leukemia; VEGF: vascular endothelium growth factor; PAR-1: protease activated receptor 1; KLF-5: Kruppel-like factor 5; PLX1DC: plexin domain containing 1; HIF-1a: hypoxia inducible factor 1a; CA: ceramidase acid; MDM2: murine double minute 2; POSTN: periostin.
[a] Murine cell model, s.c: sub-cutaneous injection, i.p: intraperitoneal injection, i.v: intravenous injection.

receptor of ephrins that takes function in cell–cell contact and cell migration by activation of MAPK pathways promoting oncogenesis and increased expression has been detected in numerous cancers [108]. Inhibitions by RNAi technology proved the anti-cancer potential of *in vitro* targeting and local *in vivo* treatment respectively in malignant mesothelioma and squamous carcinoma [109,110]. One study exposed some results on intravenous injection of mineral nanoparticles loaded with EphA2 siRNA [57]. A single injection, two weeks after cell inoculation, was sufficient to lead to a 55% decrease of tumoral volume.

Numerous cancers, as for example skin cancer [111] and prostate cancer [112] have shown disregulation of PI3K/AKT pathways. Many reviews have described oncogenic overexpression of AKT and its roles in chemoresistance [113]. SiRNA knock down of three different AKT isoforms was explored by Sasaki et al., in prostate cancer model [114]. Atelocollagen was mixed with siRNA and injected every three days during two weeks by intravenous injections. All AKT isoforms siRNA conducted to an important regression of tumoral volume, i.e. 66%, 89% and 57% for respectively AKT1, AKT2 and AKT3 isoforms [114].

Then, the PKN3 protein, named also PKNβ, has been identified a few years ago [115]. Leenders et al., demonstrated their interaction with PI3K/AKT pathways and their antiproliferative effect on prostate cell by shRNA extinction [116]. *In vivo* inhibition strategy was realized with siRNA liposomal form [117]. Repetitive intravenous injections were realized on mice bearing organotypic prostate tumor and provided 60% of tumoral volume inhibition. Moreover, metastatic process was highly inhibited with 75% of metastasis number reduction [117].

Increased focal adhesion kinase [57] levels were reported in prostate [118], and breast [119] as well as in glioma [120]. FAK can be activated by integrins and is involved in multiple pathways controlling proliferation, survival, cell migration and anoikis resistance [121]. Its overexpression has been correlated with increased invasion and migration of several metastatic tumor types [122]. Inhibition of FAK protein has been obtained by different strategies: competitive molecule (FIP200); tyrosine kinase inhibitors (TKI) (PF-228) or RNAi (siRNA) [123]. Chemical inhibitors led to the regression of tumoral volume as demonstrated by Roberts et al. [124]. Delivery systems based on chitosan nanoparticles loaded with FAK siRNA, were developed for systemic treatment [31]. Twice weekly injections of 4 μg siRNA allowed inhibiting 60% of human ovarian tumor growth in nude mice.

3.3. Cell death and survival

Pathways involved in cell death and survival have important role in cancer development [125]. Cancer cells display acquired or innate cell death resistance mechanisms (to apoptosis or other cell death pathways). Apoptosis regulation pathways form a very complex molecular network with the two intrinsic and extrinsic classically recognized triggering pathways [126]. Bcl-2 family proteins are major molecular regulators of mitochondrial pathway leading to apoptosis and clearly related with cancer progression [127]. Anti-apoptotic bcl-2 family members as Bcl-2, Bcl-xL and Mcl-1, have been shown to be overexpressed in cancer pathologies including leukemia [128] and myeloma [129]. Then, poor survival was also associated with these Bcl-2 members' up-regulation in hepatocarcinoma [130]. Moreover, chemotherapy resistance was early associated with Bcl-2 and Bcl-xL high level expression, respectively in gastric and breast cancer [131,132]. Intravenous injections of vectorized siRNA targeting these three molecules were evaluated in tumor bearing mice: Bcl-2 and Mcl-1 siRNA in pegylated cationic liposomes [27,55], and Bcl-xL siRNA complexed with atelocollagen [48]. In these studies, reduction of tumor growth reached 40%–65%. Abnormal expression or overexpression of inhibitor of apoptosis proteins (IAPs) as survivin that has been correlated with oncogenic progression was reported in hepatocellular carcinoma [133], lung cancer [134], and ovarian cancer [135]. In addition, numerous studies have evidenced higher survivin expression during metastasis development, such as in prostate cancer [136] and in poor prognosis in meningioma [137]. Different survivin inhibition strategies resulted in marked antiproliferative effects in endometrial and breast animal cancer models [138,139]. Solid lipid–PEI nanocarriers were developed by Xue et al., to carry survivin siRNA [14]. A low dose of siRNA, only 14 μg delivered in twice injections, was sufficient to obtain 30% of tumoral volume regression.

3.4. Angiogenesis

Angiogenesis is an essential step for cancer development and has thus been recognized as a hallmark of cancers [125]. Without angiogenesis, cancer could not grow up to more than 2 mm of diameter as firstly emphasized by J Folkman. In this way, stopping neoangiogenic mechanism could constitute a key strategy to inhibit tumor growth [140]. However, numerous inhibitors have already been developed to slow down angiogenesis such as antibodies and TKI (sunitinib®, sorafenib®, axitinib®, and pazopanib®) but with appearance of resistance siRNA could therefore provide an alternative strategy [141,142]. Vascular endothelium growth factors (VEGFs and VEGFA in particular) are the most described secreted molecules implicated in angiogenesis of human cancers [143]. Poly-L-lysine nanocarriers of VEGF siRNA administered intravenously reduced by 53% prostate sub-cutaneous tumors [25] while VEGF siRNA micelles led to 87% volume reduction [144].

As controversies on the benefits of such anti-angiogenic therapies arose recently, other angiogenic factors or markers could be interesting alternatives like protease activated receptor 1 (PAR-1) which is enrolled in thrombin regulation and whose expression is correlated with angiogenesis in many cancer types [145] or platelet endothelial cell adhesion molecule 1 (PECAM-1 or CD31) [146]. Both have been targeted *in vivo* by siRNA in melanoma and prostate cancer models respectively. Reduction in tumor size and metastases has been obtained [147]. Finally, plexin domain containing 1 (PLXDC1) or TEM7 (tumor endothelial marker 7) is a protein showing an overexpression in cancerous endothelium [148] and a correlation with metastasis and poor prognosis [149]. Chitosan nanoparticles were used to carry PLXDC1 siRNA in orthotopic mice ovarian cancer model [31]. Low final dose of siRNA (maximal 30 μg) injected in 10 times was sufficient to produce a strong blockage of tumoral growth with 87% of volume inhibition.

3.5. Other pathways

Hypoxia triggers angiogenesis via several cellular mediators including the well-known HIF-1α transcription factor. Wang et al., developed multi-functional peptide-based carrier to deliver anti-HIF-1α RNA that inhibited by 50% glioma tumor growth [30].

Kruppel-like factor 5 (KLF-5) is a transcriptional factor implicated in the epithelial cell proliferation and consequently in angiogenesis [150]. This protein was targeted by siRNA carried by wrapped liposomes in two sub-cutaneous cancerous models [53]. A total siRNA dose of 350 μg was injected intravenously in murine lung carcinoma and a 60% of volume reduction was obtained. Prostate model was also assessed in a KLF-5 inhibition therapy [53]. Ten injections of 150 μg siRNA were performed and decreased the tumoral volume to 48%. Moreover, this inhibition demonstrated their efficacy to prolong the survival median.

Furthermore, nucleo-cytoplasmic transport for signaling molecules and transcription factors is controlled by protein complexes situated at nucleus pore, including importin α and importin β. Ran GTPase is also implicated in this transport regulation and can contribute to pathways of cell transformation facilitating tumor progression [151]. Inhibition of Ran was assessed in sub-cutaneous murine neuroblastoma and resulted in 49% of tumoral volume regression with a single low dose of siRNA (150 μg) [29].

Considering the hallmarks of cancers as defined by Hanahan and Weinberg, bioenergetic metabolism is attractive for new therapies. Example is provided with the acid ceramidase (AC) that plays a key role in cancer development through the enhanced conversion of ceramide into the anti-apoptotic shingosine 1-phosphate [152]. A breast cancer mice model was developed to evaluate the effect of AC siRNA inhibition [63]. Results showed a strong inhibition with 75% of tumoral volume regression by using 240 μg of siRNA.

RecQL1, a human helicase, participates in DNA repair and the maintenance of genome integrity. This protein is highly up-regulated in rapidly growing cells including various kinds of cancers [153]. Pancreatic, lung and colorectal cancer models in mouse have been treated respectively by intravenous injections of 250, 400, and 500 μg of RecQL1 siRNA entrapped into non-viral delivery

systems [154]. These protocols induced alone 31%, 43% and 46% of tumor growth inhibition for pancreatic, colorectal and lung cancers. Finally, resistance mechanisms to chemotherapy include the overexpression of ABC efflux pumps such as P-glycoprotein (P-gp) that decrease intracellular chemotherapeutic agents like doxorubicin [155]. Jiang et al., worked on the effect of P-gp siRNA on doxorubicin resistant human breast cancer cells [39]. After treatment with P-gp siRNA liposomes, tumoral volumes were reduced to 63% *vs* doxorubicin alone (28%).

3.6. Virus and fusion oncogenes

As several cancer types can be induced by oncogenes from viruses, specific strategies can be developed to combat them. Examples are E6 and E7 oncogenes of human papilloma virus (HPV) that have been inhibited by siRNA strategy in murine sub-cutaneous renal carcinoma models [7] resulting in 55% of tumoral progression blockage and prolonged survival median in a metastatic model.

Genetic changes as chromosome rearrangement can cause the synthesis of abnormal fusion proteins. These later can turn out to be oncogenic and then favor the proliferation and progression of tumors. The ret/PTC1 fusion protein appears as a specific oncogene rearrangement presented in thyroid cancers [156]. de Martimprey et al., developed a siRNA strategy on ret/PTC1 protein [157]. These chitosan nanoparticles were able to strongly reduce the tumor size with 90% of volume reduction. EWS-FLI1 is another chimeric gene produced by abnormal chromosomal rearrangement, associated with Ewing sarcoma and targeted to develop a new therapeutic treatment [158,159]. The inhibition of EWS-FLI1 by siRNA was conducted by Hu-Lieskovan and coworkers [70]. Cyclodextrin based nanoparticles were injected 8 times until total siRNA dose of 400 μg and proved an effective inhibition of tumoral progression with 80% of tumoral volume reduction. Finally, targeting of SS18–SSX, a fusion protein [160], described in synovial sarcoma by a consistent chromosome translocation (X; 18) was tested by Takenaka et al., in wrapped liposomes with repetitive intravenous injections. Their protocol allowed a strong volume diminution estimated at 83% [52].

4. Perspectives

4.1. RNAi in clinics: introduction

To date, very few nucleotide-based drugs reached the market. The first one was an antisense oligonucleotide from Isis Pharmaceuticals in 1998 to treat CMV retinitis (Formivirsen; Vitravene®) but the company stopped it because of its very limited market. This drug is the first proof that local delivery of RNAi-based treatment can be envisaged. The aptamer Pegaptanib (Macugen®) is the second example of nucleotide-based therapy approved by the FDA in 2004 for the acute macular degeneration (AMD) with local administration.

Despite more than 60 clinical trials conducted with antisense oligonucleotides to combat cancer (clinicaltrials.gov) and 589 publications in pubmed database on "oligonucleotide and cancer" in "clinical trials", (April 2013), no one reached the market. Among the most promising ones, anti-Bcl-2 antisense (Oblimersen®) did not get FDA approval after the phase III randomized trial for chronic lymphocytic leukemia [161] because of lack of efficacy in terms of intent-to-treat survival benefits. Great hope has been placed in siRNA that emerges now in clinical trials as detailed hereafter.

4.2. Clinical trials

Pubmed references 31 publications related to "siRNA and cancer" in "clinical trials" (April 2013) but only few clinical trials (all in phase I clinical status) are listed on clinicaltrials.gov for solid tumor treatment. CALAA-01 is an siRNA that reduced the expression of the M2 ribonucleotide reductase subunit (R2) and was shown to inhibit/reduce melanoma tumor growth *in vivo* in mice [162]. The CALAA-01 siRNA was protected from nuclease degradation within stabilized cyclodextrin-based nanoparticles targeted to tumor cells via transferrin [163]. These nanoparticles were injected intravenously in three patients and proved effective against tumor tissues [164]. Nowadays, the Phase I trial is in progress on the safety and the adapted dose of these siRNA nanoparticles.

A second non-viral siRNA delivery system, Atu027, is in its prospective phase of clinical trials. As described before, this nanoscale system has proved its *in vitro* and *in vivo* efficacy [117,147]. Moreover, these liposomes loaded with a PKN3 siRNA were injected intravenously for 4 h in a single dose in 24 human patients. The first results showed the good tolerance to Atu027 by patients [165]. Further studies will be conducted to determine the siRNA efficacy in terms of anti-cancer effects.

Phase I trial with a liposome-carried EphA2 siRNA associated with promising results in mice [57] has just started recruitment in summer 2012. A dose of 450 μg/m^2 of siRNA into nanomedicines will be injected intravenously twice weekly during 3 week cycles in patients diagnosed with ovarian cancer. The aim of Phase I will be the study of the safety of these siRNA–EphA2–DOPC and their maximal tolerated dose (MTD).

While these clinical trials were inconceivable ten years ago, they are nowadays ongoing and showing good tolerance levels with no evidence of side effects. Also encouraging results obtained with concomitant treatment in cancer have thus suggested the possibility to undertake personalized treatment in the future (early stage diagnosis, tumor screening, siRNA pool specific for the patient…).

4.3. Concomitant treatments

The transitory effects of siRNA are adapted to chronic disease [166] however, concomitant treatments allowed by the use of synthetic delivery systems (different siRNA, chemo and radiotherapy…) are necessary. The poor results obtained with single siRNA delivery have encouraged the development of concomitant strategies by combining several siRNA to target simultaneously different pathways or to use single siRNA with other therapeutic agents. For example, three siRNA were co-formulated in liposomes by Huang et al. [8,64]. These siRNA targeted MDM2, c-myc and VEGF proteins that were all implicated in the development of cancerous pathologies. Two intravenous injections of 9 μg siRNA were able to produce 30% volume regression in a mouse melanoma metastasis model [64]. Moreover, double doses of siRNA increased the survival median by 6 days corresponding to 30% compared to the control group in the same cancer model [8].

Association and synergy between siRNA and other drugs could potentially improve their therapeutic effect. SiRNA delivery systems have been already tested in association with classic chemotherapeutic agents. Multifunctional nanoparticles, transporting siRNA and doxorubicin, were developed by Chen et al., to demonstrate their effect [65,68]. A colon cancer model was used to test this concomitant treatment based on doxorubicin and c-myc siRNA. While siRNA or doxorubicin treatment alone led respectively to 35% and 8% of inhibition contrary to siRNA associated with doxorubicin that led to a 60% synergic volume regression [65]. Similar results were obtained in a second study conducted with different siRNA against c-myc and VEGF with or without chemotherapy [68].

Other chemotherapeutic agents have been tested in such combination, e.g. docetaxel with periostin (POSTN) siRNA entrapped into chitosan nanoparticles [31]. Periostin plays a significant role in cell invasion, survival, and angiogenesis, leading to metastasis

[167]. In an ovarian cancer model, injections of POSTN siRNA with docetaxel increased tumoral regression (90% reduction in comparison to 70% and 50% regression when siRNA or docetaxel was used alone) and decreased also significantly the number of tumoral nodules [31].

Acknowledgments

We would like to thank the foundation "Association de Recherche contre le Cancer" and "La Ligue contre le cancer 49 et 35", "Conseil Régional de Bretagne", the "Structure Fédératif de Recherche de Brest" (SFR 148 ScInBioS), "Association Française contre les Myopathies" (AFM, Evry, France), "Vaincre La Mucoviscidose" (Paris, France), and "Association de transfusion sanguine et de biogénétique Gaétan Saleün" (Brest, France).

References

[1] Ratcliff F, Harrison BD, Baulcombe DC. A similarity between viral defense and gene silencing in plants. Science 1997;276:1558–60.
[2] Fire A, Xu S, Montgomery MK, Kostas SA, Driver SE, Mello CC. Potent and specific genetic interference by double-stranded RNA in *Caenorhabditis elegans*. Nature 1998;391:806–11.
[3] Winter J, Jung S, Keller S, Gregory RI, Diederichs S. Many roads to maturity: microRNA biogenesis pathways and their regulation. Nat Cell Biol 2009;11:228–34.
[4] Pushparaj PN, Aarthi JJ, Manikandan J, Kumar SD. siRNA, miRNA, and shRNA: in vivo applications. J Dent Res 2008;87:992–1003.
[5] de Martimprey H, Vauthier C, Malvy C, Couvreur P. Polymer nanocarriers for the delivery of small fragments of nucleic acids: oligonucleotides and siRNA. Eur J Pharm Biopharm 2009;71:490–504.
[6] David S, Pitard B, Benoit JP, Passirani C. Non-viral nanosystems for systemic siRNA delivery. Pharmacol Res 62:100–14.
[7] Wu SY, Singhania A, Burgess M, Putral LN, Kirkpatrick C, Davies NM, et al. Systemic delivery of E6/7 siRNA using novel lipidic particles and its application with cisplatin in cervical cancer mouse models. Gene Ther 2011;18:14–22.
[8] Li SD, Chono S, Huang L. Efficient oncogene silencing and metastasis inhibition via systemic delivery of siRNA. Mol Ther 2008;16:942–6.
[9] Tagami T, Suzuki T, Matsunaga M, Nakamura K, Moriyoshi N, Ishida T, et al. Anti-angiogenic therapy via cationic liposome-mediated systemic siRNA delivery. Int J Pharm 2012;422:280–9.
[10] Gao J, Sun J, Li H, Liu W, Zhang Y, Li B, et al. Lyophilized HER2-specific PEGylated immunoliposomes for active siRNA gene silencing. Biomaterials 2010;31:2655–64.
[11] Li J, Chen YC, Tseng YC, Mozumdar S, Huang L. Biodegradable calcium phosphate nanoparticle with lipid coating for systemic siRNA delivery. J Control Release 2010;142:416–21.
[12] Pittella F, Zhang M, Lee Y, Kim HJ, Tockary T, Osada K, et al. Enhanced endosomal escape of siRNA-incorporating hybrid nanoparticles from calcium phosphate and PEG-block charge-conversional polymer for efficient gene knockdown with negligible cytotoxicity. Biomaterials 2011;32:3106–14.
[13] David S, Resnier P, Guillot A, Pitard B, Benoit JP, Passirani C. siRNA LNCs – a novel platform of lipid nanocapsules for systemic siRNA administration. Eur J Pharm Biopharm 2012;81:448–52.
[14] Xue HY, Wong HL. Solid lipid-PEI hybrid nanocarrier: an integrated approach to provide extended, targeted, and safer siRNA therapy of prostate cancer in an all-in-one manner. ACS Nano 2011;5:7034–47.
[15] Shahzad MM, Mangala LS, Han HD, Lu C, Bottsford-Miller J, Nishimura M, et al. Targeted delivery of small interfering RNA using reconstituted high-density lipoprotein nanoparticles. Neoplasia 2011;13:309–19.
[16] Susa M, Iyer AK, Ryu K, Choy E, Hornicek FJ, Mankin H, et al. Inhibition of ABCB1 (MDR1) expression by an siRNA nanoparticulate delivery system to overcome drug resistance in osteosarcoma. PLoS One 2010;5:e10764.
[17] de Martimprey H, Bertrand JR, Malvy C, Couvreur P, Vauthier C. New core-shell nanoparticules for the intravenous delivery of siRNA to experimental thyroid papillary carcinoma. Pharm Res 2010;27:498–509.
[18] Yang XZ, Dou S, Sun TM, Mao CQ, Wang HX, Wang J. Systemic delivery of siRNA with cationic lipid assisted PEG-PLA nanoparticles for cancer therapy. J Control Release 2011;156:203–11.
[19] Huh MS, Lee SY, Park S, Lee S, Chung H, Choi Y, et al. Tumor-homing glycol chitosan/polyethylenimine nanoparticles for the systemic delivery of siRNA in tumor-bearing mice. J Control Release 2010;144:134–43.
[20] Abbasi S, Paul A, Prakash S. Investigation of siRNA-loaded polyethylenimine-coated human serum albumin nanoparticle complexes for the treatment of breast cancer. Cell Biochem Biophys 2011;61:277–87.
[21] Palanca-Wessels MC, Convertine AJ, Cutler-Strom R, Booth GC, Lee F, Berguig GY, et al. Anti-CD22 antibody targeting of pH-responsive micelles enhances small interfering RNA delivery and gene silencing in lymphoma cells. Mol Ther 2011;19:1529–37.
[22] Kim HJ, Oba M, Pittella F, Nomoto T, Cabral H, Matsumoto Y, et al. PEG-detachable cationic polyaspartamide derivatives bearing stearoyl moieties for systemic siRNA delivery toward subcutaneous BxPC3 pancreatic tumor. J Drug Target 2012;20:33–42.
[23] Xiong XB, Lavasanifar A. Traceable multifunctional micellar nanocarriers for cancer-targeted co-delivery of MDR-1 siRNA and doxorubicin. ACS Nano 2011;5:5202–13.
[24] Hillaireau H, Couvreur P. Nanocarriers' entry into the cell: relevance to drug delivery. Cell Mol Life Sci 2009;66:2873–96.
[25] Guo J, Cheng WP, Gu J, Ding C, Qu X, Yang Z, et al. Systemic delivery of therapeutic small interfering RNA using a pH-triggered amphiphilic poly-l-lysine nanocarrier to suppress prostate cancer growth in mice. Eur J Pharm Sci 2011.
[26] Sakurai Y, Hatakeyama H, Sato Y, Akita H, Takayama K, Kobayashi S, et al. Endosomal escape and the knockdown efficiency of liposomal-siRNA by the fusogenic peptide shGALA. Biomaterials 2011;32:5733–42.
[27] Shim G, Han SE, Yu YH, Lee S, Lee HY, Kim K, et al. Trilysinoyl oleylamide-based cationic liposomes for systemic co-delivery of siRNA and an anti-cancer drug. J Control Release 2011;155:60–6.
[28] Sun TM, Du JZ, Yao YD, Mao CQ, Dou S, Huang SY, et al. Simultaneous delivery of siRNA and paclitaxel via a "two-in-one" micelleplex promotes synergistic tumor suppression. ACS Nano 2011;5:1483–94.
[29] Tietze N, Pelisek J, Philipp A, Roedl W, Merdan T, Tarcha P, et al. Induction of apoptosis in murine neuroblastoma by systemic delivery of transferrin-shielded siRNA polyplexes for downregulation of Ran. Oligonucleotides 2008;18:161–74.
[30] Wang XL, Xu R, Wu X, Gillespie D, Jensen R, Lu ZR. Targeted systemic delivery of a therapeutic siRNA with a multifunctional carrier controls tumor proliferation in mice. Mol Pharm 2009;6:738–46.
[31] Han HD, Mangala LS, Lee JW, Shahzad MM, Kim HS, Shen D, et al. Targeted gene silencing using RGD-labeled chitosan nanoparticles. Clin Cancer Res 2010;16:3910–22.
[32] Meier R, Henning TD, Boddington S, Tavri S, Arora S, Piontek G, et al. Breast cancers: MR imaging of folate-receptor expression with the folate-specific nanoparticle P1133. Radiology 2010;255:527–35.
[33] Varkouhi AK, Scholte M, Storm G, Haisma HJ. Endosomal escape pathways for delivery of biologicals. J Control Release 2011;151:220–8.
[34] Wasungu L, Hoekstra D. Cationic lipids, lipoplexes and intracellular delivery of genes. J Control Release 2006;116:255–64.
[35] Wang XL, Ramusovic S, Nguyen T, Lu ZR. Novel polymerizable surfactants with pH-sensitive amphiphilicity and cell membrane disruption for efficient siRNA delivery. Bioconjug Chem 2007;18:2169–77.
[36] Felber AE, Castagner B, Elsabahy M, Deleavey GF, Damha MJ, Leroux JC. siRNA nanocarriers based on methacrylic acid copolymers. J Control Release 2011;152:159–67.
[37] Yessine MA, Lafleur M, Meier C, Petereit HU, Leroux JC. Characterization of the membrane-destabilizing properties of different pH-sensitive methacrylic acid copolymers. Biochim Biophys Acta 2003;1613:28–38.
[38] Morille M, Passirani C, Vonarbourg A, Clavreul A, Benoit JP. Progress in developing cationic vectors for non-viral systemic gene therapy against cancer. Biomaterials 2008;29:3477–96.
[39] Jiang J, Yang SJ, Wang JC, Yang LJ, Xu ZZ, Yang T, et al. Sequential treatment of drug-resistant tumors with RGD-modified liposomes containing siRNA or doxorubicin. Eur J Pharm Biopharm 2010;76:170–8.
[40] Cardarelli F, Pozzi D, Bifone A, Marchini C, Caracciolo G. Cholesterol-dependent macropinocytosis and endosomal escape control the transfection efficiency of lipoplexes in CHO living cells. Mol Pharm 2012.
[41] Fang N, Wang J, Mao H-Q, Leong KW, Chan V. BHEM-Chol/DOPE liposome induced perturbation of phospholipid bilayer. Colloids Surf B Biointerfaces 2003;29:233–45.
[42] Miyata K, Oba M, Nakanishi M, Fukushima S, Yamasaki Y, Koyama H, et al. Polyplexes from poly(aspartamide) bearing 1,2-diaminoethane side chains induce pH-selective, endosomal membrane destabilization with amplified transfection and negligible cytotoxicity. J Am Chem Soc 2008;130:16287–94.
[43] Canine BF, Wang Y, Ouyang W, Hatefi A. Development of targeted recombinant polymers that can deliver siRNA to the cytoplasm and plasmid DNA to the cell nucleus. J Control Release 2011;151:95–101.
[44] Kawakami S, Hashida M. Targeted delivery systems of small interfering RNA by systemic administration. Drug Metab Pharmacokinet 2007;22:142–51.
[45] White PJ. Barriers to successful delivery of short interfering RNA after systemic administration. Clin Exp Pharmacol Physiol 2008;35:1371–6.
[46] Grzelinski M, Urban-Klein B, Martens T, Lamszus K, Bakowsky U, Hobel S, et al. RNA interference-mediated gene silencing of pleiotrophin through polyethylenimine-complexed small interfering RNAs in vivo exerts antitumoral effects in glioblastoma xenografts. Hum Gene Ther 2006;17:751–66.
[47] Hobel S, Koburger I, John M, Czubayko F, Hadwiger P, Vornlocher HP, et al. Polyethylenimine/small interfering RNA-mediated knockdown of vascular endothelial growth factor in vivo exerts anti-tumor effects synergistically with bevacizumab. J Gene Med 2010;12:287–300.
[48] Mu P, Nagahara S, Makita N, Tarumi Y, Kadomatsu K, Takei Y. Systemic delivery of siRNA specific to tumor mediated by atelocollagen: combined therapy using siRNA targeting Bcl-xL and cisplatin against prostate cancer. Int J Cancer 2009;125:2978–90.

[49] Werth S, Urban-Klein B, Dai L, Hobel S, Grzelinski M, Bakowsky U, et al. A low molecular weight fraction of polyethylenimine (PEI) displays increased transfection efficiency of DNA and siRNA in fresh or lyophilized complexes. J Control Release 2006;112:257–70.
[50] Montazeri Aliabadi H, Landry B, Mahdipoor P, Uludag H. Induction of apoptosis by survivin silencing through siRNA delivery in a human breast cancer cell line. Mol Pharm 2011;8:1821–30.
[51] Crombez L, Morris MC, Dufort S, Aldrian-Herrada G, Nguyen Q, Mc Master G, et al. Targeting cyclin B1 through peptide-based delivery of siRNA prevents tumour growth. Nucleic Acids Res 2009;37:4559–69.
[52] Takenaka S, Naka N, Araki N, Hashimoto N, Ueda T, Yoshioka K, et al. Downregulation of SS18-SSX1 expression in synovial sarcoma by small interfering RNA enhances the focal adhesion pathway and inhibits anchorage-independent growth in vitro and tumor growth in vivo. Int J Oncol 2010;36:823–31.
[53] Yagi N, Manabe I, Tottori T, Ishihara A, Ogata F, Kim JH, et al. A nanoparticle system specifically designed to deliver short interfering RNA inhibits tumor growth in vivo. Cancer Res 2009;69:6531–8.
[54] Wu SY, Putral LN, Liang M, Chang HI, Davies NM, McMillan NA. Development of a novel method for formulating stable siRNA-loaded lipid particles for in vivo use. Pharm Res 2009;26:512–22.
[55] Sonoke S, Ueda T, Fujiwara K, Sato Y, Takagaki K, Hirabayashi K, et al. Tumor regression in mice by delivery of Bcl-2 small interfering RNA with pegylated cationic liposomes. Cancer Res 2008;68:8843–51.
[56] Bartlett DW, Davis ME. Physicochemical and biological characterization of targeted, nucleic acid-containing nanoparticles. Bioconjug Chem 2007;18: 456–68.
[57] Tanaka T, Mangala LS, Vivas-Mejia PE, Nieves-Alicea R, Mann AP, Mora E, et al. Sustained small interfering RNA delivery by mesoporous silicon particles. Cancer Res 2010;70:3687–96.
[58] Taratula O, Garbuzenko OB, Kirkpatrick P, Pandya I, Savla R, Pozharov VP, et al. Surface-engineered targeted PPI dendrimer for efficient intracellular and intratumoral siRNA delivery. J Control Release 2009;140:284–93.
[59] Halma C, Daha MR, van Es LA. In vivo clearance by the mononuclear phagocyte system in humans: an overview of methods and their interpretation. Clin Exp Immunol 1992;89:1–7.
[60] Meerasa A, Huang JG, Gu FX. CH(50): a revisited hemolytic complement consumption assay for evaluation of nanoparticles and blood plasma protein interaction. Curr Drug Deliv 2011;8:290–8.
[61] Boraschi D, Costantino L, Italiani P. Interaction of nanoparticles with immunocompetent cells: nanosafety considerations. Nanomedicine (Lond) 2012;7:121–31.
[62] Vonarbourg A, Saulnier P, Passirani C, Benoit JP. Electrokinetic properties of noncharged lipid nanocapsules: influence of the dipolar distribution at the interface. Electrophoresis 2005;26:2066–75.
[63] Mao CQ, Du JZ, Sun TM, Yao YD, Zhang PZ, Song EW, et al. A biodegradable amphiphilic and cationic triblock copolymer for the delivery of siRNA targeting the acid ceramidase gene for cancer therapy. Biomaterials 2011;32: 3124–33.
[64] Chen Y, Zhu X, Zhang X, Liu B, Huang L. Nanoparticles modified with tumor-targeting scFv deliver siRNA and miRNA for cancer therapy. Mol Ther 2010;18:1650–6.
[65] Chen Y, Wu JJ, Huang L. Nanoparticles targeted with NGR motif deliver c-myc siRNA and doxorubicin for anticancer therapy. Mol Ther 2010;18:828–34.
[66] Maeda H, Wu J, Sawa T, Matsumura Y, Hori K. Tumor vascular permeability and the EPR effect in macromolecular therapeutics: a review. J Control Release 2000;65:271–84.
[67] Halder J, Kamat AA, Landen Jr CN, Han LY, Lutgendorf SK, Lin YG, et al. Focal adhesion kinase targeting using in vivo short interfering RNA delivery in neutral liposomes for ovarian carcinoma therapy. Clin Cancer Res 2006;12: 4916–24.
[68] Chen Y, Bathula SR, Li J, Huang L. Multifunctional nanoparticles delivering small interfering RNA and doxorubicin overcome drug resistance in cancer. J Biol Chem 2010;285:22639–50.
[69] Kaestner P, Aigner A, Bastians H. Therapeutic targeting of the mitotic spindle checkpoint through nanoparticle-mediated siRNA delivery inhibits tumor growth in vivo. Cancer Lett 2011;304:128–36.
[70] Hu-Lieskovan S, Heidel JD, Bartlett DW, Davis ME, Triche TJ. Sequence-specific knockdown of EWS-FLI1 by targeted, nonviral delivery of small interfering RNA inhibits tumor growth in a murine model of metastatic Ewing's sarcoma. Cancer Res 2005;65:8984–92.
[71] Pasqualini R, Koivunen E, Ruoslahti E. Alpha v integrins as receptors for tumor targeting by circulating ligands. Nat Biotechnol 1997;15:542–6.
[72] Corti A, Curnis F, Arap W, Pasqualini R. The neovasculature homing motif NGR: more than meets the eye. Blood 2008;112:2628–35.
[73] Hashida H, Takabayashi A, Kanai M, Adachi M, Kondo K, Kohno N, et al. Aminopeptidase N is involved in cell motility and angiogenesis: its clinical significance in human colon cancer. Gastroenterology 2002;122: 376–86.
[74] Oku N, Asai T, Watanabe K, Kuromi K, Nagatsuka M, Kurohane K, et al. Anti-neovascular therapy using novel peptides homing to angiogenic vessels. Oncogene 2002;21:2662–9.
[75] Maeda N, Takeuchi Y, Takada M, Namba Y, Oku N. Synthesis of angiogenesis-targeted peptide and hydrophobized polyethylene glycol conjugate. Bioorg Med Chem Lett 2004;14:1015–7.
[76] Asai T, Matsushita S, Kenjo E, Tsuzuku T, Yonenaga N, Koide H, et al. Dicetyl phosphate-tetraethylenepentamine-based liposomes for systemic siRNA delivery. Bioconjug Chem 2011;22:429–35.
[77] Harrison GS, Wierman ME, Nett TM, Glode LM. Gonadotropin-releasing hormone and its receptor in normal and malignant cells. Endocr Relat Cancer 2004;11:725–48.
[78] Liu SV, Liu S, Pinski J. Luteinizing hormone-releasing hormone receptor targeted agents for prostate cancer. Expert Opin Investig Drugs 2011;20: 769–78.
[79] Jaracz S, Chen J, Kuznetsova LV, Ojima I. Recent advances in tumor-targeting anticancer drug conjugates. Bioorg Med Chem 2005;13:5043–54.
[80] Toole BP, Hascall VC. Hyaluronan and tumor growth. Am J Pathol 2002;161: 745–7.
[81] Toole BP. Hyaluronan promotes the malignant phenotype. Glycobiology 2002;12:37R–42R.
[82] Toole BP. Hyaluronan-CD44 interactions in cancer: paradoxes and possibilities. Clin Cancer Res 2009;15:7462–8.
[83] Daniels TR, Delgado T, Helguera G, Penichet ML. The transferrin receptor part II: targeted delivery of therapeutic agents into cancer cells. Clin Immunol 2006;121:159–76.
[84] Daniels TR, Delgado T, Rodriguez JA, Helguera G, Penichet ML. The transferrin receptor part I: biology and targeting with cytotoxic antibodies for the treatment of cancer. Clin Immunol 2006;121:144–58.
[85] Pirollo KF, Zon G, Rait A, Zhou Q, Yu W, Hogrefe R, et al. Tumor-targeting nanoimmunoliposome complex for short interfering RNA delivery. Hum Gene Ther 2006;17:117–24.
[86] Hartwell LH, Weinert TA. Checkpoints: controls that ensure the order of cell cycle events. Science 1989;246:629–34.
[87] Donjerkovic D, Scott DW. Regulation of the G1 phase of the mammalian cell cycle. Cell Res 2000;10:1–16.
[88] Nozoe T, Korenaga D, Kabashima A, Ohga T, Saeki H, Sugimachi K. Significance of cyclin B1 expression as an independent prognostic indicator of patients with squamous cell carcinoma of the esophagus. Clin Cancer Res 2002;8:817–22.
[89] Soria JC, Jang SJ, Khuri FR, Hassan K, Liu D, Hong WK, et al. Overexpression of cyclin B1 in early-stage non-small cell lung cancer and its clinical implication. Cancer Res 2000;60:4000–4.
[90] Ikuerowo SO, Kuczyk MA, Mengel M, van der Heyde E, Shittu OB, Vaske B, et al. Alteration of subcellular and cellular expression patterns of cyclin B1 in renal cell carcinoma is significantly related to clinical progression and survival of patients. Int J Cancer 2006;119:867–74.
[91] Kallakury BV, Sheehan CE, Rhee SJ, Fisher HA, Kaufman Jr RP, Rifkin MD, et al. The prognostic significance of proliferation-associated nucleolar protein p120 expression in prostate adenocarcinoma: a comparison with cyclins A and B1, Ki-67, proliferating cell nuclear antigen, and p34cdc2. Cancer 1999;85:1569–76.
[92] Strebhardt K, Ullrich A. Targeting polo-like kinase 1 for cancer therapy. Nat Rev Cancer 2006;6:321–30.
[93] Kneisel L, Strebhardt K, Bernd A, Wolter M, Binder A, Kaufmann R. Expression of polo-like kinase (PLK1) in thin melanomas: a novel marker of metastatic disease. J Cutan Pathol 2002;29:354–8.
[94] Wolf G, Elez R, Doermer A, Holtrich U, Ackermann H, Stutte HJ, et al. Prognostic significance of polo-like kinase (PLK) expression in non-small cell lung cancer. Oncogene 1997;14:543–9.
[95] Takahashi T, Sano B, Nagata T, Kato H, Sugiyama Y, Kunieda K, et al. Polo-like kinase 1 (PLK1) is overexpressed in primary colorectal cancers. Cancer Sci 2003;94:148–52.
[96] Wolf G, Hildenbrand R, Schwar C, Grobholz R, Kaufmann M, Stutte HJ, et al. Polo-like kinase: a novel marker of proliferation: correlation with estrogen-receptor expression in human breast cancer. Pathol Res Pract 2000;196: 753–9.
[97] Reagan-Shaw S, Ahmad N. Silencing of polo-like kinase (Plk) 1 via siRNA causes induction of apoptosis and impairment of mitosis machinery in human prostate cancer cells: implications for the treatment of prostate cancer. FASEB J 2005;19:611–3.
[98] Gumireddy K, Reddy MV, Cosenza SC, Boominathan R, Baker SJ, Papathi N, et al. ON01910, a non-ATP-competitive small molecule inhibitor of Plk1, is a potent anticancer agent. Cancer Cell. 2005;7:275–86.
[99] Cleveland DW, Mao Y, Sullivan KF. Centromeres and kinetochores: from epigenetics to mitotic checkpoint signaling. Cell 2003;112:407–21.
[100] Mapelli M, Massimiliano L, Santaguida S, Musacchio A. The Mad2 conformational dimer: structure and implications for the spindle assembly checkpoint. Cell 2007;131:730–43.
[101] Zhang SH, Xu AM, Chen XF, Li DH, Sun MP, Wang YJ. Clinicopathologic significance of mitotic arrest defective protein 2 overexpression in hepatocellular carcinoma. Hum Pathol 2008;39:1827–34.
[102] Alizadeh AA, Eisen MB, Davis RE, Ma C, Lossos IS, Rosenwald A, et al. Distinct types of diffuse large B-cell lymphoma identified by gene expression profiling. Nature 2000;403:503–11.
[103] Kato T, Daigo Y, Aragaki M, Ishikawa K, Sato M, Kondo S, et al. Over-expression of MAD2 predicts clinical outcome in primary lung cancer patients. Lung Cancer 2011;74:124–31.
[104] Rimkus C, Friederichs J, Rosenberg R, Holzmann B, Siewert JR, Janssen KP. Expression of the mitotic checkpoint gene MAD2L2 has prognostic significance in colon cancer. Int J Cancer 2007;120:207–11.

[105] Yu L, Guo WC, Zhao SH, Tang J, Chen JL. Mitotic arrest defective protein 2 expression abnormality and its clinicopathologic significance in human osteosarcoma. APMIS 2010;118:222–9.
[106] Johnson GL, Lapadat R. Mitogen-activated protein kinase pathways mediated by ERK, JNK, and p38 protein kinases. Science 2002;298:1911–2.
[107] Katso R, Okkenhaug K, Ahmadi K, White S, Timms J, Waterfield MD. Cellular function of phosphoinositide 3-kinases: implications for development, homeostasis, and cancer. Annu Rev Cell Dev Biol 2001;17:615–75.
[108] Pasquale EB. Eph receptors and ephrins in cancer: bidirectional signalling and beyond. Nat Rev Cancer 2010;10:165–80.
[109] Mohammed KA, Wang X, Goldberg EP, Antony VB, Nasreen N. Silencing receptor EphA2 induces apoptosis and attenuates tumor growth in malignant mesothelioma. Am J Cancer Res 2011;1:419–31.
[110] Liu Y, Yu C, Qiu Y, Huang D, Zhou X, Zhang X, et al. Downregulation of EphA2 expression suppresses the growth and metastasis in squamous-cell carcinoma of the head and neck in vitro and in vivo. J Cancer Res Clin Oncol 2012;138:195–202.
[111] Rho O, Kim DJ, Kiguchi K, Digiovanni J. Growth factor signaling pathways as targets for prevention of epithelial carcinogenesis. Mol Carcinog 2011;50:264–79.
[112] Pommery N, Henichart JP. Involvement of PI3K/Akt pathway in prostate cancer – potential strategies for developing targeted therapies. Mini Rev Med Chem 2005;5:1125–32.
[113] McCubrey JA, Steelman LS, Abrams SL, Lee JT, Chang F, Bertrand FE, et al. Roles of the RAF/MEK/ERK and PI3K/PTEN/AKT pathways in malignant transformation and drug resistance. Adv Enzyme Regul 2006;46:249–79.
[114] Sasaki T, Nakashiro K, Tanaka H, Azuma K, Goda H, Hara S, et al. Knockdown of Akt isoforms by RNA silencing suppresses the growth of human prostate cancer cells in vitro and in vivo. Biochem Biophys Res Commun 2010;399:79–83.
[115] Mukai H. The structure and function of PKN, a protein kinase having a catalytic domain homologous to that of PKC. J Biochem 2003;133:17–27.
[116] Leenders F, Mopert K, Schmiedeknecht A, Santel A, Czauderna F, Aleku M, et al. PKN3 is required for malignant prostate cell growth downstream of activated PI 3-kinase. EMBO J 2004;23:3303–13.
[117] Aleku M, Schulz P, Keil O, Santel A, Schaeper U, Dieckhoff B, et al. Atu027, a liposomal small interfering RNA formulation targeting protein kinase N3, inhibits cancer progression. Cancer Res 2008;68:9788–98.
[118] Lark AL, Livasy CA, Calvo B, Caskey L, Moore DT, Yang X, et al. Overexpression of focal adhesion kinase in primary colorectal carcinomas and colorectal liver metastases: immunohistochemistry and real-time PCR analyses. Clin Cancer Res 2003;9:215–22.
[119] Theocharis SE, Klijanienko JT, Padoy E, Athanassiou S, Sastre-Garau XX. Focal adhesion kinase (FAK) immunocytochemical expression in breast ductal invasive carcinoma (DIC): correlation with clinicopathological parameters and tumor proliferative capacity. Med Sci Monit 2009;15:BR221–6.
[120] Jones G, Machado Jr J, Merlo A. Loss of focal adhesion kinase (FAK) inhibits epidermal growth factor receptor-dependent migration and induces aggregation of nh(2)-terminal FAK in the nuclei of apoptotic glioblastoma cells. Cancer Res 2001;61:4978–81.
[121] Frisch SM, Vuori K, Kelaita D, Sicks S. A role for Jun-N-terminal kinase in anoikis; suppression by bcl-2 and crmA. J Cell Biol 1996;135:1377–82.
[122] Akasaka T, van Leeuwen RL, Yoshinaga IG, Mihm Jr MC, Byers HR. Focal adhesion kinase (p125FAK) expression correlates with motility of human melanoma cell lines. J Invest Dermatol 1995;105:104–8.
[123] Li S, Hua ZC. FAK expression regulation and therapeutic potential. Adv Cancer Res 2008;101:45–61.
[124] Roberts WG, Ung E, Whalen P, Cooper B, Hulford C, Autry C, et al. Antitumor activity and pharmacology of a selective focal adhesion kinase inhibitor, PF-562,271. Cancer Res 2008;68:1935–44.
[125] Hanahan D, Weinberg RA. Hallmarks of cancer: the next generation. Cell 2011;144:646–74.
[126] Ghobrial IM, Witzig TE, Adjei AA. Targeting apoptosis pathways in cancer therapy. CA Cancer J Clin 2005;55:178–94.
[127] Reed JC. Bcl-2-family proteins and hematologic malignancies: history and future prospects. Blood 2008;111:3322–30.
[128] Shangary S, Johnson DE. Recent advances in the development of anticancer agents targeting cell death inhibitors in the Bcl-2 protein family. Leukemia 2003;17:1470–81.
[129] Le Gouill S, Podar K, Amiot M, Hideshima T, Chauhan D, Ishitsuka K, et al. VEGF induces Mcl-1 up-regulation and protects multiple myeloma cells against apoptosis. Blood 2004;104:2886–92.
[130] Watanabe J, Kushihata F, Honda K, Sugita A, Tateishi N, Mominoki K, et al. Prognostic significance of Bcl-xL in human hepatocellular carcinoma. Surgery 2004;135:604–12.
[131] Miyake H, Hara I, Yamanaka K, Arakawa S, Kamidono S. Synergistic enhancement of resistance to cisplatin in human bladder cancer cells by overexpression of mutant-type p53 and Bcl-2. J Urol 1999;162:2176–81.
[132] Liu R, Page C, Beidler DR, Wicha MS, Nunez G. Overexpression of Bcl-x(L) promotes chemotherapy resistance of mammary tumors in a syngeneic mouse model. Am J Pathol 1999;155:1861–7.
[133] Ito T, Shiraki K, Sugimoto K, Yamanaka T, Fujikawa K, Ito M, et al. Survivin promotes cell proliferation in human hepatocellular carcinoma. Hepatology 2000;31:1080–5.
[134] Choi N, Baumann M, Flentjie M, Kellokumpu-Lehtinen P, Senan S, Zamboglou N, et al. Predictive factors in radiotherapy for non-small cell lung cancer: present status. Lung Cancer 2001;31:43–56.
[135] Sui L, Dong Y, Ohno M, Watanabe Y, Sugimoto K, Tokuda M. Survivin expression and its correlation with cell proliferation and prognosis in epithelial ovarian tumors. Int J Oncol 2002;21:315–20.
[136] Shariat SF, Lotan Y, Saboorian H, Khoddami SM, Roehrborn CG, Slawin KM, et al. Survivin expression is associated with features of biologically aggressive prostate carcinoma. Cancer 2004;100:751–7.
[137] Sasaki T, Lopes MB, Hankins GR, Helm GA. Expression of survivin, an inhibitor of apoptosis protein, in tumors of the nervous system. Acta Neuropathol 2002;104:105–9.
[138] Ai Z, Yin L, Zhou X, Zhu Y, Zhu D, Yu Y, et al. Inhibition of survivin reduces cell proliferation and induces apoptosis in human endometrial cancer. Cancer 2006;107:746–56.
[139] Blanc-Brude OP, Mesri M, Wall NR, Plescia J, Dohi T, Altieri DC. Therapeutic targeting of the survivin pathway in cancer: initiation of mitochondrial apoptosis and suppression of tumor-associated angiogenesis. Clin Cancer Res 2003;9:2683–92.
[140] Ferrara N, Kerbel RS. Angiogenesis as a therapeutic target. Nature 2005;438:967–74.
[141] Ebos JM, Lee CR, Cruz-Munoz W, Bjarnason GA, Christensen JG, Kerbel RS. Accelerated metastasis after short-term treatment with a potent inhibitor of tumor angiogenesis. Cancer Cell 2009;15:232–9.
[142] Paez-Ribes M, Allen E, Hudock J, Takeda T, Okuyama H, Vinals F, et al. Antiangiogenic therapy elicits malignant progression of tumors to increased local invasion and distant metastasis. Cancer Cell. 2009;15:220–31.
[143] Zhan P, Wang J, Lv XJ, Wang Q, Qiu LX, Lin XQ, et al. Prognostic value of vascular endothelial growth factor expression in patients with lung cancer: a systematic review with meta-analysis. J Thorac Oncol 2009;4:1094–103.
[144] Kim SH, Jeong JH, Lee SH, Kim SW, Park TG. Local and systemic delivery of VEGF siRNA using polyelectrolyte complex micelles for effective treatment of cancer. J Control Release 2008;129:107–16.
[145] Schaffner F, Ruf W. Tissue factor and protease-activated receptor signaling in cancer. Semin Thromb Hemost 2008;34:147–53.
[146] Woodfin A, Voisin MB, Nourshargh S. PECAM-1: a multi-functional molecule in inflammation and vascular biology. Arterioscler Thromb Vasc Biol 2007;27:2514–23.
[147] Santel A, Aleku M, Keil O, Endruschat J, Esche V, Durieux B, et al. RNA interference in the mouse vascular endothelium by systemic administration of siRNA-lipoplexes for cancer therapy. Gene Ther 2006;13:1360–70.
[148] Lu C, Bonome T, Li Y, Kamat AA, Han LY, Schmandt R, et al. Gene alterations identified by expression profiling in tumor-associated endothelial cells from invasive ovarian carcinoma. Cancer Res 2007;67:1757–68.
[149] Fuchs B, Mahlum E, Halder C, Maran A, Yaszemski M, Bode B, et al. High expression of tumor endothelial marker 7 is associated with metastasis and poor survival of patients with osteogenic sarcoma. Gene 2007;399:137–43.
[150] Dong JT, Chen C. Essential role of KLF5 transcription factor in cell proliferation and differentiation and its implications for human diseases. Cell Mol Life Sci 2009;66:2691–706.
[151] Rensen WM, Mangiacasale R, Ciciarello M, Lavia P. The GTPase Ran: regulation of cell life and potential roles in cell transformation. Front Biosci 2008;13:4097–121.
[152] Saad AF, Meacham WD, Bai A, Anelli V, Elojeimy S, Mahdy AE, et al. The functional effects of acid ceramidase overexpression in prostate cancer progression and resistance to chemotherapy. Cancer Biol Ther 2007;6:1455–60.
[153] Furuichi Y. Premature aging and predisposition to cancers caused by mutations in RecQ family helicases. Ann N Y Acad Sci 2001;928:121–31.
[154] Futami K, Kumagai E, Makino H, Sato A, Takagi M, Shimamoto A, et al. Anticancer activity of RecQL1 helicase siRNA in mouse xenograft models. Cancer Sci 2008;99:1227–36.
[155] Bradley G, Ling V. P-glycoprotein, multidrug resistance and tumor progression. Cancer Metastasis Rev 1994;13:223–33.
[156] Nikiforov YE. RET/PTC rearrangement in thyroid tumors. Endocr Pathol 2002;13:3–16.
[157] de Martimprey H, Bertrand JR, Fusco A, Santoro M, Couvreur P, Vauthier C, et al. siRNA nanoformulation against the ret/PTC1 junction oncogene is efficient in an in vivo model of papillary thyroid carcinoma. Nucleic Acids Res 2008;36(1):e2.
[158] Erkizan HV, Uversky VN, Toretsky JA. Oncogenic partnerships: EWS-FLI1 protein interactions initiate key pathways of Ewing's sarcoma. Clin Cancer Res 2010;16:4077–83.
[159] Toub N, Bertrand JR, Tamaddon A, Elhamess H, Hillaireau H, Maksimenko A, et al. Efficacy of siRNA nanocapsules targeted against the EWS-Fli1 oncogene in Ewing sarcoma. Pharm Res 2006;23:892–900.
[160] Smith S, Reeves BR, Wong L, Fisher C. A consistent chromosome translocation in synovial sarcoma. Cancer Genet Cytogenet 1987;26:179–80.
[161] O'Brien S, Moore JO, Boyd TE, Larratt LM, Skotnicki AB, Koziner B, et al. 5-Year survival in patients with relapsed or refractory chronic lymphocytic leukemia in a randomized, phase III trial of fludarabine plus cyclophosphamide with or without oblimersen. J Clin Oncol 2009;27:5208–12.

[162] Heidel JD, Liu JY, Yen Y, Zhou B, Heale BS, Rossi JJ, et al. Potent siRNA inhibitors of ribonucleotide reductase subunit RRM2 reduce cell proliferation in vitro and in vivo. Clin Cancer Res 2007;13:2207–15.
[163] Heidel JD. Linear cyclodextrin-containing polymers and their use as delivery agents. Expert Opin Drug Deliv 2006;3:641–6.
[164] Davis ME, Zuckerman JE, Choi CH, Seligson D, Tolcher A, Alabi CA, et al. Evidence of RNAi in humans from systemically administered siRNA via targeted nanoparticles. Nature 2010;464:1067–70.
[165] Strumberg D, Schultheis B, Traugott U, Vank C, Santel A, Keil O, et al. Phase I clinical development of Atu027, a siRNA formulation targeting PKN3 in patients with advanced solid tumors. Int J Clin Pharmacol Ther 2012;50:76–8.
[166] Folkman J, Kalluri R. Cancer without disease. Nature 2004;427:787.
[167] Kudo Y, Siriwardena BS, Hatano H, Ogawa I, Takata T. Periostin: novel diagnostic and therapeutic target for cancer. Histol Histopathol 2007;22:1167–74.
[168] Villares GJ, Zigler M, Blehm K, Bogdan C, McConkey D, Colin D, et al. Targeting EGFR in bladder cancer. World J Urol 2007;25:573–9.

CHAPITRE I

DÉVELOPPEMENT ET CARACTÉRISATION DES NANOCAPSULES LIPIDIQUES CHARGÉES EN siRNA

CHAPITRE I: DÉVELOPPEMENT ET CARACTÉRISATION DES NANOCAPSULES LIPIDIQUES CHARGÉES EN siRNA

L'utilisation des siRNA en thérapeutique apparaît comme une alternative de plus en plus intéressante afin de modifier l'expression de protéines impliquées dans des processus pathologiques. Pour cela, leur encapsulation au sein d'un nanovecteur est indispensable du fait, premièrement, de la présence de nucléases dans le plasma, et, deuxièmement, du caractère hydrophile des siRNA empêchant leur passage à travers les membranes plasmiques. Le développement des nanocapsules lipidiques offre donc la possibilité de i) protéger le principe actif, ii) favoriser son accumulation au sein de la tumeur ainsi que iii) être internalisé dans les cellules tumorales. Des travaux de thèses antérieurs se sont focalisés sur l'ADN et l'encapsulation de plasmide, démontrant ainsi le potentiel des LNC à encapsuler ces molécules par l'utilisation de lipides cationiques. Cependant, si les siRNA restent des acides nucléiques, la formulation développée pour l'ADN appliquée telle quelle à ces derniers n'a pas montré de résultats satisfaisants. Ce premier chapitre développe donc les différents travaux de formulation galénique effectués sur les nanocapsules lipidiques qui nous ont permis d'obtenir une encapsulation du siRNA au sein d'une nanomédecine stable.

La première publication fait état du procédé de formulation et de son adaptation nécessaire pour encapsuler efficacement les siRNA. Ces travaux se focalisent également sur l'utilisation de différents lipides ainsi que sur la mise au point d'une méthode de dosage du siRNA au spectrophotomètre UV.

Les études de stabilité ainsi que d'optimisation du procédé se retrouvent dans la publication n°2. L'objectif de ces nouveaux travaux a été d'expliciter la structure des LNC siRNA ainsi que d'améliorer le rendement, en faisant varier les différents constituants. Une caractérisation par microscopie électronique à transmission cryogénique (Cryo-TEM) a permis de visualiser ces objets et valider une méthode de purification efficace des LNC siRNA.

Enfin, la dernière partie de ce chapitre présente les formulations nous ayant permis d'améliorer significativement la stabilité de ces nano-objets et ayant fait l'objet d'une demande de brevet.

Ces travaux ont fait l'objet de deux publications acceptées, la première dans European Journal of Pharmaceutics and Biopharmaceutics en 2012 et la seconde sous presse dans Biotechnology Journal en 2014.

PUBLICATION N°1: siRNA LNCs – A NOVEL PLATFORM OF LIPID NANOCAPSULES FOR SYSTEMIC siRNA ADMINISTRATION

European Journal of Pharmaceutics and Biopharmaceutics 81 (2012) 448–452

Contents lists available at SciVerse ScienceDirect

European Journal of Pharmaceutics and Biopharmaceutics

journal homepage: www.elsevier.com/locate/ejpb

Note

siRNA LNCs – A novel platform of lipid nanocapsules for systemic siRNA administration

Stephanie David [a,b,c], Pauline Resnier [a,b], Alexis Guillot [a,b], Bruno Pitard [c], Jean-Pierre Benoit [a,b], Catherine Passirani [a,b,*]

[a] LUNAM Université, Université d'Angers, Angers, France
[b] INSERM U1066 MINT, Micro et Nanomedecines biomimétiques, Angers, France
[c] INSERM, UMR915, Université de Nantes, Nantes, France

ARTICLE INFO

Article history:
Received 24 November 2011
Accepted in revised form 13 February 2012
Available online 21 February 2012

Keywords:
Nanocarrier
Lipoplexes
Formulation
siRNA quantification
Cationic lipids
Systemic administration

ABSTRACT

Several siRNA (small interfering RNA) therapeutics are undergoing clinical trials for cancer, respiratory diseases or macular degeneration, but most are administrated locally. In order to overcome the different barriers to attain an efficient siRNA action after systemic administration, nanocarriers able to carry and protect siRNA are awaited. With this aim, we developed a new platform of siRNA lipid nanocapsules (LNCs) using different cationic lipids, combining the properties of LNCs (siRNA protection and targeting) and lipoplexes (efficient siRNA delivery into the cell). The formulation was revealed to contain different compartments. A siRNA quantification method based on UV spectroscopy was developed to locate and quantify siRNA in each compartment. All in all, these novel siRNA LNCs presented sizes of about 55 nm with a neutral surface charge and siRNA encapsulation efficiencies up to 65% representing appropriate characteristics for systemic administration.

1. Introduction

siRNA is rapidly broken down by nucleases and other blood components after intravenous administration. Moreover, between the administration and action site, different barriers have to be overcome. Therefore, different siRNA modifications and siRNA vectors have already been described in the literature, with a view to finding the "ideal" vector [1].

Lipid nanocapsules (LNCs), consisting of a lipid liquid core of triglycerides and a rigid shell of lecithin and polyethylene glycol, were developed in our laboratory [2]. The simple formulation process is based on phase inversions of an emulsion. These LNCs were recently modified to encapsulate DNA, complexed with cationic lipids, forming lipoplexes. These DNA LNCs were efficient for *in vitro* and *in vivo* transfection [3–5] in contrast to lipoplexes that were only efficient *in vitro*.

The association between LNCs and lipoplexes should combine LNC properties (nucleic acid protection, prolonged circulation time, possibility of active or passive targeting) with lipoplex properties (internalisation in cells, permitting nucleic acid action). With this in mind, the objective of this work was to develop siRNA LNCs allowing efficient systemic siRNA administration. In this study, various ratios of different cationic lipids were used to formulate siRNA LNCs, and the size, charge and payload characteristics of these novel promising nanocarriers were assessed.

2. Materials and methods

2.1. siRNA LNC formulation

Basic lipid nanocapsules (LNCs) were formulated, as described before [2], by mixing 20% w/w Labrafac WL 1349 (caprylic-capric acid triglycerides, Gatefossé SA, Saint-Priest, France), 1.5% w/w Lipoid S75-3 (Lipoid GmbH, Ludwigshafen, Germany), 17% w/w Solutol HS 15 (BASF, Ludwigshafen, Germany), 1.8% w/w NaCl (Prolabo, Fontenay-sous-Bois, France) and 59.8% w/w water (obtained from a Milli-Q system, Millipore, Paris, France) together under magnetic stirring. Three temperature cycles between 60 and 95 °C were performed to obtain phase inversions of the emulsion obtained after mixing all the components. Then, a rapid cooling and dilution with ice-cooled water (1:1.4) at the phase inversion temperature (PIT) led to LNC formation.

To obtain siRNA LNCs, the water in the last step was replaced by lipoplexes which were prepared by adding equal volumes of siRNA (here a model siRNA targeted against PCSK9, (sense sequence: GGAAGAUCAUAAUGGACAGdTdT) Eurogenetec, Seraing, Belgium) and liposomes in a defined charge ratio of cationic lipid charge

* Corresponding author. Inserm U646, Université d'Angers, IBS-CHU, 4 rue Larrey, 49933 Angers Cedex 9, France. Tel.: +33 244 688534; fax: +33 244 688546.
E-mail address: catherine.passirani@univ-angers.fr (C. Passirani).

0939-6411/$ - see front matter © 2012 Elsevier B.V. All rights reserved.
doi:10.1016/j.ejpb.2012.02.010

versus anionic siRNA charge. NaCl was added during preparation to obtain a final concentration of 0.15 M.

For liposome preparation, a cationic lipid DOSP (dioleylamine-succinyl paromomycin) (synthesis previously described in [6]), bis(guanidinium)-tris(2-aminoethyl)amine-cholesterol (BGTC) (synthesis previously described in [7]) or DOTAP (1.2-dioleyl-3-trimethylammoniumpropane) (Avanti® Polar Lipids Inc., Alabaster, AL, USA), solubilised in chloroform, was weighted in the ratio 1/1 (M/M), 3/2 (M/M) or 1/1 (M/M), respectively, with the neutral lipid 1.2-dioleyl-sn-glycero-3-phosphoethanolamine (DOPE) (Avanti® Polar Lipids Inc., Alabaster, AL, USA) to obtain a final concentration of 20 mM of cationic lipid charge, considering the number of lipid charges per molecule (4 for DOSP, 2 for BGTC and 1 for DOTAP). After chloroform evaporation under vacuum, deionised water was added to hydrate the lipid film overnight at 4 °C which was sonicated the next day.

DOSP micelles were prepared in the same way without the addition of DOPE.

3. Characterisation

3.1. Size and zeta potential measurements

Size and zeta potential of siRNA LNCs were measured using a Malvern Zetasizer® (Nano Series ZS, Malvern Instruments SA, Worcestershire, UK) at 25 °C, in triplicate, after dilution in a ratio of 1:100 with deionised water.

3.2. Agarose gel electrophoresis

To verify siRNA encapsulation in LNC, Triton® X100 (Sigma, Saint-Quentin Fallavier, France) was added to destroy LNCs. Samples were mixed with OrangeBlue loading dye (Promega, Madison, WI, USA) before deposition on 1% agarose gel containing ethidium bromide (Sigma, Saint-Quentin Fallavier, France) and migration at 100 V for 30 min.

3.3. siRNA LNC purification

Five hundred microlitre of siRNA LNC formulation was deposited on a 1.5 × 40 cm Sepharose CL-4B column and were eluted with HEPES buffer (pH 7.4). Fractions of 500 µl or 1 ml were collected in glass tubes for further analysis; 100 µl of each fraction was used for turbidity measurements and analysed at 580 nm. PEG (polyethylene glycol) was quantified using 20 µl of each fraction, which was mixed with 5 µl KI/I_2 and 180 µl H_2O milli-Q before analysing at 492 nm using a Multiskan Ascent microplate reader (Thermo Fisher Scientific Cergy-Pontoise, France). Size and zeta potential measurements were taken as described above, and siRNA was evidenced using gel electrophoresis experiments.

3.4. siRNA quantification

One volume of the formulation was mixed with three volumes water (obtained from a Milli-Q-plus® system, Millipore, Paris, France), six volumes 1 M NaOH and two volumes chloroform, vortexed and immediately centrifuged for 15 min at 20,000 g and 4 °C. The aqueous phase, containing free siRNA and siRNA liberated from lipoplexes outside LNCs, was removed and analysed with a UV spectrophotometer (UVIKON 922, Kontron Instruments, Munich, Germany) at 260 nm. The volume removed for free siRNA quantification was replaced by ethanol. Then two volumes water and 10 volumes NaOH 1 M were added before vortexing and centrifuged a second time for 15 min at 20,000 g and 4 °C. The aqueous phase, containing the liberated siRNA from lipoplexes inside siRNA LNCs, was removed and analysed as previously mentioned at 260 nm. To analyse free and encapsulated siRNA quantity in siRNA LNCs, the same procedure was used using two volumes of formulation and replacing water by 1 M NaOH. The first aqueous phase contained free siRNA; the second aqueous phase contained siRNA encapsulated in siRNA LNCs. The siRNA quantity was calculated using a calibrating curve with different siRNA concentrations and compared to the total siRNA amount encapsulated in theory in siRNA LNCs. All samples were prepared in duplicate.

Table 1
Characteristics of siRNA lipoplexes used for siRNA LNC formulations.

Electrophoresis experiments	Lipid	CR	Mean diameter (nm)	Zone
	DOSP	2	1818	B
		2.5	1423	B
		3	1858	B
		4	1122	B
		5	605	C
	DOSP/DOPE	2	2229	B
		2.5	2026	B
		5	234	C
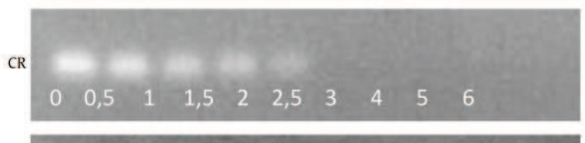	BGTC/DOPE	2.5	1314	B
		3	770	B
		4	344	C
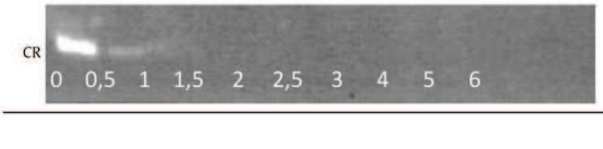	DOTAP/DOPE	2.5	1110	B
		5	680	C

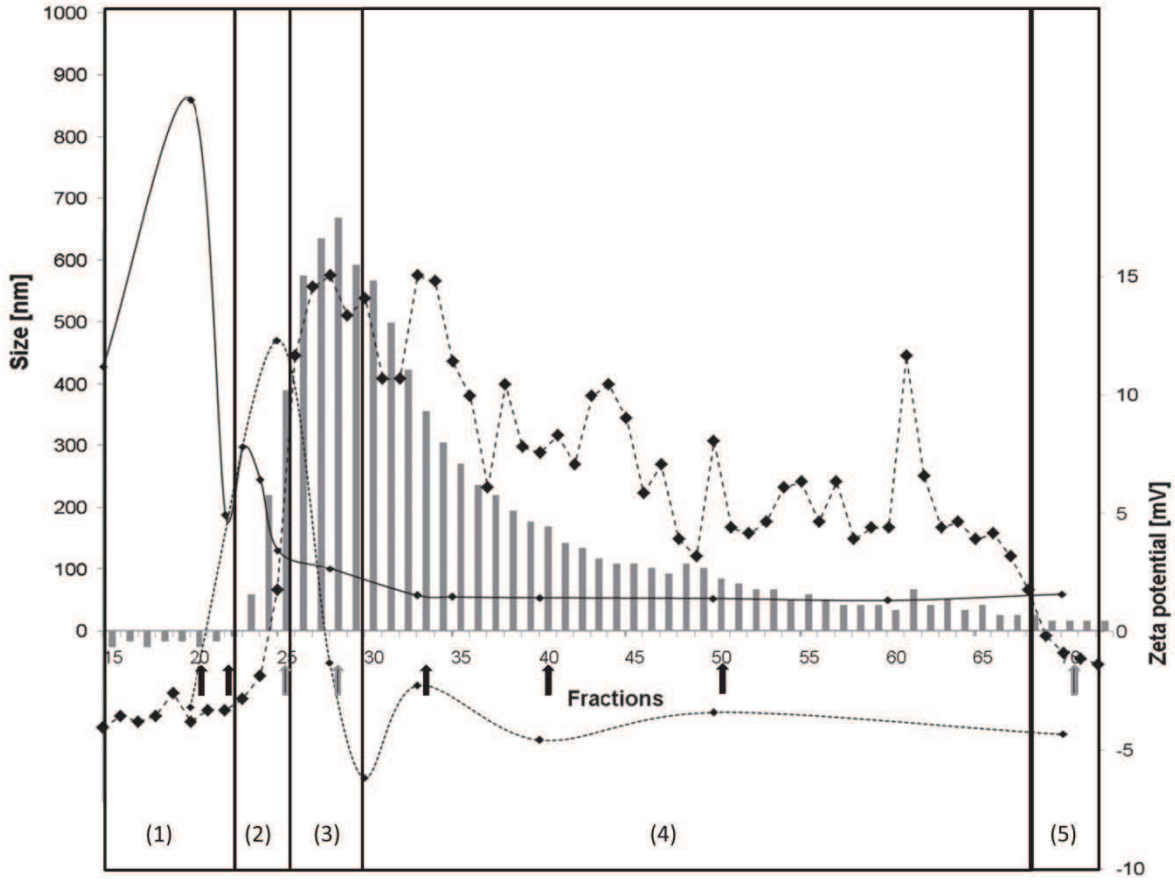

	(1) lipo	(2) lpx	(3) siLNC	(4) LNC/PEG	(5) siRNA
Size	850 nm	200 - 300 nm	100 nm	50 nm	50 nm
Zeta potential	-	5 – 10 mV	-5 – 5 mV	-5 mV	-5 mV
Turbidity	-	+	+	+	-
PEG	-	-	+	+	-
siRNA	-	+	+	-	+
Conclusion	empty liposomes	Lipoplexes	siRNA LNCs	empty LNCs/ free PEG	free siRNA

Fig. 1. Purification of DOTAP/DOPE/siRNA LNC formulation (CR 2.5) on Sepharose columns.

4. Results and discussion

4.1. Lipoplex characterisation

The colloidal stability of lipoplexes was determined at different charge ratios (CR = cationic lipid charge/siRNA charge (+/−)) for various cationic lipids (DOSP, DOSP/DOPE, BGTC/DOPE and DOTAP/DOPE) using size, fluorescence and electrophoresis analysis (Table 1). In the way as for DNA lipoplexes, three different zones of colloidal stability A, B and C could be determined with specific properties in each zone [8]. In summary, in zone A, the quantity of cationic lipid is not sufficient to complex all nucleic acids, so they are still detectable. In this zone, lipoplexes possess a small size and a negative surface charge. In zone B, all nucleic acids are complexed and are no longer detectable. The surface charge is neutral, which leads to aggregation and an augmented size. This was the case for all lipoplexes tested at CR 2 and 2.5, for DOSP/siRNA lipoplexes at CR 3 and 4 and for BGTC/DOPE/siRNA lipoplexes at CR 3. They presented a size over the arbitrary value of 700 nm and only a slight fluorescence in electrophoresis experiments. In zone C, the quantity of cationic lipids is predominant, and thus, the surface charge is positive leading to repulsion and smaller lipoplexes, which was observed for all lipoplexes tested at the CR 5 and for BGTC/DOPE/siRNA lipoplexes at CR 4. To encapsulate lipoplexes in the

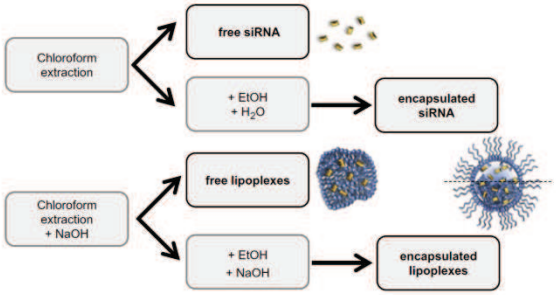

Fig. 2. Schematic representation of siRNA quantification. (For interpretation of the references to colour in this figure legend, the reader is referred to the web version of this article.)

liquid lipid core of LNCs, lipoplexes of zone B and C were chosen as, in zone B, the neutral surface charge, and the aggregation of lipoplexes suggests rather a lipophilic affinity; moreover, DNA lipoplexes of zone C were already encapsulated efficiently in LNCs.

5. siRNA LNC formulation and characterisation

Basic LNCs were developed by Heurtault et al. [2]. Their easy formulation process and their good characterisation make these nanocarriers attractive. To formulate them, the components were mixed together, and temperature cycles around the phase inversion temperature (PIT) were performed. In the last step, a large quantity of water was added at the PIT of the last cycle, resulting in the rapid cooling and dilution of the emulsion and the formation of LNCs. The addition of lipoplexes in the cooling water at the end of the formulation process contributed to siRNA LNC formulation and had the advantage of avoiding their exposure to high temperatures during the formulation.

siRNA encapsulation in LNCs was checked using electrophoresis experiments. As sometimes a low fluorescence band was visible, indicating an incomplete complexation or encapsulation, purification of siRNA LNCs DOTAP/DOPE CR 2.5 was performed on Sepharose columns. This also made it possible to determine whether siRNA was encapsulated in LNCs or simply complexed in lipoplexes. The collected fractions were then analysed by performing size and zeta potential measurements, PEG quantification, turbidity measurements and gel electrophoresis. The final result of these analyses (Fig. 1) suggested the presence of five different compartments in the formulation: (1) empty liposomes, (2) lipoplexes, (3) siRNA LNCs, (4) empty LNCs and (5) free siRNA. In the first compartment, empty liposomes were suspected as no PEG and no siRNAs were found and a size of about 850 nm was measured. In the second compartment, the size diminished, siRNAs were detected, the turbidity augmented and a slightly positive zeta potential was measured, indicating the presence of DOTAP/DOPE lipoplexes (CR 2.5). In the third compartment, PEG and siRNA were detected with a size of about 100 nm, and a near neutral zeta potential was measured, suggesting the presence of siRNA LNCs. In the fourth compartment, PEG but no siRNA was detected, and sizes about 50 nm and a slightly negative zeta potential were measured, indicating empty LNCs and/or free PEG. In the last compartment, no PEG was detected, but siRNAs were found, indicating free siRNA.

According to these results, our hypothesis is that siRNA can be situated in 4 different compartments: in the second compartment in lipoplexes outside LNCs; in the third compartment either (3a) complexed with cationic lipids in LNCs or (3b) associated with other components of the LNC formulation but dissociated from cationic lipids; or in the fifth compartment as free siRNA. To quantify and locate siRNA in the formulation, a quantification method using UV spectrometry analysis at 260 nm was developed (Fig. 2). Free siRNA was quantified using a simple chloroform extraction to separate other constituents of the formulation which interfered during UV spectroscopy analysis. siRNAs in lipoplexes outside LNCs were quantified in the same way, but NaOH was added to dissociate lipoplexes. siRNAs in LNCs were quantified using the "separated" formulations (without free siRNA and/or without lipoplexes) by addition of ethanol, to dissociate LNCs, and NaOH, to dissociate siRNAs from cationic lipids. To determine the siRNA quantity, calibrating curves for the different treatments were performed using siRNA quantities between 0 and the maximal theoretical charge in one volume siRNA LNC formulation (c = 0.25 g/l).

Afterwards, siRNA LNCs were formulated with different cationic lipids, and their size, zeta potential and encapsulation efficiency were determined (Table 2). The basic LNC formulation presented a size of 55 nm with limited distribution indicated by a very low polydispersity index (PDI) of 0.04 and a slightly negative zeta potential of about −5 mV. The zeta potential of formulations prepared by the novel process was comprised between −25 and +25 mV, and the encapsulation efficiencies in LNCs were situated between 4% and 65%. Both varied in relation to the cationic lipids used for lipoplex formation and the CR. The sizes were around 55 nm with a very low PDI with the exception of siRNA LNCs using DOTAP/DOPE/siRNA lipoplexes. Indeed, at CR 2.5, they showed two distinct populations of about 55 and 185 nm, and at CR 5, a size of 125 nm with the highest siRNA encapsulation efficiency at 65%. These lipids and CR were also previously used for DNA encapsula-

Table 2
Size, zeta potential measurements and encapsulation efficiency of siRNA LNC formulations.

LNC formulation		Size (nm)	PDI	Zeta potential (mV)	Encapsulation efficiency (%)					Total siRNA found (%)
Basic LNC formulation		55.5 ± 0.5	0.04 ± 0.01	−5.2 ± 0.5						
LNC siRNA					Compartment 1				siLNC (3a + 3b)	
Cationic lipids	CR [±]				(5) siRNA	(2) Lpx	(3a²) siLNC	(3b³) siLNC		
BGTC/DOPE	2.5	55.3 ± 0.1	0.13 ± 0.03	1.5 ± 0.7	20 ± 0	66 ± 3	3 ± 1	10 ± 4	13 ± 3	108 ± 4
DOSP	2	51.6 ± 0.2	0.07 ± 0.00	−2.4 ± 0.7	2 ± 1	94 ± 5	0	4 ± 6	4 ± 6	107 ± 7
	2.5	60.4 ± 1.0	0.10 ± 0.02	−1,1 ± 0.1	8 ± 9	75 ± 18	13 ± 9	4 ± 1	17 ± 10	117 ± 14
	5	52.8 ± 0.0	0.08 ± 0.00	24.1 ± 1.7 10.1 ± 3.2 −3.7 ± 4.3	20 ± 12	65 ± 13	11 ± 1	3 ± 0	14 ± 1	126 ± 8
DOSP/DOPE	2	53.3 ± 0.2	0,03 ± 0.01	−25.7 ± 1.9	4 ± 1	80 ± 8	8 ± 12	7 ± 2	15 ± 10	75 ± 9
	2.5	59.7 ± 0.5	0.09 ± 0.01	−1.5 ± 0.4	2 ± 2	91 ± 0	2 ± 2	5 ± 0	7 ± 2	88 ± 2
	5	61.4 ± 0.3	0.15 ± 0.03	7.8 ± 0.9	12 ± 4	73 ± 1	11 ± 4	3 ± 0	15 ± 5	105 ± 6
DOTAP/DOPE	2.5	53.5 ± 6.8 184.1 ± 28.4	0.29 ± 0.03	−0.3 ± 0.5	0	73 ± 19	11 ± 16	16 ± 3	27 ± 19	100 ± 5
	5	124.8 ± 0.6	0.24 ± 0.00	1.6 ± 0.3	0	34 ± 1	20 ± 4	45 ± 5	65 ± 2	79 ± 7

tion in DNA LNCs forming efficient nanocarriers for *in vitro* [3] and *in vivo* [4] transfection. The size of DOTAP/DOPE siRNA LNCs (CR 5) was similar to that of other promising siRNA vectors (100–170 nm), with efficient transfection *in vivo* after systemic administration [9]. However, the first siRNA nanocarriers for systemic administration that are in phase I clinical trials (CALAA-01 [10]) have sizes of about 70 nm. This corresponds to siRNA LNC formulations containing the other lipids, but in contrast, they present only half or lower encapsulation efficiencies.

In summary, we developed a new platform of siRNA LNCs showing appropriate characteristics for systemic administration with good encapsulation efficiencies and/or small sizes and neutral surface charges. However, further investigations need now to be carried out to test their transfection efficiency *in vitro* and *in vivo* and to find a compromise between a small size and a high siRNA payload.

References

[1] S. David, B. Pitard, J.P. Benoit, C. Passirani, Non-viral nanosystems for systemic siRNA delivery, Pharmacol. Res. 62 (2010) 100–114.
[2] B. Heurtault, P. Saulnier, B. Pech, J.E. Proust, J.P. Benoit, A novel phase inversion-based process for the preparation of lipid nanocarriers, Pharm. Res. 19 (2002) 875–880.
[3] M. Morille, C. Passirani, E. Letrou-Bonneval, J.P. Benoit, B. Pitard, Galactosylated DNA lipid nanocapsules for efficient hepatocyte targeting, Int. J. Pharm. 379 (2009) 293–300.
[4] M. Morille, C. Passirani, S. Dufort, G. Bastiat, B. Pitard, J.L. Coll, J.P. Benoit, Tumor transfection after systemic injection of DNA lipid nanocapsules, Biomaterials (2010).
[5] A. Vonarbourg, C. Passirani, L. Desigaux, E. Allard, P. Saulnier, O. Lambert, J.P. Benoit, B. Pitard, The encapsulation of DNA molecules within biomimetic lipid nanocapsules, Biomaterials 30 (2009) 3197–3204.
[6] L. Desigaux, M. Sainlos, O. Lambert, R. Chevre, E. Letrou-Bonneval, J.P. Vigneron, P. Lehn, J.M. Lehn, B. Pitard, Self-assembled lamellar complexes of siRNA with lipidic aminoglycoside derivatives promote efficient siRNA delivery and interference, Proc. Natl. Acad. Sci. USA 104 (2007) 16534–16539.
[7] J.P. Vigneron, N. Oudrhiri, M. Fauquet, L. Vergely, J.C. Bradley, M. Basseville, P. Lehn, J.M. Lehn, Guanidinium-cholesterol cationic lipids: efficient vectors for the transfection of eukaryotic cells, Proc. Natl. Acad. Sci. USA 93 (1996) 9682–9686.
[8] B. Pitard, Supramolecular assemblies of DNA delivery systems, Somat. Cell Mol. Genet. 27 (2002) 5–15.
[9] K.P. Mahon, K.T. Love, K.A. Whitehead, J. Qin, A. Akinc, E. Leshchiner, I. Leshchiner, R. Langer, D.G. Anderson, Combinatorial approach to determine functional group effects on lipidoid-mediated siRNA delivery, Bioconjug. Chem. 21 (2010) 1448–1454.
[10] M.E. Davis, J.E. Zuckerman, C.H.J. Choi, D. Seligson, A. Tolcher, C.A. Alabi, Y. Yen, J.D. Heidel, A. Ribas, Evidence of RNAi in humans from systemically administered siRNA via targeted nanoparticles, Nature 464 (2010) 1067–1070.

PUBLICATION N°2:

EFFICIENT *IN VITRO* GENE THERAPY WITH PEG siRNA LIPID NANOCAPSULES FOR PASSIVE TARGETING STRATEGY FOR MELANOMA

PUBLICATION N°2:
EFFICIENT *IN VITRO* GENE THERAPY WITH PEG siRNA LIPID NANOCAPSULES FOR PASSIVE TARGETING STRATEGY FOR MELANOMA

Pauline Resnier[1,2], Pierre LeQuinio[1,2], Nolwenn Lautram[1,2], Emilie André[1,2], Cédric Gaillard[3], Guillaume Bastiat[1,2], Jean-Pierre Benoit[1,2] and Catherine Passirani[1,2*]

[1] PRES LUNAM – Université d'Angers, F-49933 Angers, France

[2] INSERM U1066 – Micro et Nanomédecines Biomimétiques, 4 rue Larrey, F-49933 Angers, France

[3] INRA – UR1268 Biopolymères Interactions Assemblages, B.P. 71627, F-44316 Nantes, Cedex 3, France

* Corresponding author

Pr. Catherine Passirani

INSERM U1066, IBS-IRIS, 4 rue Larrey, F-49933 Angers Cedex 9, France

Tel.: +33 244 688534, Fax: +33 244688 546, E-mail: catherine.passirani@univ-angers.fr

Ces travaux ont fait l'objet d'une publication acceptée actuellement sous presse dans Biotechnology Journal en septembre 2014.

Abbreviation list

AAV: Associated adenoviruses

CMV: Cytomegalovirus

CR: Charge ratio

Cryo-TEM: Cryogenic transmission electron microscopy

DLS: Dynamic light scattering

DOPE: 1,2-dioleoyl-sn-glycero-3-phosphoethanolamine

DOTAP: 1,2-dioleoyl-3- trimethylammoniumpropane

DSPE-PEG2000: 1,2-distearoyl-sn-glycero-3-phosphoethanolamine-N-[methoxy (polyethylene-glycol)-2000

EDOPC: dioleoyl-*sn*-glycerol-3-ethylphosphocholine or *O*-ethyldioleoylphophatidylcholine

EE: Encapsulation efficiency

EtB: Ethidium bromide

LNC: Lipid nanocapsules

MTS: 3-(4,5-dimethylthiazol-2-yl)-5-(3-carboxymethoxyphenyl)-2-(4-sulfophenyl)-2H tetrazolium

NHS: Normal human serum

OD: Optical density

PEG: Polyethylene glycol

PIT: Phase inversion temperature

siRNA: Small interfering RNA

Abstract

SiRNA-mediated gene therapy is a promising strategy to temporarily inhibit the expression of proteins implicated in carcinogenesis or chemotherapy resistance. Although intra-tumoral administration could be envisaged, studies are currently focused on formulating nanomedicines for intravenous injection to target the tumor site as well as metastases. The development of synthetic nanoparticles and liposomes has advanced greatly during the last decade. The objective of this work consists in formulating and optimizing the encapsulation of siRNA into lipid nanocapsules (LNCs) for efficient gene therapy on melanoma cells. SiRNA LNCs were prepared from DOTAP/DOPE lipoplexes, and the siRNA dose and lipid/siRNA charge ratio were assayed to improve the stability and encapsulation yield. Cryo-TEM imaging of the siRNA lipoplexes and LNC morphology revealed a specific organization of the siRNA DOTAP/DOPE lipoplexes as well as specific lipid microstructures. No cytotoxicity of the siRNA LNCs against the melanoma SK-Mel28 cell line was observed at concentrations of up to 500 ng/mL siRNA and in vitro siRNA transfection experiments, compared to oligofectamine, demonstrated interesting target gene silence effects. Finally, complement activation assays confirmed the feasibility of the PEGylation of siRNA LNCs as part of a passive targeting strategy for future melanoma in vivo experiments and metastasis targeting.

Keywords

Nanomedicine, Cryo-TEM, drop tensiometer, stability, CH50

Introduction

Gene therapy is a rapidly emerging field. Initial gene therapy strategies sought to increase the expression of deficient genes in monogenic diseases by the efficient transfection of DNA plasmids. A more recent gene therapy strategy aims to transiently inhibit the expression of a target gene in chronic diseases such as cancer. In this strategy, the use of a small interfering RNA (siRNA) in place of a DNA plasmid produces a partial or total extinction of messenger RNA (mRNA) and protein levels of the targeted gene [1]. Proof of concept of siRNA action has been provided by commercial transfection agents that can suppress the expression of proteins in vitro in tumor cell cultures, resulting in decreased tumor cell proliferation [2, 3]. However, the application of this strategy is limited by the ability to systemically inject these nucleic acids. In this way, our objectives were to obtain i) high encapsulation and stability of siRNA in the nanocarrier, ii) efficient protection from innate immune system present in the blood and iii) improved uptake into the targeted cells with efficient transfection.

Initial studies involved viruses such as cytomegalovirus (CMV) or associated adenoviruses (AAV). However, high costs, risks of genome rearrangement, possible crossing with natural viruses, and inflammatory and immunogenic reactions have limited the use of these viral forms and encouraged the development of non-viral carriers, such as synthetic nanoparticles. Over the last few years, some nanomedicines have been formulated to efficiently encapsulate siRNA and deliver it into the blood stream without degradation [4]. Nanoparticles and liposomes are the most-studied siRNA delivery systems. Nanoparticles with an oily core and a monolayer shell are usually based on polymers such as polyethylene glycol (PEG) and can protect nucleic acids from degradation by nucleases and cells of the innate immune system [5-7]. Liposomes composed of bilayers of cationic charged lipid components, such as cholesterol, DOTAP (1,2-dioleoyl-3- trimethylammoniumpropane), or DOPE (1,2-dioleoyl-sn-glycero-3-phosphoethanolamine), enable i) the fixation of siRNA by electrostatic forces; ii) the interaction of siRNA with cell membranes and the improvement of cellular uptake; and iii) the endosomal escape of the siRNA [8-10]. Polymers and lipids have frequently been employed in tandem in the formulation of new siRNA delivery systems to combine the advantages of both components, as in the siRNA lipid nanocapsules (siRNA LNCs) presented here.

Lipid nanocapsules (LNCs), which consist of a lipid liquid core of triglycerides and a rigid shell of lecithin and PEG, were developed in our laboratory [11]. The simple formulation process is based on the phase inversion of an emulsion. Firstly used to load DNA [12-15], these LNCs were recently modified to encapsulate siRNA complexed with DOTAP/DOPE lipids, resulting in efficient encapsulation of up to 60 % siRNA [16]. Transfection of U87MG glioma cells with these siRNA LNCs resulted in inhibition of EGFR protein expression by 63 % [17]. In the present study, siRNA LNCs were characterized by specific microscopic methods to provide insights into siRNA organization and LNC structure. Moreover, the process was optimized to improve the siRNA payload

and the stability of siRNA LNCs over time. The cytotoxicity of the siRNA LNCs was then assessed against the SK-Mel28 human melanoma cell line. The final aim was to produce a partial or total extinction of messenger RNA (mRNA) and protein levels of the targeted gene using siRNA LNCs. So, the in vitro experiment about the ability of LNCs carrying siRNA to transfect cell and suppress protein levels of the targeted gene was carried out. Finally, with the aim of designing stealth nanocarriers for in vivo systemic administration, the addition of long PEG chains at the LNC surface was evaluated by complement activation assays.

1. Materials and methods

1.1. Formulation of siRNA LNCs

1.1.1. Liposomes and lipoplexes

For liposome preparation, the cationic lipid DOTAP (1,2-dioleoyl-3- trimethylammoniumpropane) (Avanti® Polar Lipids Inc., Alabaster, AL, USA) dissolved in chloroform and combined at a 1:1 mole ratio with the neutral lipid DOPE (1,2-dioleoyl-sn-glycero-3-phosphoethanolamine) (Avanti® Polar Lipids Inc., Alabaster, AL, USA) to obtain a final concentration of 30 mM cationic lipid charge based on the number of lipid charges per molecule, i.e., 1 for DOTAP. After evaporation of chloroform under vacuum, deionized water was added to rehydrate the lipid film overnight at 4 °C. The lipid film was then sonicated for 30 min.

Lipoplexes were formulated as a simple equivolume mixture of siRNA and liposomes. The complexes were characterized by their charge ratio (CR) [17], i.e., the ratio between the positive charges of the lipids and negative charges of the nucleic acids (+/- ratio), which ranged from 5 to 15.

1.1.2. siRNA LNCs

LNCs were formulated as described previously [11] by combining 20.5 % w/w Labrafac WL 1349 (caprylic-capric acid triglycerides, Gatefossé S.A. Saint-Priest, France), 1.5 % w/w Lipoid S75-3 (Lipoid GmbH, Ludwigshafen, Germany), 16.9 % w/w Kolliphor® HS 15 (BASF, Ludwigshafen, Germany), 1.8 % w/w NaCl (Prolabo, Fontenay-sous-Bois, France), and 59.8 % w/w water (obtained from a Milli-Q system, Millipore, Paris, France) with magnetic stirring. The temperature was cycled three times between 60 and 95 °C to produce phase inversions of the emulsion. Subsequent rapid cooling and dilution with ice-cooled water after the last phase inversion temperature (PIT) led to the formation of blank LNCs.

To obtain siRNA LNCs, the aqueous solution was replaced during the last temperature cycle with lipoplexes, i.e., α1 subunit siRNA (sense sequence: 5'- GGGCAGUGUUUCAGGCUUATT -3';

antisense sequence: 5'- UUAGCCUGAAACACUGCCCTT -3'; Eurogentec, Seraing, Belgium), complexed with cationic liposomes in a defined charge ratio, as described above.

1.2. Surface modification by post-insertion

The polymer used for post-insertion was 1,2-distearoyl-sn-glycero-3-phosphoethanolamine-N-[methoxy(polyethyleneglycol)-2000] (DSPE-mPEG2000) (Mean Molecular Weight (MMw = 2805 g/mol) (Avanti Polar Lipids, Inc., Alabaster, USA). This polymer was added to LNCs to obtain a final concentration of 10 mM DSPE-mPEG2000. Pre-formed siRNA LNCs and DSPE-mPEG2000 were co-incubated for 4 h at 37 °C. The mixture was vortexed every 15 min and then quenched in an ice bath for 1 min.

1.3. Filtration and purification

After formulation and/or the DSPE-PEG2000 post-insertion, the LNCs were filtered with a 0.2 µm filter (Acrodisc PALL GHP, VWR, Radnor, USA) or purified using PD10 Sephadex columns (Amersham Biosciences Europe, Orsay, France). Purifications were performed in water or with low concentrations of sodium hydroxide (0.15 M) to disrupt the interaction between lipids and siRNA. After this purification step, the salt concentration of the suspension was adjusted to a physiological NaCl concentration (150 mM).

1.4. Characterization of siRNA LNCs

1.4.1. Size and Zeta potential

The size and Zeta potential of the LNCs were measured by Dynamic Light Scattering (DLS) using a Malvern Zetasizer® apparatus (Nano Series ZS, Malvern Instruments S.A., Worcestershire, UK) in triplicate at 25 °C after dilution at a ratio of 1:200 in deionized water [18]. These parameters were measured daily over the course of one month.

1.4.2. Encapsulation efficiency (EE)

Qualitative ethidium bromide (EtB) electrophoresis detection: The EE and integrity of the siRNA molecules after nanocapsule formulation and post-insertion were evaluated by EtB agarose gel electrophoresis. Samples of LNC suspension equivalent to 2.5 µg of siRNA were tested with or without Triton® X100 (Sigma, Saint-Quentin Fallavier, France), mixed with gel-loading solution (Sigma, Saint-Quentin Fallavier, France) and loaded in each well of a 1 % agarose gel containing EtB

(Sigma, Saint-Quentin Fallavier, France) [12]. Free siRNA (2.5 µg) in solution was used as a control. The samples were migrated for 20 min at 125 V in a Tris–EDTA buffer (Sigma, Saint-Quentin Fallavier, France).

Quantitative UV detection: A spectrophotometric method based on recent work by David et al., (2012) was used to evaluate the EE [16]. Briefly, siRNA LNCs were mixed with chloroform and water to separate hydrophilic and lipophilic components, respectively. Sodium hydroxide was then added to destabilize the lipoplexes, and finally, absolute ethanol was added to destroy the LNCs [16]. After two centrifugation steps, four fractions were obtained: free siRNA, free lipoplexes (i.e., siRNA associated with liposomes), siRNA encapsulated by LNCs, and lipoplexes encapsulated by LNCs. To determine the concentration of siRNA, the optical density of each sample was determined in triplicate at 260 nm (UV-2600, Shimadzu, Noisiel, France). The EE was measured every week for one month using these two methods.

1.5. Cryogenic transmission electron microscopy (cryo-TEM) [19]

Specimens for cryo-TEM imaging were prepared using a cryo-plunge cryo-fixation device (Gatan, Pleasanton USA) in which a drop of the aqueous suspension was deposited on a carbon-coated grid (Ted Pella Inc., Redding, USA). The TEM grid was then prepared by blotting the drop containing the specimen so that a thin liquid layer remained across the holes of the carbon support film. The liquid film was vitrified by rapidly plunging the grid into liquid ethane cooled by liquid nitrogen. The vitrified specimens were mounted in a Gatan 910 specimen holder (Gatan, Pleasanton, USA), which was inserted into the microscope using a CT-3500-cryotransfer system (Gatan, Pleasanton, USA) and cooled with liquid nitrogen. The TEM images were then obtained from specimens preserved in vitreous ice and suspended across a hole in the supporting carbon substrate [20, 21]. The samples were observed under low-dose conditions (<10 e-/Å2), at -178 °C, using a JEM 1230 “Cryo” microscope (Jeol, Akishima, Japan) operated at 80 kV and equipped with a LaB6 filament. All micrographs were recorded on a Gatan 1.35Kx1.04Kx 12 bit ES500W CCD camera.

1.6. Drop tensiometry

Oil–water interface (Labrafac®-water) behavior was measured using a drop tensiometer (Tracker, ITConcept, Longessaigne, France) and a water drop containing different quantities of liposome, lipoplex, or siRNA in bulk Labrafac® [22]. The quantities of liposome and lipoplex were calculated based on the masses used in the formulation of the LNCs. The tested concentrations varied from 2 to 12 mg of lipid per gram of Labrafac®, and the observed lipid concentration in siRNA LNCs was 11.36 mg/g. A 5 µL (~12.5 mm²) rising drop of water, with or without liposomes or lipoplexes, was

formed using an Exmire microsyringe and a gauge (Prolabo, Paris, France) in a glass vial filled with an oily phase (Labrafac®). The axially symmetric shape (Laplacian profile) of the drop was analyzed using a camera connected to a computer. From the analysis of the digital image and integration of the drop profile according to the Laplace equation, the interfacial tension and surface area could be simultaneously calculated and recorded in real time. The volume was controlled by a motor operating the micro-syringe. To enable adsorption of liposomes and lipoplexes onto the interface, the drop was equilibrated for 12 h (at 25 °C), with the surface area kept constant with the help of the syringe motor. At the end of the equilibration time, the equilibrium surface tension was recorded.

1.7. Human SK-Mel28 melanoma cell culture

Human SK-Mel28 melanoma cell lines were obtained from ATCC (LGC Promochem, Molsheim, France). The cell lines were grown in RPMI medium (Lonza, Verviers, Belgium) supplemented with 10 % fetal bovine serum (Lonza, Verviers, Belgium), 1 % antibiotics (10 units of penicillin, 10 mg of streptomycin, and 25 µg of amphotericin B/mL; Sigma-Aldrich, St. Louis, USA), and 1 % non-essential amino acids (Lonza). Cell lines were cultured according to ATCC protocol and maintained at 37 °C in a humidified atmosphere with 5 % CO2.

1.8. Viability assay

Cells were seeded onto 24-well plates at a density of 5 x 10^4 cells/well and precultured overnight. Before incubation, the medium was changed to a fresh medium without serum. The cells were treated with blank or siRNA LNCs at siRNA concentrations of 50 to 500 mg/mL for 4 h. After removing the LNCs, the cells were cultured for two days before determining the IC50. Cytotoxicity assays were performed using MTS (3-(4,5-dimethylthiazol-2-yl)-5-(3-carboxymethoxyphenyl)-2-(4-sulfophenyl)-2Htetrazolium) (Promega, Madison, USA). Each well contained 100 µL of MTS, and the plates were incubated for 2.5 h at 37 °C in a humidified atmosphere with 5 % CO2. The OD was measured at 492 nm with a Multiskan Ascent (Labsystems, Fisher Scientific, Wilmington, USA).

1.9. Transfection experiments

SK-Mel28 cells were seeded onto 6-well plates at the density of 2 x 10^5 cells/well or in flask (25cm2) with 5 x 10^6 cells/flask and pre-cultured overnight. Before transfection, the medium was changed to a fresh one containing no serum. Different treatments (control, scramble siRNA LNCs and alpha 1 siRNA LNCs) were incubated with cells and removed 8 h post-transfection. Positive control

was realized with Oligofectamine® according to the manufacturer protocol with scramble and alpha 1 siRNA. Transfection was realized three days consecutively.

1.10. Western blot

After three transfections, total proteins were extracted from melanoma cells by scraping with a cell lysis buffer (10 mmol/L Tris-Base, 1 mmol/L Na_3O_4, and 1 % SDS, pH 7.4) and stored at -20°C. Twenty micrograms of proteins were resolved on 10% (v/v) SDS-PAGE gel and transferred to a nitrocellulose membrane (0.45-µm pore size) (Amersham GE Healthcare). Mouse anti-human Na/K ATPase α1 (clone C464.6; Millipore) and mouse anti-human actine (Clone C4; Millipore), used as loading controls, were diluted, respectively, at ratios of 1:1,000 and 1:5,000 according to the manufacturer's instructions and incubated over night at 4°C. A second mouse antibody (Dako) was used at a dilution of 1:2,000. Detection (using LAS4000, GE HealthCare) was performed using enhanced chemiluminescence (ECL; Fisher Scientific, Pierce).

1.11. RT-q-PCR

Total RNA of cells were extracted and purified using RNeasy Microkit (Qiagen, Courtaboeuf, France), and treated with DNase (10 U DNase I/µg total RNA). RNA concentrations were determined using a ND-2000 NanoDrop (Thermo Fisher Scientific, Wilmington, Delaware USA) and used for normalization of the input RNA in the Reverse transcription. First strand cDNA synthesis was performed with a SuperScript™ II Reverse Transcriptase (Invitrogen), in combination with random hexamers, according to the manufacturer's instructions. Following first-strand cDNA synthesis, cDNAs were purified (Qiaquick PCR purification kit, Qiagen, Courtaboeuf, France) and eluted in 40 µL RNAse free water (Gibco). 3ng of cDNA was mixed with Maxima™ SYBR Green qPCR Master Mix (Fermentas) and primer mix (0.3 µM) in a final volume of 10 µL. Amplification was carried out on a LightCycler 480 (Roche) with a first denaturation step at 95°C for 10 min and 40 cycles of 95°C for 15 s, 60°C for 30 s. After amplification, a melting curve of the products determined the specificity of the primers for the targeted genes. A mean cycle threshold value (Cq) was obtained from 2 measurements for each cDNA. Specific gene expression was calculated using the $2^{-\Delta\Delta CT}$ method using GAPDH as calibrator.

1.12. CH50 assay

Complement consumption was assessed in normal human serum (NHS) (provided by the Etablissement Français du Sang, Pays de la Loire - Angers, France) by measuring the residual hemolytic capacity of the complement system after contact with LNCs. The final dilution of NHS in the mixture was 1:4 (V/V), corresponding to 100 µL of NHS in 400 µL of reactive media. The amount of serum required to lyse 50 % of a fixed number of sensitized sheep erythrocytes using rabbit anti-sheep erythrocyte antibodies (CH50) was determined according to a procedure described elsewhere [23]. Complement activation was first expressed as a function of the surface area of the LNCs to compare different formulations. Nanoparticle surface areas were estimated using the equation: $S = 3 m/r\rho$, where S is the surface area [cm^2], m is the weight [g] in 1 mL of suspension, r is the average radius [cm] determined by DLS, and ρ is the volumetric mass [g/cm^3] of the nanoparticles estimated at 1 g/cm^3.

2. Results and Discussion

2.1. siRNA LNC characterization

2.1.1. Charge ratio and siRNA amount influence the stability of siRNA LNCs

LNCs were prepared with three different amounts of lipids/siRNA charge ratio (CR) (Figure 1). At Day 0, all samples had an LNC size of approximately 110 nm with a polydispersity index (PdI) of less than 0.3 (Figure 1A). Over time, the size of the LNCs decreased depending on the amount of siRNA, to a minimum size of 60 nm. The sizes were stabilized in 7 to 14 days for high and low amounts of siRNA, respectively. A direct correlation between size and zeta potential was observed (Figure 1A). While the size decreased, the zeta potential increased up to + 30 mV, confirming siRNA LNC reorganization. Despite perturbation of size and zeta level, the yield was constant for 1 month, indicating a strong interaction between the siRNA and LNCs (Figure 1E). Interestingly, the siRNA-encapsulated yield differed depending on the amount siRNA introduced into the formulation (Figure 1F). Saturation of siRNA incorporation during the encapsulation process was not observed below 750 µg siRNA, leading to an estimated maximal encapsulation efficiency (EE) of 53 %, which corresponds to 130 µg siRNA per mL of LNC suspension. Many formulations reported in the literature that have been based on electrostatic interactions, such as with lipoplexes, have a yield greater than 90 % complexation after electrophoresis or centrifugation [24, 25]. However, our siRNA LNC synthesis more closely resembles the calcium phosphate (CaP) nucleic acid nanoparticle synthesis developed by Zhang et al. This process includes a nanoencapsulation step for lipoplexes and leads to a yield of 55 % (radioactive dosage with tritium), similar to our results [26].

A positive CR greater than 3 has been used previously for complexation of siRNA and lipids [27]. In initial studies of siRNA LNC formulation, superior encapsulation was observed for DOTAP/DOPE lipoplexes with a CR of 5 compared to those with a CR of 2.5 [16, 17]. In the present study, no significant improvement of the EE and stability was observed for a CR of 10 (Figure 1B, 1F). Unexpectedly, the highest CR tested (15) led to small nanocapsules of approximately 50 nm and no encapsulation of siRNA (Figure 1B, 1F). At a high CR, the substantial excess of positive charges seems to prevent efficient siRNA encapsulation. Consequently, the large size (100 nm) obtained at Day 0 for lower CRs might indicate siRNA incorporation into LNCs. The quantities of siRNA and liposomes used to formulate the LNCs appears to be a key factor in improving the stability and EE of siRNA LNCs. Based on these results, a medium siRNA content of 375 µg and a low CR (5) were selected for subsequent experiments.

2.1.2. siRNA stability evaluation in function of manufacturing and storage conditions

Storage temperature is a key parameter in ensuring the stability of nanomedicines over time with scale-up and industrialization. Temperatures of 25 and 37 °C were tested to predict the behavior of siRNA LNCs at room and physiological conditions, respectively (Figure 1D). Our results demonstrated the necessity of 4°C storage compared to room or physiological temperature to retain the siRNA in the LNCs (Figure 1F). Room and physiological temperatures induced a rapid decrease in LNC size, and electrophoresis studies revealed that siRNA delivery began 8 h after incubation and was complete at 24 h at 37 °C (*data not shown*). In this case, the size reduction was associated with siRNA delivery and demonstrated the reversibility of the electrostatic interactions between the siRNA and LNCs. Thus, the siRNA LNCs were stored at 4 °C.

To avoid the possible denaturation of siRNA during the process, lipoplexes were added during the third temperature cycle at the PIT, which corresponded to 75 °C which is the dilution temperature typically used in the LNC formulation process. Lipoplexes were also introduced at lower temperatures: at 40 °C, during the phase inversion at 75 °C, and at 4 °C with stirring, after the completion of blank LNC formation. No major differences in physico-chemical characteristics or EE levels were observed at the varying temperatures (Figure 1C, 1F), indicating that the encapsulation of siRNA by LNCs is not dependent on the dilution temperature. This result suggests that lipoplexes can interact with LNCs during and/or after complete LNC formation, indicating that lipoplexes are most likely located within the shell, at the interface between the LNC core and water. Similarly, Pitaksuteepong et al. also reported an interfacial localization of hydrophilic compounds when introduced into a water-in-oil emulsion [28].

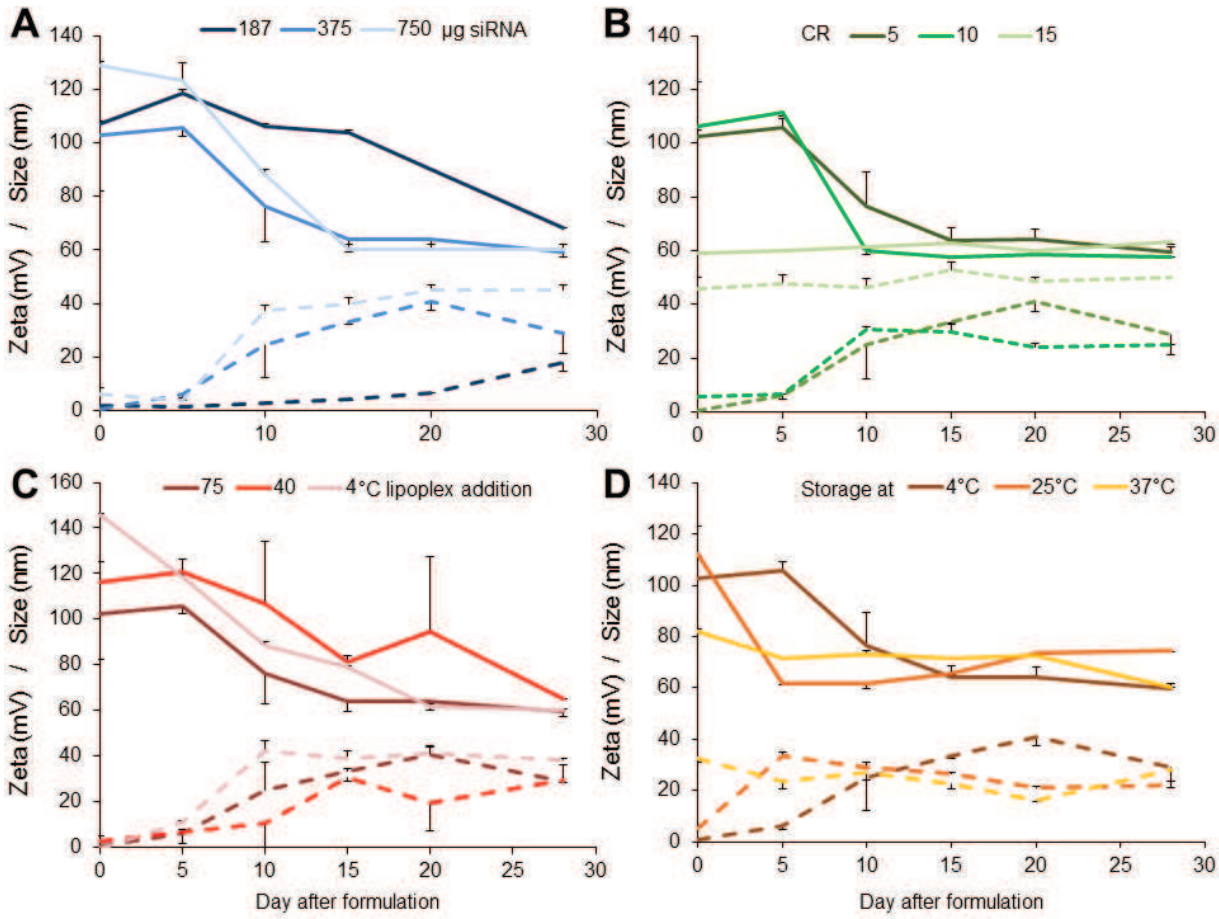

E

LNC alpha 1 – CR 5 – 375µg - lipoplex addition at 75°C

Days after formulation	0	7	14	21	28
EE (%)	40	27	31	39	38
Electrophoresis					

Lane 1 2
Intact LNCs
Destruction of LNCs by Triton 100X

F

siRNA dose (µg)	187	375	750
EE (%)	20	38	53
Electrophoresis			ND

CR	5	10	15
EE (%)	38	45	17
Electrophoresis		ND	

Lipoplex addition Temperature	4°C	40°C	75°C
EE (%)	46	48	38
Electrophoresis			

Storage Temperature	4°C	25°C	37°C
EE (%)	38	25	17
Electrophoresis			

Figure 1: **Size (____) and zeta potential (……) of siRNA LNCs over time for different siRNA quantities (A), charge ratios (B), temperatures of lipoplex addition (C), and storage temperatures (D).** The encapsulation efficiency (EE) was determined by UV spectroscopy and EtB electrophoresis of blank LNCs over the course of 1 month (E), while the other parameters were tested after 1 month of storage (F). ND: non-determined. Size and zeta measures were expressed as mean ± standard deviation (n=3).

2.2. siRNA LNC structure

2.2.1. Tensiometry study evidence interfacial localization of siRNA

To explain LNC instability, surface tension studies were conducted at an oil-water interface. siRNA, liposomes, and lipoplexes were diluted in a water drop introduced into bulk Labrafac® oil. Application of siRNA alone only slightly modified the surface tension, even at the highest tested concentration, which can be attributed to the hydrophilic structure of the siRNA (Figure 2A). DOTAP/DOPE lipids strongly reduced surface tension due to their amphiphilic structures, which feature polar heads and hydrophobic carbon chains. The lipoplexes had a stronger effect on surface tension than did the liposomes, confirming the interaction of lipoplexes with the water/oil interface. This phenomenon has also been described with another cationic lipid, EDOPC (O-ethyl-dioleoylphosphatidylcholine), in association with DNA plasmids. The importance of the CR on interfacial properties has been demonstrated previously [29]. The tensio-active profile of EDOPC/DNA was obtained only at a high CR, i.e., 6, as opposed to 1, similar to that obtained here for DOTAP/DOPE lipoplexes at a CR of 5, suggesting their interfacial position.

The siRNA LNCs were purified by passage through a PD10 column in water and again in NaOH (0.15 M). NaOH was used to disrupt non-LNC-encapsulated lipoplexes potentially containing siRNA by destabilizing electrostatic interactions [16]. After purification in water, the size, zeta potential, and EE of the siRNA LNCs were unchanged, while the PdI decreased by half. Taken together with the results of the UV assay, these results confirmed the removal of non-encapsulated siRNA. After purification with NaOH, the size of the siRNA LNCs decreased to 61 nm, while the surface charge became negative and similar to that of blank LNCs (Figure 2B). In addition, the final encapsulation was estimated at 21 %, versus 40 % without NaOH (Figure 2B). This result demonstrated that the encapsulated lipoplexes were sensitive to NaOH treatment, supporting lipoplex incorporation into the LNC shell. siRNA LNCs could be represented by a core-shell structure in which the tensio-active properties of the lipoplexes enable incorporation of siRNA into the shell, as previously reported for other siRNA delivery systems (Figure 2C) [30-32].

2.2.2. Specific structure of siRNA LNCs observed by cryo-TEM

All components of the siRNA LNCs were examined by transmission electron microscopy using a cryogenic stage (cryo-TEM) with vitreous samples to ensure optimal preservation of the hydrated structures [19]. DOTAP/DOPE liposomes displayed the uni- or multilamellar structures classically observed for liposomes, with diameters ranging from 100 to 1000 nm (Figure 3A) [33]. The siRNA lipoplexes exhibited a typical “onion-like” structure, with large sizes up to a micrometer, confirming the association of siRNA with cationic lipids via electrostatic interaction (Figure 3B, 3C) [34]. The narrow size distribution and spherical structure of blank and siRNA LNCs were also evidenced

(Figure 3D, 3E). This microscopy study confirmed the size range of the siRNA and blank LNCs measured by DLS (approximately 100 nm and 50 nm, respectively). Lipid microstructures organized as multilamellar structures similar to the lipoplex edifices were also observed in non-purified suspensions of the siRNA LNCs (Figure 3F). These structures might contain non-LNC-encapsulated siRNA, potentially explaining the observed EE of 40 %.

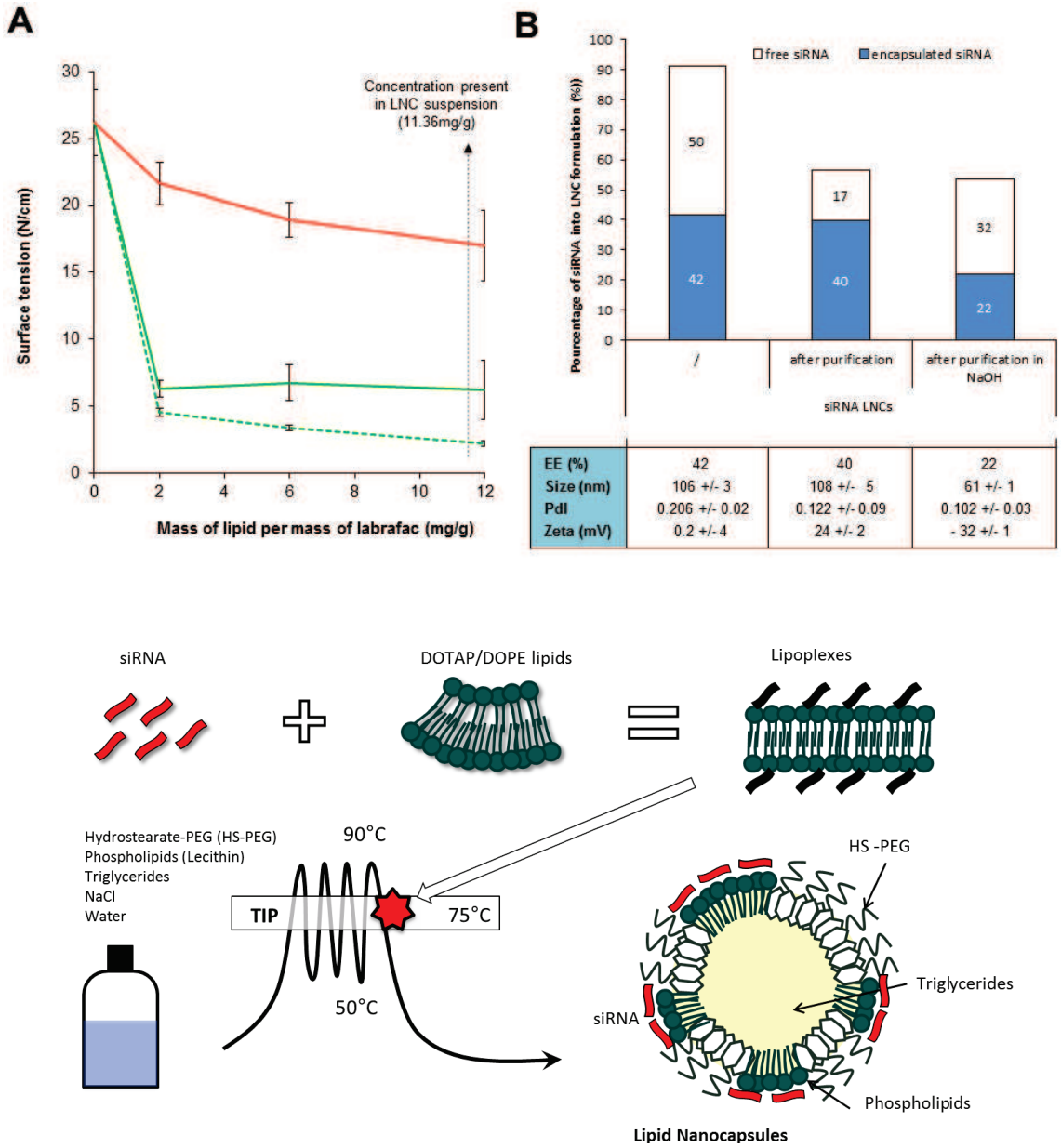

Figure 2: A: Drop tensiometer analysis of DOTAP/DOPE liposomes (——), lipoplexes (.....), and siRNA (——) at different concentrations of DOTAP/DOPE in Labrafac (mg/g). B: Determination of siRNA encapsulation by UV spectroscopy and DLS-determined physico-chemical parameters of siRNA LNCs at day 0, after column purification, and after column purification in sodium hydroxide solution (0.15 M). C: Process for siRNA LNC formulation by the phase inversion method, with schematic representation of liposome, lipoplexes, and siRNA LNC organization. Surface tension, size and zeta measures were expressed as mean ± standard deviation (n=3).

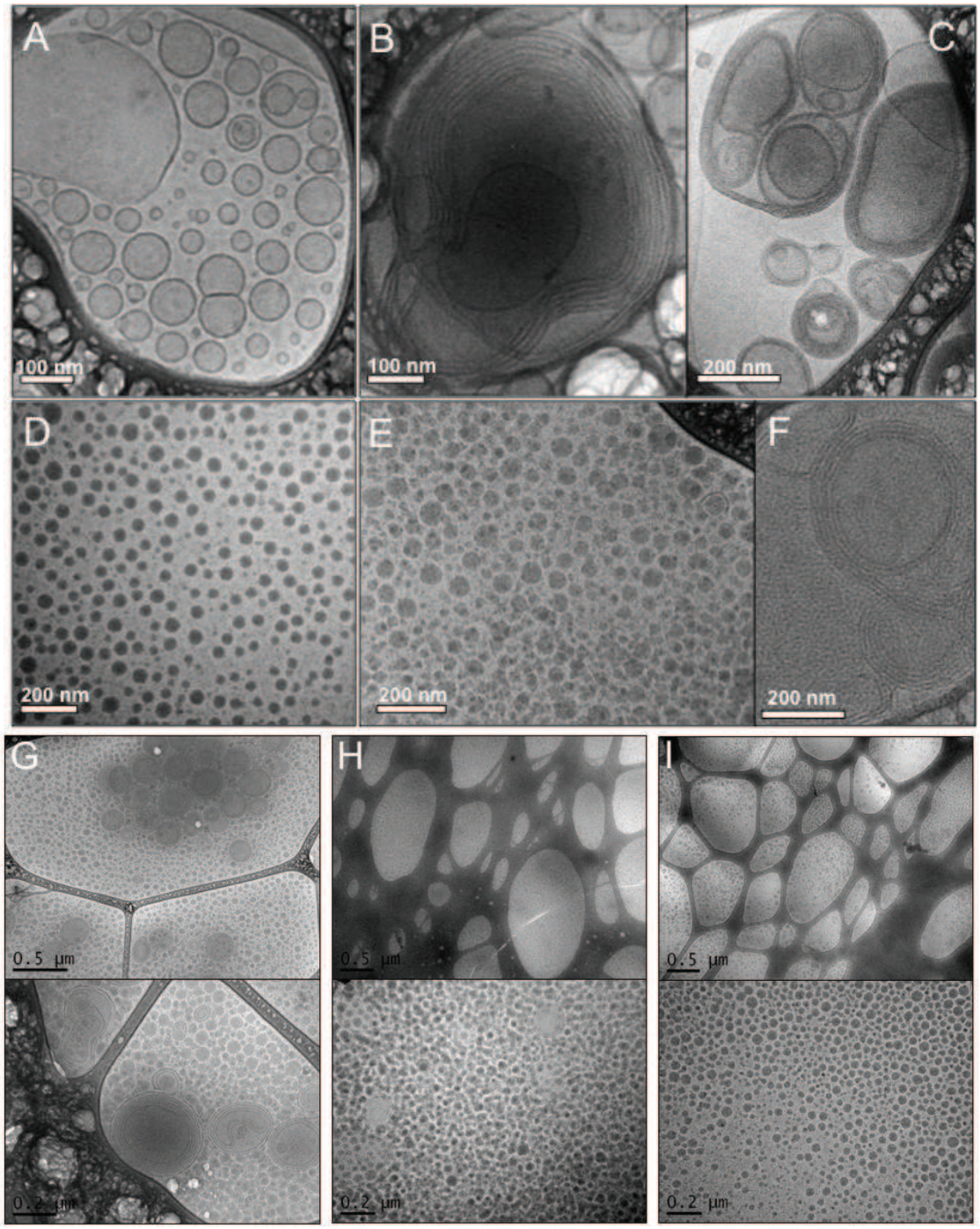

J

Formulation	Day 0	Filtred	Purified
Size (nm)	106 +/- 3	119 +/- 2	108 +/- 5
PdI	0.206 +/- 0.02	0.110 +/- 0.01	0.200 +/- 0.05
Zeta potential (mV)	0.2 +/- 4	7 +/- 3	24 +/- 2
EE (%)	42	ND	40

Figure 3: Cryo-TEM imaging of siRNA LNC components: DOTAP/DOPE liposomes at 30 mM+ (A), lipoplexes (B, C), blank LNCs (D), siRNA LNCs (E), and lipid microstructures in the siRNA LNC suspension (F). The siRNA LNC suspension was characterized before filtration (G), after filtration (H), and after purification on a column (I). The corresponding physico-chemical characteristics are given in (J).

2.2.3. Elimination of lipid microstructures by purification method

As suggested in our previous studies of DNA LNCs [15], prior to in vivo administration, the siRNA LNCs must be purified to eliminate non-encapsulated siRNA and, consequently, the lipid microstructures observed by cryo-TEM. Two methods were tested: filtration at 0.2 µm and purification with a Sephadex® column (Figure 3H, 3I). For siRNA LNCs at Day 0, we observed classical physico-chemical parameters with an EE of approximately 40 % (Figure 3J). As described previously, numerous lipid microstructures were observed in the LNC suspension by cryo-TEM (Figure 3G). After filtration, no significant variation of the physico-chemical parameters was observed compared to the suspension at Day 0, with the exception of a decrease in the PdI (Figure 3H). At low blowback, analysis by cryo-TEM demonstrated that the large majority of lipid microstructures were eliminated (Figure 3I). However, at high blowback, a few vesicles, smaller than 200 nm, passed through the filter and were observed in the LNC suspension. The presence of these vesicles is related to the extrusion method classically used to disrupt liposomes and obtain monodisperse populations [35]. After column purification, electron microscopy analysis revealed that the siRNA LNCs remained intact and that the lipid microstructures had been removed. The column system appears to be the most effective method for the elimination of non-encapsulated siRNA retained in the lipid microstructures for the purification of siRNA LNC suspensions for in vivo experiments.

2.3. In vitro assays

2.3.1. Cytotoxicity evaluation and efficient transfection on melanoma cells

Alpha 1 subunit of sodium pump NaK ATPase is an essential part of protein complex allowing the active transport of sodium and potassium ions to regulate the osmosis [36]. This protein has been involved in cancerogenesis in melanoma by interaction with abnormal proliferation and survival via MAPKinase pathway. Moreover, the inhibition of this protein by chemical inhibitor has shown interestingly anticancerous effect with chemosensitivity [37]. However, this inhibitor appears as strong cardiotoxic drug. In this context, siRNA LNCs could represent a promising tool to inhibit specifically this alpha 1 subunit and promote the activity of subsequent chemotherapy in melanoma model.

The effects of blank and siRNA LNCs on cell viability were evaluated on human melanoma SK-Mel28 cells. No cytotoxicity was observed after 4 h of incubation of siRNA LNCs with SK-Mel28, whatever the kind of LNCs, even at a siRNA concentration of 500 ng/mL (equivalent to 32 nM), corresponding to a LNC concentration of 0.6 mg/mL (Figure 4A). In contrast to chemical inhibitors, inhibition by alpha 1 siRNA alone at 3 days after 4h transfection did not induce cell death in SK-Mel28 cells as observed in Figure 4A [36]. Similarly, Karpova et al. (2010) observed no impact of alpha 1 siRNA on viability four days even after 72 h transfection in neuroblastoma cells [38]. SiRNA efficacy was validated with commercial transfection reagent Oligofectamine® inducing a total

inhibition of targeted protein (Figure 4B/4C). Concerning siRNA LNCs, at low concentration corresponding to a 150 ng/mL, protein and gene analysis confirmed the efficacy of siRNA LNCs to induce partial inhibition of alpha 1 subunit after transfection on SK-Mel28 (30 % of mRNA inhibition versus 70% with Oligofectamine®) (Figure 4B/4C).

Karpova *et al*. demonstrated the partial inhibition of mRNA with Lipofectamine® reagent in neuroblastoma cells similarly to our result with LNCs. In their case, this inhibition was sufficient to obtain significant result by studying the combination with antineoplasic drugs [38]. In literature, the transfection efficiency of nanoparticles is usually comprised between 30% and total inhibition, in function of cell models and transfection protocols [4]. In future works, siRNA LNCs could be combined with dacarbazine or other anticancerous drugs. If necessary, the amount of siRNA could be increased as described before and in vivo protocols adapted for a synergic effect.

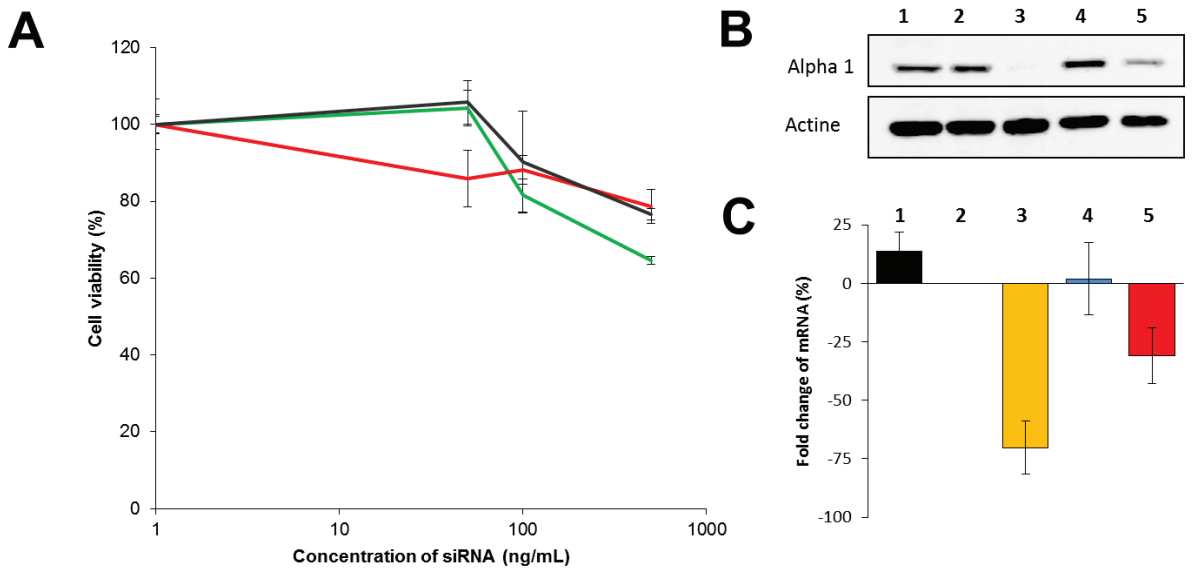

Figure 4: Efficient inhibition of alpha 1 subunit by siRNA LNCs without cytotoxicity on SK-Mel28. (A) No difference was evidenced on cytotoxicity of blank LNCs (—), 75 °C siRNA LNCs (—), and 40 °C siRNA LNCs (—) after evaluation of cell viability by MTS assay on human SK-Mel28 melanoma cell line until a concentration at 500ng/mL. (B) The protein inhibition of alpha 1 subunit was confirmed by positive control using oligofectamine® et also demonstrated using the LNCs: 1 SK-Mel28 cells, 2 Oligofectamine® with control siRNA, 3 Oligofectamine® with alpha 1 siRNA, 4 control siRNA LNCs, and 5 alpha 1 siRNA LNCs. (C) Gene analysis by RT-q-PCR showed the decrease of alpha 1 mRNA with Oligofectamine® and LNCs. Viability and alpha 1 mRNA fold change were expressed as mean ± standard error of the mean (SEM) (n=3).

A

Formulation at 75°C	PEGylated	PEGylated and purified
Size (nm)	104 +/- 2	73 +/- 4
PdI	0.293 +/- 0.10	0.167 +/- 0.02
Zeta potential (mV)	- 13 +/- 6	- 12 +/- 7
EE (%)	41	46

Formulation at 40°C	PEGylated	PEGylated and purified
Size (nm)	110 +/- 5	89 +/- 6
PdI	0.331 +/- 0.15	0.232 +/- 0.04
Zeta potential (mV)	- 14 +/- 3	-18 +/- 2
EE (%)	45	52

B

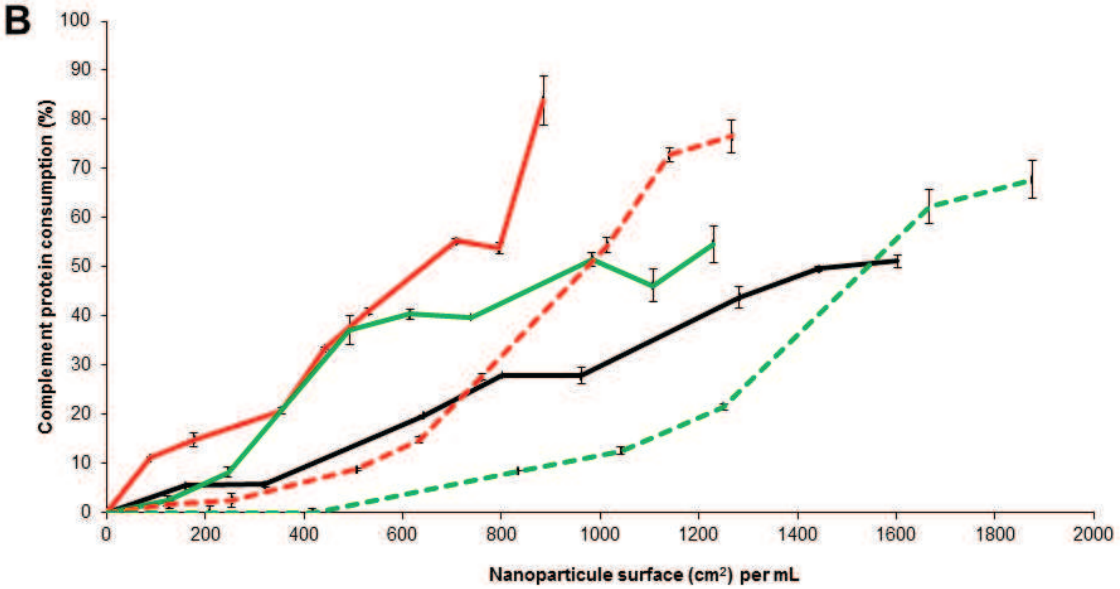

Figure 5: A: Physico-chemical parameters of two PEGylated LNC formulations (75 °C and 40 °C) before (left column) and after (right column) purification. B: Activation profile of complement consumption evaluated by CH50 assay of different formulations: blank LNCs (—), 75 °C siRNA LNCs (—), 40 °C siRNA LNCs (—), PEG 75 °C siRNA LNCs (– –), and PEG 40 °C siRNA LNCs (– –). Percentage values were expressed as mean ± standard error of the mean (n=3).

2.3.2. PEGylation step induces low complement protein consumption

To enable long circulation time in the blood, LNCs were modified by the addition of long PEG chain (2000 kDa) to create a hydrophilic ring around the LNCs by a post-insertion method described elsewhere [12, 15]. Two formulations were tested, corresponding to lipoplex addition temperatures of 75 °C and 40 °C (Figure 5A). After PEGylation, the surface charge decreased to approximately -14 mV for both siRNA LNC formulations due to the presence of the negative PEG dipoles [39]. A higher PdI was observed after PEGylation due to the presence of free PEG chains in the LNC suspensions. Elimination of the free PEG chains by column purification reduced the PdI to less than 0.25, while maintaining the negative surface charge and adequate EE of the siRNA LNCs (Figure 5A). Thus, this PEGylation method, which was initially developed for DNA LNCs, is also suitable for siRNA LNCs.

To determine the efficacy of PEGylation, in vitro CH50 tests evaluating complement protein consumption were performed on blank, 75 °C siRNA, and 40 °C siRNA LNCs and on the PEGylated form of both siRNA LNCs (Figure 5B). No activation of complement proteins was observed for

siRNA alone (*data not shown*). The low activation profile of blank LNCs was previously ascribed to their low negative surface charge. Compared to blank LNCs, positively charged surface of siRNA LNCs led to a greater consumption of complement proteins, with a higher response for 75 °C siRNA LNCs. The negative charge of the PEGylated forms led to reduced consumption for the PEGylated siRNA LNCs compared to both non-PEGylated siRNA LNC formulations (75 °C and 40 °C). These results confirm the integration of PEG on the siRNA LNC surface to produce "stealth" nanomedicines. The addition of PEG is a classic surface modification employed to improve the lifetime of nanomedicines in the blood [12, 40, 41]. In fact, the passive targeting of tumor sites via long-circulating drug delivery systems can be obtained via the enhanced permeability and retention (EPR) effect [42, 43].

3. Concluding remarks

The development of nanomedicine carriers for systemic administration of siRNA is a major challenge. Lipid nanocapsules appear to be good candidates for siRNA delivery. This study confirmed the impact of the relative quantities of siRNA and lipid as well as storage conditions on the physico-chemical stability of siRNA LNCs. In addition, tensiometer analysis revealed the tensio-active properties of lipoplexes and supported the hypothesis of lipoplex shell localization. Cryo-TEM imaging validated the spherical structure of the siRNA LNCs as well as the removal by column purification of lipid microstructures formed during the manufacture of the nanomedicine suspensions. No cytotoxicity against SK-Mel28 melanoma cells was observed at siRNA concentrations as high as 500 ng/mL. At a concentration under the threshold of toxicity, an promising extinction of alpha 1 protein was obtained with LNCs. Finally, the low complement activation of siRNA LNCs was demonstrated by CH50 assay. These results encourage the pursuit of in vitro and in vivo research to enable the application of this nanotechnology for cancer chemotherapy by co-encapsulating siRNA into the shell and a chemotherapeutic agent in the oily core.

Acknowledgements

The authors thank Veronique Mathieu for alpha 1 siRNA design and melanoma cell line. We gratefully thank the platform "SFR ICAT" available at Angers who perform the RT-q-PCR analysis, and in particular Dr Jérôme Cayon. This work was supported by special grants from the "Association de la Recherche contre le Cancer" (reference n°: SFI20121205972) and by "La Ligue contre le cancer 49 et 35" (Reference n°: R12164NN). The author reports no conflicts of interest in this work.

References

[1] Fire, A.; Xu, S.; Montgomery, M. K.; Kostas, S. A., et al.,, Potent and specific genetic interference by double-stranded RNA in Caenorhabditis elegans. Nature. 1998, 391, 806-11.

[2] Yuan, X.; Naguib, S.; Wu, Z., Recent advances of siRNA delivery by nanoparticles. Expert Opin Drug Deliv. 2011, 8, 521-36.

[3] Lee, J. M.; Yoon, T. J.; Cho, Y. S., Recent Developments in Nanoparticle-Based siRNA Delivery for Cancer Therapy. Biomed Res Int. 2013, 2013, 782041.

[4] Resnier, P.; Montier, T.; Mathieu, V.; Benoit, J. P., et al.,, A review of the current status of siRNA nanomedicines in the treatment of cancer. Biomaterials. 2013, 34, 6429-43.

[5] Ambardekar, V. V.; Wakaskar, R. R.; Sharma, B.; Bowman, J., et al.,, The efficacy of nuclease-resistant Chol-siRNA in primary breast tumors following complexation with PLL-PEG(5K). Biomaterials. 2013, 34, 4839-48.

[6] Ravina, M.; Cubillo, E.; Olmeda, D.; Novoa-Carballal, R., et al.,, Hyaluronic acid/chitosan-g-poly(ethylene glycol) nanoparticles for gene therapy: an application for pDNA and siRNA delivery. Pharm Res. 2010, 27, 2544-55.

[7] Hadinoto, K.; Sundaresan, A.; Cheow, W. S., Lipid-polymer hybrid nanoparticles as a new generation therapeutic delivery platform: A review. Eur J Pharm Biopharm. 2013.

[8] Terp, M. C.; Bauer, F.; Sugimoto, Y.; Yu, B., et al.,, Differential efficacy of DOTAP enantiomers for siRNA delivery in vitro. Int J Pharm. 2012, 430, 328-34.

[9] Martino, S.; di Girolamo, I.; Tiribuzi, R.; D'Angelo, F., et al.,, Efficient siRNA delivery by the cationic liposome DOTAP in human hematopoietic stem cells differentiating into dendritic cells. J Biomed Biotechnol. 2009, 2009, 410260.

[10] Mochizuki, S.; Kanegae, N.; Nishina, K.; Kamikawa, Y., et al.,, The role of the helper lipid dioleoylphosphatidylethanolamine (DOPE) for DNA transfection cooperating with a cationic lipid bearing ethylenediamine. Biochim Biophys Acta. 2013, 1828, 412-8.

[11] Heurtault, B.; Saulnier, P.; Pech, B.; Proust, J. E., et al.,, A novel phase inversion-based process for the preparation of lipid nanocarriers. Pharm Res. 2002, 19, 875-80.

[12] Morille, M.; Montier, T.; Legras, P.; Carmoy, N., et al.,, Long-circulating DNA lipid nanocapsules as new vector for passive tumor targeting. Biomaterials. 2010, 31, 321-9.

[13] Morille, M.; Passirani, C.; Dufort, S.; Bastiat, G., et al.,, Tumor transfection after systemic injection of DNA lipid nanocapsules. Biomaterials. 2011, 32, 2327-33.

[14] David, S.; Montier, T.; Carmoy, N.; Resnier, P., et al.,, Treatment efficacy of DNA lipid nanocapsules and DNA multimodular systems after systemic administration in a human glioma model. J Gene Med. 2012, 14, 769-75.

[15] David, S.; Carmoy, N.; Resnier, P.; Denis, C., et al.,, In vivo imaging of DNA lipid nanocapsules after systemic administration in a melanoma mouse model. Int J Pharm. 2012, 423, 108-15.

[16] David, S.; Resnier, P.; Guillot, A.; Pitard, B., et al.,, siRNA LNCs--a novel platform of lipid nanocapsules for systemic siRNA administration. Eur J Pharm Biopharm. 2012, 81, 448-52.

[17] Resnier, P.; David, S.; Lautram, N.; Delcroix, G. J., et al.,, EGFR siRNA lipid nanocapsules efficiently transfect glioma cells in vitro. Int J Pharm. 2013.

[18] Bastiat, G.; Pritz, C. O.; Roider, C.; Fouchet, F., et al.,, A new tool to ensure the fluorescent dye labeling stability of nanocarriers: A real challenge for fluorescence imaging. J Control Release. 2013, 170, 334-42.

[19] Gaillard, C.; Douliez, J.-P., Cryo-TEM and AFM for the characterization of vesicle-like nanoparticle dispersions and self-assembled supramolecular fatty-acid-based structures: a few examples. A. Méndez-Vilas, Ed. Current Microscopy Contributions to Advances in Science and Technology 2012, 5, 912-922.

[20] Tonelli, G.; Oumzil, K.; Nallet, F.; Gaillard, C., et al.,, Amino acid-nucleotide-lipids: effect of amino acid on the self-assembly properties. Langmuir. 2013, 29, 5547-55.

[21] Anton, N.; Saulnier, P.; Gaillard, C.; Porcher, E., et al.,, Aqueous-core lipid nanocapsules for encapsulating fragile hydrophilic and/or lipophilic molecules. Langmuir. 2009, 25, 11413-9.

[22] Hirsjarvi, S.; Bastiat, G.; Saulnier, P.; Benoit, J. P., Evaluation of surface deformability of lipid nanocapsules by drop tensiometer technique, and its experimental assessment by dialysis and tangential flow filtration. Int J Pharm. 2012, 434, 460-7.

[23] Vonarbourg, A.; Passirani, C.; Desigaux, L.; Allard, E., et al.,, The encapsulation of DNA molecules within biomimetic lipid nanocapsules. Biomaterials. 2009, 30, 3197-204.

[24] Nishimura, Y.; Mieda, H.; Ishii, J.; Ogino, C., et al.,, Targeting cancer cell-specific RNA interference by siRNA delivery using a complex carrier of affibody-displaying bio-nanocapsules and liposomes. J Nanobiotechnology. 2013, 11, 19.

[25] Wei, W.; Lv, P. P.; Chen, X. M.; Yue, Z. G., et al.,, Codelivery of mTERT siRNA and paclitaxel by chitosan-based nanoparticles promoted synergistic tumor suppression. Biomaterials. 2013, 34, 3912-23.

[26] Zhang, Y.; Peng, L.; Mumper, R. J.; Huang, L., Combinational delivery of c-myc siRNA and nucleoside analogs in a single, synthetic nanocarrier for targeted cancer therapy. Biomaterials. 2013, 34, 8459-68.

[27] Alaaeldin, E.; Abu Lila, A. S.; Moriyoshi, N.; Sarhan, H. A., et al.,, The Co-Delivery of Oxaliplatin Abrogates the Immunogenic Response to PEGylated siRNA-Lipoplex. Pharm Res. 2013, 30, 2344-54.

[28] Pitaksuteepong, T.; Davies, N. M.; Tucker, I. G.; Rades, T., Factors influencing the entrapment of hydrophilic compounds in nanocapsules prepared by interfacial polymerisation of water-in-oil microemulsions. Eur J Pharm Biopharm. 2002, 53, 335-42.

[29] Macdonald, R. C.; Gorbonos, A.; Momsen, M. M.; Brockman, H. L., Surface properties of dioleoyl-sn-glycerol-3-ethylphosphocholine, a cationic phosphatidylcholine transfection agent, alone and in combination with lipids or DNA. Langmuir. 2006, 22, 2770-9.

[30] de Martimprey, H.; Bertrand, J. R.; Malvy, C.; Couvreur, P., et al.,, New core-shell nanoparticules for the intravenous delivery of siRNA to experimental thyroid papillary carcinoma. Pharm Res. 2010, 27, 498-509.

[31] Palanca-Wessels, M. C.; Convertine, A. J.; Cutler-Strom, R.; Booth, G. C., et al.,, Anti-CD22 antibody targeting of pH-responsive micelles enhances small interfering RNA delivery and gene silencing in lymphoma cells. Mol Ther. 2011, 19, 1529-37.

[32] Kim, H. J.; Oba, M.; Pittella, F.; Nomoto, T., et al.,, PEG-detachable cationic polyaspartamide derivatives bearing stearoyl moieties for systemic siRNA delivery toward subcutaneous BxPC3 pancreatic tumor. J Drug Target. 2012, 20, 33-42.

[33] Yan, J.; Berezhnoy, N. V.; Korolev, N.; Su, C. J., et al.,, Structure and internal organization of overcharged cationic-lipid/peptide/DNA self-assembly complexes. Biochim Biophys Acta. 2012, 1818, 1794-800.

[34] Hsu, S. H.; Yu, B.; Wang, X.; Lu, Y., et al.,, Cationic lipid nanoparticles for therapeutic delivery of siRNA and miRNA to murine liver tumor. Nanomedicine. 2013.

[35] Lasic, D. D., Liposomes in gene delivery. CRC Press. 1997.

[36] Mathieu, V.; Pirker, C.; Martin de Lassalle, E.; Vernier, M., et al.,, The sodium pump alpha1 sub-unit: a disease progression-related target for metastatic melanoma treatment. J Cell Mol Med. 2009, 13, 3960-72.

[37] Lefranc, F.; Kiss, R., The sodium pump alpha1 subunit as a potential target to combat apoptosis-resistant glioblastomas. Neoplasia. 2008, 10, 198-206.

[38] Karpova, L.; Eva, A.; Kirch, U.; Boldyrev, A., et al.,, Sodium pump alpha1 and alpha3 subunit isoforms mediate distinct responses to ouabain and are both essential for survival of human neuroblastoma. FEBS J. 2010, 277, 1853-60.

[39] Vonarbourg, A.; Saulnier, P.; Passirani, C.; Benoit, J. P., Electrokinetic properties of noncharged lipid nanocapsules: influence of the dipolar distribution at the interface. Electrophoresis. 2005, 26, 2066-75.

[40] Sandiford, L.; Phinikaridou, A.; Protti, A.; Meszaros, L. K., et al.,, Bisphosphonate-anchored PEGylation and radiolabeling of superparamagnetic iron oxide: long-circulating nanoparticles for in vivo multimodal (T1 MRI-SPECT) imaging. ACS Nano. 2013, 7, 500-12.

[41] Perry, J. L.; Reuter, K. G.; Kai, M. P.; Herlihy, K. P., et al.,, PEGylated PRINT nanoparticles: the impact of PEG density on protein binding, macrophage association, biodistribution, and pharmacokinetics. Nano Lett. 2012, 12, 5304-10.

[42] Maeda, H., The enhanced permeability and retention (EPR) effect in tumor vasculature: the key role of tumor-selective macromolecular drug targeting. Adv Enzyme Regul. 2001, 41, 189-207.

[43] Maeda, H.; Wu, J.; Sawa, T.; Matsumura, Y., et al.,, Tumor vascular permeability and the EPR effect in macromolecular therapeutics: a review. J Control Release. 2000, 65, 271-84.

BREVET : NANOCAPSULES LIPIDIQUES CHARGÉES EN siRNA

BREVET : NANOCAPSULES LIPIDIQUES CHARGÉES EN SIRNA

Les LNC siRNA sont formulées en utilisant le procédé d'inversion de phase classiquement décrit pour la formulation des LNC (premier brevet en 2000). Cette formulation est composée de Solutol® (hydroxystéarate de polyéthylène glycol, HS-PEG), Labrafac® (triglycérides), Lipoid® (lécithine), de chlorure de sodium et d'eau. Pour permettre l'encapsulation des siRNA, ceux-ci sont tout d'abord complexés à des lipides cationiques (DOTAP/DOPE) afin de former des lipoplexes. Ces lipoplexes sont ajoutés à la formulation au niveau de la zone d'inversion de phase (ZIP) après trois cycles de chauffage/refroidissement, ce procédé menant à la formation des LNC siRNA.

En réalisant ce procédé de formulation, les LNC chargées en siRNA montrent une stabilité très courte de l'ordre d'une semaine démontrant le caractère instable de la formulation de base pour encapsuler ces molécules hydrophiles chargées négativement (siRNA) (Figure 15). Aux vues des résultats détaillés dans ce premier chapitre, des essais complémentaires ont été réalisés. Les modifications dans le procédé de formulation ont permis d'améliorer significativement la stabilité des LNC siRNA sans altérer leur capacité d'encapsulation des siRNA (Figure 15). Suite à cette découverte, une procédure de dépôt de brevet a été initiée en collaboration avec la SATT Grand Ouest (Société d'accélération du transfert technologique). La demande d'invention a été déposée en Janvier 2014 et le dépôt de brevet a été effectué auprès de l'INPI (Institut national de la propriété intellectuelle) au mois de septembre 2014.

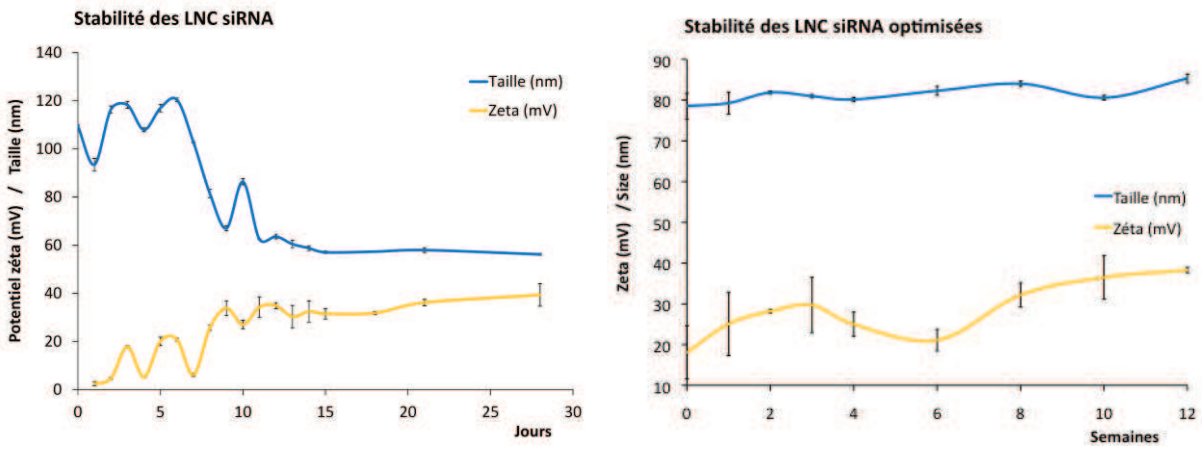

Figure 15 : Comparaison de la stabilité des LNC siRNA avant et après optimisation. Le suivi de la taille et du potentiel zêta révèle une amélioration de la stabilité passant de 7 jours à 3 mois.

CHAPITRE II

NANOCAPSULES LIPIDIQUES DE SIRNA ET CIBLAGE TUMORAL

CHAPITRE II: NANOCAPSULES LIPIDIQUES DE siRNA ET CIBLAGE TUMORAL

Les formulations nanoparticulaires permettent de modifier la biodistribution naturelle d'un principe actif. En effet, une fois au sein du nanosystème, l'efficacité du principe actif dépend alors des propriétés de la nanoparticule permettant, par exemple, aux siRNA de traverser les membranes biologiques.

Le ciblage tumoral reste à l'heure actuelle un des grands challenges du monde des nanomédecines. La compréhension du microenvironnement tumoral est indispensable pour adapter et développer correctement les médicaments de demain. L'une des découvertes majeures des années 2000 est la mise en évidence de l'effet EPR « Enhanced permeability and retention effect » par Maeda. En effet, la présence d'un endothélium défectueux et lacunaire relié à une angiogenèse trop rapide ainsi qu'un drainage lymphatique limité, permettent l'accumulation passive des nanoparticules circulant longtemps dans le compartiment sanguin. Le mélanome ne déroge pas à la règle et le ciblage dit « passif » a pu être démontré à l'aide de nombreux vecteurs. Cependant, si une circulation prolongée est permise par l'ajout de longues chaines de polyéthylène glycol (PEG), leur présence limite voire empêche fortement l'internalisation des nanocapsules au sein des cellules. Il s'agit donc aujourd'hui de développer de nouvelles alternatives efficaces combinant les avantages du ciblage passif sans les inconvénients. Pour cela, de récentes stratégies de ciblage se basent sur des caractéristiques micro-environnementales de la tumeur comme l'hyperthermie, l'acidité, la présence d'enzyme... Ce ciblage dit « intelligent » consiste à rendre les particules thermo ou pH-sensibles afin de favoriser la libération du principe actif au site d'action souhaité.

L'objectif de ces travaux a été de concevoir différentes modifications de surface des LNC siRNA telles que la pegylation ou l'ajout de peptide à leur surface. Puis, notre étude s'est focalisée sur l'impact de ces différentes modifications de surface sur le procédé d'internalisation et de libération du siRNA au sein des cellules de mélanome. Enfin, des expérimentations animales ont été conduites dans le but d'étudier également l'influence de ces recouvrements sur la biodistribution et le ciblage tumoral dans un modèle de mélanome humain implanté en sous-cutané chez la souris nude.

Ces travaux ont donné lieu à une publication actuellement soumise dans Journal of Controlled Release

PUBLICATION N°3:

INNOVATIVE AFFITIN AND PEG MODIFICATIONS ONTO siRNA LIPID NANOCAPSULES INFLUENCE CELL UPTAKE, *IN VIVO* BIODISTRIBUTION AND TUMOR TARGETING

PUBLICATION N°3 :

INNOVATIVE AFFITIN AND PEG MODIFICATIONS ONTO SIRNA LIPID NANOCAPSULES INFLUENCE CELL UPTAKE, *IN VIVO* BIODISTRIBUTION AND TUMOR TARGETING

Pauline Resnier[1,2], Anthea Lucrezia Emina[1,2], Natacha Galopin[3], Jérôme Bejaud[1,2], Stephanie David[4], Thierry Benvegnu[5], Frédéric Pecorari[6], Igor Chourpa[4], Jean-Pierre Benoit[1,2], Catherine Passirani[1,2]

[1]PRES LUNAM – Université d'Angers, F-49933 Angers, France

[2]INSERM U1066 – Micro et Nanomédecines biomimétiques, 4 rue Larrey, F-49933 Angers, France

[3]SCAHU – Faculté de Médecine, Pavillon Ollivier, rue haute de reculée, F-49933 Angers, France

[4]EA6295 – Nanosondes et Nanomédicaments, avenus Monge, F-37000 Tours, France

[5]Ecole Nationale Supérieure de Chimie de Rennes – CNRS - UMR 6226, 11 Allée de Beaulieu, CS 50837, F-35708 Rennes, France

[6]UMR CNRS 629 - INSERM U892, CRCNA, F-44007 Nantes, France

* Corresponding author

C. Passirani

INSERM U1066, IBS-IRIS, 4 rue Larrey, 49 933 Angers Cedex 9, France

Tel : +33 244 688 534, Fax : +33 244 688 546 : E-mail : catherine.passirani@univ-angers.fr

Ces travaux ont donné lieu à une publication actuellement soumise pour publication dans Journal of Controlled Release

Abbreviation list

BFI	Biofluorescence imaging
DiD	1,1'-Dioctadecyl-3,3,3',3'-Tetramethylindodicarbocyanine Perchlorate
DiI	1,1'-Dioctadecyl-3,3,3',3'-Tetramethylindocarbocyanine Perchlorate
DOPE	1,2-dioleoyl-sn-glycero-3-phosphoethanolamine
DOTAP	1,2-dioleoyl-3- trimethylammoniumpropane
DSPE-PEG	1,2-distearoyl-sn-glycero-3-phosphoethanolamine-N-[methoxy(polyethyleneglycol)-2000]
DTT	Dithiothréitol
FRET	Fluorescence/Förster Resonance Energy Transfer
I.V.	Intravenous
LNCs	Lipid nanocapsules
MalDSPE-PEG	1,2-distearoyl-sn-glycero-3-phosphoethanolamine-N-[maleimide(polyethyleneglycol)-2000]
siRNA	Small interfering RNA
TE-PEG	Tetraether-polyethylene glycol

Abstract

Malignant melanoma is an aggressive tumor associated to the presence of local and/or distance metastasis. The development of gene therapy by the use of small interfering RNA (siRNA) represents a potential new treatment. However, a protection of siRNA, for example via its incorporation into a nanomedicine, is necessary before injecting them into blood stream. In parallel to the passive targeting usually obtained by pegylation, more and more studies aimed at developing "smart" nanomedicines to deliver efficiently the drug into tumor sites and cells. In this work, siRNA-loaded lipid nanocapsules (LNCs) were modified with DSPE-polyethylene glycol (DSPE-PEG), Tetraether-PEG (TE-PEG), and/or with a model Affitins with no specificity to melanoma tumors, a new high affinity protein, to assay multiple targeting strategies on siRNA LNCs. The uptake of fluorescently labelled LNCs, the nanocarrier integrity and the siRNA release were studied into SK-Mel28 melanoma by flow cytometry, conventional confocal microscopy and confocal spectral imaging in a Förster Resonance Energy Transfer (FRET) mode. SiRNA LNC detection after Human plasma incubation and after intravenous injection were evaluated to compare the protection effect and the stealth properties after surface modifications. Finally, the biodistribution of the different siRNA LNCs in healthy and subcutaneous melanoma mice model was assessed by in vivo biofluorescence imaging (BFI), in order to evaluate the tumor targeting. The insertion of DSPE-PEG induced a strong limitation of the internalization into melanoma cells compared to TE-PEG. The two PEG polymers induced a great plasma protection of siRNA but only DSPE-PEG led to stealth properties, even at low concentration (5mM). The Affitin grafting by thiolation of DSPE-PEG was validated on siRNA LNCs. While DSPE-PEG-Affitin LNCs were not detected in these tumors on subcutaneous melanoma model and did not show unspecific accumulation in organs, DSPE-PEG and TE-PEG LNCs induced significant intratumoral accumulation of modified LNCs. In conclusion, PEG LNC is a promising tool providing an adaptable platform for multiple siRNA targeting strategies.

Keywords

Nanomedicine, melanoma, biofluorescence imaging, stealth properties, passive targeting, active targeting, Affitin

1. Introduction

Malignant melanoma is the most aggressive form of melanoma, causing 80% of death by cancer over the world. Chemotherapy or immunotherapy still fails to cure the high stage of disease with local or distance metastasis. In fact, the maximal response rate is obtained with dacarbazine, the reference treatment, and is limited to 16% of patient. In this way, the use of small interfering RNA (siRNA) could offer the opportunity to play on the expression of protein involved into melanoma resistance to chemotherapy. As described in literature, siRNA can specifically interact with targeted mRNA by RISC (RNA-induced silencing complex) pathways and transitory inhibit the production of protein into cytoplasm [1]. However, this hydrophilic entity is not able to cross alone the cellular membrane. Recently, new nanomedicines have been developed to complex and improve the passage of siRNA through lipid biological membrane such as lipid nanocapsules (LNCs) [2].

In our previous works, LNC formulation, based on emulsion phase inversion, was adapted for siRNA encapsulation via strong electrostatic interactions [3, 4]. Moreover, the transfection efficacy of siRNA LNCs was demonstrated on glioma and melanoma cells with a significant inhibition of the targeted protein in both cases [5].

In the aim of metastasis targeting, the intravenous injection of siRNA appears as an evident administration way. In this case, the encapsulation of siRNA into LNCs should provide its i) protection against blood nucleases, ii) accumulation into tumor site and iii) penetration into intracellular compartment. In this study, the surface of the LNCs was modified by pharmacokinetic modulating moieties. The pegylation, i.e., the addition of long chains of polyethylene glycol (PEG), has been known to play an important role in the efficacy of passive targeting strategy in solid tumor models [6, 7]. This common polymer confers a long time circulation into blood, by limiting the recognition and the massive destruction by innate immune system and then the elimination via the liver. LNCs already showed their capacity to accumulate into tumor microenvironment characterized by leaky junctions of the neovessels and a poor lymphatic drainage by EPR effect (Enhanced Permeability and Retention Effect) [8]. DSPE-PEG (or 1,2-distearoyl-sn-glycero-3-phosphoethanolamine-N-[methoxy(polyethyleneglycol)-2000]) has been usually used in LNCs to improve this passive targeting.

In parallel, emerging archaeal tetraether PEG (TE-PEG) molecules are able to form stable and stealth liposomes [9, 10]. The TE natural lipid has shown strong stability in several conditions such as high temperature, acidic pH and serum media [11]. This lipid, found in Archaea, has been studied for potential application in drug/gene delivery system. It could be a promising candidate for LNC pegylation.

In order to overcome the limits of passive targeting, more and more studies have worked on the development of active targeting strategies by post-insertion of innovative pharmacokinetic modulating

moieties to improve their half-life time, their targeting efficiency or stimuli-sensitivity, and then, their intracellular delivery [12]. Ligands as sugars, peptides or antibodies grafted on nanomedicine surface have been used to recognize specifically tumor antigen in a targeting strategy. Recently, archaeal extremophilic proteins from the "7 kDa DNA-binding" family, such as Sac7d, were developed as scaffold to derive small artificial binding proteins (Affitins) [13, 14]. Binders with high stability and affinity have been isolated by associating the generation of combinatorial libraries of Sac7d variants of the surface originally involved in the binding of DNA and selections against different targets [13-15]. Affitins appear as an alternative to the use of antibody.

In this study, surface modifications of siRNA LNCs were assessed with these innovative TE-PEG polymers and an Affitin model in comparison to classic DSPE-PEG LNCs. Flow cytometry and confocal fluorescence microscopy were used to determine the LNC capacity to deliver the siRNA into cytoplasm. The LNC integrity after contact with SK-Mel28 human melanoma cells was evaluated by fluorescence confocal spectral imaging (FCSI) using LNCs co-loaded with two fluorophores forming a FRET couple (DiI/DiD) and fluorescently labelled siRNA (siRNA Alexa488). Moreover, the protection against nucleases and blood behavior was determined by vitro and vivo experiments on mice. Finally, biodistribution studies of modified siRNA LNCs on healthy and melanoma tumor graft nude mice were performed to evaluate the elimination and then the tumor targeting potential of these surface modified LNCs.

2. Materials and Methods

2.1. siRNA LNC formulation

2.1.1. Lipids and lipoplexes

For lipid preparation, the cationic lipid DOTAP (1,2-dioleoyl-3- trimethylammoniumpropane) (Avanti® Polar Lipids Inc., Alabaster, AL, USA), solubilized in chloroform, was weighted at the ratio 1/1 (Mol/Mol) with the neutral lipid DOPE (1,2-dioleoyl-sn-glycero-3-phosphoethanolamine) (Avanti® Polar Lipids Inc., Alabaster, AL, USA) to obtain a final concentration of 30 mM of cationic lipid charge, based on the number of lipid charges per molecule, i.e., 1 for DOTAP. After evaporation of chloroform under vacuum, deionized water was added to rehydrate the lipid film overnight at 4 °C. The lipid film was then sonicated for 30 min. Lipoplexes were formulated as a simple equivolume mix of siRNA and lipids. The complexes were characterized by the charge ratio (CR), i.e., the ratio between the positive charges of the lipids and negative charges of the nucleic acids (+/- ratio) fixed to 5 considering our previous results [3].

2.1.2. siRNA LNCs

LNCs were formulated as described previously [16], by combining 20.5 % w/w Labrafac WL 1349 (caprylic-capric acid triglycerides, Gatefossé S.A. Saint-Priest, France), 1.5 % w/w Lipoid S75-3 (Lipoid GmbH, Ludwigshafen, Germany), 16.9 % w/w Kolliphor® HS 15 (BASF, Ludwigshafen, Germany), 1.8 % w/w NaCl (Prolabo, Fontenay-sous-Bois, France), and 59.8 % w/w water (obtained from a Milli-Q system, Millipore, Paris, France) with magnetic stirring. Three temperature cycles between 60 and 95 °C were performed to obtain phase inversions of the emulsion. Subsequent rapid cooling and dilution with ice-cooled water at the last phase inversion temperature (PIT) led to formation of blank LNCs.

To obtain siRNA LNCs, the ice-cooled water introduced during the last temperature cycle, was replaced by aqueous solution containing the lipoplexes. To formulate fluorescent siRNA LNCs, a solution of DiD (1,1′-dioctadecyl-3,3,3′,3′-tetramethylindodicarbocyanine perchlorate; em. = 644 nm; exc. = 665 nm) or DiI (1,1'-Dioctadecyl-3,3,3',3'-Tetramethylindocarbocyanine Perchlorate; em. = 549 nm; exc. = 565 nm) (Invitrogen, Cergy-Pontoise, France) in acetone at 25 mg/mL was prepared, incorporated in Labrafac® and acetone was evaporated before use. In this study, the Na/K ATPase alpha1 subunit siRNA (sense sequence: 5'- GGGCAGUGUUUCAGGCUAAdTdT -3'; antisens: 5'-UUAGCCUGAAACACUGCCCdTdT -3'; Eurogentec, Seraing, Belgium) was used. The coupling of Alexa488 was realized during the synthesis of siRNA to obtain a fluorescent Alexa488 siRNA (em. = 488 nm; exc. = 524 nm, Eurogentec).

2.2. Purification and post-insertion of PEG polymers

Purifications were performed in water (obtained from a Milli-Q system, Millipore, Paris, France) with PD10 Sephadex column (Amersham Biosciences Europe, Orsay, France) to remove the non-encapsulated siRNA and lipoplexes [4]. At the end, the NaCl concentration was adjusted to physiological concentration (150 mM).

The polymers used for post-insertion were 1,2-distearoyl-sn-glycero-3-phosphoethanolamine-N-[methoxy(polyethyleneglycol)-2000] (DSPE-PEG) (Mean Molecular Weight (MMw = 2805 g/mol), 1,2-distearoyl-sn-glycero-3-phosphoethanolamine-N-[maleimide(polyethyleneglycol)-2000] (malDSPE-PEG) (Mean Molecular Weight (MMw = 2942 g/mol) (Avanti Polar Lipids, Inc, Alabaster, USA) and tetraether-[methoxy(polyethyleneglycol)-2000] (TE-PEG) (MMw = 3217 g/mol) synthesized according to Barbeau et al., [11]. Polymers and siRNA LNCs were co-incubated 4h at 37 °C with final polymer concentration adjusted to 5 or 10 mM.

2.3. Affitin coupling on DSPE-PEG LNCs

The Affitins H4 used in this study is specific for chicken hen egg white lysozyme, and has been described previously [15]. To allow coupling via thiol chemistry, a cysteine residue was added to C-terminus of this Affitin by directed mutagenesis. The resulting Affitin (H4-Ct) was coupled to LNC according to Bourseau et al., [17]. Briefly, a solution at 1 mg/mL (corresponding to 110 µM) of Affitins was prepared in water and mixed with DTT (Dithiothreitol, Sigma-Aldrich), a small-molecule redox reagent, at 0.012 mg/mL (corresponding to 80 µM) under stirring at room temperature during 1 h. Affitins with DTT were purified using PD10 Sephadex column (Amersham Biosciences Europe, Orsay, France). PEGylated siRNA LNCs with 10 mM MalDSPE-PEG were mixed with purified Affitins under stirring at room temperature overnight. DSPE-PEG-Affitin LNCs were purified by CL4B sepharose column (Sigma Aldrich). The presence of LNCs was evidenced with turbidity lecture at 580 nm and Affitins by microBCA test (Thermo Fisher, Waltham, MA, USA) according to the manufacturer protocol.

2.4. Characterization of siRNA LNCs

2.4.1. Size and Zeta potential

The size and Zeta potential of LNCs were measured by using the Dynamic Light Scattering (DLS) method using a Malvern Zetasizer® apparatus (Nano Series ZS, Malvern Instruments S.A., Worcestershire, UK) at 25 °C, in triplicate, after dilution at a ratio of 1:200 with deionized water [18].

2.4.2. Encapsulation efficiency (EE)

A spectrophotometric method based on a work recently described by David et al., was used to evaluate the EE [3]. Briefly, siRNA LNCs were mixed with chloroform and water to separate hydrophilic and lipophilic components, respectively. Sodium hydroxide was added to destabilize lipoplexes, and finally absolute ethanol was added to destroy the LNCs. After two centrifugations, four fractions were obtained: free siRNA, free lipoplexes, encapsulated siRNA and encapsulated lipoplexes into LNCs. To determine the concentration of siRNA, the optical density of each sample was determined at 260 nm (UV-2600, Shimadzu, Noisiel, France) in triplicate conditions.

2.5. Cell culture

The SK-Mel28 human melanoma cell lines were grown in Roswell Park Memorial Institute (RPMI) 1640 medium (Lonza, Verviers, Belgium) supplemented with 10 % fetal bovine serum

(Lonza, Verviers, Belgium), 1 % antibiotics (10 units of penicillin, 10 mg of streptomycin, 25 µg of amphotericin B/mL ; Sigma-Aldrich, Saint louis, USA) and 1 % non-essential amino acids (Lonza). Cell lines were cultured according to ATCC protocol and maintained at 37 °C in a humidified atmosphere with 5 % CO_2.

2.6. Cellular uptake

2.6.1. Flow cytometry

Melanoma cells were seeded onto 6-well plates at the density of 50 x 10^4 cells/well and precultured overnight. Before transfection, the medium was changed to a fresh medium without serum. The cells were treated with double fluorescent siRNA LNCs (DiD and Alexa488 siRNA) at siRNA concentration of 0.25 µg/mL for 4h to 48h. Immunostaining was performed to evaluate the internalisation of LNCs and siRNA into SK-Mel28 cells. After kinetic point (4, 8, 24 et 28h), cells were washed twice with PBS (Lonza) and incubation with trypan blue (Lonza) was performed during 1 min following by three PBS washing. Cell suspensions were fixed with PBS/Azide 0.02 %/Formaldehyde 1 %, protected from light and stored at 4 °C. Analyses were performed with a FACScalibur flow cytometer (BD Bioscience, San José, USA) in collaboration with PACeM platform (Angers).

2.6.2. Fluorescence microscopy

Melanoma cells were seeded onto CC2 Labtek 4 chambers (Dominique Dutcher, France) at the density of 50 x 10^4 cells/chamber and precultured overnight. Before transfection, the medium was changed to a fresh medium without serum. The cells were treated with double fluorescent siRNA LNCs (DiD and Alexa488 siRNA) at siRNA concentration of 0.25 µg/mL for 4h to 48h. To stop the reaction, cells were incubated with solution of paraformaldehyde 4 % at 4 °C. Cells were then washed twice with PBS 1X (Lonza) and incubation with DAPI (Sigma, Saint-Louis, MO, États-Unis) was performed during 1 min following by three PBS washing. Cells were analyzed under a fluorescence microscope (Axioscope® 2 optical, Zeiss, Le Pecq, Germany).

2.7. Fluorescence confocal spectral imaging (FCSI)

To follow the nanocarrier behavior in the presence of melanoma cells, siRNA-loaded LNCs were formulated with three different fluorochromes. Two fluorescent probes, DiI and DiD were used respectively as donor and acceptor partners to obtain a FRET (Fluorescence/Förster Resonance Energy Transfer) signal. DiI (abs max at 550 nm, em max at ca 565 nm) was excited with a 488 nm line of a

laser described below. With this excitation wavelength, the DiD fluorescence (abs max at 645 nm, em max at ca 665 nm) can mainly result from FRET. To observe FRET, the LNCs were co-loaded with DiI:DiD mixture at 2:1 molar ratio. In addition, the LNCs were loaded with siRNA conjugated to Alexa488 fluorophore (exc at 488 nm; em max at 520 nm). Therefore, with the triple-labelled LNCs, we excited simultaneously the DiI/DiD FRET couple and the green fluorescence of Alexa488 in order to follow both the LNC integrity and the siRNA distribution.

SK-Mel28 cells were seeded onto CC2 Labtek 4 chambers (Dominique Dutcher, France) at the density of 30 x 10^3 cells/chamber and precultured for 96 h. The medium was then replaced by a suspension of triple-labelled siRNA LNCs in the culture medium at the concentration of 0.50 µg/mL of siRNA and the cells incubated for 0.5, 3.5, 5, or 15 h at 37 °C/5% CO_2. After the treatment, SK-Mel28 cells were washed twice in HBSS supplemented with Ca^{2+} and Mg^{2+}. Then the media chambers were removed, some HBSS supplemented with Ca^{2+} and Mg^{2+} was added to keep the cells alive during the fluorescence confocal spectral imaging (FCSI), and finally the cells were recovered by a lamella.

The FCSI measurements were carried out using a LabRam confocal microspectrometer (Horiba Jobin Yvon, Villeneuve d'Ascq, France) equipped with an automated X–Y–Z scanning stage, a low dispersion grating (300 grooves/mm) and an air-cooled CCD detector. The fluorescence spectra were excited using a 488 nm line of an Ar+ laser (Melles Griot, France) and collected in a confocal mode, through the 50× LWD objective (NA 0.5). For each cell analysis, an equatorial optical section (x–y plane situated at half-thickness of the cell) was scanned with a step of 0.7 µm that provided maps containing typically ≈900 spectra. The cellular auto-fluorescence was completely neglected, because of the absence of any significant fluorescence of the untreated cells under the conditions used (laser power on the sample ca 5 µW, 0.03 s per spectrum). No sample photodegradation was observed.
Both acquisition and treatment of multispectral maps were performed with LabSpec software. Subcellular LNC and siRNA distribution maps were established via analysis of both the intensity and shape of intracellular fluorescence spectra. Briefly, each experimental spectrum was fitted using the least-squares method to a sum of three reference spectra described below. The fitting errors were below 5% (typically 2–4%).

2.8. Plasma protection

SiRNA, siRNA LNCs and surface modified formulations containing 30 µg siRNA were incubated for different time intervals in 50% (v/v) Normal Human Serum (NHS) at 37 °C [19]. Following incubation, samples were stored at -20 °C. Electrophoresis into 1 % (m/vol) agarose gels in TBE buffer containing ethidium bromide (EtB) was performed at 125 V for 20 min and the resulting gels were photographed under UV light.

2.9. *In vivo* experiments

2.9.1. Orthotopic mouse model of melanoma

Six- to eight-week-old female, nude NMRI mice (Elevage Janvier, France) were housed and maintained at the SCAHU; they were processed in accordance with the Laboratory Animal Care Guidelines (NIH Publication 85-23, revised 1985) and with the agreement of the national ethic committee (national authorization N°01315.01, France). Tumor bearing mice were prepared by injecting subcutaneously a suspension of 3×10^6 SK-Mel28 melanoma cells in 100 µl of RPMI medium into the right flank of athymic nude NMRI mice (6-8 week-old females, 20–24 g).

2.9.2. Determination of graphical half-life time

To determine the half-life of formulations, 150 µl of DiD fluorescent siRNA LNCs or surface modified LNCs were administered by single intravenous injection into the tail vein of the healthy mice. Blood samples were collected into heparin microtubes (Sarstedt, Marney, France), centrifuged and plasma were stored at -20 °C. DiD fluorescence of samples was evaluated by Fluoroskan Ascent (Labsystems, Fischer Scientific, Wilmington, USA). The DiD fluorescence of sample was compared to range of fluorescent LNCs diluted into mice plasma. Graphical determination was used for the half-life time, corresponding to the time where 50% of fluorescent LNCs where found in blood.

2.9.3. Biofluorescent imaging

Non-invasive fluorescent imaging (BFI) was performed 15min, 30min, 45min, 1 h, 3 h, 5 h, 8h, 24 h and 48 h post-injection, using the BFI system of the MaestroTM II (CRi, Woburn, USA) equipped with cooled CCD camera and lipid crystal tunable filter (LCTF) and driven with the Maestro 2 software (Cambridge Research & Instrumentation, Inc, USA). Considering the fluorescent characteristics of the DiD fluorescent tag used to follow the LNCs, wavelength spectrum choose is from 600 to 700 nm. In parallel, the light beam was kept constant for each fluorescent measurement, which was ideal with the ringlight, and epi-illumination. As the ringlight was always set at the same height, the excitation energy on the sample would always be the same. Each mouse was anesthetized with a 4% air-isofluran blend. Once placed in the acquisition chamber, the anesthesia of the mice was maintained with a 2% air-isofluran mixture throughout the experiment as described above. With the BFI system, the fluorescent acquisition time was 5 s. Animals were sacrificed at last time acquisition (48h) and dissection of organs was performed to evaluate individually their fluorescence. All data were analysed on Maestro II software to obtain the average fluorescence signal for each organ (photon/sec/cm^2). Ratio between autofluorescence of control organ (without injection of fluorescent

LNCs) and fluorescence of organs receiving the different DiD LNCs were performed to compare all formulations.

2.10. Statistical analysis

Comparisons between all groups, supposed with normal distribution, were performed using a classical analysis of variance (one-way ANOVA) followed by a Tukey's *post-hoc* analysis. The encapsulation efficiencies for modified LNCs and non-modified LNC were compared using a t-test. Statistical significance was ascribed to a threshold p-value of 0.05.

Formulations	Size (nm)	PDI	Zeta potential (mV)	EE (%)
LNCs	74 ±4	0.05 ±0.01	+ 13 ±6	35 ±5
TE-PEG LNCs	74 ±3	0.074 ±0.04	+ 15 ±1	30 ±5
5mM DSPE-PEG LNCs	85 ±2	0.13 ±0.05	- 10 ±4	33 ±4
10mM DSPE-PEG LNCs	94 ±14	0.16 ±0.08	- 16 ±4	36 ±7
10mM DSPE-PEG Affitins LNCs	103 ±13	0.16 ±0.02	- 16 ±4	36 ±3

Table 1: Physico-chemical characterization and encapsulation yield of modified siRNA LNCs. LNCs are incubated with 10mM of tetraether-polyethyleneglycol-2000 (TE-PEG) and 5 or 10mM of 1,2-distearoyl-sn-glycero-3-phosphoethanolamine-N-[methoxy(polyethyleneglycol)-2000] (DSPE-PEG). Grafting of the Affitins (110µM) is performed on 10mM maleimideDSPE-PEG post-inserted LNCs. Results (n=3) are expressed as mean measure ± standard deviation (SD). No difference was demonstrated on encapsulation efficiency (EE) using ANOVA 1F, *post-hoc* Tukey.

3. Results

3.1. Surface modified LNCs

Formulation of siRNA LNCs led to nanoparticles measuring 75 nm and characterized by positive charge (+ 13 mV) (Table 1). The post-insertion of TE-PEG, which structure is described in Table 2, did not induce modifications compared to non-modified siRNA LNCs. With DSPE-PEG, described in Table 2, at 5 and 10 mM concentrations, the size increased proportionally and the zeta potential became negative (- 10 mV ; - 16 mV respectively). The presence of a maleimide group on DSPE-PEG led to the same size than DSPE-PEG LNC one, but with a lower negative zeta potential (- 9 mV *versus* -16 mV) (*Data not shown*). The incorporation of fluorescent probes as DiD, DiI and Alexa488 siRNA did not modify the physico-chemical properties of siRNA LNCs (*Data not shown*).

The Affitin was grafted on 10 mM malDSPE-PEG siRNA LNCs. Turbidity and protein detection confirmed the efficient grafting of the Affitins on DSPE-PEG LNC surface, as obtained previously with the grafting of an antibody by the same chemical reaction in Bourseau *et al.,* [17]. The resulting formulation had a larger size than 10 mM DSPE-PEG LNCs (103 and 94 nm, respectively), while the other parameters did not change (Table 1).

All the different surface modified siRNA LNCs were monodispersed (PDI < 0.2) and the encapsulation efficiency of siRNA was evaluated around 35 % in all cases.

Polymer	Structure	PEG Length (kDa)
TE-PEG	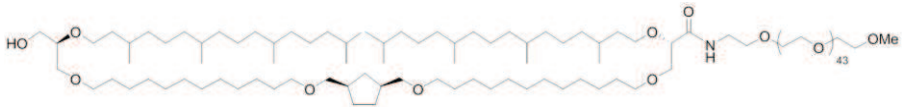	2000
DSPE-PEG	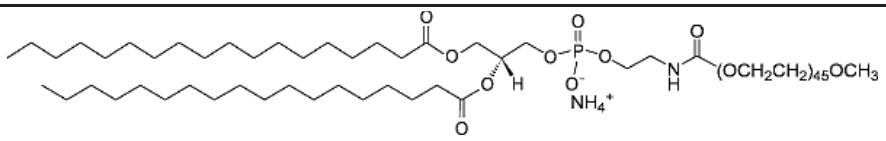	2000
malDSPE-PEG	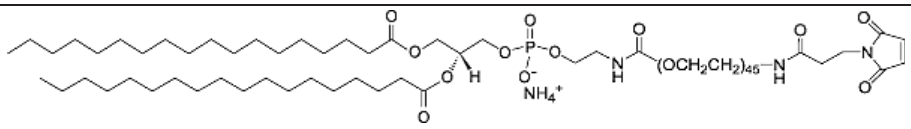	2000

Table 2: Structure of TE-PEG and DSPE-PEG used for siRNA LNCs post-insertion. All polyethylene glycol (PEG) polymer (Tetraether-[methoxy(polyethyleneglycol)-2000] (TE-PEG) and 1,2-distearoyl-sn-glycero-3-phospho ethanolamine-N-[methoxy(polyethyleneglycol)-2000] (DSPE-PEG)) have same PEG length evaluated at 2000 kDa. Two functional groups are used on DSPE-PEG such as methoxy (lane 2) and maleimide (lane 3) with thiol function for the grafting of Affitins via cystein amino acid.

3.2. Behavior of FRET siRNA LNCs in SK-Mel28 cells

The mechanism of siRNA delivery by LNCs was studied on living melanoma cells by fluorescence confocal multispectral imaging, FCSI (Figure 1). In order to follow both the LNC integrity and the siRNA distribution, triple-labelled LNCs were generated by loading them with the DiI/DiD FRET couple and with the siRNA-Alexa488 (see the experimental section). With a 488 nm excitation, both the green Alexa488 fluorescence and the strong FRET of the DiI/DiD couple were recorded simultaneously (black spectrum in Figure 1A: I_{669nm}/I_{569nm} ratio 1.28). Once LNCs were completely disintegrated, for instance by dissolving them in organic solvents, the FRET was lost and the DiD emission band disappeared (I_{669nm}/I_{569nm} ratio decreased to 0.19, *data not shown*).

Using the above considerations, spectral analysis allowed us to distinguish the intracellular situations corresponding to the three model spectra (Figure 1A) and to generate the corresponding merged maps shown in pseudocolors (Figure 1B): i) the blue spectrum and the blue zones

corresponded to 75% of the initial FRET; ii) the green spectrum and the green zones corresponded to 44% of FRET, and iii) the red spectrum and the red zones corresponded to free Alexa488-siRNAs, not co-localized with DiI/DiD (0% FRET).

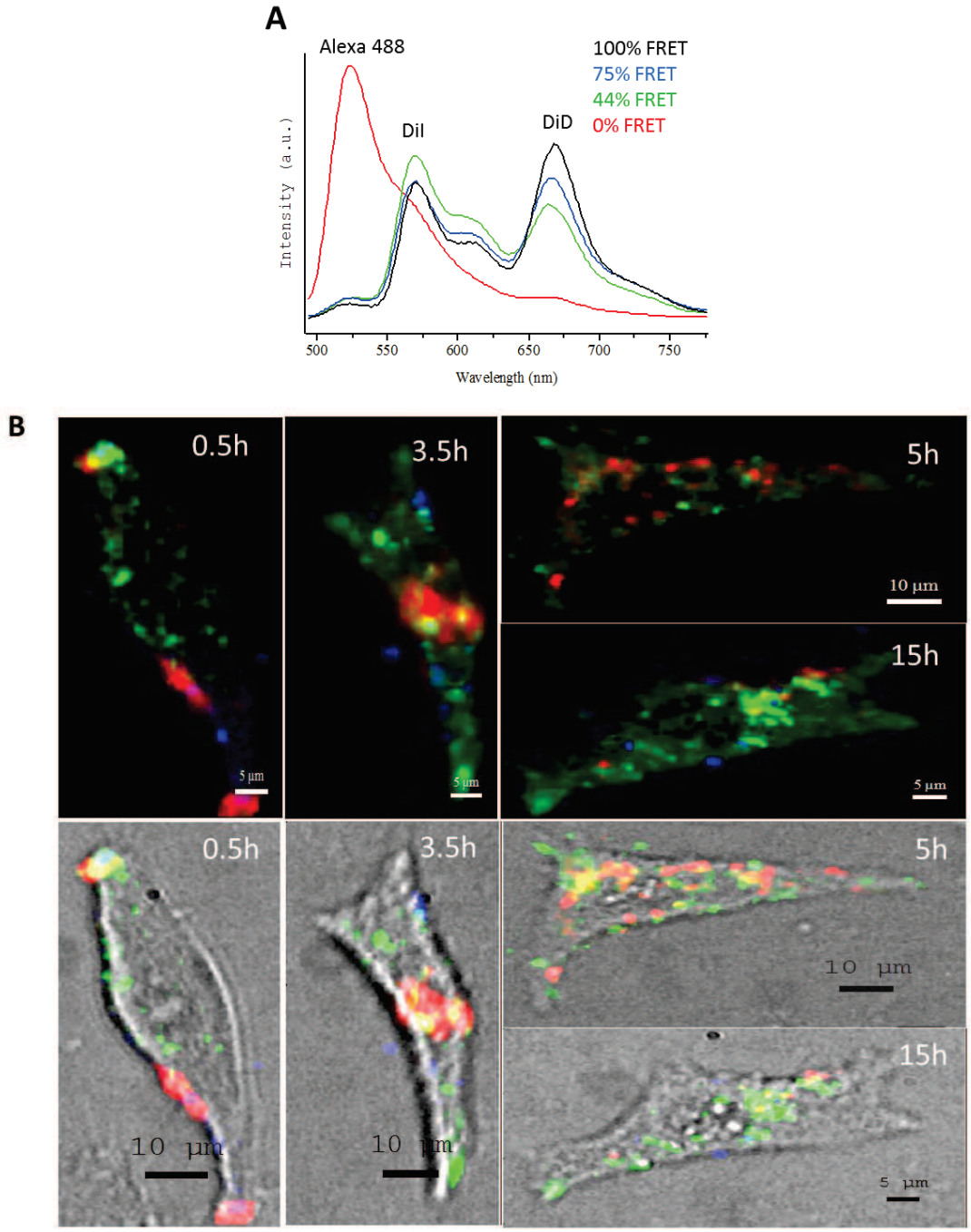

Figure 1: Behavior of siRNA LNCs in SK-Mel28 cells over time as followed by fluorescence confocal spectral imaging, FCSI. (A) Model spectra of triple-labelled control LNCs (100% FRET signal in black), partially degraded LNCs (75% FRET signal in blue and 44% FRET signal in green) and Alexa 488-labeled siRNAs (0% FRET signal in red). (B) Spectral maps (upper panel) and the spectral maps merged with the white light images of the cells (lower panel) of different SK-Mel28 cells over time. The red color represents free siRNA (corresponding to the red spectrum) and the green and blue colors represent the degraded LNCs (corresponding to the green and blue spectra respectively).

The results showed that at 0.5 h of incubation time, LNCs were mostly observed at the cell membrane and only few of them were found in the cytosol. Compared to the initial LNCs, a partial FRET decrease was observed, to 75 % for the LNCs in the cell membranes and to 44 % in the cytosol of cells (respectively blue and green spectra in Figure 1A and blue and green zones in Figure 1B). Although the LNC degradation in membranes was not yet strong at 0.5 h, it gave rise to the appearance of the free siRNA released from the LNCs as shown by the red zones found in the membranes.

At 3.5 h, the cytosol of the cells was significantly enriched with LNCs, while most of the cytosolic LNCs were strongly degraded (green zones). As a result of this degradation, a massive accumulation of free siRNA released from LNCs (large red zones) was observed in the cytosol (Figure 1B). A fraction of the less degraded LNCs (blue zones) was still observed mainly at the periphery membrane of the cell. At 5 h, instead of the massive cytosolic staining of free siRNA commented at 3.5 h, one observed the siRNA localization in numerous small zones distributed in the cytosol. The dissociation of LNCs in cytosol led to the fact that blue zones became rare, even on membranes. At 15 h, only few free siRNA (red spots) were observed in the cell, close to its periphery, while the fluorescence of DiI released from the degraded LNCs was still readily detected in the large zones of cytosol.

3.3. Cellular uptake into melanoma cells

The internalization of LNCs and siRNA was evaluated after modification of LNC surface by different PEG (5 mM DSPE-PEG, 10 mM DSPE-PEG, 10 mM TE-PEG, 10 mM DSPE-PEG-Affitins) in comparison to non-modified LNCs by fluorescent microscopy and flow cytometry (Figure 2 and 3). With microscopy, Alexa488 and DiD encapsulated into LNCs was evidenced in SK-Mel28 cells after contact with LNCs and TE-PEGs. At the opposite, no signal was detected after incubation with LNC DSPE-PEG formulations (5, 10 mM and DSPE-PEG-Affitins) (Figure 2). To evaluate the proportion of positive cells, flow cytometry was realized and a quenching of Alexa488 was performed with trypan blue to discriminate the adsorbed/internalized siRNA (Figure 3). The analysis confirmed the large proportion of positive cells after incubation with non-modified and TE-PEG post-inserted LNCs such as fluorescent microscopy (Figure 2 and 3B). After 4 h of contact, 90 % of cells were Alexa488 positive with non-modified and TE-PEG LNCs and the proportion was constant until 48 h. In this case, the proportion of absorbed siRNA was limited to 20 % at 4 h and decreased over time to few percent (Figure 3B). For DSPE-PEG LNCs, flow cytometry proved the significant lower percentage of cells that internalized the siRNA (lower than 10 %), even at low concentration in DSPE-PEG. Moreover, compared to 10 mM DSPE-PEG LNCs, the presence of Affitin model, which has no specificity for melanoma tumors, at the surface, did not change significantly the interaction of siRNA LNCs with melanoma cells.

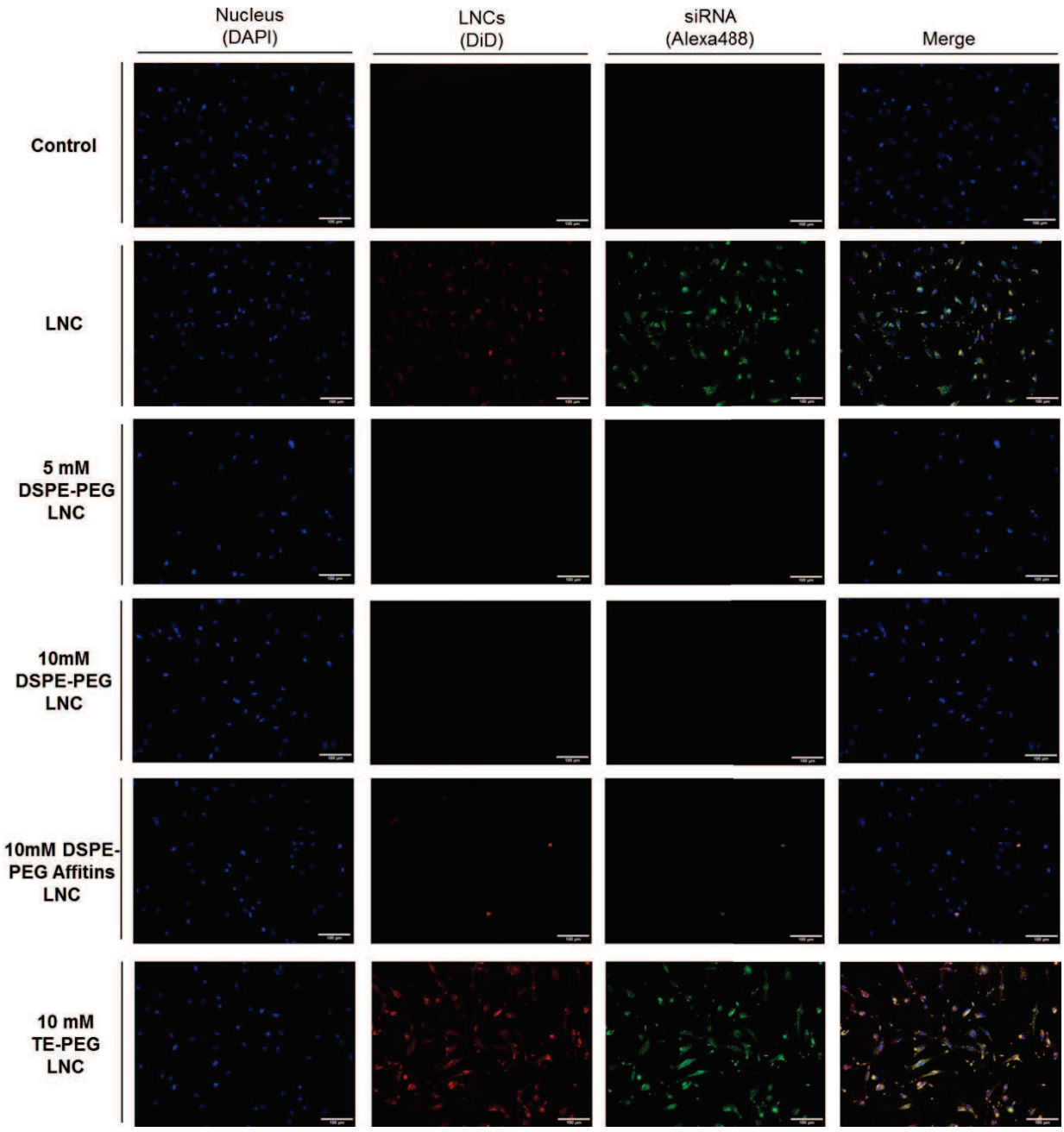

Figure 2: Cellular uptake of siRNA LNCs in melanoma cells in function of surface modification. After two days incubation, fluorescent microscopy was performed with siRNA LNCs on SK-Mel28 human melanoma cells. Cells are fixed on Labtek slide and nucleus staining was performed with DAPI (blue). Double fluorescent probes are used to following siRNA LNCs: lipophilic DiD (red) and Alexa488 siRNA (green). Analysis confirmed the internalization of siRNA LNCs without surface modification or after post-insertion of TE-PEG. At the opposite, all DSPE-PEG LNCs showed no fluorescent signal. Scale bar represents 100µm.

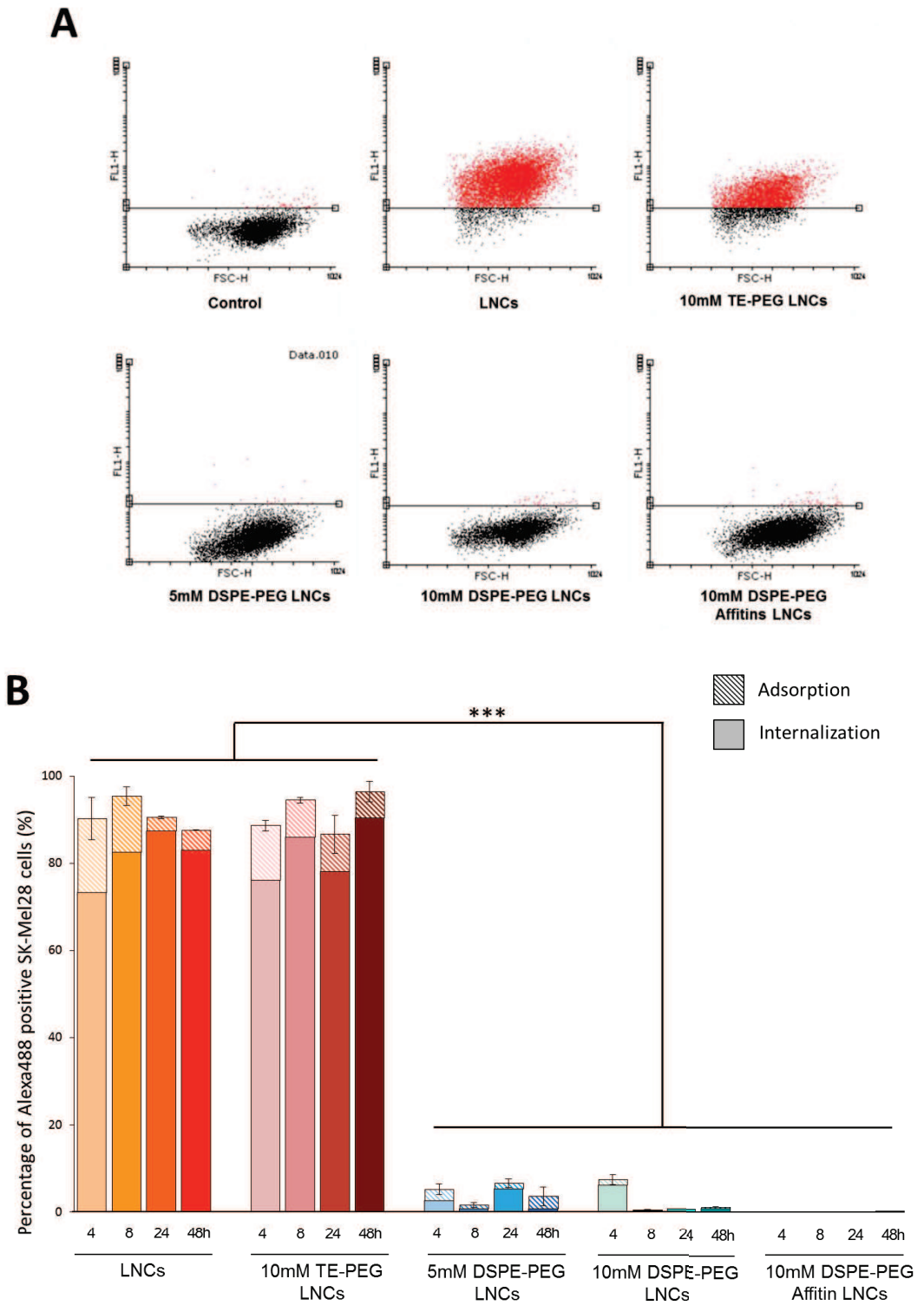

Figure 3: Evaluation of siRNA positive cell by flow cytometry analysis over time thank to lipid nanocapsules. (A) Dot plot analysis evidenced the large uptake of Alexa488 siRNA into melanoma cells for LNCs and TE-PEG LNCs such as fluorescent microscopy. (B) Histograms analysis showed the difference between internalized and adsorbed (hatchted part of barr) siRNA with trypan blue quenching. Data confirmed the large proportion of positive cells with LNCs and TE-PEG LNC with low absorption phenomenon (>10%) contrary to 5 and 10 mM DSPE-PEG LNCs and 10 mM DSPE-PEG-Affitins LNCs at 48h. The mean percentage of fluorescent cells was compared to control cell without fluorescence ± standard error of mean SEM (n=3). Statistical analysis performed with ANOVA 1F, *post-hoc* Tukey, ***p=0.001.

3.4. Plasma protection and blood behavior

Protection of siRNA was evaluated after incubation with human plasma at physiological temperature (Figure 4A). In control conditions with siRNA alone, a rapid degradation by plasmatic nucleases was observed with large degradation at 30 min. Our lipid nanocapsules proved their efficacy to protect the siRNA against nucleases for at less 8 h and longer times up to 24 h or 48 h for all PEGylated LNCs (TE-PEG, 5 and 10 mM DSPE-PEG). The presence of Affitins on DSPE-PEG LNCs did not modify the protection effect against nucleases.

Intravenous injection (i.v) of DiD fluorescent LNCs was performed in tail vein of mice. Blood samples were collected over time to determine the behavior of modified LNCs (5 mM, 10 mM DSPE-PEG, 10 mM TE-PEG, 10 mM DSPE-PEG-Affitins) (Figure 4B). Fluorescence analysis showed that the most rapid elimination profile concerned the LNCs without surface modification. On the figure 4B, TE-PEG LNCs showed a similar profile than non-modified LNCs with a graphical half-life time estimated at 2.5 h, but the elimination was slightly slower. For DSPE-PEG LNCs, the presence of this PEG increased proportionally the graphical half-life time to 6 h and 10 h for 5 and 10 mM of DSPE-PEG respectively. Concerning 10 mM DSPE-PEG-Affitins LNCs, the profile was intermediate with a first part displaying a rapid elimination such as for non-modified LNCs, but a slow elimination such as for 10 mM DSPE-PEG LNCs. In this case, the graphical half-life time was estimated inferior to 4 h.

3.5. Biodistribution on healthy mice

Biofluorescence imaging on animals was realized with Maestro II to evaluate the biodistribution of DiD siRNA LNCs with or without surface modification, after i.v. injection in healthy mice (Figure 5). For siRNA LNC without modification, the maximal signal was obtained after 1 h injection. Non-modified siRNA LNC injection induced a strong hepatic accumulation after 3 h and until 8 h (Figure 5A). The DSPE-PEG post-inserted LNCs showed an important liver localization from 5 h up to 24 h for low concentration (5 mM) with a peak at 8 h. The high concentration of DSPE-PEG (10 mM) on LNCs seemed to limit the liver accumulation and fluorescence signal was diffused in whole mice (Figure 5A). However, after animal dissection at 48 h, results of organ fluorescence evidenced the high level of fluorescence with 5 and 10 mM DSPE-PEG LNCs, especially in liver, spleen, kidneys and bladder (Figure 5B). Surprisingly, very high fluorescence signal was observed in ovary with 5 and 10 mM DSPE-PEG LNCs. Otherwise, the grafting of Affitins at 10 mM DSPE-PEG LNCs modified the biodistribution with liver accumulation contrary to 10 mM DSPE-PEG LNCs between 1 h until 24 h (Figure 5A). However, the global fluorescence signal of DSPE-PEG-Affitin LNC showed no important retention in undesirable organs (Figure 5B). Concerning the TE-PEG siRNA LNCs, biofluorescence imaging on mice and organs dissection demonstrated the accumulation into liver over time with higher signal at 48 h (Figure 5). Moreover, the organ analysis confirmed also the high level

of fluorescence into other organs such as spleen, kidney or bladder for all pegylated LNCs (5 mM, 10 mM DSPE-PEG and TE-PEG LNCs) (Figure 5B).

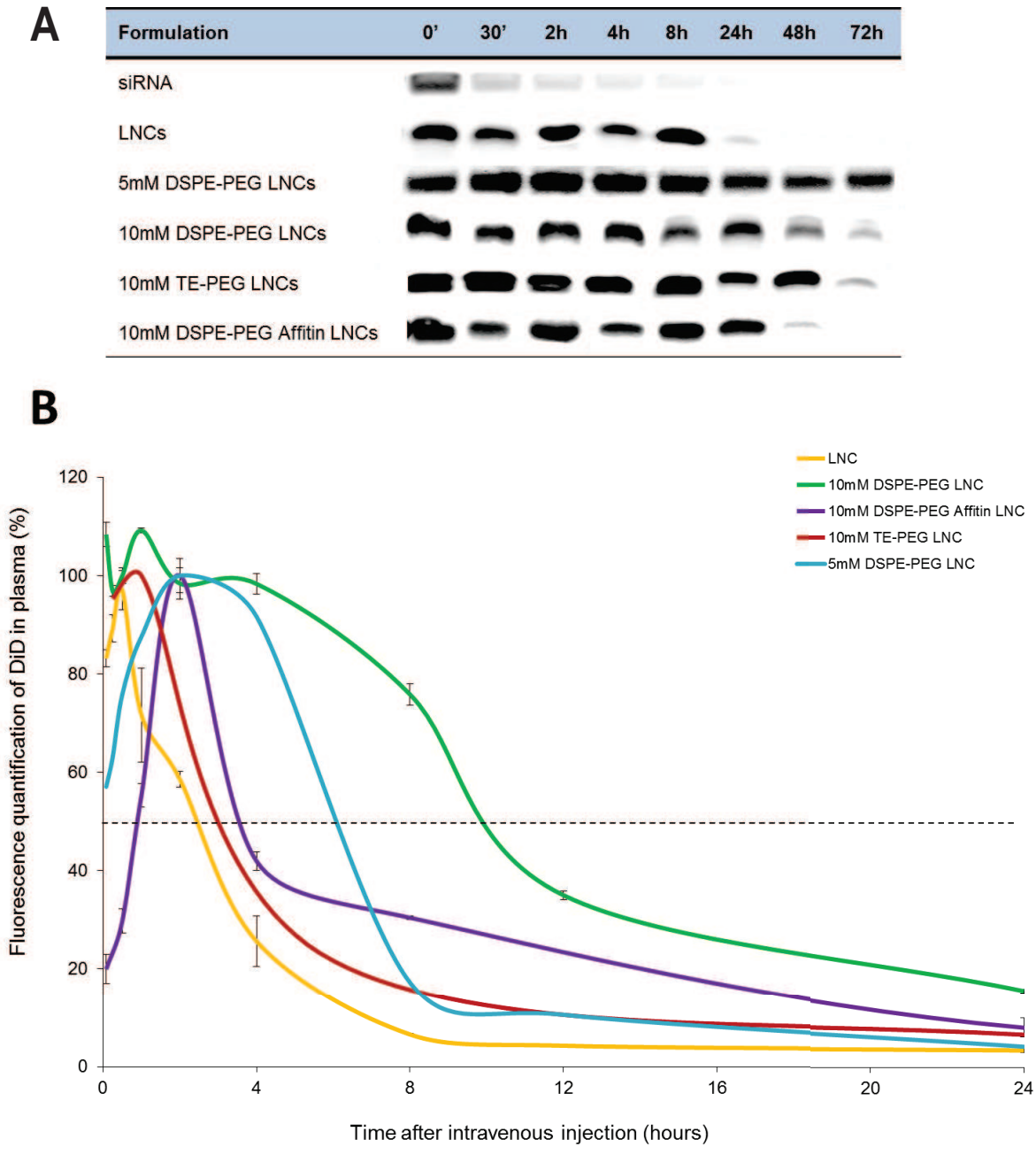

Figure 4: Evaluation of plasmatic protection and blood behavior of siRNA LNCs with different surface modifications. (A) UV light detection of siRNA thank to ethidium bromide (EtB) electrophoresis after incubation with human plasma at 37°C showed the efficient nuclease protection of siRNA with pegylated LNCs. (B) Fluorescence analysis of DiD siRNA LNCs after intravenous injection into tail vein of NMRI Nude mice (female, 6-8 week-old) evidenced the longer plasma detection for pegylated LNCs (n=3).

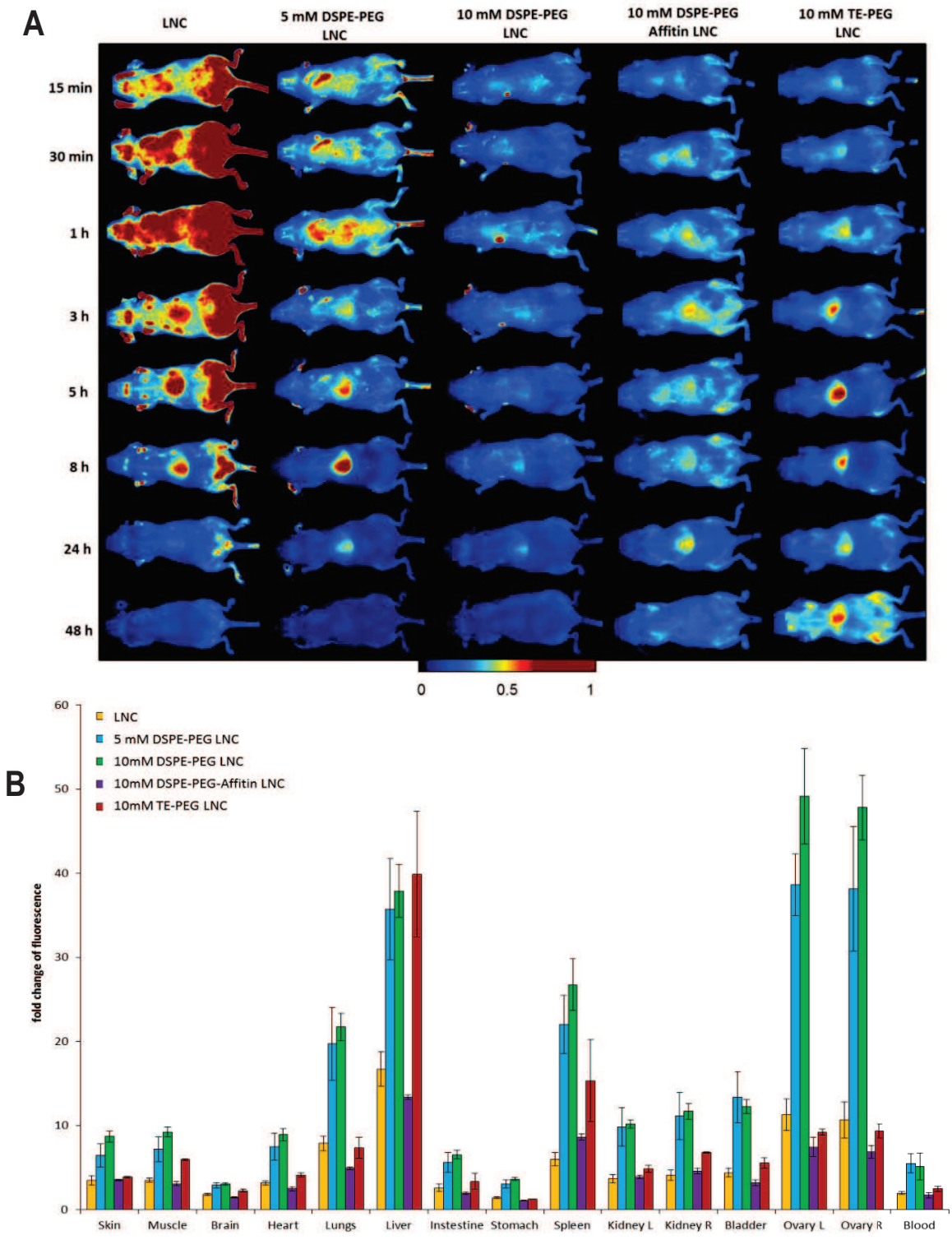

Figure 5: Evaluation of siRNA LNCs biodistribution after intravenous injection in healthy NRMI nude female mice. (A) LNCs (yellow), 5mM DSPE-PEG LNCs (blue), 10mM DSPE-PEG LNCs (green), 10mM DSPE-PEG-Affitin LNCs (violet) and 10mM TE-PEG LNCs (red), encapsulating a fluorescent tracer, DiD, were injected intravenously in healthy mice (n=4) and *vivo* biofluorescence imaging (BFI) were taken at different times (15min, 30min, 1, 3, 5, 8, 24 and 48 hours after injection) from decubitus dorsal views to follow their biodistribution. BFI revealed over time the specific biodistribution and the hepatic elimination of LNCs. (B) Two days after injection; biodistribution in organs was evaluated proving the high liver accumulation for pegylated LNCs compared to LNCs and 10mM DSPE-PEG-Affitins LNCs which was completely eliminated. PEG, polyethylene glycol; TE: tetraether, DSPE: 1,2-distearoyl-sn-glycero-3-phosphoethanolamine-N-[methoxy (polyethylene glycol)-2000]. Mean fluorescence ± Standard error of the mean (SEM).

3.6. Biodistribution on subcutaneous melanoma mice model

Biofluorescence imaging was performed on mice after implantation of subcutaneous melanoma model in right flank (Figure 6). In order to better visualize the tumor, animals were positioned on the left flank, limiting however the visualization of the biodistribution in some of the other organs in comparison to figure 5. Non-modified LNCs presented a spread repartition of fluorescence with liver accumulation such as in healthy animals. However, no specific fluorescence signal was co-localized with tumor site and fluorescence in organs at 48 h confirmed the important hepatic accumulation (Figure 6B). Biofluorescence imaging of DSPE-PEG LNCs showed tumor targeting at early time (1 h and 5 h, for 10 mM and 5 mM DSPE-PEG LNCs respectively) with co-localization at the tumor site. The significant passive accumulation of siRNA LNCs modified with DSPE-PEG was confirmed by tumor fluorescence at 48 h and evidenced also the absence of difference between the two PEG concentrations (Figure 6). Moreover, DSPE-PEG LNC biodistribution in tumor bearing animals showed similar profile than in healthy animals (Figure 6A). Concerning DSPE-PEG-Affitin LNCs, no signal on tumor was observed by biofluorescence imaging and organ biodistribution evidenced the large elimination of this formulation at 48 h compared to other forms such as in healthy animals (Figure 6B). Finally, LNC modified with TE-PEG showed tumor localization later than DSPE-PEG LNCs, 24 h after intravenous injection (Figure 6A). Interestingly, at 48 h, TE-PEG LNCs obtained the higher fluorescence signal in tumor significantly different compared to non-modified and DSPE-PEG-Affitin LNCs (Figure 6B).

4. Discussion

The mechanism of siRNA delivery with LNCs was studied on living melanoma cells by fluorescence confocal multispectral imaging (FCSI). The loss of FRET should correlate with a partial release of the dyes and/or nanocapsule degradation. These results showed that from short incubation times (0.5 h) at 37 °C, LNCs seemed to be degraded by the contact with the cell membrane, represented by a decrease of the DiD component of the FRET signal. This fact may be due to the destructuration of LNCs by fusion at the cell membrane supported by DOTAP/DOPE lipids and leading to the efficient cytoplasm delivery of the siRNAs. In fact, localization of fluorescence was spread into the cytoplasm contrary to concentrated spots that can be observed after endocytosis phenomenon such as with calcium phosphate particles developed recently by Xie et al., [20]. The siRNA transfection seemed to reach a maximum at 3.5 h, where the siRNAs were stained over large cytosolic regions. At 5 h, the siRNAs seemed to be dispatched in the whole cell and the fluorescence signal decreased clearly at longer incubation times (15 h), indicating a release of siRNAs as the signal was observed at the periphery of the cell. Same intracellular trafficking and kinetic was observed for

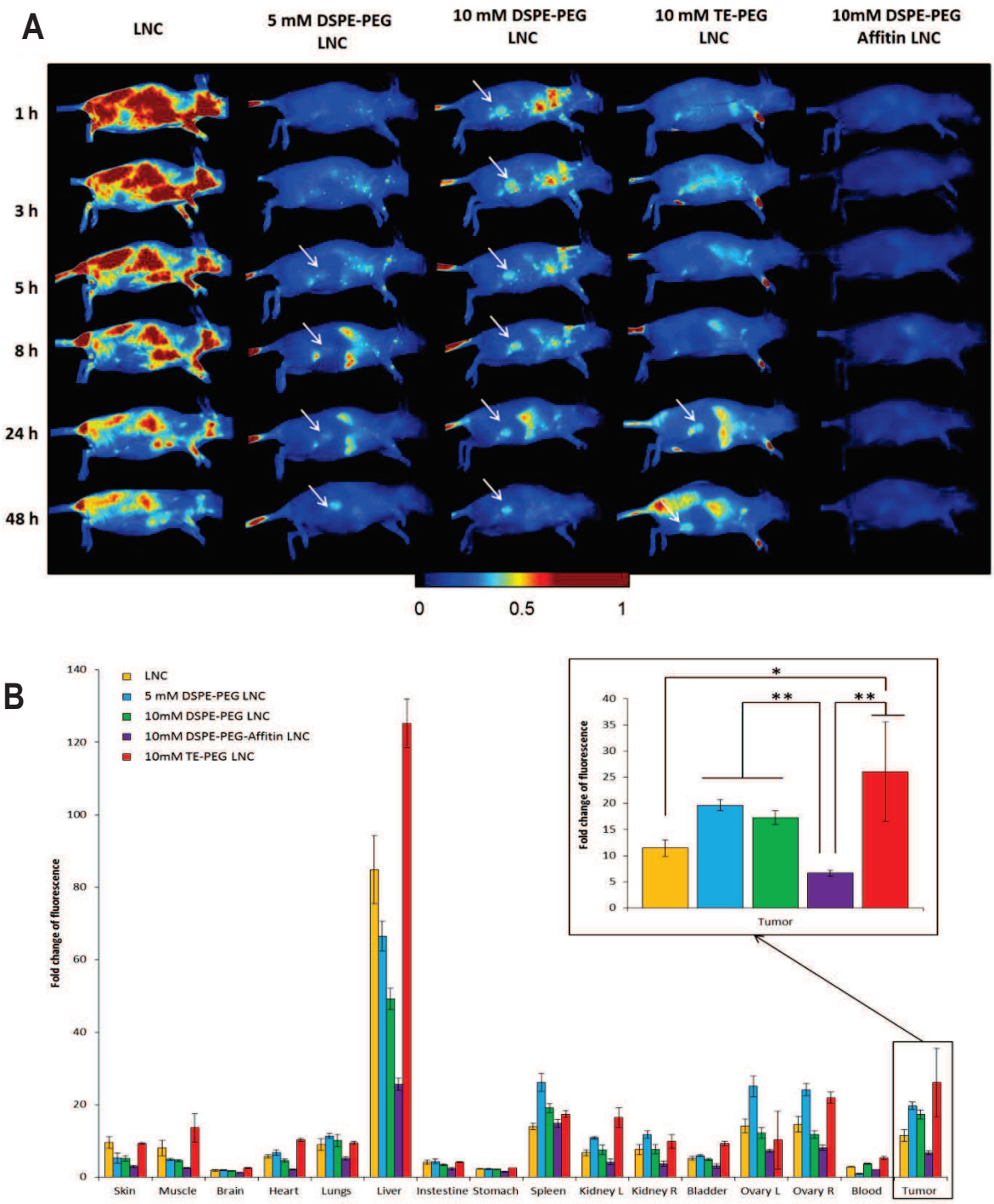

Figure 6: Evaluation of siRNA LNCs biodistribution after intravenous injection in subcutaneous tumor bearing NRMI nude female mice. (A) LNCs (yellow), 5mM DSPE-PEG LNCs (blue), 10mM DSPE-PEG LNCs (green), 10mM DSPE-PEG-Affitin LNCs (violet) and 10mM TE-PEG LNCs (red), encapsulating a fluorescent tracer, DiD, were injected intravenously in mice (n=4) and vivo biofluorescence imaging (BFI) were taken at different times (1, 8, 24 and 48 hours after injection) from lateral views to follow their biodistribution and the tumor targeting. BFI revealed over time the specific tumor targeting in subcutaneous melanoma model for pegylated LNCs. (B) Two days after injection; biodistribution in organs was evaluated proving the high liver accumulation for LNCs and TE-PEG LNCs compared to DSPE-PEG LNCs and 10mM DSPE-PEG-Affitins LNCs. Fluorescence analysis in tumor demonstrated the best signal for TE-PEG and DSPE-PEG LNCs. PEG, polyethylene glycol; TE: tetraether, DSPE: 1,2-distearoyl-sn-glycero-3-phosphoethanolamine-N-[methoxy (polyethylene glycol)-2000]. Mean fluorescence ± Standard error of the mean (SEM), ANOVA 1F, post-hoc Tukey, *$p<0.05$ and **$p<0.01$.

calcium phosphate particles with maximal cytoplasmic loading 4 h after incubation [20]. Furthermore, the mechanism of cellular uptake for blank LNCs (without drug encapsulation) was investigated by Paillard *et al.,* [21]. Interestingly, his result showed clearly that the internalization of blank LNCs passed through energy dependent mechanism such as clathrin pathways or caveole to reach endosomes into cells. Our study evidenced the difference of cellular uptake mechanism with siRNA LNCs in comparison to blank LNCs: the siRNA-loaded nanocarriers seemed to interact more strongly with the cellular membranes. This result could be explained by the siRNA loading, but also by the presence of new excipient in siRNA LNC formulation corresponding to cationic DOTAP and zwiterrionic DOPE lipids. These lipids have proved their interest in nanomedicine fields [2]. In fact, the fusiogenic property of DOPE was demonstrated and attributed to its ability to undergo transition from bilayer to inverted hexagonal structures at low pH, which are known to catalyze the fusion process with the endosomal membrane [22, 23].

The surface modification of nanomedicines with innovative polymers represents an important challenge to improve the tumor targeting after intravenous injection. In this work, various surface coatings (PEG and Affitin protein grafting) were applied on siRNA LNCs and validated without loading modifications. The pegylation was known to improve the half-life time of DNA LNCs and same results were obtained here for siRNA LNCs [6]. However, the addition of DSPE-PEG induced considerable limitation of in vitro cellular uptake avoiding the intracellular siRNA delivery. Actually, this result could be explained by steric interactions between grafted chains and the cell membrane in function of PEG concentration, length and conformation [21, 24, 25]. The comparison of two PEG concentrations in biodistribution and tumor targeting potential evidenced the advantage of choosing the lower tested concentration of PEG inducing a comparable fluorescence. A theoretical calculation estimated that 5 mM led to a surface coating of 10 molecules/nm² or approximatively 3000 PEG molecules/LNC [6].

The grafting of Affitins at the LNC surface, a small artificial binding protein, which is a potent tool for specific recognition of molecules with high affinity, modified the behavior of LNCs as already observed for nanomedicines modified with peptides [21, 26]. As a first step toward active targeting with LNCs, we wanted to study if a model Affitins, i.e. without any affinity for a melanoma biomarker, had intrinsic properties compatible with our goals. In our work, the Affitins did not alter the plasma protection of siRNA in 10 mM DSPE-PEG LNCs. Moreover, Affitin presence on LNCs was associated to the lowest fluorescence signals observed 48 h after injection, confirming the rapid elimination and the absence of accumulation in undesirable organs in healthy and melanoma bearing mice. Ten mM DSPE-PEG-Affitin LNCs induced, at early times, a higher hepatic accumulation than for the 10 mM DSPE-PEG LNCs, probably caused by the recognition of the peptide by the Kupffer cells. In addition, the low fluorescence signal in tumor with 10 mM DSPE-PEG-Affitin LNCs could be related to two causes: i) the absence of expected passive targeting despite the presence of the

DSPE-PEG, and ii) the absence of active target for this control Affitin used in this work. A study of Rangger et al., showed the necessity to study the balance between pegylation and ligand grafting to achieve an efficient and optimized targeting [21]. In conclusion, these results highlight one of the most challenging problems in the targeted delivery of nanoparticles which is to develop high-quality formulations that can give rise to more specific accumulation of nanoparticles in tumors than in other tissues [27].

Finally, the tetraether-PEG (TE-PEG) appears as an innovative solution to replace DSPE-PEG lipid nanocapsules with low influence on cellular uptake and a good plasma protection compared to non-modified LNCs. This archaeal lipid is known to improve the stability of liposomes [11]. Interestingly, TE-PEG LNCs had a short half-life time in blood, but biodistribution profile evidenced their liver and higher tumor accumulation over time. These results are at once interesting, concerning the tumor accumulation and surprising, as the liver accumulation is very late. This efficacy could be explained by a different PEG conformation at LNC surface or different TE interaction with LNC reinforcing the shell. Beyond classic surface modifications of nanomedicines that give longevity in blood stream, some efforts have been recently directed towards developing “smart” nanocarriers [12, 28]. Smart nanomedicines consisted in designing stimuli-sensitive drug delivery system in response to various internal micro-environments such as acidic pH, hyperthermia, or external signal, as magnetism or ultrasound [12]. This TE-PEG appears as a good candidate to create smart targeting with a pH sensitive link adapted to melanoma acidic microenvironment [10, 29]. Affitins display a high stability for acidic pHs [13], and future works should test efficiency of TE-PEG-Affitin formulations using specific Affitins for a melanoma biomarker.

5. Conclusion

Lipid nanocapsules (LNCs) previously demonstrated their capacity to encapsulate efficiently siRNAs. In this study, FRET experiments proved the efficient, time-dependent delivery of free siRNA to the cytosol of human melanoma cells thanks to strong interaction/fusion of LNCs within the cellular membranes. In addition, different surface modifications with PEG chains were assessed on LNCs. While the tested DSPE-PEG LNCs were not able to penetrate into cell, experiments showed the efficient internalization of siRNA and LNCs with TE-PEG LNCs and non-modified LNCs. The biodistribution on melanoma mice model showed the better tumor targeting for pegylated LNCs at 48 h and specifically for TE-PEG LNCs. Moreover, this TE-PEG, recently modified thanks to the addition of pH sensitive link between the PEG and TE molecule, could represent an innovative smart nanomedicine. Finally, the results obtained with an Affitin are encouraging as its presence on LNCs did not induce undesirable side effect. It remains to study if the use of a melanoma specific Affitin combined with an optimized balance of DSPE or TE-PEG/Affitin will allow efficient active targeting.

Acknowledgements

The authors thank SFR ICAT concerning the PACEM platform for flow cytometry and especially Catherine GUILLET for their expertise in this field. We are also grateful to the Dr Joel EYER and Dr Franck LETOURNEL for their collaboration in using the Maestro II, and Dr Guillaume Bastiat for their expertise in statistical analysis. This work was supported by special grants from the "Association de la Recherche contre le Cancer" and by "La Ligue contre le cancer 49 et 35". Frédéric Pecorari is inventor of a patent application (PCT/IB2007/004388), owned by Institut Pasteur and Centre National de Recherche Scientifique (CNRS) related to generation of Affitins. Frédéric Pecorari is a co-founder of a spin-off company of the institute Pasteur/ CNRS/ Université de Nantes that has a licence agreement related to this application.

References

[1] A. Fire, S. Xu, M.K. Montgomery, S.A. Kostas, S.E. Driver, C.C. Mello, Potent and specific genetic interference by double-stranded RNA in Caenorhabditis elegans, Nature, 391 (1998) 806-811.

[2] P. Resnier, T. Montier, V. Mathieu, J.P. Benoit, C. Passirani, A review of the current status of siRNA nanomedicines in the treatment of cancer, Biomaterials, 34 (2013) 6429-6443.

[3] S. David, P. Resnier, A. Guillot, B. Pitard, J.P. Benoit, C. Passirani, siRNA LNCs--a novel platform of lipid nanocapsules for systemic siRNA administration, Eur J Pharm Biopharm, 81 (2012) 448-452.

[4] P. Resnier, P. LeQuinio, N. Lautram, E. André, C. Gaillard, G. Bastiat, J.P. Benoit, C. Passirani, Formulation and structural characterization of siRNA lipid nanocapsules for efficient in vitro gene therapy, Biotechnology Journal, in press (2014).

[5] P. Resnier, S. David, N. Lautram, G.J. Delcroix, A. Clavreul, J.P. Benoit, C. Passirani, EGFR siRNA lipid nanocapsules efficiently transfect glioma cells in vitro, Int J Pharm, 454 (2013) 748-755.

[6] M. Morille, T. Montier, P. Legras, N. Carmoy, P. Brodin, B. Pitard, J.P. Benoit, C. Passirani, Long-circulating DNA lipid nanocapsules as new vector for passive tumor targeting, Biomaterials, 31 (2010) 321-329.

[7] S. David, N. Carmoy, P. Resnier, C. Denis, L. Misery, B. Pitard, J.P. Benoit, C. Passirani, T. Montier, In vivo imaging of DNA lipid nanocapsules after systemic administration in a melanoma mouse model, Int J Pharm, 423 (2012) 108-115.

[8] H. Maeda, J. Wu, T. Sawa, Y. Matsumura, K. Hori, Tumor vascular permeability and the EPR effect in macromolecular therapeutics: a review, J Control Release, 65 (2000) 271-284.

[9] C. Laine, E. Mornet, L. Lemiegre, T. Montier, S. Cammas-Marion, C. Neveu, N. Carmoy, P. Lehn, T. Benvegnu, Folate-equipped pegylated archaeal lipid derivatives: synthesis and transfection properties, Chemistry, 14 (2008) 8330-8340.

[10] T. Benvegnu, L. Lemiegre, S. Cammas-Marion, New generation of liposomes called archaeosomes based on natural or synthetic archaeal lipids as innovative formulations for drug delivery, Recent Pat Drug Deliv Formul, 3 (2009) 206-220.

[11] J. Barbeau, S. Cammas-Marion, P. Auvray, T. Benvegnu, Preparation and Characterization of Stealth Archaeosomes Based on a Synthetic PEGylated Archaeal Tetraether Lipid, J Drug Deliv, 2011 (2011) 396068.

[12] A. Jhaveri, P. Deshpande, V. Torchilin, Stimuli-sensitive nanopreparations for combination cancer therapy, J Control Release, (2014).

[13] G. Behar, M. Bellinzoni, M. Maillasson, L. Paillard-Laurance, P.M. Alzari, X. He, B. Mouratou, F. Pecorari, Tolerance of the archaeal Sac7d scaffold protein to alternative library designs: characterization of anti-immunoglobulin G Affitins, Protein Eng Des Sel, 26 (2013) 267-275.

[14] B. Mouratou, F. Schaeffer, I. Guilvout, D. Tello-Manigne, A.P. Pugsley, P.M. Alzari, F. Pecorari, Remodeling a DNA-binding protein as a specific in vivo inhibitor of bacterial secretin PulD, Proc Natl Acad Sci U S A, 104 (2007) 17983-17988.

[15] A. Correa, S. Pacheco, A.E. Mechaly, G. Obal, G. Behar, B. Mouratou, P. Oppezzo, P.M. Alzari, F. Pecorari, Potent and specific inhibition of glycosidases by small artificial binding proteins (Affitins), PLoS One, 9 (2014) e97438.

[16] B. Heurtault, P. Saulnier, B. Pech, J.E. Proust, J.P. Benoit, A novel phase inversion-based process for the preparation of lipid nanocarriers, Pharm Res, 19 (2002) 875-880.

[17] E. Bourseau-Guilmain, J. Bejaud, A. Griveau, N. Lautram, F. Hindre, M. Weyland, J.P. Benoit, E. Garcion, Development and characterization of immuno-nanocarriers targeting the cancer stem cell marker AC133, Int J Pharm, 423 (2012) 93-101.

[18] G. Bastiat, C.O. Pritz, C. Roider, F. Fouchet, E. Lignieres, A. Jesacher, R. Glueckert, M. Ritsch-Marte, A. Schrott-Fischer, P. Saulnier, J.P. Benoit, A new tool to ensure the fluorescent dye labeling stability of nanocarriers: a real challenge for fluorescence imaging, J Control Release, 170 (2013) 334-342.

[19] W.J. Kim, J.W. Yockman, J.H. Jeong, L.V. Christensen, M. Lee, Y.H. Kim, S.W. Kim, Anti-angiogenic inhibition of tumor growth by systemic delivery of PEI-g-PEG-RGD/pCMV-sFlt-1 complexes in tumor-bearing mice, J Control Release, 114 (2006) 381-388.

[20] Y. Xie, H. Qiao, Z. Su, M. Chen, Q. Ping, M. Sun, PEGylated carboxymethyl chitosan/calcium phosphate hybrid anionic nanoparticles mediated hTERT siRNA delivery for anticancer therapy, Biomaterials, 35 (2014) 7978-7991.

[21] C. Rangger, A. Helbok, E. von Guggenberg, J. Sosabowski, T. Radolf, R. Prassl, F. Andreae, G.C. Thurner, R. Haubner, C. Decristoforo, Influence of PEGylation and RGD loading on the targeting properties of radiolabeled liposomal nanoparticles, Int J Nanomedicine, 7 (2012) 5889-5900.

[22] A. Elouahabi, J.M. Ruysschaert, Formation and intracellular trafficking of lipoplexes and polyplexes, Mol Ther, 11 (2005) 336-347.

[23] Y. Ma, Z. Wang, W. Zhao, T. Lu, R. Wang, Q. Mei, T. Chen, Enhanced bactericidal potency of nanoliposomes by modification of the fusion activity between liposomes and bacterium, Int J Nanomedicine, 8 (2013) 2351-2360.

[24] Y. Li, M. Kroger, W.K. Liu, Endocytosis of PEGylated nanoparticles accompanied by structural and free energy changes of the grafted polyethylene glycol, Biomaterials, 35 (2014) 8467-8478.

[25] E.C. Cho, Q. Zhang, Y. Xia, The effect of sedimentation and diffusion on cellular uptake of gold nanoparticles, Nat Nanotechnol, 6 (2011) 385-391.

[26] W. Dai, Y. Fan, H. Zhang, X. Wang, Q. Zhang, X. Wang, A comprehensive study of iRGD-modified liposomes with improved chemotherapeutic efficacy on B16 melanoma, Drug Deliv, (2014).

[27] A.D. Friedman, S.E. Claypool, R. Liu, The smart targeting of nanoparticles, Curr Pharm Des, 19 (2013) 6315-6329.

[28] N.T. Huynh, E. Roger, N. Lautram, J.P. Benoit, C. Passirani, The rise and rise of stealth nanocarriers for cancer therapy: passive versus active targeting, Nanomedicine (Lond), 5 (2010) 1415-1433.

[29] Y. Kato, S. Ozawa, C. Miyamoto, Y. Maehata, A. Suzuki, T. Maeda, Y. Baba, Acidic extracellular microenvironment and cancer, Cancer Cell Int, 13 (2013) 89.

CHAPITRE III

EVALUATION DU POTENTIEL THERAPEUTIQUE DES NANOCAPSULES LIPIDIQUES DE siRNA

CHAPITRE III:

EVALUATION DU POTENTIEL THERAPEUTIQUE DES NANOCAPSULES LIPIDIQUES DE siRNA

La thérapie génique est une stratégie apparue en clinique au milieu des années 90 avec les premiers essais sur les bébés bulles et autres maladies dites monogéniques. La découverte des ARN interférents, permettant une régulation négative de l'expression des gènes, a alors ouvert de nouvelles perspectives, notamment dans le traitement des pathologies cancéreuses.

Le mélanome métastatique, cancer de la peau de stade IV, est une des formes les plus réfractaires aux traitements chimio-thérapeutiques actuels. Ces résistances peuvent s'expliquer par une incapacité des cellules tumorales à mourir due à un blocage du mécanisme de mort cellulaire qu'est l'apoptose. Des études ont démontré que diverses protéines, impliquées dans le processus d'apoptose, étaient surexprimées dans les mélanomes. Le ciblage de la protéine anti-apoptotique Bcl-2 peut donc se révéler comme un choix judicieux pour un ciblage via les siRNA.

Si l'inhibition de Bcl-2 permet de rétablir la balance entre les signaux pro et anti-apoptotiques, elle n'entraine pas systématiquement la cellule dans un processus de mort cellulaire. En revanche, l'association avec des agents chimio-thérapeutiques pourrait être l'élément déclencheur d'un processus de mort cellulaire. De plus en plus d'études combinent donc les siRNA avec des agents chimio-thérapeutiques afin d'améliorer l'effet de ces agents par synergie.

L'objectif de ces derniers travaux de thèse a été d'utiliser des LNC chargées avec un siRNA ciblant la protéine Bcl-2 afin de démontrer son potentiel antiprolifératif sur le mélanome. Par ailleurs, une association avec de nouvelles molécules anticancéreuses, les ferrocifènes, a été testée avec les LNC siRNA Bcl-2. Des études de co-encapsulation ont été réalisées afin d'étendre les possibilités d'action de ce type de nanomédecines. Enfin, les expérimentations animales ont été effectuées sur un modèle de mélanome humain implanté en sous-cutané chez la souris Nude.

Ces travaux n'ont pas encore été soumis, des manipulations sont en cours pour compléter la partie de co-traitement chez la souris.

PUBLICATION N°4:

EFFICIENT FERROCIFEN ANTICANCER DRUG AND BCL-2 GENE THERAPY USING LIPID NANOCAPSULES FOR *IN VIVO* MELANOMA TREATMENT

PUBLICATION N°4:

EFFICIENT FERROCIFEN ANTICANCER DRUG AND BCL-2 GENE THERAPY USING LIPID NANOCAPSULES FOR *IN VIVO* MELANOMA TREATMENT

Pauline Resnier[1,2], Natacha Galopin[3], Yann Sibiril[4], Alessandro Briganti[1,2], Pierre Legras[3], Anne Vessières[5], Tristan Montier[4], Gérard Jaouen[5], Jean-Pierre Benoit[1,2], Catherine Passirani[1,2]

[1]PRES LUNAM – Université D'Angers, F-49933 Angers, France

[2]INSERM U1066 – Micro et Nanomédecines biomimétiques, 4 rue Larrey, F-49933 Angers, France

[3]SCAHU – Faculté de Médecine, Pavillon Ollivier, rue haute de reculée, F-49933 Angers, France

[4]INSERM U1078 – Transfert de gènes et thérapie génique, Faculté de médecine, 22 avenue Camille Desmoulins, F-29200 Brest, France

[5]CNRS, UMR 7223, Ecole Nationale Supérieure de Chimie de Paris, Paris, France

* Corresponding author

C. Passirani

INSERM U1066, IBS-IRIS, 4 rue Larrey, 49 933 Angers Cedex 9, France

Tel : +33 244 688 534, Fax : +33 244 688 546 : E-mail : catherine.passirani@univ-angers.fr

Ces travaux ont donné lieu à une publication en cours de rédaction.

Abstract

Metastatic melanoma has been described as a high resistance cancer against most chemotherapeutic agents with a best response rate for 16% of patients with dacarbazine. Molecular analysis evidenced the role of apoptosis in resistance of melanoma and especially of the key regulator, Bcl-2. In addition, new metal based drugs, ferrocen derivatives (ferrocifens), showed interesting anticancer potential in resistant cancer model such as triple negative breast cancer. The objective of this study was to combine the two strategies by the use of siRNA for Bcl-2 inhibition and ferrocen-based drug as new potential anticancer agent encapsulated together into lipid nanocapsules (LNCs). The co-encapsulation of siRNA and two ferrocifens (ferrociphenol (FcDiOH) or ansa-ferrociphenol (ansa-FcDiOH)) was assessed into LNCs. The cytotoxicity of ferrocifens and specific extinction of Bcl-2 thanks to siRNA were tested on human melanoma cells after individual encapsulation into LNCs. Cell model and subcutaneous model of melanoma implanted in nude mice were assessed with Bcl-2 siRNA LNCs and ferrocifen LNCs as well as with the combination of ferrocifen and Bcl-2 siRNA in the same LNCs.

The co-encapsulation of each ferrocifen with siRNA was successfully performed and even led to a better encapsulation of siRNA. Experiments on human melanoma cells confirmed the gene extinction of Bcl-2 thanks to LNCs and the ferrocifen anticancer property. Concomitant assays on melanoma cells confirmed the potential of Bcl-2 and ansa-FcDiOH association. Subcutaneous melanoma model was reduced using Bcl-2 LNCs and also with ansa-FcDiOH LNCs but the association of both components into the same nanocapsules did not induce any synergic effect after repeated intravenous injections on one week. LNCs appeared as a promising tool for the co-encapsulation of a metal-based drug and siRNA. Each component showing a reduction of the tumor, a co-encapsulated LNC injection followed by ansa-FcDiOH LNC injection over a longer time should be envisaged in order to evaluate the synergic potential of these nanomedicines.

Keywords

Gene therapy, metal based drug, SK-Mel28, nanoparticles, passive targeting, bio-organometallic

1. Introduction

Malignant melanoma has been the leading cause of death from skin cancer with a 5-year survival rate of less than 10 % [1]. Unfortunately, dacarbazine (DTIC), the FDA approved chemotherapeutic treatment for metastatic melanoma has been known to induce a low response rate (16%) [2]. Since 2011, two targeted therapies, vemurafenib and ipilumimab, which correspond to B-Raf inhibitor and CTLA-4 blocking antibody respectively, have been also evaluated on melanoma patients. However, resistance phenomenon was rapidly described for B-Raf inhibitor with recurrence of metastasis and CTLA-4 showed low response rate as DTIC [3, 4], with a survival median inferior to 13 months. The challenge of melanoma therapy consists in bypassing the high resistance phenomenon limiting or avoiding completely the efficacy of chemotherapy.

The low effect of anticancer drugs was explained by the intrinsic resistance to apoptosis, one of the important hallmarks of cancer, and especially in melanoma [5, 6]. This cell death mechanism is controlled by pro-apoptotic (Bax, Bak) and anti-apoptotic members (Bcl-2, Bcl-$_{XL}$, Mcl-1) [7]. Bcl-2 (B-cell lymphoma 2) is a key regulator in apoptosis pathways blocking the effective oligomerization of Bax and Bak, and thus protecting against cell death [8]. Molecular analysis evidenced the up-regulation of Bcl-2 in melanoma metastasis and this high level was associated to chemoresistance [9, 10]. Interestingly, overexpression of Bcl-2 has been correlated with poor prognosis and short survival [9, 11, 12].

Bcl-2 inhibition was early assessed by antisense oligonucleotide (Oblimersen®) in cancer application and especially in melanoma [13]. While Oblimersen® increased apoptosis in melanoma xenografts and improved their sensitivity to dacarbazine [14-15], the clinical trials did not prove significant difference on patient survival revealing the disillusion [16]. This failure can be explained by i) the use of antisens oligonucleotide that now could be replaced by powerfull tool such as siRNA to modulate specifically the expression of Bcl-2 protein, and ii) the absence of adaptable nanocarriers improving the tumor targeting and then limiting side effect after intravenous administration.

Nowadays, innovative nanomedicines can improve the bioavailability of encapsulated drugs such as anticancer drugs, or nucleic acids [17]. Lipid nanocapsules (LNCs), nanomedicines based on emulsion phase inversion, were adapted recently for small interfering RNA (siRNA) encapsulation providing specific gene extinction. They showed efficient targeting of subcutaneous melanoma cells after intravenous injection [18]. In addition, these nanoparticles have an oily core suitable for the encapsulation and the delivery of lipophilic drugs such as anticancer compounds [19].

Metal based drug represents a promising family of compounds for cancer application and especially ferrocen based drugs (ferrocifens) [20]. These bio-organometallic molecules are defined as active molecules that contain at least one carbon directly bound to a metal or metalloid. In ferrocifens, the metal studied is iron (Fe), and the metallocen derivative is ferrocen [η5-Fe(C_5H_5)$_2$] chemically

grafted on a polyphenolic skeleton, resulting as ferrocenyl phenol derivatives [21]. Ferrocifens have been successfully encapsulated into LNCs and demonstrated interesting anticancer property on resistant cancer such as triple negative breast and glioma cancer model [22].

The association of Bcl-2 siRNA and a new anticancer drug as ferrocifen compounds represent a new opportunity for melanoma treatment. For this, two different ferrocifens were used corresponding to ferrociphenol (FcDiOH) and ansa-ferrociphenol (ansa-FcDiOH). The objective of this work consisted in developing lipid nanocapsules as nanomedicines for an new and efficient double application, i.e., gene therapy with siRNA and anticancer drug delivery with ferrocifens. The efficacy of LNCs to deliver Bcl-2 siRNA and ferrocifens was tested on human SK-Mel28 melanoma cells. Finally, subcutaneous melanoma model implanted in nude mice was used to study their *in vivo* anticancer properties and possible synergic effects.

2. Material and Methods

2.1. Chemical materials

Ferrociphenol (FcDiOH) and ansa-ferrociphenol (ansa-FcDiOH) were prepared by a McMurry cross-coupling reaction as previously described (Table 1) [23]. The lipophilic Labrafac® WL1349 (caprylic-capric acid triglycerides) was purchased from Gattefosse S.A. (Saint-Priest, France), Solutol® HS15 (a mixture of free polyethylene glycol 660 and polyethylene glycol 660 hydroxystearate) by BASF (Ludwigshafen, Germany), Lipoïd® S75-3 (corresponding to soybean lecithin at 69% of phosphatidylcholine) by Lipoïd Gmbh (Ludwigshafen, Germany) and NaCl by Prolabo (Fontenay-sous-bois, France). Deionized water was acquired from a Milli-Q plus system (Millipore, Paris, France).

1,2-DiStearoyl-sn-glycero-3-PhosphoEthanolamine-N-[methoxy-(polyethyleneglycol)-2000] (DSPE-PEG) (Mean Molecular Weight (MMW) = 2805 g/mol), cationic lipid as 1,2-dioleoyl-3-trimethylammoniumpropane (DOTAP) and zwitterionic lipid as 1,2-dioleoyl-sn-glycero-3-phosphoethanolamine (DOPE) were purchased from Avanti Polar Lipids (Alabaster, USA). In this study, the siRNA sequence targeting Bcl-2 protein (sens sequence: 5'-GUGAUGAAGUACAUCCAUUdTdT-3'; antisens: 5'- AAUGGAUGUACUUCAUCACdTdT-3') and scramble sequence as control (sense sequence: 5'-UCUACGAGGCACGAGACUUdTdT-3'; antisens: 5'-AACUCUCGUGCCUCGUAGAdTdT-3') were purchased from Eurogentec (Seraing, Belgium).

Ferrociphenol (FcDiOH)	Ansa-ferrociphenol (ansa-FcDiOH)
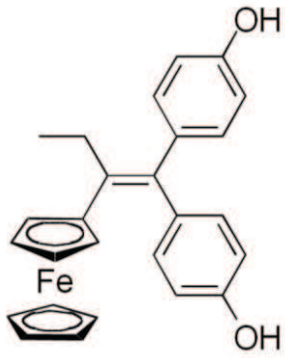	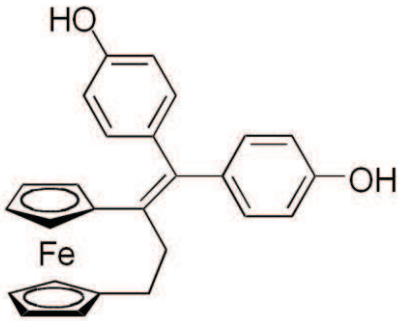

Table 1: Chemical structure of two ferrocifens: ferrociphenol (FcDiOH) and ansa-ferrociphenol (ansa-FcDiOH). Chemical structure evidenced the presence of a characteristic ferrocen group in these two derivatives.

2.1.1. siRNA LNCs

siRNA LNCs were prepared according to a phase inversion method as previously described [25]. Briefly, the preparation process involved 2 steps. Step I consisted of mixing all the excipients (Kolliphor® HS15 (17.2% w/w), Labrafac® (20.8% w/w), NaCl (1.8% w/w), Lipoïd® S75-3 (1.5 % w/w) and water (60.2% w/w) under magnetic stirring and heating from room temperature to 90 °C. Three cycles of progressive cooling and heating between 90 and 60 °C were then carried out. Step II was an irreversible shock induced by rapid dilution with water (33% (v/v)) applied to the mixture at 70–72 °C. Slow magnetic stirring was then applied to the suspension for 5 min. For siRNA encapsulation, lipoplexes in aqueous solution, described above, were introduced during step II as developed in our previous works [18, 26].

2.1.2. Ferrocifen LNCs

Ferrocifen LNCs were prepared according to a phase inversion method as previously described [25]. Ferrocifen compounds (FcdiOH and ansa-FcDiOH), as solid powders, were added at step I with other excipients in order to obtain a final concentration of 6 mg/mL (2% w/w) [22]. The drugs were solubilized during the heating step and ultimately encapsulated over the last cooling step.

2.1.3. Ferrocifen-siRNA LNCs

Ferrocifen-siRNA LNCs were formulated by combining the processes of ferrocifen and siRNA encapsulation. For this, ferrocifen powder was added at step I with all excipients and temperature cycles were performed between 60°C to 90°C. The siRNAs, complexed with lipids in aqueous

solution, were introduced during the step II inducing the irreversible shock in order to formulate the Ferrocifen-siRNA LNCs.

2.2. Purification and post-insertion with DSPE-PEG

Purifications were performed in water (obtained from a Milli-Q system, Millipore, Paris, France) with PD10 Sephadex column (Amersham Biosciences Europe, Orsay, France) to remove the non-encapsulated siRNA and lipoplexes [18]. The NaCl concentration was adjusted after this purification to physiological concentration (150 mM). The post-insertion of 1,2- distearoyl – sn – glycerol – 3 – phosphoethanolamine –N- [methoxy(polyethyleneglycol)-2000] (DSPE-PEG) (Mean Molecular Weight (MMw = 2805 g/mol) was performed by incubation of LNCs at 37 °C during 4h with final PEG polymer concentration at 5 mM.

2.3. Characterization of siRNA LNCs

2.3.1. Size and Zeta potential

The size and Zeta potential of LNCs were measured by using the Dynamic Light Scattering (DLS) method using a Malvern Zetasizer® apparatus (Nano Series ZS, Malvern Instruments S.A., Worcestershire, UK) at 25 °C, in triplicate, after dilution at a ratio of 1:200 with deionized water [27].

2.3.2. Encapsulation efficiency

siRNA quantification - A spectrophotometric method based on a work recently described by David et al., (2012) was used to evaluate the encapsulation efficiency (EE) [24]. Briefly, siRNA LNCs were mixed with chloroform and water to separate hydrophilic and lipophilic components, respectively. Sodium hydroxide was added to destabilize lipoplexes, and finally absolute ethanol was added to destroy the LNCs. After two centrifugations, four fractions were obtained: free siRNA, free lipoplexes, encapsulated siRNA and encapsulated lipoplexes into LNCs. To determine the concentration of siRNA, the optical density of each sample was determined at 260 nm (UV-2600, Shimadzu, Noisiel, France) in triplicate conditions.

Ferrocifen quantification - The determination of the ferrocifen loading into LNCs was achieved by spectrophotometry at 254 nm after dissolving 10 µL of LNCs into 5 mL of methanol (Fisher chemical) before and after LNC filtration on 0.2µm filter (GHP Pall, Acrodisc, VWR international, Fontenay-sous-bois, France). The calibration curve, ranged from 10 µM to 100 µM, was also prepared in methanol.

2.4. SK-Mel28 melanoma cell culture

The SK-Mel28 human melanoma cell line was grown in Roswell Park Memorial Institute (RPMI) 1640 medium (Lonza, Verviers, Belgium) supplemented with 10 % fetal bovine serum (Lonza, Verviers, Belgium), 1 % antibiotics (10 units of penicillin, 10 mg of streptomycin, 25 µg of amphotericin B/mL ; Sigma-Aldrich, Saint louis, USA) and 1 % non-essential amino acids (Lonza). Cell lines were cultured according to ATCC protocol and maintained at 37 °C in a humidified atmosphere with 5 % CO_2.

2.5. Western blot

After transfections or *vivo* experiments, total proteins were extracted from melanoma cells by scraping with a cell lysis buffer (10 mmol/L Tris-Base, 1 mmol/L Na3O4, and 1 % SDS, pH 7.4) and stored at -20°C, or melanoma tumor were grinded with Ultra-turrax (Ika imlab, Lille, France) in same buffer lysis. Twenty micrograms of proteins were resolved on 10% (v/v) SDS-PAGE gel and transferred to a nitrocellulose membrane (0.45-µm pore size) (Amersham GE Healthcare). Mouse anti-human Bcl-2 (ab694, Abcam) and mouse anti-human actine (Clone C4; Millipore), used as loading controls, were diluted, respectively, at ratios of 1:500 and 1:5,000 according to the manufacturer's instructions and incubated over night at 4°C. A second mouse antibody (Dako) was used at a dilution of 1:2,000. Detection (using LAS4000, GE HealthCare) was performed using enhanced chemoluminescence (ECL; Fisher Scientific, Pierce).

2.6. RT-q-PCR

Total RNA of cells were extracted and purified using RNeasy Microkit (Qiagen, Courtaboeuf, France), and treated with DNase (10 U DNase I/µg total RNA). RNA concentrations were determined using a ND-2000 NanoDrop (Thermo Fisher Scientific, Wilmington, Delaware USA) and used for normalization of the input RNA in the Reverse transcription. First strand cDNA synthesis was performed with a SuperScript™ II Reverse Transcriptase (Invitrogen), in combination with random hexamers, according to the manufacturer's instructions. Following first-strand cDNA synthesis, cDNAs were purified (Qiaquick PCR purification kit, Qiagen, Courtaboeuf, France) and eluted in 40 µL RNAse free water (Gibco). 3ng of cDNA was mixed with Maxima™ SYBR Green qPCR Master Mix (Fermentas) and primer mix (0.3 µM) in a final volume of 10 µL. Amplification was carried out on a LightCycler 480 (Roche) with a first denaturation step at 95°C for 10 min and 40 cycles of 95°C for 15 s, 60°C for 30 s. After amplification, a melting curve of the products determined the specificity of the primers for the targeted genes. A mean cycle threshold value (Cq) was obtained from 2

measurements for each cDNA. Specific gene expression was calculated using the $2^{-\Delta\Delta CT}$ method using GAPDH as calibrator.

2.7. Determination of cell viability

Melanoma cells were seeded onto 24-well plates at a density of 5 x10^4 cells/well and pre-cultured overnight. Dose dependent transfection was realized as described above to determine the IC_{50} and cells were subsequently cultured during two days. Cytotoxicity assays were performed using MTS (3-(4,5-dimethylthiazol-2-yl)-5-(3-carboxymethoxyphenyl)-2-(4-sulfophenyl)-2Htetrazolium) (Promega, Madison, USA). For this, 100 µL of MTS/well were disposed and plates were incubated 2.5 h à 37 °C in a humidified atmosphere with 5 % CO_2. The OD was evaluated by Mutliskan Ascent (Labsystems, Fisher Scientific, Wilmington, USA) at 492 nm.

2.8. Orthotopic mouse model of melanoma

Six- to eight-week-old female, nude NMRI mice (Elevage Janvier, France) were housed and maintained at the SCAHU; they were processed in accordance with the Laboratory Animal Care Guidelines (NIH Publication 85-23, revised 1985) and with the agreement of the national ethic committee (authorization N°01315.01, 12/2013, France). Tumor bearing mice were prepared by injecting subcutaneously a suspension of 3 × 10^6 SK-Mel28 melanoma cells in 100 µl of PBS 1X into the right flank of mice (20–24 g). After three weeks of tumoral growth, treatments (PBS, blank LNCs, ferrociphenol-LNCs, siRNA LNCs) were applied intravenously with daily injections during one or three weeks. To determine the tumor volume, each mouse was monitored at the indicated time by measurement of tumor size and tumor volume was estimated using the formula: $V= 6/\pi*length*width^2$.

2.9. ALAT—ASAT determination

Blood samples were collected from the lateral saphenous vein from animals receiving no injections (n = 4), siRNA LNCs (n = 8), and PEG siRNA LNCs (n = 8). Blood was collected before and day 2, 4 and 9 after LNC injections on different animals (two per condition per day) to prevent a too great loss of blood, and were collected in Microvette collection tubes (Sarstedt, Numbrecht, Germany). Afterwards, the samples were centrifuged for 2 minutes at 10,000 g at 4 °C and the plasma removed for further analysis. ALAT and ASAT values were determined using a Selectra-E (Elitech, Signes, France).

2.10. Statistical analysis

Comparisons between all groups, supposed with normal distribution, were performed using a classical analysis of variance (one-way ANOVA) followed by a Tukey's *post-hoc* analysis. Statistical significance was ascribed to a threshold p-value of 0.05.

3. Results

3.1. Description of LNCs and co-encapsulation

The size of LNCs was not significantly modified by the encapsulation of all tested drugs (Table 2). At the opposite, the zeta potential was influenced in function of encapsulated drugs. Contrary to negative blank and ferrocifen LNCs, the cationic lipid used for siRNA binding induced a positive charge of LNCs. Concerning the encapsulation, siRNA and the two ferrocifen drugs alone were efficiently encapsulated individually such as in our previous works [18, 22]. The formulation led to an encapsulation efficiency of siRNA evaluated at 35 % and more than 90% for ferrociphenol (FcDiOH) and ansa-ferrociphenol (ansa-FcDiOH) (Table 2). Interestingly, the co-encapsulation of siRNA and ferrocifens induced a significant higher encapsulation efficiency of siRNA (Table 1). However, this co-encapsulation induced slightly, but significant, lower encapsulation of ferrocifens.

Formulation	Size (nm)	PDI	Zeta (mV)	siRNA EE (%)	Fc EE (%)
Blank LNCs	77 ±2	0.08 ±0.01	- 7 ±2	/	/
siRNA LNCs	74 ±4	0.05 ±0.01	+ 13 ±2	35 ±5	/
FcDiOH LNCs	65 ±2	0.07 ±0.01	- 4 ±1	/	92 ±2
ansa LNCs	64 ±4	0.05 ±0.01	- 4 ±2	/	96 ±1
si+FcDiOH LNCs	65 ±1	0.04 ±0.01	+ 15 ±15	63 ±5 *	82 ±5 *
si+ansa LNCs	69 ±5	0.11 ±0.03	+ 11 ±13	49 ±12 *	85 ±7 *

Table 2: Physico-chemical characterization and encapsulation yield of siRNA LNCs, each ferrocifen LNCs and their co-encapsulated forms. All lipid nanocapsules (LNCs) led to monodispersed nanomedicines with size ranging between 60 and 80 nm. SiRNA encapsulation conducted to a positive zeta potential, contrary to blank and ferrocifen encapsulation into LNCs. Interestingly, the co-encapsulation of siRNA and ferrocifen induced a significant higher siRNA encapsulation. Results are expressed as mean measure ± standard deviation (SD) (n=3). Statistical analysis, to compare the co-encapsulation form to single encapsulation, was performed using a t-test, *p=0.05. FcDiOH: ferrociphenol, ansa-FcDiOH: ansa-ferrociphenol, LNCs: lipid nanocapsules.

3.2. Extinction of Bcl-2

The extinction of Bcl-2 protein was tested using siRNA tools. The transfection efficacy of LNCs was compared to a commercial agent one (Oligofectamine®) (Figure 1). Protein and gene analysis evidenced the similar inhibition of Bcl-2 protein with Oligofectamine® and siRNA LNCs (50% vs 45%) with a mRNA level significantly reduced compared to control conditions (45 % vs 0 %, respectively) (Figure 1).

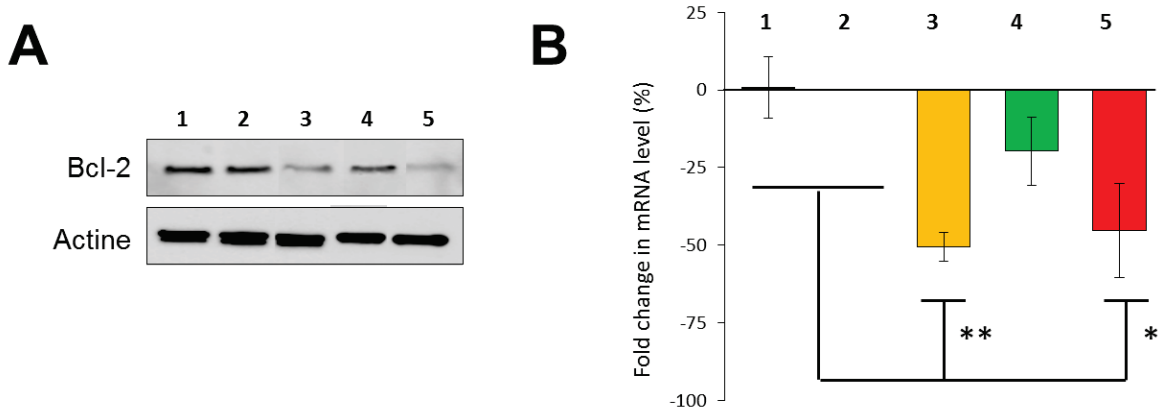

Figure 1: Protein and gene extinction of Bcl-2 by siRNA lipid nanocapsules. Bcl-2 expression was tested by western blot (A) and RT-q-PCR analysis (B). 1: Cells, 2: Oligofectamine® siRNA scramble, 3: Oligofectamine® siRNA Bcl-2, 4: scramble siRNA LNCs; 5: Bcl-2 siRNA LNCs. mRNA levels are expressed as mean measure ± standard error of the mean (SEM) (n=3). Statistical analysis was performed by ANOVA 1F, *post-hoc* Tukey, ** $p<0.01$, *$p<0.05$.

3.3. Ferrocifen activity on melanoma cells

The action of FcDiOH and ansa-FcDiOH was tested and compared to reference chemotherapy used for metastatic melanoma, dacarbazine (DTIC). Human SK-Mel28 melanoma cells showed resistance to DTIC, even at high concentration (superior to 100 µg/mL) (Figure 2). FcDiOH and ansa-FcDiOH compounds showed significantly high cytotoxicity compared to DTIC on melanoma cells, with an IC_{50} estimated at 1.3 µg/mL and 0.5 µg/mL respectively (corresponding to 3 µM and 1.2 µM) (Figure 2).

Interestingly, the best efficacy was evidenced on melanoma cells with ansa-FcDiOH. Encapsulated forms of FcDiOH and ansa-FcDiOH into LNCs presented the same toxicity profiles than free drugs, evidencing the capacity of LNCs to deliver ferrocifens into melanoma cells.

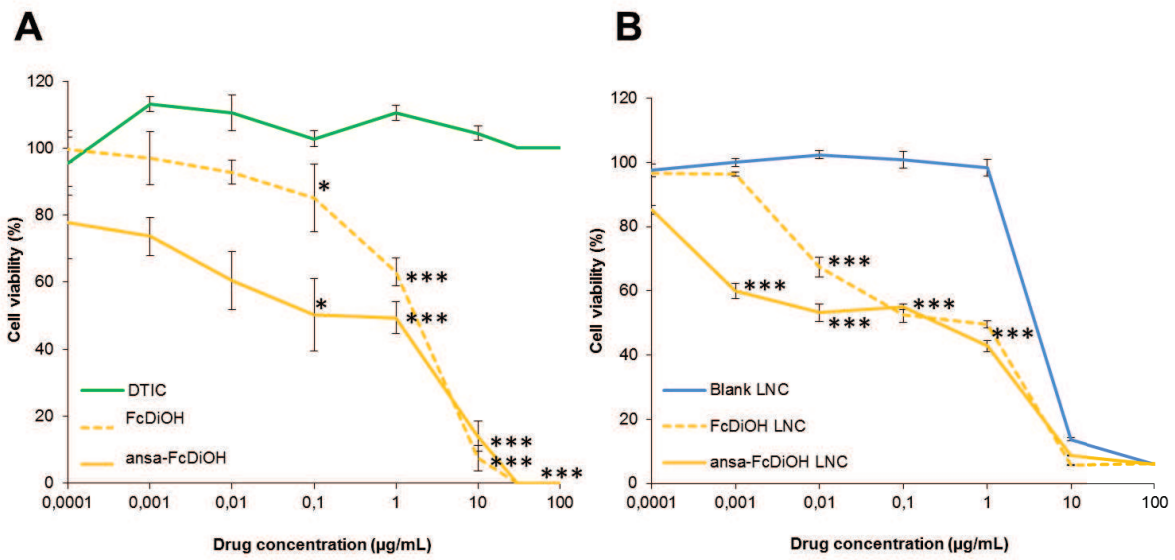

Figure 2: Cytotoxicity of free and LNC-encapsulated ferrocifens on human melanoma cell line Sk-Mel28. (A) Free FcDiOH (yellow dotted line) and ansa-FcDiOH (yellow line) solubilized in organic solvent showed significant toxicity on melanoma cell line compared to reference chemotherapy (DTIC, solubilized in water) (green line). Ansa-FcDiOH had the lower IC_{50} values estimated at 1 µM (compared to 3µM for FcDiOH). (B) Encapsulated FcDiOH (yellow dotted line) and ansa-FcDiOH (yellow line) into lipid nanocapsules (LNCs) induced a significant specific toxicity compared to blank LNCs (blue line). Percentage of cell viability was expressed as mean percentage ± standard error of the mean (SEM) (n=3). Statistical analysis compared to control condition (DTIC or blank LNCs) was performed by ANOVA *post-hoc* Tukey, ***p<0.001, **p<0.01, *p<0.05. DTIC: dacarbazine, FcDiOH: ferrociphenol, ansa-FcDiOH: ansa-ferrociphenol.

3.4. Chemo-sensitization of melanoma cells

The combination of Bcl-2 siRNA and ferrocifens was assessed on human melanoma cells in order to study a possible synergic effect (Figure 3). The association of Bcl-2 siRNA was assessed with DTIC, FcDiOH and ansa-FcDiOH. The transfection of Bcl-2 LNCs siRNA did not induce strong toxicity such as scramble and blank LNCs (79 % *versus* 89 % and 94 %). The combination of Bcl-2 siRNA with DTIC or FcDiOH did not show any synergic effect. Finally, the concomitant treatment with Bcl-2 siRNA and ansa-FcDiOH conducted to important cytotoxicity compared to individual treatment (46 % *versus* 79 % for Bcl-2 and 90 % for ansa-FcDiOH), demonstrating a significant synergic effect compared to control conditions.

3.5. Bcl-2 siRNA treatment on tumor growth

Three weeks after cell implantation, repeated intravenous injections of siRNA LNCs were performed in tail vein of nude mice during 5 days (1 IV/day) corresponding to 0.75 mg/kg/day of siRNA/day. No toxicity was observed on mice during all experiment protocols. Control group (without treatment, n=10) was compared to blank LNCs (n=10), control siRNA LNCs (n=8) and Bcl-2 siRNA LNCs (n=8) (Figure 4A). Evaluation of tumor volume evidenced the absence of effect using blank and control siRNA LNCs compared to Bcl-2 LNCs inducing 30 % of volume reduction.

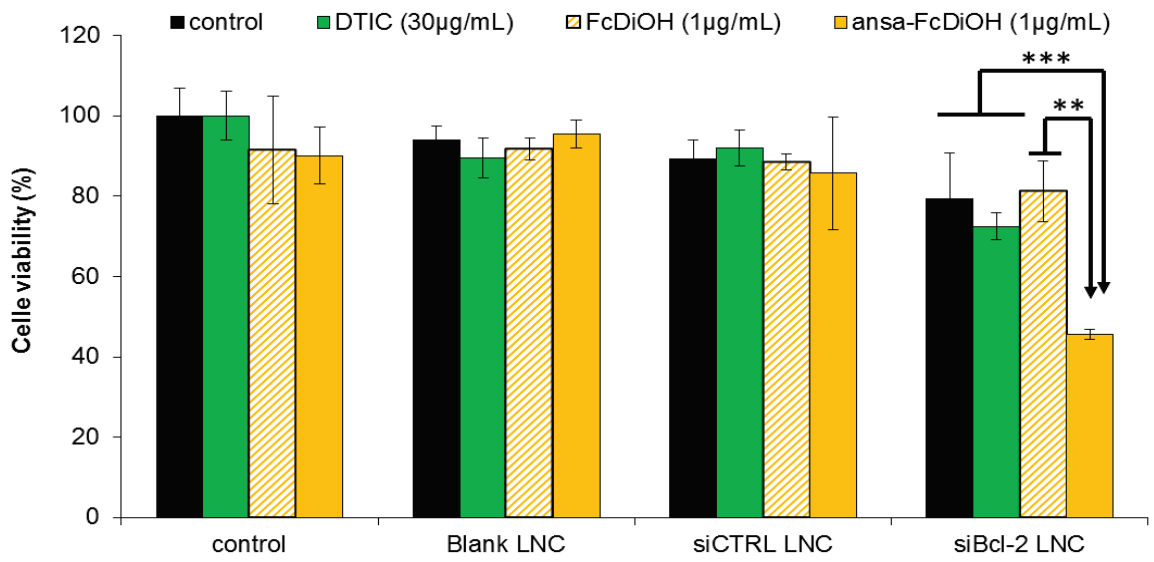

Figure 3: Association of siRNA LNCs with reference chemotherapy or ferrocifens on melanoma cell line. Control, blank, control siRNA and Bcl-2 siRNA LNCs were associated to chemotherapeutic drugs such as DTIC (green), FcDiOH (yellow, striped), and ansa-FcDiOH (yellow) to evidence a possible additive or synergic effect of concomitant treatment. Results showed the potential of synergic association of Bcl-2 with ansa-FcDiOH. Percentage of cell viability was expressed as mean percentage ± standard error of the mean (SEM) (n=1). Statistical analysis was performed by ANOVA 1F *post-hoc* Tukey, *** p=0.001, **p=0.01. DTIC: dacarbazine, FcDiOH: ferrociphenol, ansa-FcDiOH: ansa-ferrociphenol.

Finally, the dissection of the tumor at D21 confirmed their lower mass for the group that received the Bcl-2 siRNA LNCs (-32 % compared to control group and -28 % compared to scramble and blank LNCs) (Figure 4B). Extraction of proteins in tumor at D5 and D21 was performed to study the *vivo* transfection efficacy of siRNA LNCs. While any inhibition was observed at D21 (*data not shown*), at early time (Day 6), after repeated intravenous injections of Bcl-2 siRNA LNCs, the specific inhibition was evidenced on one half of the animals (Figure 4C) demonstrating the potential *in vivo* transfection efficacy of siRNA LNCs after intravenous injections.

3.6. Ferrocifen treatment on tumor growth

Ferrocifens were tested on subcutaneous melanoma model induced in nude mice. Repeated intravenous injections were performed during three weeks (1 IV/day, 5 days consecutively, 3 weeks). FcDiOH LNCs (n=8) and ansa-FcDiOH LNCs (n=8) at 45 mg/kg were compared to control groups (n=10) and positive control (n=10) with single i.p. injection of DTIC at 100 mg/kg (Figure 5A). Tumor volume analysis demonstrated the efficacy of ansa-FcDiOH LNCs to reduce the progression contrary to FcDiOH LNCs and control group estimated at -30% and -38%, respectively. Interestingly, ansa-FcDiOH LNCs showed superior efficacy to DTIC confirmed by tumor mass analysis with a reduction of 36% vs 27% respectively (Figure 5B).

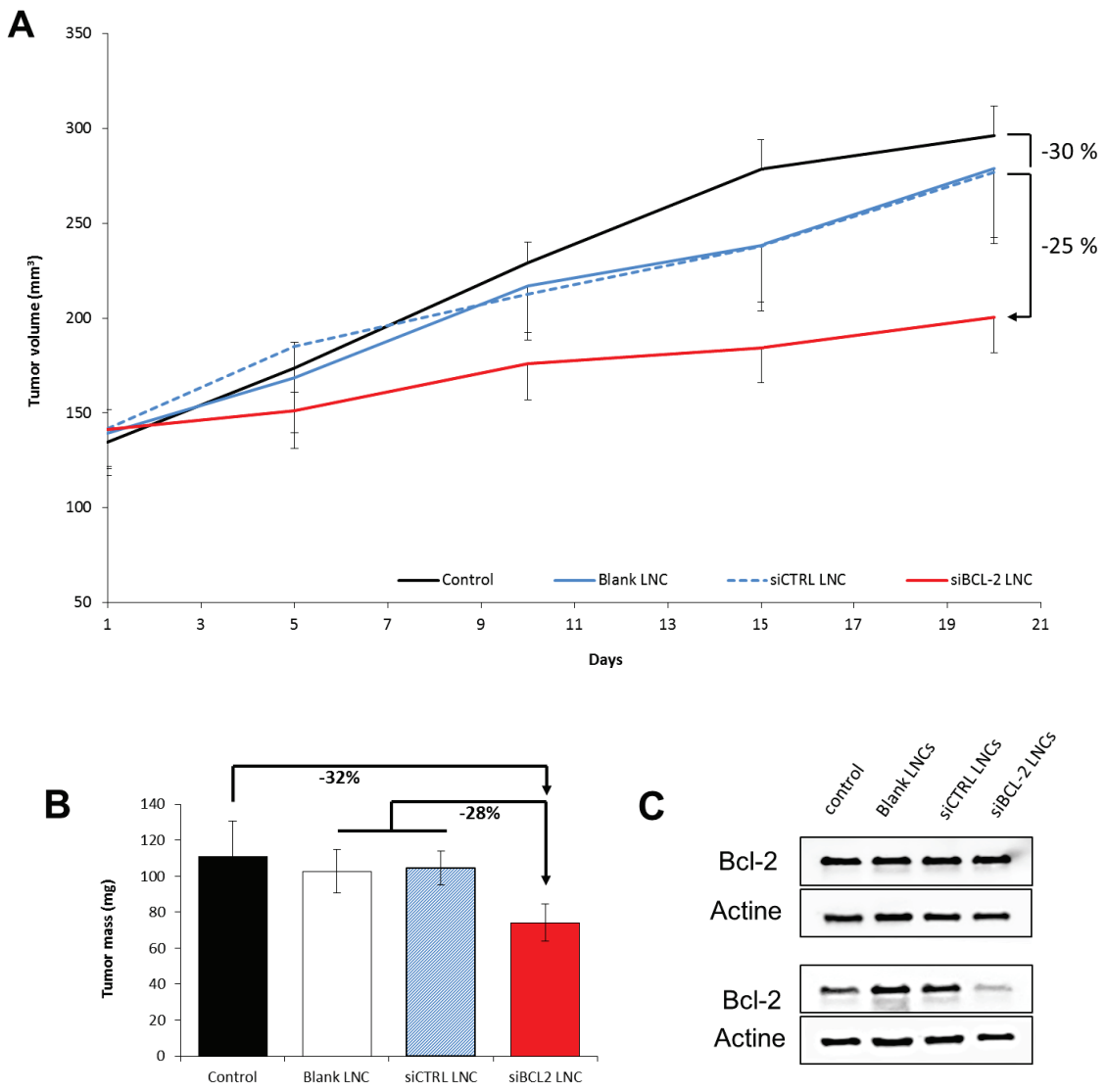

Figure 4: Tumor progression after repeated intravenous injections of siRNA LNCs in nude mice. (A) Evaluation of subcutaneous melanoma progression was performed with estimation of tumoral volume over time after treatment. Lipid nanocapsules with Bcl-2 siRNA (red line) proved a reduction of at less 30 % of tumor volume compared to control conditions (black line), blank LNCs (blue line) and control siRNA LNCs (blue dotted line). (B) Tumors were dissected and weighted at D21 after treatment and tumor mass analysis confirmed the reduction of 25% for animal receiving the Bcl-2 siRNA LNCs compared to other control groups. (C) Protein analysis was performed on tumor at D6 illustrating the heterogeneity of Bcl-2 response in melanoma tumor (n=4). Bcl-2 inhibition was proved in one-half of the animal receiving the Bcl-2 siRNA LNCs. Tumor volumes and mass were expressed as mean values ± standard error of the mean (SEM) (n=8).

3.7. Concomitant treatment on tumor growth

Ansa-FcDiOH and siRNA co-encapsulated into LNCs were tested on subcutaneous melanoma model induced in nude mice. Repeated intravenous injections were performed during one week (1 IV/day, 5 days consecutively) (Figure 6). However, the reduction effect was comparable to ansa-FcDiOH alone one. In conclusion, the co-encapsulated LNCs did not improve the efficacy of each component (ansa-FcDiOH and Bcl-2 siRNA alone).

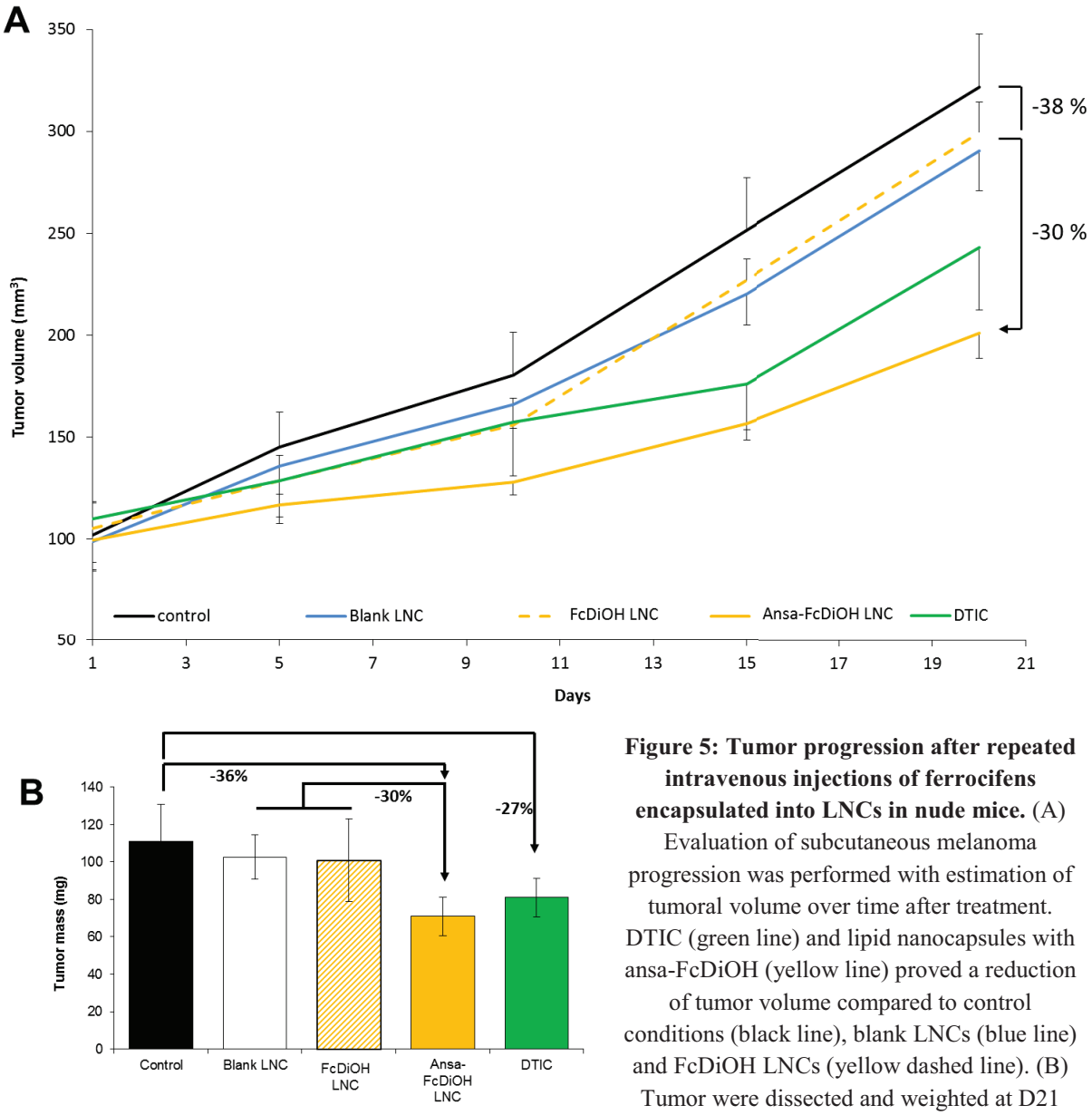

Figure 5: Tumor progression after repeated intravenous injections of ferrocifens encapsulated into LNCs in nude mice. (A) Evaluation of subcutaneous melanoma progression was performed with estimation of tumoral volume over time after treatment. DTIC (green line) and lipid nanocapsules with ansa-FcDiOH (yellow line) proved a reduction of tumor volume compared to control conditions (black line), blank LNCs (blue line) and FcDiOH LNCs (yellow dashed line). (B) Tumor were dissected and weighted at D21 after treatment and tumor mass analysis confirmed the reduction of 30% for animal receiving the ansa-FcDiOH LNCs and 20% for animals receiving DTIC (i.p. injection) compared to control group. Tumor volumes and mass were expressed as mean values ± standard error of the mean (SEM) (n=8).

3.8. Hepatotoxicity of repeated IV of LNCs

To determine the hepatotoxicity of siRNA LNCs comparatively to blank LNCs after repeated injections (D1-D5), blood samples were collected regularly during the observation period (D0, D2, D4, D9) and the enzyme activity of alanine aminotransferase (ALAT) and aspartate aminotransferase (ASAT) were quantified (Figure 7). For control group (without injections), ALAT and ASAT showed a basal constant level around 55 U/L. For each group receiving LNCs, ASAT and ALAT values

showed a slight increase corresponding to a maximum of 90 U/L between D2 and D4. At D9, basal level was recovered for all conditions.

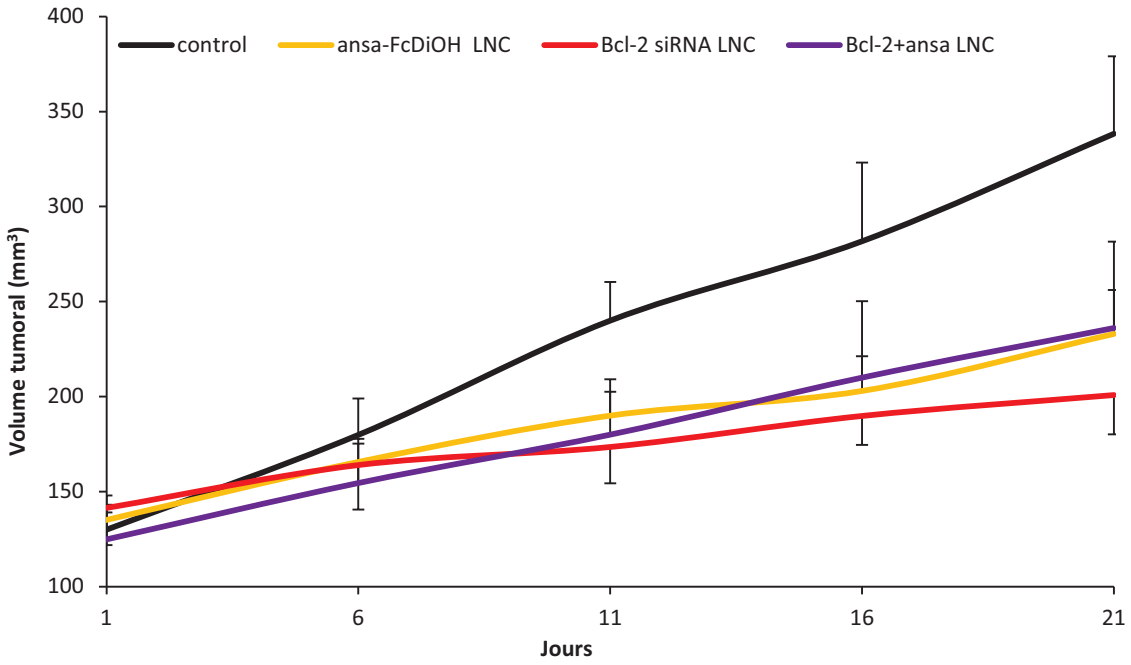

Figure 6: Impact of ansa-FcDiOH and Bcl-2 siRNA co-encapsulated LNCs on subcutaneous melanoma model. Evaluation of subcutaneous melanoma progression was performed with estimation of tumoral volume over time after treatment: control (black line), Bcl-2 siRNA LNCs (red line), ansa-FcDiOH LNCs (yellow line) and ansa-Bcl-2 LNCs (violet line). Tumor volumes were expressed as mean values ± standard error of the mean (SEM) (n=8).

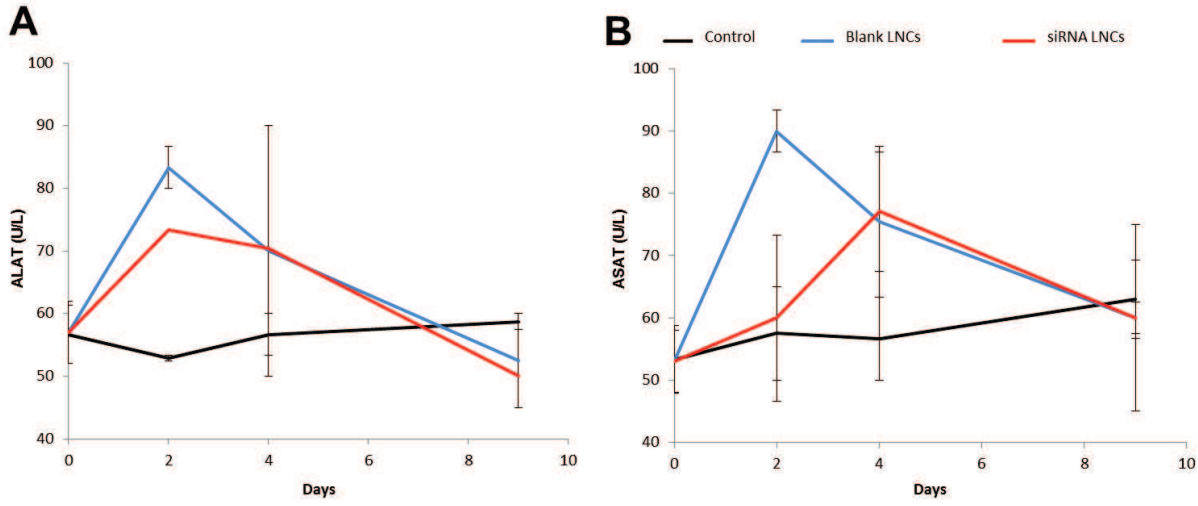

Figure 7: Evaluation of hepatotoxicity with ALAT/ASAT enzymatic quantification after repeated intravenous injections of LNCs in mice. Blood samples of animals receiving no injection (control, black line), blank LNCs (blue line), and siRNA LNCs (red line) were collected D0, D2, D4 and D9 during the observation period to analyze the hepatotoxicity of these siRNA LNCs, represented by ALAT (A) and ASAT values (B) (n = 2 for untreated animals and n = 4 for treated animals). ALAT: alanine aminotransferase; ASAT: aspartate aminotransferase; LNCs: lipid nanocapsule.

4. Discussion

Non-specific distribution and resistance mechanism cause many limitations that may result in reduced effectiveness of the chemotherapeutic agents in cancer treatment such as melanoma [28, 29]. Combination therapy has been recommended due to its advantage of increased efficacy by additive or synergic possible effects [30]. The down-regulation of gene by the use of siRNA has emerged as one of the most promising strategy for anticancer therapy [29]. However, their biological instability in blood stream involved their encapsulation into nanomedicines [17]. The encapsulation of siRNA, in order to have an efficient cellular and tumor delivery of nucleic acids, represents an important challenge in cancer research [31]. Previous work on siRNA LNCs demonstrated the efficient encapsulation and the interfacial localization of siRNA into LNCs by interaction with DOTAP/DOPE lipids and evidenced, by imaging, an efficient melanoma targeting [18]. In parallel, considering the poor water soluble property of ferrocifens, LNCs represented a suitable drug delivery system for this kind of drugs thanks to its oily core [32]. As shown in table 2, LNCs appeared as a promising nanomedicine for the co-encapsulation of poor soluble ferrocifens and hydrophilic siRNA, with a significant higher siRNA encapsulation. This better encapsulation efficiency could be explained by hypothetic interactions between ferrocifens and DOTAP/DOPE lipids boosting the siRNA entrapment.

Moreover, Bcl-2 siRNA LNCs in melanoma cells induced significant gene extinction comparable to commercial agent one at low siRNA concentrations. It was also comparable to block copolymer or cationic micelle ones described in the literature (16 nM vs 25 nM or 50 nM respectively) [31, 33]. However, the effect on apoptosis was not verified in our work, but similar study on siRNA Bcl-2 transfection thanks to PEG coated lipoplexes, demonstrated the increase rate of apoptotic cells after Bcl-2 extinction in colorectal cancer cells [34]. DTIC showed no *in vitro* cytotoxic effect compared to ferrocifen and the association of Bcl-2 siRNA LNCs with DTIC on melanoma cells did not induce any interesting additive effect either. Then, the experiments in nude mice confirmed the absence of synergy of DTIC with Bcl-2 siRNA LNCs on subcutaneous melanoma model (*data not shown*). Similarly, the addition of Oblimersen® (Bcl-2 antisens oligonucleotide) with DTIC did not improve the overall survival or progression-free survival and increased the side effects in patients with advanced melanoma [16].

In this way, as shown in figure 2, the *in vitro* assay with new promising ferrocifens evidenced interesting anti-proliferative effect on melanoma cell line. The concentration, which inhibits the cell growth at 50% (IC_{50}), was evaluated respectively at 1 µM and 3 µM for ansa-FcDiOH and FcDiOH, demonstrating the better efficiency of ansa-FcDiOH on melanoma. This last compound was also demonstrated as the most efficient derivative in breast cancer cell line and evidenced comparable IC_{50} values [22]. For the first time, the association of ferrocifen with siRNA therapy was tested, showing *in vitro* interesting additive cytotoxicity with ansa-FcDiOH contrary to FcDiOH. The benefit of

ferrocifen and Bcl-2 siRNA association could be explained by an action on mitochondrial stress. In fact, Bcl-2 inhibition results in the oligomerization of pro-apoptotic proteins (Bax/Bad) in order to induce the release of cytochrome C to mitochondria. Moreover, recent study showed that ferrocifen action induced the production of reactive oxygen species in breast cancer cells [35]. Thus, these two molecules are able to interact directly on mitochondrial metabolism and could promote a synergic effect under this way.

For *in vivo* experiments, formulations were post-inserted with long chains of PEG to ensure a melanoma passive targeting after intravenous targeting. According to our results on melanoma targeting, the optimal PEG concentration of 5 mM has been determined in function of tumor accumulation [36]. This surface modification confers stealth properties to siRNA LNCs allowing a passive targeting strategy. Repeated injections of Bcl-2 siRNA LNCs, described in figure 4, induced a promising reduction of melanoma tumor growth compared to control conditions. However, the variation of Bcl-2 extinction, evidenced by protein analysis of tumor at D5, could explain the tendency (and a non significant effect) observed. Thus, this *in vivo* transfection result could be improved: i) by increasing the amount of delivered siRNA with optimization of the encapsulation process [18], and ii) by a higher targeting efficiency with active or smart targeting strategies for specific melanoma cell uptake [36].

Considering the biodistribution profile, liver appeared as the major organ for LNC elimination. Hepatotoxicity is one of the major issues encountered with many nanomedicines due to capitation by liver [37]. ALAT and ASAT quantification revealed no significant increased level even with repeated intravenous injections of siRNA LNCs, demonstrating the absence of hepatotoxicity. For comparison, a single injection of DNA LNCs induced higher level of ALAT and ASAT (max 160 U/L versus 90 U/L) [38]. These results evidenced the good tolerance of siRNA LNCs, even after multiple injections.

Otherwise, Bcl-2 targeting is nowadays controversial as explained by recent clinical trials [16]. In fact, apoptosis pathways represent a complex protein-protein network regulated by numerous anti and pro-apoptotic members, leading to deficiency apoptosis in melanoma [39, 40]. Recent publications evidenced the fact that inhibiting proteins (i.e. Bcl-2) could promote the expression of other anti-apoptotic members (Mcl-1, A1, Bcl-$_{XL}$) to replace Bcl-2 and ensure the survival of melanoma cells [41]. The perspective of this work could consist in associating a multiple apoptosis targeting such as Bcl-2, Bcl-$_{XL}$ or Mcl-1 to improve the sensitivity to chemotherapy. For this, the solution could be the combination of different siRNA or microRNA (miRNA). In fact, a single miRNA can, contrary to siRNA, inhibit different protein synthesis [42]. In the recent years, it has become evident that miRNAs play an important role in cancer, including melanoma [43].

5. Conclusion

The association of chemotherapy and gene therapy has appeared as a promising opportunity to improve the efficacy of chemotherapy on melanoma. The objectives of this work were to develop efficient nanomedicines for the co-delivery of Bcl-2 siRNA and ferrocifens in melanoma treatment. The co-encapsulation was efficiently performed thanks to lipid nanocapsules (LNCs) with efficient gene therapy and anti-proliferative effect on SK-Mel28 melanoma cell line. *In vitro* chemosensitive effect of Bcl-2 siRNA was confirmed in association with ansa-FcDiOH. Subcutaneous human melanoma bearing mice received Bcl-2 siRNA LNCs or ansa-FcDiOH LNCs inducing an interesting reduction of tumor volume of 25 % and 30 % respectively. In conclusion, the combination of Bcl-2 siRNA and innovative ansa-FcDiOH anticancer drug encapsulation together into LNCs can appear as a future promising alternative treatment for melanoma.

Acknowledgements

The authors would like to thank Dr. Guillaume Bastiat (INSERM U1066) for its skill in statistical analysis and Pascal Pigeon (ENSCP) for the synthesis of FcDiOH and ansa-FcDiOH. We are also grateful to PACeM platform for their expertise in RT-q-PCR, and especially Dr. Jérôme Cayon. We want to thanks Pierre Legras and Jérôme Roux for their background in animal experiments. This work was supported by special grants from the “Association de la Recherche contre le Cancer” and by “La Ligue contre le cancer 49 et 35”. The authors declare no conflict of interest.

References

[1] G. Grazia, I. Penna, V. Perotti, A. Anichini, E. Tassi, Towards combinatorial targeted therapy in melanoma: from pre-clinical evidence to clinical application (review), Int J Oncol, 45 (2014) 929-949.

[2] L.B. Jilaveanu, S.A. Aziz, H.M. Kluger, Chemotherapy and biologic therapies for melanoma: do they work?, Clin Dermatol, 27 (2009) 614-625.

[3] L. Finn, S.N. Markovic, R.W. Joseph, Therapy for metastatic melanoma: the past, present, and future, BMC Med, 10 (2012) 23.

[4] L. Tentori, P.M. Lacal, G. Graziani, Challenging resistance mechanisms to therapies for metastatic melanoma, Trends Pharmacol Sci, 34 (2013) 656-666.

[5] J. Eberle, L.F. Fecker, A.M. Hossini, B.M. Kurbanov, H. Fechner, Apoptosis pathways and oncolytic adenoviral vectors: promising targets and tools to overcome therapy resistance of malignant melanoma, Exp Dermatol, 17 (2008) 1-11.

[6] D. Hanahan, R.A. Weinberg, Hallmarks of cancer: the next generation, Cell, 144 (2011) 646-674.

[7] X. Wang, The expanding role of mitochondria in apoptosis, Genes Dev, 15 (2001) 2922-2933.

[8] D. Grossman, D.C. Altieri, Drug resistance in melanoma: mechanisms, apoptosis, and new potential therapeutic targets, Cancer Metastasis Rev, 20 (2001) 3-11.

[9] U. Leiter, R.M. Schmid, P. Kaskel, R.U. Peter, G. Krahn, Antiapoptotic bcl-2 and bcl-xL in advanced malignant melanoma, Arch Dermatol Res, 292 (2000) 225-232.

[10] F. Tas, D. Duranyildiz, H. Oguz, H. Camlica, V. Yasasever, E. Topuz, Circulating levels of vascular endothelial growth factor (VEGF), matrix metalloproteinase-3 (MMP-3), and BCL-2 in malignant melanoma, Med Oncol, 25 (2008) 431-436.

[11] J. Utikal, U. Leiter, M. Udart, P. Kaskel, R.U. Peter, G.M. Krahn, Expression of c-myc and bcl-2 in primary and advanced cutaneous melanoma, Cancer Invest, 20 (2002) 914-921.

[12] S. Ilmonen, M. Hernberg, S. Pyrhonen, J. Tarkkanen, S. Asko-Seljavaara, Ki-67, Bcl-2 and p53 expression in primary and metastatic melanoma, Melanoma Res, 15 (2005) 375-381.

[13] N. Mohana-Kumaran, D.S. Hill, J.D. Allen, N.K. Haass, Targeting the intrinsic apoptosis pathway as a strategy for melanoma therapy, Pigment Cell Melanoma Res, 27 (2014) 525-539.

[14] A. Watanabe, S. Yasuhira, T. Inoue, S. Kasai, M. Shibazaki, K. Takahashi, T. Akasaka, T. Masuda, C. Maesawa, BCL2 and BCLxL are key determinants of resistance to antitubulin chemotherapeutics in melanoma cells, Exp Dermatol, 22 (2013) 518-523.

[15] B. Jansen, V. Wacheck, E. Heere-Ress, H. Schlagbauer-Wadl, C. Hoeller, T. Lucas, M. Hoermann, U. Hollenstein, K. Wolff, H. Pehamberger, Chemosensitisation of malignant melanoma by BCL2 antisense therapy, Lancet, 356 (2000) 1728-1733.

[16] A.Y. Bedikian, M. Millward, H. Pehamberger, R. Conry, M. Gore, U. Trefzer, A.C. Pavlick, R. DeConti, E.M. Hersh, P. Hersey, J.M. Kirkwood, F.G. Haluska, Bcl-2 antisense (oblimersen sodium) plus dacarbazine in patients with advanced melanoma: the Oblimersen Melanoma Study Group, J Clin Oncol, 24 (2006) 4738-4745.

[17] P. Resnier, T. Montier, V. Mathieu, J.P. Benoit, C. Passirani, A review of the current status of siRNA nanomedicines in the treatment of cancer, Biomaterials, 34 (2013) 6429-6443.

[18] P. Resnier, P. LeQuinio, N. Lautram, E. André, C. Gaillard, G. Bastiat, J.P. Benoit, C. Passirani, Efficient in vitro gene therapy with PEG siRNA lipid nanocapsules for passive targeting strategy in melanoma, Biotechnology journal, in press (2014).

[19] N.T. Huynh, C. Passirani, P. Saulnier, J.P. Benoit, Lipid nanocapsules: a new platform for nanomedicine, Int J Pharm, 379 (2009) 201-209.

[20] A.L. Laine, C. Passirani, Novel metal-based anticancer drugs: a new challenge in drug delivery, Curr Opin Pharmacol, 12 (2012) 420-426.

[21] E. Allard, D. Jarnet, A. Vessieres, S. Vinchon-Petit, G. Jaouen, J.P. Benoit, C. Passirani, Local delivery of ferrociphenol lipid nanocapsules followed by external radiotherapy as a synergistic treatment against intracranial 9L glioma xenograft, Pharm Res, 27 (2009) 56-64.

[22] A.L. Laine, E. Adriaenssens, A. Vessieres, G. Jaouen, C. Corbet, E. Desruelles, P. Pigeon, R.A. Toillon, C. Passirani, The in vivo performance of ferrocenyl tamoxifen lipid nanocapsules in xenografted triple negative breast cancer, Biomaterials, 34 (2013) 6949-6956.

[23] S. Top, A. Vessieres, G. Leclercq, J. Quivy, J. Tang, J. Vaissermann, M. Huche, G. Jaouen, Synthesis, biochemical properties and molecular modelling studies of organometallic specific estrogen receptor modulators (SERMs), the ferrocifens and hydroxyferrocifens: evidence for an antiproliferative effect of hydroxyferrocifens on both hormone-dependent and hormone-independent breast cancer cell lines, Chemistry, 9 (2003) 5223-5236.

[24] S. David, P. Resnier, A. Guillot, B. Pitard, J.P. Benoit, C. Passirani, siRNA LNCs--a novel platform of lipid nanocapsules for systemic siRNA administration, Eur J Pharm Biopharm, 81 (2012) 448-452.

[25] B. Heurtault, P. Saulnier, B. Pech, J.E. Proust, J.P. Benoit, A novel phase inversion-based process for the preparation of lipid nanocarriers, Pharm Res, 19 (2002) 875-880.

[26] P. Resnier, S. David, N. Lautram, G.J. Delcroix, A. Clavreul, J.P. Benoit, C. Passirani, EGFR siRNA lipid nanocapsules efficiently transfect glioma cells in vitro, Int J Pharm, 454 (2013) 748-755.

[27] G. Bastiat, C.O. Pritz, C. Roider, F. Fouchet, E. Lignieres, A. Jesacher, R. Glueckert, M. Ritsch-Marte, A. Schrott-Fischer, P. Saulnier, J.P. Benoit, A new tool to ensure the fluorescent dye labeling stability of nanocarriers: a real challenge for fluorescence imaging, J Control Release, 170 (2013) 334-342.

[28] W.E. Gutteridge, Existing chemotherapy and its limitations, Br Med Bull, 41 (1985) 162-168.

[29] N.S. Gandhi, R.K. Tekade, M.B. Chougule, Nanocarrier mediated delivery of siRNA/miRNA in combination with chemotherapeutic agents for cancer therapy: Current progress and advances, J Control Release, (2014).

[30] F.M. Uckun, S. Ramakrishnan, L.L. Houston, Increased efficiency in selective elimination of leukemia cells by a combination of a stable derivative of cyclophosphamide and a human B-cell-specific immunotoxin containing pokeweed antiviral protein, Cancer Res, 45 (1985) 69-75.

[31] C. Zheng, M. Zheng, P. Gong, J. Deng, H. Yi, P. Zhang, Y. Zhang, P. Liu, Y. Ma, L. Cai, Polypeptide cationic micelles mediated co-delivery of docetaxel and siRNA for synergistic tumor therapy, Biomaterials, 34 (2013) 3431-3438.

[32] A.L. Laine, A. Clavreul, A. Rousseau, C. Tetaud, A. Vessieres, E. Garcion, G. Jaouen, L. Aubert, M. Guilbert, J.P. Benoit, R.A. Toillon, C. Passirani, Inhibition of ectopic glioma tumor growth by a potent ferrocenyl drug loaded into stealth lipid nanocapsules, Nanomedicine, (2014).

[33] D. Cheng, N. Cao, J. Chen, X. Yu, X. Shuai, Multifunctional nanocarrier mediated co-delivery of doxorubicin and siRNA for synergistic enhancement of glioma apoptosis in rat, Biomaterials, 33 (2012) 1170-1179.

[34] K. Nakamura, A.S. Abu Lila, M. Matsunaga, Y. Doi, T. Ishida, H. Kiwada, A double-modulation strategy in cancer treatment with a chemotherapeutic agent and siRNA, Mol Ther, 19 (2011) 2040-2047.

[35] C. Lu, J.M. Heldt, M. Guille-Collignon, F. Lemaitre, G. Jaouen, A. Vessieres, C. Amatore, Quantitative analyses of ROS and RNS production in breast cancer cell lines incubated with ferrocifens, ChemMedChem, 9 (2014) 1286-1293.

[36] P. Resnier, A.L. Emina, N. Galopin, J. Bejaud, S. David, C. Ballet, T. Benvegnu, F. Pecorari, I. Chourpa, J.P. Benoit, C. Passirani, Innovative Affitin and PEG modifications onto siRNA lipid nanocapsules influence cell uptake, in vivo biodistribution and tumor targeting, submit to Journal of Controlled Realease, (2014).

[37] Q. Chen, Y. Xue, J. Sun, Kupffer cell-mediated hepatic injury induced by silica nanoparticles in vitro and in vivo, Int J Nanomedicine, 8 (2013) 1129-1140.

[38] S. David, T. Montier, N. Carmoy, P. Resnier, A. Clavreul, M. Mevel, B. Pitard, J.P. Benoit, C. Passirani, Treatment efficacy of DNA lipid nanocapsules and DNA multimodular systems after systemic administration in a human glioma model, J Gene Med, 14 (2012) 769-775.

[39] M.L. Hartman, M. Czyz, Anti-apoptotic proteins on guard of melanoma cell survival, Cancer Lett, 331 (2013) 24-34.

[40] M. Plotz, B. Gillissen, S.A. Quast, A. Berger, P.T. Daniel, J. Eberle, The BH3-only protein Bim(L) overrides Bcl-2-mediated apoptosis resistance in melanoma cells, Cancer Lett, 335 (2013) 100-108.

[41] R.A. Anvekar, J.J. Asciolla, D.J. Missert, J.E. Chipuk, Born to be alive: a role for the BCL-2 family in melanoma tumor cell survival, apoptosis, and treatment, Front Oncol, 1 (2011).

[42] C. Luo, C.E. Weber, W. Osen, A.K. Bosserhoff, S.B. Eichmuller, The role of microRNAs in melanoma, Eur J Cell Biol, 93 (2014) 11-22.

[43] M.V. Iorio, C.M. Croce, microRNA involvement in human cancer, Carcinogenesis, 33 (2012) 1126-1133.

DISCUSSION GENERALE

DISCUSSION GENERALE

1. Genèse des travaux

Le cancer se caractérise par l'acquisition de propriétés biologiques spécifiques qui sont à l'origine de la complexité de cette pathologie telles le maintien des signaux de prolifération, la possibilité illimitée de division, la résistance aux processus de mort cellulaire, l'induction de l'angiogenèse, l'échappement aux gènes suppresseurs de tumeur et enfin la capacité de migration et d'invasion menant à la formation de métastases [1]. Le mélanome, forme la plus courante du cancer de la peau, répond à toutes les caractéristiques du développement tumoral via l'apparition progressive de mutations touchant ces différentes voies moléculaires comme décrit précédemment (cf. Introduction, §2.1), et plus particulièrement la résistance aux processus de mort cellulaire qu'est l'apoptose [2].

La dégénérescence de ce programme dit de « suicide cellulaire » est primordiale dans le développement du mélanome. En effet, la peau, soumise aux rayonnements UV, connait de nombreuses mutations provoquées par des expositions répétées et/ou intenses. Dans ce cas, la cellule enclenche un processus de réparation de l'ADN afin d'effacer la mutation acquise. Cependant, si la mutation n'est pas réparée, la cellule déclenche alors normalement le processus d'apoptose via le gène suppresseur de tumeur p53 [2, 3]. Certaines cellules de la peau court-circuitent alors ce processus et conservent la mutation entrainant alors une dérive potentiellement tumorale allant vers un mélanome. Cette autonomie spontanément acquise entraine une résistance importante envers les traitements chimiothérapeutiques actuellement disponibles en clinique [2].

Il s'agit donc aujourd'hui de lever cette résistance par l'intermédiaire de nouvelles thérapies afin de rétablir le processus de mort cellulaire. Si les inhibiteurs chimiques restent un challenge au niveau de leur conception, de nouveaux outils, tels que les petits ARN interférents (siRNA), sont désormais disponibles pour moduler aisément l'expression de protéines spécifiques. Cependant, le défi consiste alors à transporter jusqu'au site souhaité ces siRNA sensibles aux nucléases plasmatiques et incapables de franchir seuls les membranes biologiques.

Les nanomédecines répondent alors à la nécessité de protéger et de diriger spécifiquement les siRNA vers le(s) site(s) tumoral(aux) comme la revue bibliographique détaillée en amont a pu le montrer (cf. revue bibliographique) [4]. Les nanocapsules lipidiques (LNC) développées au sein du laboratoire ont pu précédemment démontrer leur capacité pour encapsuler des plasmides d'ADN dans le cadre des travaux de thèse du Dr. Arnaud Vonarbourg [5]. Cette thématique a ensuite été poursuivie par le Dr. Marie Morille. Ses travaux se sont orientés sur l'utilisation des LNC ADN post-insérées avec de longues chaînes de polyéthylène glycol (PEG), via l'utilisation de deux types de polymères

amphiphiles : le DSPE-PEG et le copolymère F108 [6]. La pegylation des LNC ADN a permis l'obtention d'un vecteur furtif capable de s'accumuler de manière significative au niveau des tissus tumoraux, grâce à un effet EPR (Enhanced permeability and retention) et d'engendrer une transfection sur un modèle luciférase [7]. Suite à cette preuve de concept sur les LNC ADN, les travaux suivants réalisés par le Dr. Stephanie David, se sont focalisés sur le développement d'une stratégie thérapeutique en utilisant les LNC ADN en cancérologie. La stratégie du gène suicide a été développée sur un modèle sous-cutané de gliome montrant des résultats intéressants [8]. De plus, le ciblage passif des LNC ADN a été démontré dans un modèle sous-cutané de mélanome. Enfin, la dernière partie des expérimentations à laquelle j'ai participé dans le cadre de mon master 2 s'est concentrée sur l'adaptation des LNC ADN pour l'encapsulation d'une seconde forme d'acide nucléique que sont les siRNA [9].

Mes travaux de thèse se sont donc intégrés, dans la continuité des travaux cités ci-dessus, selon trois problématiques principales :

- La première problématique s'est inscrite dans la poursuite des travaux de formulation initiés par le Dr. Stephanie David. L'objectif est alors de comprendre la formulation des LNC siRNA afin d'optimiser l'encapsulation des siRNA et d'améliorer la stabilité de telles nanomédecines pour une transposition clinique.
- La seconde partie étudie les différentes stratégies de ciblage possibles dans un modèle de mélanome sous-cutané. Les études se sont orientées vers l'impact des modifications de surface des LNC siRNA sur l'internalisation au niveau cellulaire, ainsi que sur l'accumulation au niveau du site tumoral après injection intraveineuse.
- Enfin, la troisième problématique concerne les possibilités thérapeutiques des LNC siRNA *via* le ciblage de la protéine Bcl-2. Les LNC siRNA ont été testées en association ou non avec des chimiothérapies innovantes que sont les ferrocifènes sur un modèle animal de mélanome sous-cutané.

2. Formulation et optimisation du procédé

2.1. L'encapsulation des siRNA

Aujourd'hui, de nombreuses formulations sont développées pour délivrer par voie intraveineuse les siRNA telles que les dendrimères, les micelles, les liposomes, les nanoparticules à base de lipides et/ou de polymères [10, 11]. Si les structures et les composants changent, la littérature s'accorde sur des propriétés communes indispensables aux nanomédecines pour l'encapsulation et la libération des siRNA par injection systémique. Le premier critère concerne la taille : elle doit être comprise entre 20 et 100 nm permettant de limiter une clairance rénale trop rapide, ainsi que la reconnaissance par le système immunitaire (cellules de Kupffer). Le second critère est la charge de surface des particules qui

doit idéalement être proche de la neutralité afin d'éviter les phénomènes d'agrégations avec les protéines sanguines. Enfin, le dernier critère concerne la nécessité de développer un ciblage spécifique du site tumoral (cf. Revue bibliographique, § 2.3).

Au vu des propriétés hydrophiles des siRNA, leur encapsulation reste limitante et nécessite un développement de nanomédecines appropriées et une optimisation des procédés. A l'heure actuelle, l'encapsulation des siRNA passe principalement par l'utilisation de polymères ou de lipides cationiques permettant la formation d'interactions électrostatiques avec les siRNA anioniques [4]. Il ne s'agit donc pas à proprement dit « d'encapsulation », mais plutôt d'adsorption des siRNA à la surface de micelles ou de liposomes cationiques [4]. Dans ce cas, la complexation consiste à effectuer un simple mélange entre les formulations et les siRNA. Différentes techniques d'adsorption des siRNA ou microRNA (miRNA) ont été mises au point sur les nanocapsules lipidiques (LNC) en réalisant préalablement un recouvrement avec du chitosan ou avec des peptides cationiques [12, 13]. Cela permet, en effet, d'obtenir avec succès une adsorption du matériel génétique à la surface des LNC. A contrario, la surface étant déjà modifiée pour adsorber les siRNA, elle n'est plus entièrement disponible pour effectuer des modifications de surface en vue d'un ciblage passif, actif ou intelligent par injection intraveineuse.

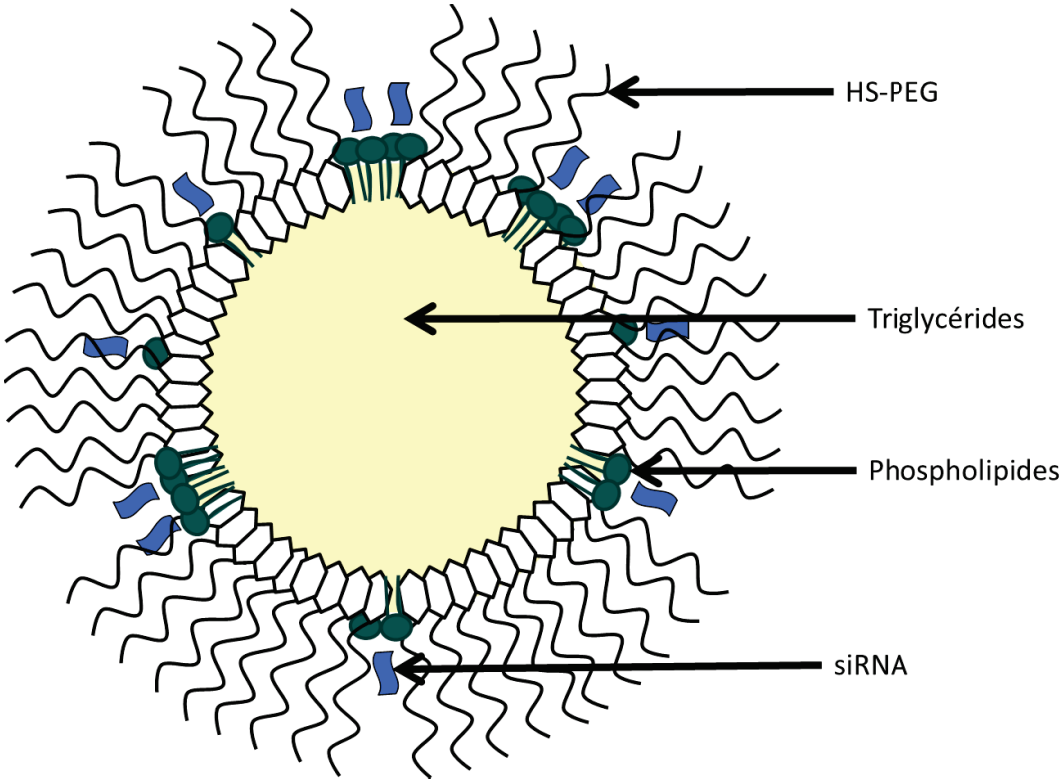

Figure 16 : Représentation schématique des LNC siRNA. Les nanocapsules lipidiques sont formées d'un cœur huileux (triglycérides) avec une coque d'hydroxystéarate de polyéthylène glycol (HS-PEG) et de phospholipides incluant la lécithine ainsi que le DOTAP/DOPE. Les siRNA se positionnent au niveau de la coque grâce à des interactions électrostatiques avec les phospholipides.

Au vu de cette importante limitation, l'adaptation du procédé de formulation pour encapsuler les siRNA est indispensable afin d'élargir les applications des LNC siRNA. Pour cela, l'usage de lipoplexes apparait comme une alternative innovante et prometteuse pour la complexation des siRNA avec les LNC (cf. Chapitre 1). Les études de tensiométrie démontrent un positionnement des lipoplexes de siRNA à l'interface entre l'huile et l'eau, qui pourrait, comme les stratégies d'adsorption décrites précédemment, les rendre accessibles aux nucléases et limiter les possibilités de modifications de surface (Figure 16). Pourtant, les études menées par la suite ont prouvé que les acides nucléiques sont tout de même protégés des nucléases et que les modifications de surface diverses n'entachent en rien l'encapsulation du siRNA (cf. Chapitre 2). On peut supposer qu'avec une première association avec les lipides cationiques, les siRNA sont amenés à proximité du cœur des nanocapsules, au sein même de la coque et non à la surface de la coque comme ce qui est observé par adsorption. Dans ce cas, les chaînes de polyéthylène glycol (660 kDa), constituant la coque primaire des LNCs, agissent comme un manteau hydrophile protecteur, empêchant ainsi l'accès aux siRNA. Contrairement à l'adsorption avec le chitosan ou avec les peptides, la formulation des LNC siRNA se fait en une seule étape et rend alors la surface des nanocapsules disponible pour différentes stratégies de ciblage.

Par ailleurs, cette organisation particulière laisse le cœur huileux des LNC disponible pour l'encapsulation d'autres molécules thérapeutiques. Un nombre grandissant d'études fait part de l'utilisation de nanomédecines pour l'encapsulation simultanée de siRNA et d'agent anti-cancéreux [14]. Dans la majorité des cas, la chimiothérapie utilisée est la doxorubicine [14]. Plusieurs études démontrent des effets synergiques obtenus *in vitro* et *in vivo* avec un siRNA ciblant la protéine Bcl-2 [15-17]. Nos travaux mettent en évidence une nouvelle utilisation d'un siRNA Bcl-2 avec la co-encapsulation possible avec des agents anticancéreux tels que les composés organométalliques au sein des LNC (cf. Chapitre 3). Par ailleurs, ces expériences de co-encapsulation démontrent également que la présence de ferrocifènes améliore l'efficacité d'encapsulation des siRNA pour les deux dérivés utilisés. Cette amélioration de l'encapsulation du siRNA reste aujourd'hui mal comprise. On peut supposer que la présence des composés organométalliques favorise l'intégration des lipides à la coque des LNC et ainsi l'attraction du siRNA.

Les LNC pourraient donc encapsuler simultanément différents agents chimiothérapeutiques, ainsi que des siRNA, qui théoriquement peuvent cibler toutes les protéines du vivant, offrant alors un champ illimité de possibilités et d'applications.

2.2. Dépôt de brevet et industrialisation

La recherche et l'approfondissement des connaissances sur la structure et le comportement des systèmes nanoparticulaires permet de mieux les comprendre et ainsi de les améliorer. Le procédé de formulation des LNC fait l'objet d'une protection sous brevet depuis 2000 (FR2805761 (A1)) [18]).

Depuis ce premier brevet, huit autres brevets sur les LNC ont été déposés (www.inpi.fr). Par ailleurs, les LNC siRNA ont fait l'objet d'un travail important de formulation.

En effet, suite aux premiers travaux de formulation effectués par le Dr Stephanie David, les LNC siRNA permettent une encapsulation efficace de siRNA, mais les études de stabilité démontrent une perturbation du système après une semaine de conservation à 4°C. Grâce à diverses modifications du procédé de formulation, une amélioration considérable de la stabilité a pu être obtenue lors de ces travaux donnant lieu au dépôt d'un brevet (cf. Chapitre 1). Les démarches en collaboration avec la SATT Ouest Valorisation (Société d'accélération du transfert de technologie) ont débuté au printemps de cette année et le dépôt du brevet a eu lieu cet automne. L'exploitation des brevets concernant les LNC est détenue par la Start-up Carlina Technologies basée à Angers. Une valorisation sera donc possible si les études réalisées à l'avenir montrent le potentiel des LNC siRNA.

3. Preuve de concept

Le développement de ces nanomédecines a pour but de permettre et d'aider le passage des siRNA à travers les barrières biologiques telles que les membranes cellulaires afin d'atteindre le cytoplasme, passage indispensable à l'efficacité des siRNA ou, de façon plus complexe, les endothéliums pour accéder au site tumoral.

3.1. L'internalisation des siRNA

L'internalisation des siRNA au sein du cytoplasme est une preuve de concept essentielle. Les travaux ici réalisés ont prouvé, *via* l'utilisation de techniques de microscopie confocale utilisant le FRET, que les LNC sont capables de délivrer les siRNA au niveau du cytoplasme des cellules tumorales issues de mélanome humain (cf. chapitre 2). De façon surprenante, ces analyses ont montré un comportement très différent du comportement initialement observé par Paillard *et al.,* avec les LNC non chargées [19]. En effet, les différences entre les deux procédés de formulation semblent engendrer des voies d'internalisation diamétralement opposées. Des phénomènes d'endocytose ont été premièrement décrits impliquant les voies des cavéoles et des clathrines [19]. Ces mécanismes entrainent alors une accumulation dans les vésicules d'endocytose, puis dans les lysosomes. Ce phénomène est classiquement décrit dans la littérature avec les différentes nanoparticules et pose d'ailleurs la problématique de l'échappement endosomal afin d'éviter la dégradation des siRNA [4, 20]. Les LNC siRNA, quant à elles, semblent directement fusionner avec la membrane plasmique et ainsi échapper à la problématique des lysosomes. Cependant, des études complémentaires doivent démontrer la non-colocalisation avec les vésicules d'endocytose ou les lysosomes, afin d'affirmer que les voies d'entrée sont totalement dissociées. Cette interaction membranaire peut être due à la présence supplémentaire de lipides cationiques et zwitterioniques nécessaire à la formulation des LNC siRNA.

En effet, ces lipides sont classiquement décrits pour avoir des comportements fusiogéniques avec la membrane [21].

Par ailleurs, les LNC siRNA modifiées en surface avec le tetraéther de polyéthylène glycol (TE-PEG) ont montré une internalisation importante du siRNA au sein des cellules de mélanome contrairement aux autres formes de LNC siRNA pegylées (cf. Chapitre 2). Ces LNC modifiées empreintent-elles la voie d'internalisation des LNC siRNA ou des LNC non chargées ? Cette modification améliore-t-elle l'efficacité de transfection ? Les réponses à ces questions sont indispensables pour évaluer si la modification de surface avec les TE-PEG est réellement intéressante. Cependant, on peut déjà penser que la présence des PEG risque de modifier le processus de prise en charge des LNC à la surface des cellules et limiter l'effet de fusion possible induit par les lipides cationiques contenus dans la coque.

3.2. Le ciblage tumoral

Le ciblage tumoral après injection intraveineuse reste aujourd'hui un challenge pour une application des nanomédecines en cancérologie lors d'atteinte métastatique. Si les premières générations de nanomédecines sans modification de surface entrainent une dégradation par le système immunitaire et une accumulation hépatique, la seconde génération, pegylée en surface, permet une furtivité accrue et une accumulation passive au niveau tumoral [4]. A des fins de ciblage passif, l'utilisation du polyéthylène glycol (PEG) est aujourd'hui largement décrite [22].

Les travaux détaillés dans le chapitre 2 montrent l'importance et l'influence du PEG sur la biodistribution des LNC siRNA chez les animaux sains et dans un modèle sous-cutané de mélanome humain implanté chez la souris immunodéficiente. L'influence de la concentration, ainsi que de la longueur des chaines de PEG sur le profil de biodistribution des nanomédecines a été largement étudiée dans la littérature [23, 24]. Cependant, peu d'études se sont attardées sur l'importance de la molécule d'ancrage du PEG à la surface des nanoparticules. Pourtant, la comparaison avec le TE-PEG et le DSPE-PEG met en évidence des différences essentielles sur la biodistribution des LNC siRNA.

Les LNC modifiées avec le DSPE-PEG ont été largement utilisées au sein du laboratoire dans diverses applications [6, 25]. Leur étude a démontré un ciblage passif efficace dans différents modèles cancéreux tels que le gliome et le mélanome [6, 26]. La présence de DSPE-PEG à la surface des LNC permet d'obtenir un temps de circulation prolongé dans le temps. Au bout de 48 h, une localisation dans les organes d'élimination tels que le foie, la rate, les reins et la vessie est observée. Alors que les études *in vitro* démontrent que le DSPE-PEG empêche l'internalisation des LNC au sein des cellules, l'expérimentation *in vivo* prouve une accumulation favorisée des LNC DSPE-PEG comparativement aux LNC non modifiées au niveau du site tumoral. On peut alors imaginer que les LNC pegylées s'accumulent plus facilement au niveau du site tumoral grâce à leur propriété de furtivité. Une fois arrivées dans le stroma tumoral, les chaines de PEG présentes sur les LNC pourraient être dégradées

dans la matrice extracellulaire favorisant ainsi le passage des LNC au niveau des membranes cellulaires.

De façon surprenante, une localisation au niveau des ovaires des LNC DSPE-PEG ouvre des possibilités intéressantes dans le cadre de la pathologie cancéreuse correspondante. Ce ciblage spécifique des LNC DSPE-PEG reste aujourd'hui peu connu et mal-caractérisé. Par ailleurs, si la circulation prolongée des nanomédecines pegylées limite l'accumulation hépatique ou encore les effets sur la myélosuppression, on observe pour ces formes une accumulation non souhaitée au niveau de la peau (cf. chapitre 2) [27]. De manière similaire, des études cliniques ont montré que le Doxyl® (liposome pegylé de doxorubicine) entraine l'apparition d'un syndrome main-pied (érythrodysthésie palmo-plantaire), limitant son utilisation [28].

Contrairement au DSPE-PEG, les LNC contenant le TE-PEG semblent posséder un profil de biodistribution bien distinct. Pourtant, les premières analyses physico-chimiques montrent que la post-insertion de TE-PEG ne modifie pas la taille, la monodispersité, ni la charge des LNC siRNA. La question de l'efficacité de post-insertion s'est alors posée. Pour cela, des analyses de chromatographie sur couche mince ont été réalisées au laboratoire et ont révélé la présence du TE-PEG avec les LNC siRNA après purification. Cependant, la quantification du PEG reste impossible via ces techniques et le dosage par d'autres méthodes tels que l'HPLC ou ULPC reste aujourd'hui complexe à mettre en place. De façon assez surprenante, les LNC TE-PEG possèdent à la fois des propriétés similaires aux LNC non-modifiées mais également aux LNC DSPE-PEG. On montre, par exemple, que les LNC TE-PEG permettent une protection prolongée du siRNA contre les nucléases tout comme les LNC DSPE-PEG (cf. Chapitre 2, Figure 4). Pourtant, les analyses de temps de demi-vie mettent en évidence un comportement sanguin proche des LNC non-modifiées avec une élimination rapide. Cependant, les résultats d'expérimentation animale montrent l'intérêt de ces nouvelles molécules caractérisées par une accumulation hépatique très retardée (48 h), ce qui permet de favoriser l'accumulation tumorale. Ce polymère, développé à Rennes par le groupe du Pr. Thierry Benvegnu, est issu d'une archée et a premièrement été utilisé pour ses propriétés de rigidité des liposomes, puis afin de les rendre furtifs [29]. Par ailleurs, des études récentes de cette équipe ont permis d'insérer un lien pH sensible entre la partie tetraéther et la chaine de PEG, révélant un potentiel bien plus grand d'application pour ce type de polymère [30]. Cette collaboration a donc débuté dans le but de pouvoir, à fortiori, développer une stratégie dite de « ciblage intelligent » avec les LNC siRNA [31]. En effet, les mélanomes, comme de nombreux types cancéreux, possèdent un microenvironnement tumoral légèrement acide, pouvant justifier de l'utilisation de ce type de stimuli [32].

Enfin, le greffage d'affitine a été réalisé avec succès sur les LNC siRNA suivant le protocole développé par Bourseau-Guilmain [33]. Ces séquences peptidiques, synthétisées à Nantes par le groupe du Dr. Frédéric Pecorari, permettent de reconnaitre avec une affinité similaire aux anticorps des antigènes spécifiques [34]. L'objectif consiste à déterminer l'impact des affitines sur la biodistribution et le ciblage passif des LNC siRNA, avec dans un premier temps des affitines dites

« contrôles » (pas de spécificité antigénique particulière pour le mélanome). Comme observé dans la littérature avec d'autres formes peptidiques, les résultats concernant les LNC affitines démontrent une reconnaissance facilitée des LNC par le système immunitaire, menant à une élimination hépatique (cf. chapitre 2) [35]. Par ailleurs, aucune accumulation spécifique dans les organes ni effets secondaires n'ont été mis en évidence. Il s'agit dorénavant de réaliser des affitines reconnaissant des antigènes pertinents pour le ciblage du mélanome. La superfamille de protéines MAGE (Melanoma Antigen Genes) est spécialement exprimée par un nombre réduit de cellules saines (cellules germinales), et de façon intéressante, on la retrouve fréquemment exprimée au niveau des tumeurs telles que le mélanome [36]. D'autres molécules que les MAGE sont spécifiquement retrouvées surexprimées au niveau des mélanomes telles que le récepteur à la mélanocortine [37]. Ces molécules apparaissent comme des candidats potentiellement intéressants pour viser spécifiquement le mélanome à l'aide des affitines.

3.3. Validation *via* un modèle « luciférase »

Afin de démontrer la possibilité d'une transfection *in vivo*, un modèle de cellules tumorales SK-Mel28 a été modifié afin d'exprimer la luciférase. La luciférase est une enzyme naturellement présente chez le ver luisant. En effet, cette enzyme contrôle l'oxydation de la luciférine en oxyluciférine. Cette dernière est capable alors d'émettre des photons détectables par des caméras, c'est ce que l'on nomme la bioluminescence. Ces cellules SK-Mel28 Luc+, sont donc capables après injection de luciférine d'émettre des photons. Après implantation en sous-cutané, la tumeur peut donc être visualisée par imagerie de bioluminescence.

En collaboration avec le Pr. Tristan Montier de Brest, des expérimentations, non présentées dans les parties précédentes, utilisant ce modèle « luciférase » ont été réalisées. Afin d'évaluer l'efficacité des LNC à véhiculer les siRNA, des injections répétées de LNC, encapsulant des siRNA ciblant la luciférase, sont réalisées par voie intraveineuse. Les formulations sans modification et après post-insertion de DSPE-PEG sont comparées et le signal de bioluminescence, issu des mélanomes sous-cutanés, est alors suivi au cours du temps. Malheureusement, l'analyse de la bioluminescence ne montre pas d'extinction du signal de bioluminescence malgré l'injection des LNC siRNA (Figure 17).

Comment expliquer ce résultat ? En effet, les expérimentations *in vitro* réalisées au préalable montrent pourtant une extinction de l'expression de la luciférase (Figure 18). Cependant, l'expression forcée de protéines telle que la luciférase par l'intégration de plasmide d'ADN entraine une expression très forte. On peut imaginer que la quantité de siRNA injectée n'a pas suffi à engendrer une baisse significative d'ARNm pour entrainer une baisse du signal de luminescence. De plus, le volume tumoral n'est pas corrélé avec le signal de bioluminescence obtenu. Ceci entraine une forte hétérogénéité inter individus entre les volumes tumoraux et le signal de bioluminescence qui rendent l'établissement des groupes très complexe. A l'heure actuelle, peu d'études utilisent la

bioluminescence *in vivo* avec les siRNA. Mais deux études ont d'ores et déjà démontré une stabilisation du signal de bioluminescence après injection intraveineuse de nanomédecines, telles que des dendrimères ou du polyéthylène imine (PEI), encapsulant un siRNA luciférase [38, 39]. Ces études mettent en évidence la réelle nécessité d'améliorer le ciblage des LNC siRNA.

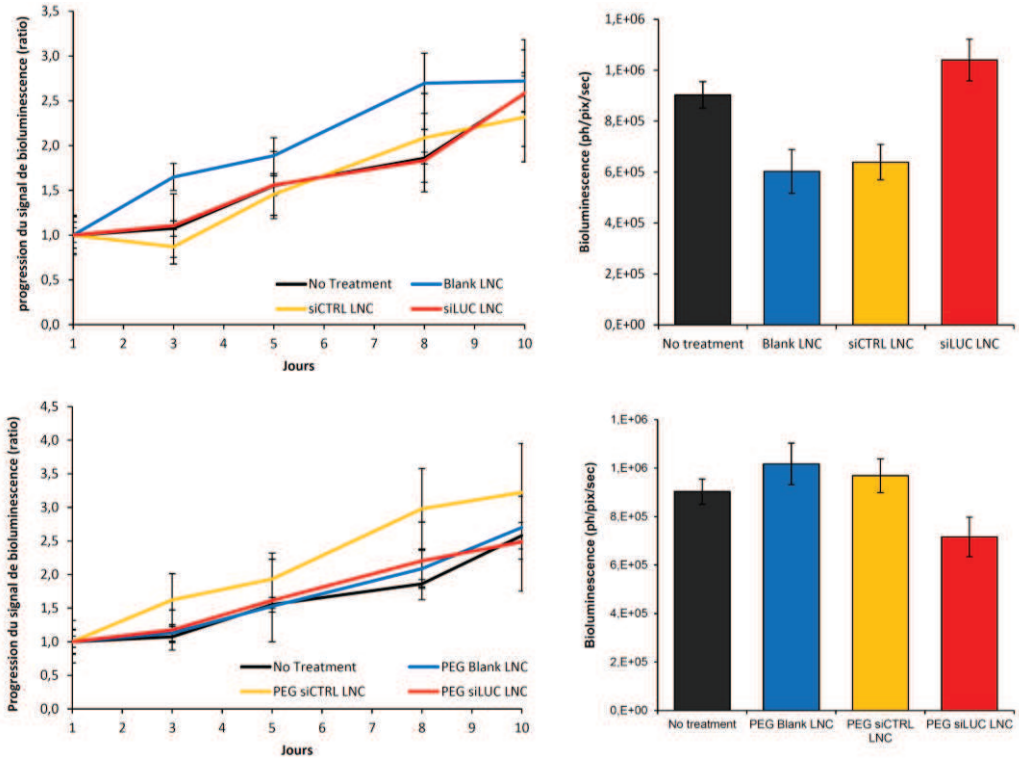

Figure 17 : Suivi du signal de bioluminescence issu de cellules de mélanome sous-cutané au cours du temps. A gauche, les graphiques montrent l'évolution du signal de bioluminescence par comparaison au signal de bioluminescence obtenu à J1 après injection intraveineuse de LNC siRNA avec ou sans pegylation. A droite, on observe le signal de bioluminescence des tumeurs extraites à J10 en fonction des groupes correspondant aux contrôles (aucune injection - noir), LNC blanches (sans siRNA - bleu), LNC siRNA Contrôle (jaune), LNC siRNA Luciférase (rouge).

Cependant, l'utilisation d'un tel modèle ouvre d'autres opportunités. Ces cellules exprimant la luciférase peuvent être en effet localisées par leur signal de bioluminescence. Une injection intraveineuse de ces cellules devrait permettre l'établissement d'un modèle métastasé représentant alors un modèle s'approchant de la réalité clinique [26]. Des études de ciblage des sites métastatiques sur un modèle luciférase sont indispensables afin d'améliorer et tester de manière fiable les différentes stratégies développées à l'avenir.

4. Application en oncologie

Le cancer est une cause majeure de décès à travers le monde. Le mélanome, cancer de la peau le plus fréquent, reste aujourd'hui une pathologie problématique avec une absence de traitements efficaces. De nouvelles thérapies telles que la thérapie génique apparaissent comme des alternatives prometteuses afin de favoriser la sensibilité aux chimiothérapies.

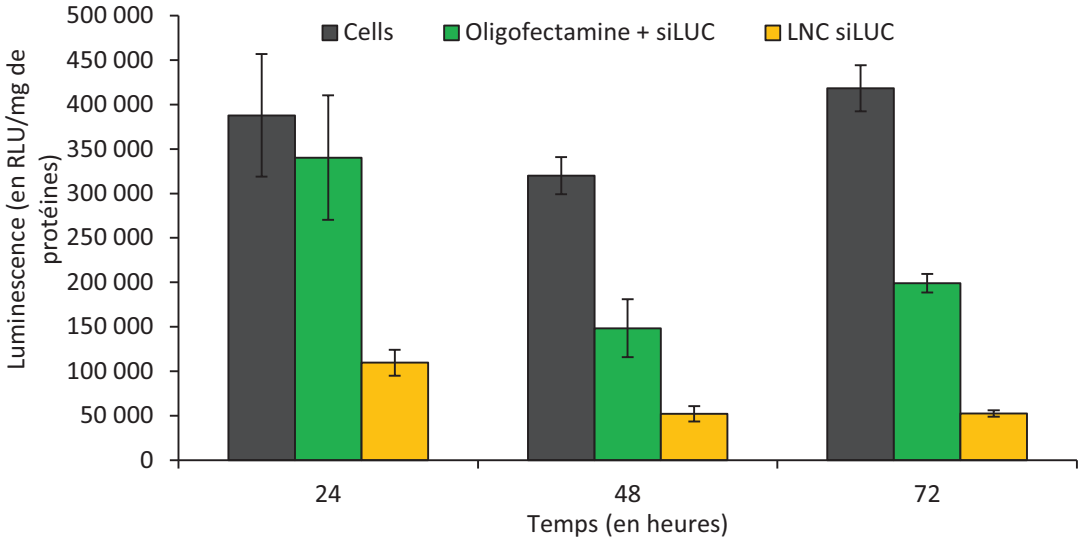

Figure 18 : **Expérience d'extinction de la luciférase exprimée par des cellules de mélanome humain transformées.** Les cellules tumorales, n'ayant reçu aucun traitement, sont comparées à la transfection d'un siRNA luciférase à l'aide d'Oligofectamine® (vert) ou de nanocapsules lipidiques (LNC, jaune). Les signaux de bioluminescence obtenus sont exprimés selon la moyenne des échantillons ± l'écart type standard (n=1).

4.1. La thérapie génique

4.1.1. La sous-unité alpha 1 et chimiosensibilité

La sous-unité alpha 1 de la pompe à sodium est un élément cellulaire clé permettant le maintien et la régulation de l'osmose *via* le contrôle des échanges d'ions Na^+ et K^+ au sein des cellules [40]. Les inhibiteurs chimiques de cette pompe, déjà sur le marché, ont montré une activité anticancéreuse intéressante [41]. Cependant, leur forte cardiotoxicité a nécessité la recherche d'autres alternatives pour cibler plus spécifiquement la sous-unité alpha 1 [42].

L'utilisation des LNC siRNA a permis d'inhiber de façon spécifique la sous-unité alpha 1 sur les cellules de mélanome sans engendrer de toxicité particulière (cf. Chapitre 1). Des études complémentaires, non présentées précédemment, ont été réalisées avec un siRNA ciblant la sous-unité alpha 1. En effet, l'association de ce ciblage est testée *in vitro* en concomitance avec différentes chimiothérapies (Figure 19). Les essais avec la chimiothérapie de référence (dacarbazine, DTIC, vert) ne montrent pas d'effet bénéfique avec une réduction de la viabilité non significative de 30 % contre 20 % pour les traitements non associés. Par contre, son association avec les composés organométalliques a montré des résultats intéressants (Figure 19). L'association avec le ferrociphénol (FcDiOH, orange) entraine une diminution de la viabilité cellulaire de 50 % contrairement aux traitements seuls qui induisent une baisse de 10 à 20 %. L'ansa-ferrociphénol (ansa-FcDiOH, jaune) montre les résultats les plus prometteurs avec une diminution de plus de 60 % de la viabilité en employant une dose plus faible d'agents anticancéreux. Comment expliquer ce résultat ? On peut supposer un effet combiné sur la régulation de l'osmose. En effet, le mécanisme supposé d'action des ferrocifènes se base sur la formation de dérivés réactifs de l'oxygène (ROS) [43].

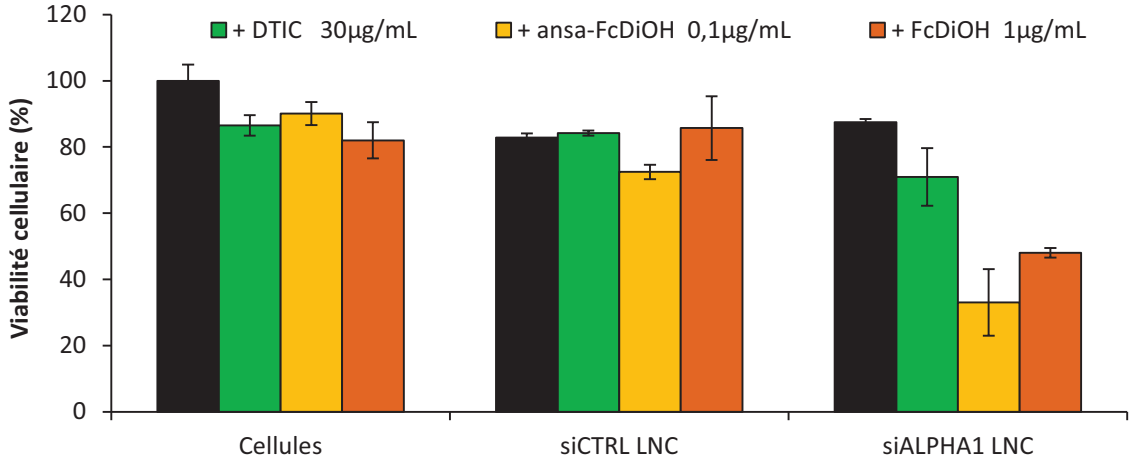

Figure 19 : Impact de l'association des nanocapsules lipidiques chargées en siRNA et de différentes chimiothérapies sur des cellules issues de mélanome humain. Les résultats démontrent une action cytotoxique lorsque le siRNA ciblant la sous-unité de la pompe à sodium est associé à des composés organométalliques tels que le ferrociphénol (FcDiOH, orange) et l'ansa-ferrociphénol (ansa-FcDiOH, jaune). A contrario, l'association avec la dacarbazine (DTIC, vert) n'entraine pas de cytotoxicité. Les pourcentages de cellules viables sont exprimés selon la moyenne des échantillons ± l'écart type standard (n=3).

Par ailleurs, l'action du siRNA prive la cellule de la régulation du flux d'ions Na/K [42]. L'association des deux traitements pourrait entrainer un stress oxydatif plus important menant à la cytotoxicité. Une seconde hypothèse pourrait être formulée concernant une action possible sur le cycle cellulaire. En effet, l'inhibition de la sous-unité alpha 1 doit empêcher la transduction du signalosome favorisant la prolifération (c-myc) [42, 44]. De plus, l'action de l'ansa-ferrociphenol pourrait également perturber le cycle cellulaire impliquant un arrêt en phase G0/G1 [45, 46]. Des études complémentaires seront nécessaires afin de déterminer le mode d'action induit par l'association de ces deux molécules.

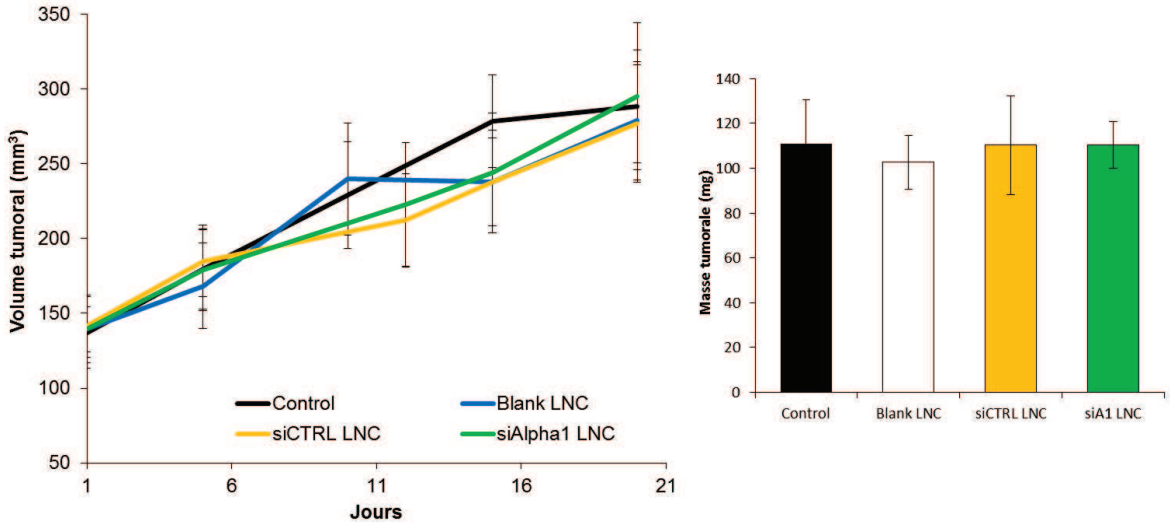

Figure 20 : Impact du ciblage de la sous-unité alpha 1 de la pompe à sodium via des LNC siRNA sur un modèle de mélanome sous-cutané. (A gauche) La progression du volume tumoral est réalisée en fonction des différents traitements : contrôle (aucune injection, noir), LNC blanches (bleu), LNC siRNA contrôle (jaune) et LNC siRNA alpha 1 (vert). (A droite) Comparaison des masses tumorales en fonction des traitements réalisés. Les résultats démontrent l'absence d'effet du ciblage de la pompe à sodium sur le développement du mélanome sous-cutané. Les valeurs sont exprimées selon la moyenne des échantillons ± l'écart type standard (n=8).

Au vu de ces résultats prometteurs, des expérimentations chez la souris NMRI Nude après implantation en sous-cutané de cellules de mélanome humain (SK-Mel28) ont également été conduites (Figure 20). Cependant, l'injection de LNC siRNA alpha 1 n'engendre aucune modification sur la progression du mélanome sous-cutané, un résultat en corrélation avec les observations *in vitro*.

Par ailleurs, l'association du siRNA alpha 1 avec la dacarbazine, ainsi qu'avec les deux composés organométalliques décrits précédemment, a été testée sur le même modèle de mélanome sous-cutané. L'association avec la dacarbazine chez l'animal a confirmé les résultats obtenus *in vitro*. De façon intéressante, la concomitance n'a pas empêché l'action de la dacarbazine, mais aucun effet additif ou synergique n'a pu être observé. De plus, l'association du siRNA alpha 1 avec les deux dérivés ferrocèniques n'a montré aucune réduction préférentielle de la tumeur, résultat confirmé par l'obtention de masses tumorales identiques à celles du groupe contrôle correspondant.

4.1.2. La protéine Bcl-2

La protéine Bcl-2 est un acteur clé dans le processus de mort cellulaire qu'est l'apoptose [47]. Les LNC siRNA ont montré leur efficacité à délivrer le siRNA Bcl-2 avec une inhibition de la progression tumorale de 30 % en comparaison avec le groupe contrôle (cf. Chapitre 3). L'efficacité du ciblage de la protéine Bcl-2 a été largement décrite pour le mélanome par de nombreuses études [48]. Plusieurs essais cliniques avec un oligonucléotide antisens (Oblimersen®) ont été menés sur des patients atteints de mélanome métastasé [49]. Cependant, les études parues récemment semblent montrer que le bénéfice de l'oligonucléotide antisens sont limités [50] malgré une association avec la dacarbazine. En effet, les premières études *in vitro* démontrent la nécessité de combiner l'Oblimersen® avec des lipides cationiques pour permettre une transfection efficace des cellules tumorales [51]. Or, les expérimentations pré-cliniques et cliniques ne font pas référence à l'utilisation d'agents de transfection comme les lipides, l'oligonucléotide étant directement injecté en intrapéritonéale chez la souris ou en intraveineux chez l'homme [50, 51]. La limitation de son effet en clinique pourrait peut-être s'expliquer par l'absence d'un vecteur efficace pour l'internalisation. D'autres vecteurs encapsulant des siRNA ciblant la protéine Bcl-2 sont actuellement à l'étude dans d'autres modèles de cancer tels que des nanoparticules à base de silice [52], des liposomes cationiques [53], des nanoparticules polymériques à base de polyéthylène imine [17] ou encore des lipoplexes [54].

Finalement, l'effet mitigé des stratégies de ciblage de Bcl-2 peut également s'expliquer par la régulation complexe du processus d'apoptose [55]. L'inhibition de la protéine Bcl-2 par le siRNA peut, en effet, être masquée ou compensée par la surexpression d'autres membres anti-apoptotiques tels que Mcl-1 ou Bcl-$_{XL}$ [55]. L'utilisation de plusieurs siRNA serait une option à envisager afin d'améliorer l'effet pro-apoptotique. Des perspectives à plus long terme pourraient concerner l'utilisation de microARN (miRNA). Ces séquences, semblables aux siRNA, sont endogènes et ont la capacité, contrairement aux siRNA, d'interagir sur plusieurs cibles [56]. Une étude plus approfondie

des différents miRNA impliqués dans la régulation de l'apoptose fournirait de nouveaux outils pour moduler plus efficacement l'expression de plusieurs protéines pro-apoptotiques.

Par ailleurs, l'association de chimiothérapies semble indispensable pour optimiser l'inhibition de Bcl-2 [14]. Les LNC siRNA Bcl-2 ont été combinées avec trois traitements anticancereux différents (cf. chapitre 3). Cependant, les travaux de concomitance avec la dacarbazine et avec le ferrociphénol n'ont pas mis à jour d'effet additif ou synergique entre les différentes associations. Des résultats encourageants ont été obtenus avec l'ansa-ferrociphénol (ansa-FcDiOH), mais la durée de traitement ne semblait pas adaptée. Un effet de courte durée (7 jours) a pu être observé avec une stabilisation de la croissance tumorale (cf. chapitre 3). Cependant, dès l'arrêt du traitement, la progression a repris son cours. Des études sont actuellement en cours afin de tester à nouveau l'association de ces deux composés sous un nouveau protocole comprenant une semaine d'injections de LNC siRNA Bcl-2-FcDiOH suivie de deux semaines de traitement avec les LNC FcDiOH.

Ces premières expérimentations chez l'animal soulèvent la problématique du protocole expérimental. En effet, l'association de plusieurs traitements nécessite la mise au point et l'optimisation du protocole d'injections. Dans un but de sensibilisation, nous pensons qu'il est nécessaire de débuter par le traitement contenant le siRNA, puis de continuer avec la chimiothérapie. Cependant, la littérature montre qu'il n'existe pas de protocole expérimental universel [4, 14]. Une étude approfondie du protocole adéquat est indispensable pour améliorer l'efficacité des traitements concomitants.

4.2. Les composés organométalliques

Les composés organométalliques tels que les ferrocifènes représentent une classe novatrice de molécules pouvant apporter de nouvelles réponses pour les cancers dits résistants [45]. Leur efficacité a d'ores et déjà été démontrée sur un modèle de cellules tumorales issues de cancer du sein triple négatif [45]. Les études *in vitro* réalisées sur les cellules de mélanome humain montrent un effet cytotoxique lié aux ferrocifènes très intéressant en comparaison avec la dacarbazine (cf. Chapitre 3). Cependant, seul l'ansa-ferrociphénol montre une activité antiproliférative sur le modèle sous-cutané de mélanome, confirmant ainsi la cytotoxicité plus élevée de ce dérivé par rapport aux autres dérivés ferrocéniques [46].

L'efficacité de ces composés sur les cellules de mélanome peut s'expliquer par un mécanisme d'action ne dépendant pas de l'apoptose. En effet, de récents travaux montrent que les ferrocifènes favorisent la production de ROS au sein des cellules créant ainsi un stress oxydatif [43]. Ces composés apparaissent donc comme une alternative aux traitements actuels. Cependant, la solubilité réduite des ferrocifènes oblige le développement de formulation pour une injection intraveineuse. Les nanocapsules lipidiques (LNC) ont démontré leur capacité à encapsuler ce type de molécules avec succès [57]. Des études antérieures ont montré des effets de radiosensibilisation des LNCs de

ferrociphénol avec des complexes lipophiles de rhénium pour le traitement du glioblastome (tumeur du système nerveux central) [58]. L'application de ces dérivés organométalliques semble donc prometteuse et de multiples études complémentaires s'imposent afin de découvrir et comprendre le mécanisme lié à leur propriété antiproliférative.

5. Un avenir en clinique ?

Les nanomédecines, ou vecteurs non viraux, semblent aujourd'hui apporter des réponses satisfaisantes pour l'encapsulation et la délivrance de siRNA par voie systémique. Qu'en est-il de leur développement au niveau clinique ? En 2010, le résultat du premier essai clinique utilisant un vecteur polymérique encapsulant un siRNA est publié [59]. Les travaux mettent en évidence une bonne tolérance du système. Depuis, cinq nouveaux essais cliniques sont actuellement en cours (*www.clinicaltrials. gov*). Et si les LNC siRNA devaient arriver demain en clinique, quel budget cela représenterait-il pour soigner un patient ? Il est assez difficile d'évaluer le coût global d'une telle thérapie. Par extrapolation par rapport aux expérimentations précliniques réalisées ici, le coût du traitement, comprenant uniquement les excipients et les molécules nécessaires à la réalisation de la formulation, représenterait déjà un budget de 17 500 € pour un patient soigné pendant une semaine. Par comparaison, le coût moyen aujourd'hui des chimiothérapies est évalué à quelques milliers d'euros pour une cure complète (Rapport de 2010, *du Service d'évaluation Médico-économique et santé publique, Haute autorité de la Santé*). Les nouvelles thérapies sont sans doute des thérapies extrêmement coûteuses, un paramètre essentiel, qui conditionnera le développement de telles stratégies en clinique.

Par ailleurs, quel recul avons-nous sur la tolérance de ces nanomédecines ? La toxicité de ces particules représente à l'heure actuelle une part des enjeux importants afin d'évaluer la faisabilité des nanomédecines en clinique [60]. L'encapsulation des siRNA passe principalement par des molécules cationiques (polymères ou lipides) connues pour leur toxicité [61]. De plus, l'inhibition transitoire à la base du système d'ARN interférent demande le plus souvent des ré-injections, pouvant alors créer une toxicité cumulée [62]. Les injections systémiques présentent le plus fort risque de toxicité due à une accessibilité à la plupart des organes vitaux et une possible accumulation comme dans le foie [60]. Dans notre étude, les analyses sur les enzymes ALAT et ASAT montrent, qu'après plusieurs injections de LNC siRNA, le taux augmente mais ne dépasse jamais plus de deux fois le niveau basal (cf. Chapitre 3). Ces nanocapsules lipidiques apparaissent donc comme très peu toxiques (hépatotoxicité). Par ailleurs, aucune mortalité n'a été observée, ni même de perte de poids supérieure à 5%, même après 1 à 3 semaines d'injection intraveineuse. Cependant, d'autres problèmes de toxicité peuvent émerger via l'utilisation des siRNA. En effet, ces séquences nucléotidiques peuvent être reconnues par les TLR (Tool-like Receptor) et les activer, favorisant ainsi l'initiation d'une réponse inflammatoire [63]. Pour le moment, aucun problème majeur de toxicité n'est à déplorer au vu des premiers essais

cliniques utilisant des siRNA. Pourtant, les recherches sur la nanotoxicité restent primordiales afin d'assurer le développement de nouvelles alternatives viables.

Bibliographie

[1] D. Hanahan, R.A. Weinberg, Hallmarks of cancer: the next generation, Cell, 144 (2011) 646-674.

[2] M.S. Soengas, S.W. Lowe, Apoptosis and melanoma chemoresistance, Oncogene, 22 (2003) 3138-3151.

[3] A.L. Gartel, Mechanisms of apoptosis induced by anticancer compounds in melanoma cells, Curr Top Med Chem, 12 (2012) 50-52.

[4] P. Resnier, T. Montier, V. Mathieu, J.P. Benoit, C. Passirani, A review of the current status of siRNA nanomedicines in the treatment of cancer, Biomaterials, 34 (2013) 6429-6443.

[5] A. Vonarbourg, C. Passirani, L. Desigaux, E. Allard, P. Saulnier, O. Lambert, J.P. Benoit, B. Pitard, The encapsulation of DNA molecules within biomimetic lipid nanocapsules, Biomaterials, 30 (2009) 3197-3204.

[6] M. Morille, T. Montier, P. Legras, N. Carmoy, P. Brodin, B. Pitard, J.P. Benoit, C. Passirani, Long-circulating DNA lipid nanocapsules as new vector for passive tumor targeting, Biomaterials, 31 (2010) 321-329.

[7] M. Morille, C. Passirani, S. Dufort, G. Bastiat, B. Pitard, J.L. Coll, J.P. Benoit, Tumor transfection after systemic injection of DNA lipid nanocapsules, Biomaterials, 32 (2010) 2327-2333.

[8] S. David, T. Montier, N. Carmoy, P. Resnier, A. Clavreul, M. Mevel, B. Pitard, J.P. Benoit, C. Passirani, Treatment efficacy of DNA lipid nanocapsules and DNA multimodular systems after systemic administration in a human glioma model, J Gene Med, 14 (2012) 769-775.

[9] S. David, P. Resnier, A. Guillot, B. Pitard, J.P. Benoit, C. Passirani, siRNA LNCs--a novel platform of lipid nanocapsules for systemic siRNA administration, Eur J Pharm Biopharm, 81 (2012) 448-452.

[10] M.S. Draz, B.A. Fang, P. Zhang, Z. Hu, S. Gu, K.C. Weng, J.W. Gray, F.F. Chen, Nanoparticle-mediated systemic delivery of siRNA for treatment of cancers and viral infections, Theranostics, 4 (2014) 872-892.

[11] J.M. Williford, J. Wu, Y. Ren, M.M. Archang, K.W. Leong, H.Q. Mao, Recent advances in nanoparticle-mediated siRNA delivery, Annu Rev Biomed Eng, 16 (2014) 347-370.

[12] K. Messaoudi, P. Saulnier, K. Boesen, J.P. Benoit, F. Lagarce, Anti-epidermal growth factor receptor siRNA carried by chitosan-transacylated lipid nanocapsules increases sensitivity of glioblastoma cells to temozolomide, Int J Nanomedicine, 9 (2014) 1479-1490.

[13] A. Griveau, J. Bejaud, S. Anthiya, S. Avril, D. Autret, E. Garcion, Silencing of miR-21 by locked nucleic acid-lipid nanocapsule complexes sensitize human glioblastoma cells to radiation-induced cell death, Int J Pharm, 454 (2013) 765-774.

[14] N.S. Gandhi, R.K. Tekade, M.B. Chougule, Nanocarrier mediated delivery of siRNA/miRNA in combination with chemotherapeutic agents for cancer therapy: Current progress and advances, J Control Release, 194C (2014) 238-256.

[15] O. Taratula, O.B. Garbuzenko, A.M. Chen, T. Minko, Innovative strategy for treatment of lung cancer: targeted nanotechnology-based inhalation co-delivery of anticancer drugs and siRNA, J Drug Target, 19 (2011) 900-914.

[16] M. Saad, O.B. Garbuzenko, T. Minko, Co-delivery of siRNA and an anticancer drug for treatment of multidrug-resistant cancer, Nanomedicine (Lond), 3 (2008) 761-776.

[17] D. Cheng, N. Cao, J. Chen, X. Yu, X. Shuai, Multifunctional nanocarrier mediated co-delivery of doxorubicin and siRNA for synergistic enhancement of glioma apoptosis in rat, Biomaterials, 33 (2012) 1170-1179.

[18] B. Heurtault, P. Saulnier, B. Pech, J.E. Proust, J.P. Benoit, A novel phase inversion-based process for the preparation of lipid nanocarriers, Pharm Res, 19 (2002) 875-880.

[19] A. Paillard, F. Hindre, C. Vignes-Colombeix, J.P. Benoit, E. Garcion, The importance of endo-lysosomal escape with lipid nanocapsules for drug subcellular bioavailability, Biomaterials, 31 (2010) 7542-7554.

[20] M. Morille, C. Passirani, A. Vonarbourg, A. Clavreul, J.P. Benoit, Progress in developing cationic vectors for non-viral systemic gene therapy against cancer, Biomaterials, 29 (2008) 3477-3496.

[21] Y. Ma, Z. Wang, W. Zhao, T. Lu, R. Wang, Q. Mei, T. Chen, Enhanced bactericidal potency of nanoliposomes by modification of the fusion activity between liposomes and bacterium, Int J Nanomedicine, 8 (2013) 2351-2360.

[22] D. Vllasaliu, R. Fowler, S. Stolnik, PEGylated nanomedicines: recent progress and remaining concerns, Expert Opin Drug Deliv, 11 (2014) 139-154.

[23] Y. Li, M. Kroger, W.K. Liu, Endocytosis of PEGylated nanoparticles accompanied by structural and free energy changes of the grafted polyethylene glycol, Biomaterials, 35 (2014) 8467-8478.

[24] C. Rangger, A. Helbok, E. von Guggenberg, J. Sosabowski, T. Radolf, R. Prassl, F. Andreae, G.C. Thurner, R. Haubner, C. Decristoforo, Influence of PEGylation and RGD loading on the targeting properties of radiolabeled liposomal nanoparticles, Int J Nanomedicine, 7 (2012) 5889-5900.

[25] A.C. Groo, P. Saulnier, J.C. Gimel, J. Gravier, C. Ailhas, J.P. Benoit, F. Lagarce, Fate of paclitaxel lipid nanocapsules in intestinal mucus in view of their oral delivery, Int J Nanomedicine, 8 (2013) 4291-4302.

[26] S. David, N. Carmoy, P. Resnier, C. Denis, L. Misery, B. Pitard, J.P. Benoit, C. Passirani, T. Montier, In vivo imaging of DNA lipid nanocapsules after systemic administration in a melanoma mouse model, Int J Pharm, 423 (2012) 108-115.

[27] A.L. Laine, J. Gravier, M. Henry, L. Sancey, J. Bejaud, E. Pancani, M. Wiber, I. Texier, J.L. Coll, J.P. Benoit, C. Passirani, Conventional versus stealth lipid nanoparticles: formulation and in vivo fate prediction through FRET monitoring, J Control Release, 188 (2014) 1-8.

[28] M. Lotem, A. Hubert, O. Lyass, M.A. Goldenhersh, A. Ingber, T. Peretz, A. Gabizon, Skin toxic effects of polyethylene glycol-coated liposomal doxorubicin, Arch Dermatol, 136 (2000) 1475-1480.

[29] A. Jacquemet, J. Barbeau, L. Lemiegre, T. Benvegnu, Archaeal tetraether bipolar lipids: Structures, functions and applications, Biochimie, 91 (2009) 711-717.

[30] J. Barbeau, S. Cammas-Marion, P. Auvray, T. Benvegnu, Preparation and Characterization of Stealth Archaeosomes Based on a Synthetic PEGylated Archaeal Tetraether Lipid, J Drug Deliv, 2011 (2011) 396068.

[31] A. Jhaveri, P. Deshpande, V. Torchilin, Stimuli-sensitive nanopreparations for combination cancer therapy, J Control Release, 190 (2014) 352-370.

[32] Y. Kato, S. Ozawa, C. Miyamoto, Y. Maehata, A. Suzuki, T. Maeda, Y. Baba, Acidic extracellular microenvironment and cancer, Cancer Cell Int, 13 (2013) 89.

[33] E. Bourseau-Guilmain, J. Bejaud, A. Griveau, N. Lautram, F. Hindre, M. Weyland, J.P. Benoit, E. Garcion, Development and characterization of immuno-nanocarriers targeting the cancer stem cell marker AC133, Int J Pharm, 423 (2012) 93-101.

[34] A. Correa, S. Pacheco, A.E. Mechaly, G. Obal, G. Behar, B. Mouratou, P. Oppezzo, P.M. Alzari, F. Pecorari, Potent and specific inhibition of glycosidases by small artificial binding proteins (affitins), PLoS One, 9 (2014) e97438.

[35] N.T. Huynh, E. Roger, N. Lautram, J.P. Benoit, C. Passirani, The rise and rise of stealth nanocarriers for cancer therapy: passive versus active targeting, Nanomedicine (Lond), 5 (2010) 1415-1433.

[36] M. Sang, L. Wang, C. Ding, X. Zhou, B. Wang, L. Wang, Y. Lian, B. Shan, Melanoma-associated antigen genes - an update, Cancer Lett, 302 (2011) 85-90.

[37] A.A. Rosenkranz, T.A. Slastnikova, M.O. Durymanov, A.S. Sobolev, Malignant melanoma and melanocortin 1 receptor, Biochemistry (Mosc), 78 (2013) 1228-1237.

[38] R. Fazzina, L. Lombardini, L. Mezzanotte, A. Roda, P. Hrelia, A. Pession, R. Tonelli, Generation and characterization of bioluminescent xenograft mouse models of MLL-related acute leukemias and in vivo evaluation of luciferase-targeting siRNA nanoparticles, Int J Oncol, 41 (2012) 621-628.

[39] P. Ofek, W. Fischer, M. Calderon, R. Haag, R. Satchi-Fainaro, In vivo delivery of small interfering RNA to tumors and their vasculature by novel dendritic nanocarriers, Faseb J, 24 (2010) 3122-3134.

[40] W. Fuller, L.B. Tulloch, M.J. Shattock, S.C. Calaghan, J. Howie, K.J. Wypijewski, Regulation of the cardiac sodium pump, Cell Mol Life Sci, 70 (2013) 1357-1380.

[41] T. Mijatovic, R. Kiss, Cardiotonic steroids-mediated Na+/K+-ATPase targeting could circumvent various chemoresistance pathways, Planta Med, 79 (2013) 189-198.

[42] V. Mathieu, C. Pirker, E. Martin de Lassalle, M. Vernier, T. Mijatovic, N. DeNeve, J.F. Gaussin, M. Dehoux, F. Lefranc, W. Berger, R. Kiss, The sodium pump alpha1 sub-unit: a disease progression-related target for metastatic melanoma treatment, J Cell Mol Med, 13 (2009) 3960-3972.

[43] C. Lu, J.M. Heldt, M. Guille-Collignon, F. Lemaitre, G. Jaouen, A. Vessieres, C. Amatore, Quantitative analyses of ROS and RNS production in breast cancer cell lines incubated with ferrocifens, ChemMedChem, 9 (2014) 1286-1293.

[44] A.N. Nguyen, K. Jansson, G. Sanchez, M. Sharma, G.A. Reif, D.P. Wallace, G. Blanco, Ouabain activates the Na-K-ATPase signalosome to induce autosomal dominant polycystic kidney disease cell proliferation, Am J Physiol Renal Physiol, 301 (2011) F897-906.

[45] A.L. Laine, E. Adriaenssens, A. Vessieres, G. Jaouen, C. Corbet, E. Desruelles, P. Pigeon, R.A. Toillon, C. Passirani, The in vivo performance of ferrocenyl tamoxifen lipid nanocapsules in xenografted triple negative breast cancer, Biomaterials, 34 (2013) 6949-6956.

[46] A.L. Laine, A. Clavreul, A. Rousseau, C. Tetaud, A. Vessieres, E. Garcion, G. Jaouen, L. Aubert, M. Guilbert, J.P. Benoit, R.A. Toillon, C. Passirani, Inhibition of ectopic glioma tumor growth by a potent ferrocenyl drug loaded into stealth lipid nanocapsules, Nanomedicine, (2014).

[47] G. Grazia, I. Penna, V. Perotti, A. Anichini, E. Tassi, Towards combinatorial targeted therapy in melanoma: from pre-clinical evidence to clinical application (review), Int J Oncol, 45 (2014) 929-949.

[48] N. Mohana-Kumaran, D.S. Hill, J.D. Allen, N.K. Haass, Targeting the intrinsic apoptosis pathway as a strategy for melanoma therapy, Pigment Cell Melanoma Res, 27 (2014) 525-539.

[49] A.A. Tarhini, J.M. Kirkwood, Oblimersen in the treatment of metastatic melanoma, Future Oncol, 3 (2007) 263-271.

[50] A.Y. Bedikian, C. Garbe, R. Conry, C. Lebbe, J.J. Grob, Dacarbazine with or without oblimersen (a Bcl-2 antisense oligonucleotide) in chemotherapy-naive patients with advanced melanoma and low-normal serum lactate dehydrogenase: 'The AGENDA trial', Melanoma Res, 24 (2014) 237-243.

[51] J. Ramanarayanan, F.J. Hernandez-Ilizaliturri, A. Chanan-Khan, M.S. Czuczman, Pro-apoptotic therapy with the oligonucleotide Genasense (oblimersen sodium) targeting Bcl-2 protein expression enhances the biological anti-tumour activity of rituximab, Br J Haematol, 127 (2004) 519-530.

[52] T.L. Cheng, C.F. Teng, W.H. Tsai, C.W. Yeh, M.P. Wu, H.C. Hsu, C.F. Hung, W.T. Chang, Multitarget therapy of malignant cancers by the head-to-tail tandem array multiple shRNAs expression system, Cancer Gene Ther, 16 (2009) 516-531.

[53] C. Zheng, M. Zheng, P. Gong, J. Deng, H. Yi, P. Zhang, Y. Zhang, P. Liu, Y. Ma, L. Cai, Polypeptide cationic micelles mediated co-delivery of docetaxel and siRNA for synergistic tumor therapy, Biomaterials, 34 (2013) 3431-3438.

[54] K. Nakamura, A.S. Abu Lila, M. Matsunaga, Y. Doi, T. Ishida, H. Kiwada, A double-modulation strategy in cancer treatment with a chemotherapeutic agent and siRNA, Mol Ther, 19 (2011) 2040-2047.

[55] R.A. Anvekar, J.J. Asciolla, D.J. Missert, J.E. Chipuk, Born to be alive: a role for the BCL-2 family in melanoma tumor cell survival, apoptosis, and treatment, Front Oncol, 1 (2011).

[56] C. Luo, C.E. Weber, W. Osen, A.K. Bosserhoff, S.B. Eichmuller, The role of microRNAs in melanoma, Eur J Cell Biol, 93 (2014) 11-22.

[57] E. Allard, N.T. Huynh, A. Vessieres, P. Pigeon, G. Jaouen, J.P. Benoit, C. Passirani, Dose effect activity of ferrocifen-loaded lipid nanocapsules on a 9L-glioma model, Int J Pharm, 379 (2009) 317-323.

[58] E. Allard, D. Jarnet, A. Vessieres, S. Vinchon-Petit, G. Jaouen, J.P. Benoit, C. Passirani, Local delivery of ferrociphenol lipid nanocapsules followed by external radiotherapy as a synergistic treatment against intracranial 9L glioma xenograft, Pharm Res, 27 (2009) 56-64.

[59] M.E. Davis, J.E. Zuckerman, C.H. Choi, D. Seligson, A. Tolcher, C.A. Alabi, Y. Yen, J.D. Heidel, A. Ribas, Evidence of RNAi in humans from systemically administered siRNA via targeted nanoparticles, Nature, 464 (2010) 1067-1070.

[60] H.Y. Xue, S. Liu, H.L. Wong, Nanotoxicity: a key obstacle to clinical translation of siRNA-based nanomedicine, Nanomedicine (Lond), 9 (2014) 295-312.

[61] J. Zhao, Y. Mi, S.S. Feng, siRNA-based nanomedicine, Nanomedicine (Lond), 8 (2013) 859-862.

[62] K. Raemdonck, R.E. Vandenbroucke, J. Demeester, N.N. Sanders, S.C. De Smedt, Maintaining the silence: reflections on long-term RNAi, Drug Discov Today, 13 (2008) 917-931.

[63] K. Singha, R. Namgung, W.J. Kim, Polymers in small-interfering RNA delivery, Nucleic Acid Ther, 21 (2011) 133-147.

CONCLUSION & PERSPECTIVES

CONCLUSION & PERSPECTIVES

Ces travaux de thèse ont premièrement permis le développement d'une formulation stable et efficace pour la délivrance de siRNA au sein de cellules tumorales, telles que les cellules issues de mélanome humain (Figure bilan 21). Ces études ont permis d'approfondir la compréhension d'un tel système et ainsi appréhender les interactions présentes entre les siRNA et les nanocapsules lipidiques (LNC). Cette formulation améliorée a donné lieu à un dépôt de brevet durant le mois de septembre 2014 afin de protéger cette invention innovante.

En ce qui concerne les travaux sur le ciblage tumoral, ils rappellent l'intérêt du ciblage passif pour le mélanome à l'aide de LNC pegylées. Cependant, la partie lipophile du polymère, qui permet l'ancrage de PEG au niveau de la coque des LNC, semble jouer un rôle important dans l'interaction avec les cellules mais également sur la biodistribution et le ciblage tumoral. Il apparait donc aujourd'hui essentiel d'étudier ce phénomène plus en détail afin de comprendre les mécanismes qui engendrent ces différences de comportement. Par ailleurs, le greffage des affitines a été initié lors de ce projet de thèse. Il s'agit maintenant de développer des affitines spécifiques qui pourront avoir une attractivité et un intérêt pour le ciblage actif du mélanome primaire, mais également pour les sites métastatiques.

La comparaison de deux cibles protéiques distinctes : la protéine anti-apoptotique Bcl-2 et la sous-unité alpha 1 de la pompe à sodium, a permis d'étudier deux stratégies d'action sur la résistance du mélanome. Les résultats d'expérimentation animale mettent en évidence un effet antiprolifératif intéressant avec le ciblage de Bcl-2, contrairement au ciblage de la sous-unité alpha 1. La chimio-sensibilité a été étudiée avec la chimiothérapie de référence prescrite actuellement (dacarbazine) ainsi qu'avec une nouvelle catégorie d'agents anticancéreux que sont les molécules organométalliques (les ferrocifènes). Les résultats obtenus *in vitro* ont montré des effets cytostatiques prometteurs et encourageants concernant les traitements concomitants. Cependant, le bénéfice *in vivo* n'a pas été à la hauteur des espérances avec la nécessité de s'attarder à l'avenir sur la mise au point du protocole d'injections. De nouvelles expérimentations pourront être conduites avec un fractionnement différent des traitements afin d'optimiser l'effet des thérapies.

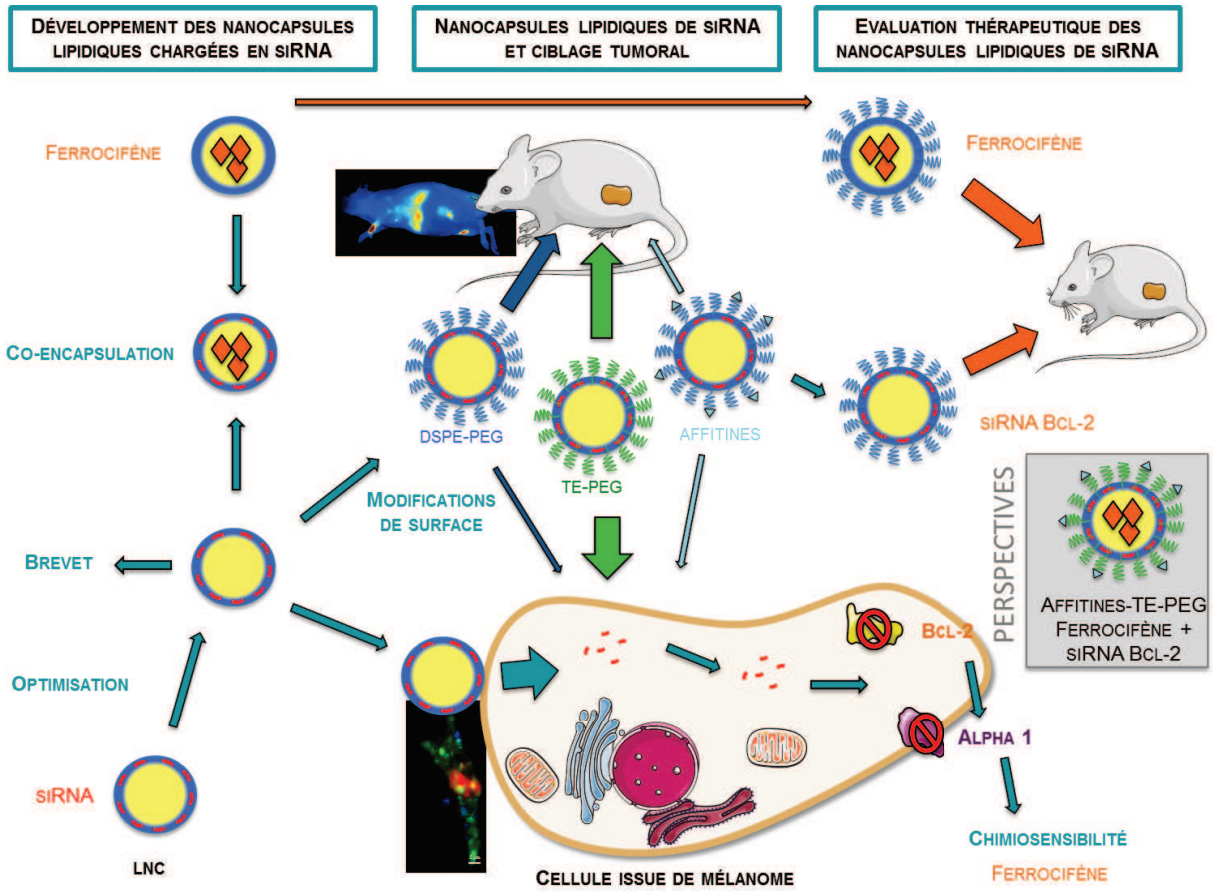

Figure 21 : Représentation schématique bilan des travaux de thèse

Finalement, la preuve de concept sur la co-encapsulation de chimiothérapie et la capacité des LNC à éteindre un gène au niveau tumoral après injection intraveineuse démontrent l'étendue des possibilités concernant l'utilisation des LNC comme co-vecteur d'acides nucléiques et d'agents anti-cancéreux. Un nombre illimité de combinaisons est alors imaginable et applicable à tout type de cellules cancéreuses pour lesquelles les LNC présentent une affinité.

ANNEXE

ANNEXE

1. Chapitre de Livre

Pauline Resnier, Anne Clavreul and Catherine Passirani. "Chapter 15: Nanocarriers for the treatment of Brain Tumours. Nanomedicine and the Nervous System". *Edition: King's College London*. 2012. ISBN 978-1-57808-728-0.

2. Publication

Pauline Resnier, Stephanie David, Nolwenn Lautram, Gaëtan Delcroix, Anne Clavreul, Jean-Pierre Benoit, Catherine Passirani. "EGFR siRNA Lipid Nanocapsules efficiently transfect glioma cells *in vitro*". *International Journal of Pharmaceutics*. 2013. 454; 748-755.

3. Curriculum vitae

CHAPITRE DE LIVRE

NANOCARRIERS FOR THE TREATMENT OF BRAIN TUMORS

NANOCARRIERS FOR THE TREATMENT OF BRAIN TUMOURS

Pauline Resnier, Anne Clavreul, Catherine Passirani [1]

[1] corresponding author

Catherine Passirani

INSERM U646, Université d'Angers

IBS-CHU ANGERS

4 rue Larrey

49933 Angers Cedex 9

E-mail: catherine.passirani@univ-angers.fr

Tel: +33 244 68 85 34. Fax: +33 244 68 85 46

Pauline Resnier

INSERM U646, Université d'Angers

IBS-CHU ANGERS

4 rue Larrey

49933 Angers Cedex 9

E-mail: pauline.resnier@etud.univ-angers.fr

Anne Clavreul

INSERM U646, Université d'Angers

IBS-CHU ANGERS

4 rue Larrey

49933 Angers Cedex 9

E-mail: anne.clavreul@univ-angers.fr

Tel : +33 244 68 85 48. Fax: +33 244 68 85 46

Abstract

Many strategies have been developed to deliver chemotherapeutic agents into the brain, especially to treat gliomas. Among them, nanostructures have appeared like new promising drug carriers thanks to their small size (<1µm) and generally lipid components that should improve the passage of the blood brain barrier (BBB). Firstly, local strategies by stereotaxy like bolus injection and convection enhanced delivery (CED) have the advantage to bypass the hurdle of BBB. However, these techniques are invasive and repeated administrations are excluded. On the other hand, nanoparticles, thanks to their stability in bloodstream and their long-circulating properties, have been developed for intravenous strategies by passive or active targeting. The passive strategy permits to target tumour thanks to the increased permeability of tumour vessels while the active strategy uses ligands that promote directly the interaction with cancer cells or indirectly facilitate the passage through the BBB. More recently, these nanostructures have appeared to be an efficient solution to deliver DNA or siRNA for gene therapy.

Abbreviations

G: Generation
CBTRUS: Central brain tumors registry of the United States
BBB: Blood-brain barrier
MNPs: Magnetic nanoparticles
SPIONs: Superparamagnetic iron oxide nanoparticles
PLA: Polylactide
PLGA : Polylactide-co-glycolide
SLNs: Solid lipid nanoparticles
LNCs: Lipid nanocapsules
PEG: Polyethylene glycol
CED: Convection enhanced delivery
TAA: Tumor associated antigen
EGFR: Epidermal growth factor receptor
EPR: Enhanced permeability retention effect
TF: Transferrin
MAN: P-aminophenyl-α-D-manopyroside
NGR: Asn-Gly-Arg
RGD: Arg-Gly-Asp
IL-13: Interleukin 13
GLUT1: Glucose transporter 1
TGFβ: Transforming growth factor β
TNFα: Tumor necrosis factor α
TRAIL: TNF-related-apoptosis-inducing-ligand

Key terms – définition

- *Blood-brain barrier (BBB)* is a specific structure observed in the brain; it regulates exchanges with the bloodstream and homeostasis.
- *Systemic strategy* consists in delivering therapeutic agents from the bloodstream after intravenous or intraperitoneal injection.
- *Local strategy* consists in injecting directly therapeutic agents into the tumour area. In the case of gliomas, this injection is executed into the brain by stereotaxy.
- *Convection-enhanced delivery (CED)* is a local technique allowing the display, *via* a constant pressure gradient, of greater volumes of distribution than by stereotaxy bolus.
- *Enhanced Permeability and Retention (EPR) effect* is a destabilisation of the vessel endothelium that causes the decrease of cell junction and the increase of the vessel permeability. This phenomenon is observed on vessels that are close to a tumour site.
- *Passive targeting* is a concept of "natural" accumulation in tumour area based on the long circulating property of nanoparticles and on the EPR effect.
- *Active targeting* is a concept that consists in functionalising nanoparticles with ligands to specifically target tumour cells or to guide carriers to the tumour site.

Key facts of nanocarriers in brain tumor therapy

- Drug-loaded nanocarriers hold great promise in the field of brain tumour therapy. They enable the control of drug characteristics such as solubility, vascular circulation time, and specific site-targeted delivery.
- Four principal types of nanocarriers are developed for brain tumour treatment: dendrimers, micelles, liposomes and nanoparticles that can be magnetic, polymer or lipid/polymer.
- *Nanocarriers* are divided in generations (G) that characterise their stabilised structure (G1), stealth (G2) or targeting (G3) properties. Stabilised nanocarriers (G1) provide controlled drug release but necessitate a local injection. Stealth nanocarriers (G2) escape the immune system recognition which enhances their longevity in the blood and their accumulation into the tumour *via* the EPR effect, leading to passive targeting. Functionalized nanocarriers (G3) enable active targeting based on the attachment of ligands at the surface of the carrier to bind specifically on over-expressed receptors of tumour cells or organs.
- Systemic (intravenous or intraperitoneal) and direct (stereotaxic bolus or CED) delivery to brain tumours have been used to administer drug-loaded nanocarriers.
- Gene-loaded nanocarriers are recently developed to increase or decrease the expression of a target gene and are opening a new field of research in glioma therapy.

Summary points

- Glioblastomas, more frequent primary brain tumours, still have a poor prognostic as the median survival rarely exceeds 1 year.
- The ineffectiveness of chemotherapy in glioblastomas is not linked to drug potency but mainly to the presence of BBB and the poor penetration of drug into the tumour. Drug-loaded nanocarriers such as dendrimers, micelles, liposomes and nanoparticles are able to protect

drugs and improve their biodistribution and therapeutic index and represent a new hope for brain treatment.

- Local delivery strategies of drug-loaded nanocarriers to brain tumour (stereotaxy bolus and CED) showed promising results because they have the advantage to bypass the BBB and to deliver high concentrations of drugs. However, they are not adaptable for repeated injections and for personalisation of patient treatment.
- Systemic delivery of drug-loaded nanocarriers offers the advantage to be non invasive and to allow repeated injections over short periods. The development of stealth and functionalized nanocarriers to allow passive and active targeting in brain tumour respectively holds great promise for systemic delivery approaches.
- The gene therapy of brain tumour is more recent but first *in vivo* results with gene-loaded nanocarriers are promising and demonstrate the therapeutic potential of this strategy for brain cancer disease.

1. Introduction

1.1. Brain tumours

Primary brain tumours include tumours of the brain parenchyma, meninges, cranial nerves, and other intracranial structures (such as the pituitary and pineal glands). The most common and malignant primary brain tumours are Grade IV astrocytomas, called glioblastomas, which are characterised by the aggressive invasion and diffuse infiltration of tumor cells into the surrounding brain tissue. According to CBTRUS (Central Brain Tumor Registry of the United States), glioblastomas accounted for about 20% of the estimated 44,500 new primary brain tumours diagnosed in the United States in 2005. The conventional therapy of glioblastomas consists of surgery followed by fractionated radiotherapy with concomitant and adjuvant chemotherapy with temozolomide (Stupp *et al.*, 2009). Despite this treatment, glioblastomas generally recur at the site of initial treatment. Median survival is around 16 months and less than 10% of patients survive for more than five years.

Numerous chemotherapeutic drugs affecting cell division or DNA synthesis have been tested to improve the prognosis of glioblastomas (Muldoon *et al.,* 2007). However, the ineffectiveness of these drugs for the treatment of brain tumours is generally not linked to drug potency, but mainly to three hurdles:

1) The presence of the blood-brain barrier (BBB) which regulates central nervous system homeostasis and controls the delivery of molecules in the brain (Figure 1). This restriction is carried out by endothelial cell-tight junctions, which are characterised by an absence of fenestration and a reduction of pinocytotic vesicles. In addition, the BBB is composed of specific anatomical elements that also limit this passage of, for example, astrocytic end-feet, pericytes and extracellular matrices. Furthermore, this normal barrier has an efflux activity due to the presence of effective efflux transporters on surface cells (Deeken *et al*., 2007).

2) Diffusion in the brain parenchyma is very weak, partially due to the high level of intercellular fluid pressure in tumours. Targeting tumour cells infiltrating the brain tissue surrounding the tumour is consequently rather difficult which leads to frequent GB recurrence.

3) The brain tissue is highly sensitive, so only limited doses of therapeutic agents can be employed.

1.2. Applications to area of health and disease

Many strategies have emerged to overcome these three obstacles. Among these, nanotechnology has been developed to protect drugs and improve their biodistribution and therapeutic index. These non-viral carriers can ideally offer optimal, controlled release and specific targeting that could limit unwanted side effects on healthy cells and deliver a therapeutic concentration of drugs only to cancerous cells. Chemotherapy is already a major point to treat cancer. The use of drug-loaded nanocarriers is expected to ameliorate the prognostic of patients hoping a curative treatment.

2. Nanocarriers

Nanocarriers regroup some models of nanostructures recognisable by their organization, size and lipid or polymer components. They are divided in generations (G) that characterise their stabilised structure (G1), stealth (G2) or targeting (G3) properties (Figure 2). The principal nanocarriers described for the treatment of gliomas are dendrimers, micelles, liposomes and different types of nanoparticles.

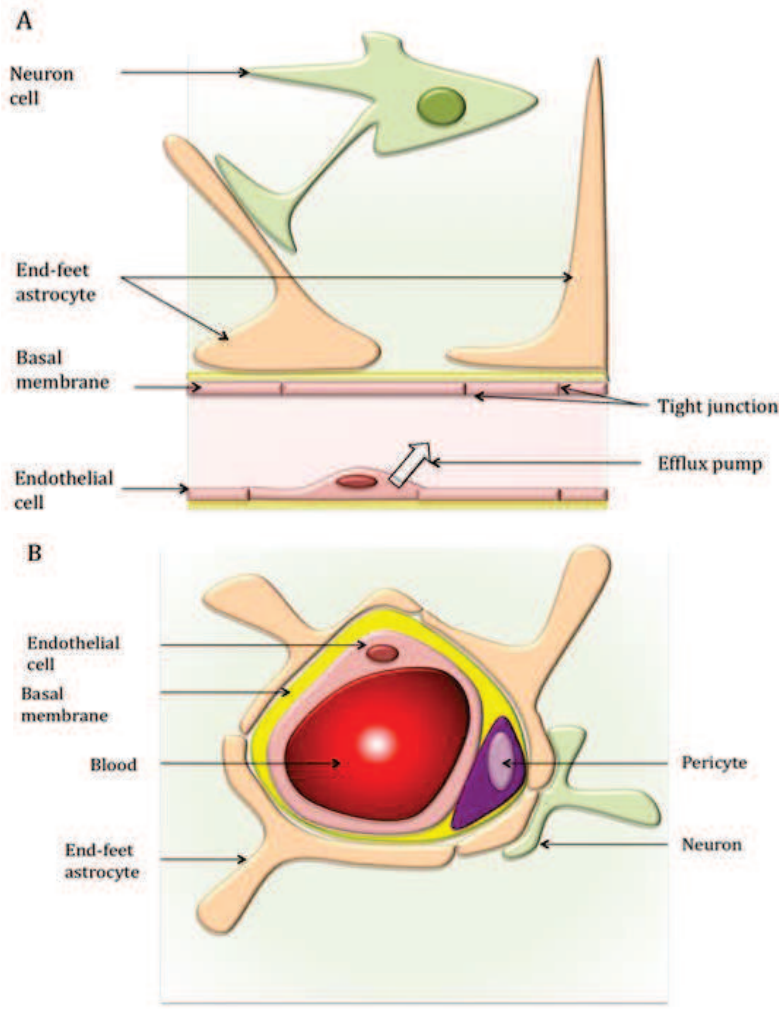

Figure 1: Schematic representation of the blood-brain barrier (A: longitudinal and B: transversal). In the brain, tight junctions bind endothelial cells; they are surrounded by pericytes and basal membrane. Moreover, end-feet of astrocytes create a second layer that surrounds basal membrane, increases te non-permeability of the BBB and allows neuron protection.

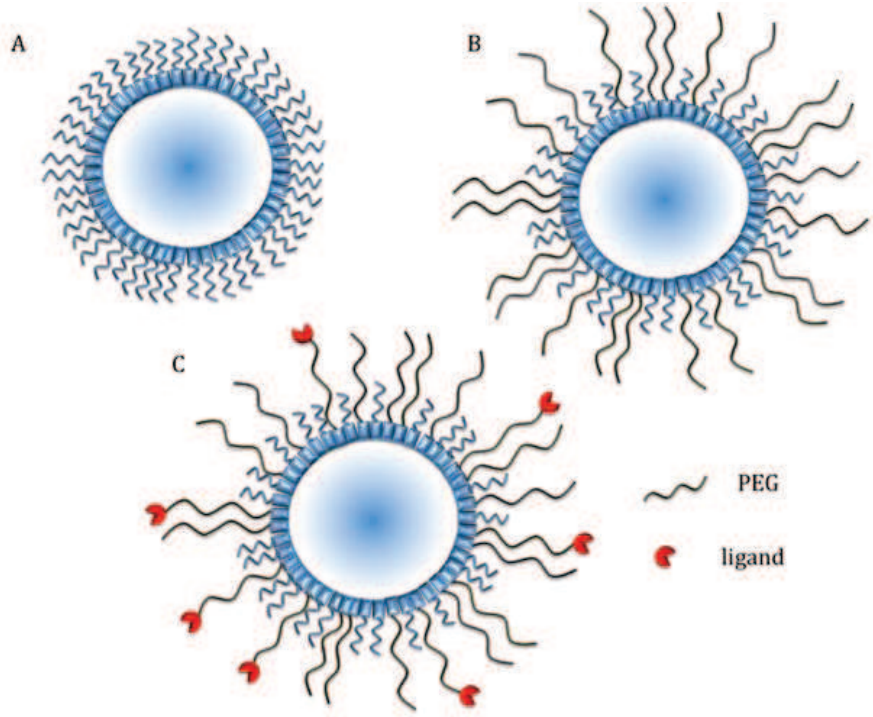

Figure 2: Representation of nanocarrier generations (G). A: G1, B: G2 and C: G3. Nanocarriers are classified into three generations (G). The first generation (G1) corresponds to vectors stabilised with surfactant for drug encapsulation. G2 corresponds to stealth nanoparticles; they have long-circulating properties and can be used for systemic delivery. G3 are nanocarriers functionalised with ligands to target specifically tumour cells or organs.

2.1. Dendrimers

Dendrimers are hierarchical, highly-branched polymers that form a spherical three-dimension structure. These "macromolecules" are built with the repetitive assembly of a unique monomer around a core. This confers a narrow degree of polydispersity and low nanometer range size. The number of layers represents the generation of a dendrimer (Figure 3A). Sizes are less than 4-5 nm for earlier generations (G0-G5) and more than 10 nm for most complex dendrimers (G9-G10). This specific shape can react with nanoscopic reagents like drugs as well as with DNA or antibodies, and form stable complexes. These very small sizes allow an improved passage through natural barriers, this being an essential point for systemic injection for the brain. Moreover, dendrimers are characterised by multivalency that confers a high capacity of reaction with all surfaces in a "molecular Velcro" behaviour (Nanjwade *et al.*, 2009). Dendrimers are often considered like "proteins" because they can adopt a "native" or "denatured" conformation depending on polarity, ionic strength and pH of the solvent.

2.2. Polymer micelles

Block copolymers that have amphiphilic properties can spontaneously form polymer micelles in aqueous media with a size of between 50 and 100 nm (Figure 3B). These are characterised by a core-shell structure whose core serves as a nanocontainer for hydrophobic drugs as anticancer drugs. Micelles provide a good alternative for poor water-soluble drugs but also for gene or siRNA thanks to electrostatic interactions. Advantages of micelles are an easy process of fabrication, efficient drug loading and a fairly narrow size distribution. They also present good thermodynamic stability in physiological solution that induces slow dissociation and controlled drug release (Nishiyama and Kataoka, 2006).

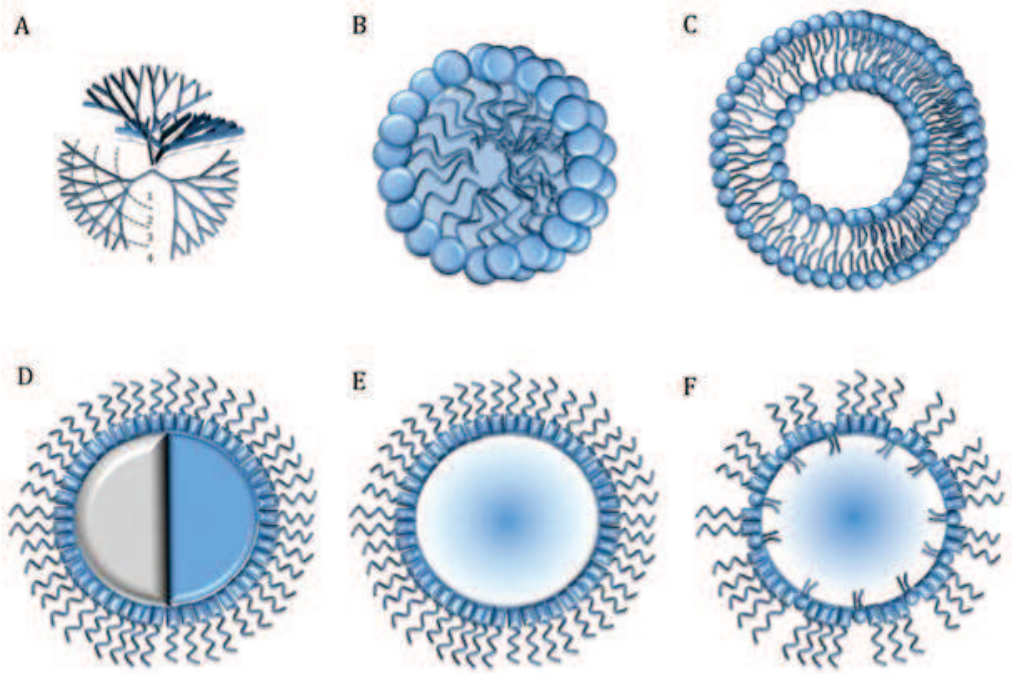

Figure 3: Representation of various nanostructures used in brain tumor therapy. Four different types of nanocarriers are mainly developed in brain tumour therapy: (A) dendrimer: highly-branched polymers; (B) micelle: diblock polymers auto-assembled; (C) liposome: bilayer of phospholipids forming a liquid aqueous core; (D) nanoparticles: polymer shell that can contain magnetic core (left), or solid polymer core (right); (E) solid lipid nanoparticle: polymer and lipid shell surrounding a solid lipid core; and (F) lipid nanocapsule: polymer and lipid shell surrounding a liquid lipid core.

2.3. Liposomes

Liposomes are nanocarriers whose structure is similar to the lipid membrane of cells (figure 3C) (Ulrich, 2002). They are composed of amphiphilic molecules, found in biological membranes (like phospholipids, cholesterol, sphingomyelin…) that spontaneously assemble into bilayers due to their poor solubility and their configuration. Liposomes are divided into two major sub-groups: multilamellar vesicles (0.1 to 10 µm) and unilamellar ones. Small unilamellar vesicles are less than 100 nm in size; large ones are from 100 nm to 500 nm and giant ones are around 1 µm. Hydrophobic and hydrophilic drugs can be encapsulated simultaneously or singly inside liposomes. This property allows lipoplexes to be created, due to electrostatic interaction between nucleic acids (DNA or siRNA) and lipids. Under pathological conditions, such as in malignant tumours, liposomes (< 100 nm) can passively pass through the lipid membrane by fusion or by receptor-mediated endocytosis. Thanks to their size, hydrophobic and hydrophilic character, biocompatibility, biodegradability, low toxicity and immunogenicity, liposomes are promising systems for drug delivery.

2.4. Nanoparticles

Nanoparticles regroup two types of nanocarriers that differ in their intern organisation: nanospheres that are characterised by a matrix structure; and nanocapsules that have a vesicular structure with an inner core surrounded by a shell. This shell can be composed of polymer and/or lipid with various proportions and sizes from 10 nm and 200-500 nm. Nanoparticles are very interesting because they are characterised by their physical stability due to the presence of polymers, good protection of incorporated, labile drugs from degradation, and good release control.

2.4.1. Magnetic nanoparticles

In this case, the shell surrounds a magnetic core. MNPs have traditionally been used for disease imaging, but recent advances have opened the door for drug delivery. This group includes metallic, bimetallic and superparamagnetic iron oxide nanoparticles (SPIONs). The latter are widely favoured because they have an inoffensive toxicity profile and a reactive surface. SPIONs are mainly made with magnetite (Fe_3O_4) and maghemite (Fe_2O_3), which form the magnetic core usually surrounded by polymer components to enhance their biocompatibility (Figure 3D). These nanoparticles are not only used for their chemical stability, but also for their possibilities in the use of targeted drug delivery. In fact, the particular physiochemical profile of SPIONs can provide specific targeting, as with Combidex®, used for imaging of lymph node metastasis (Harisinghani *et al*., 2003).

2.4.2. Polymer nanoparticles

Polymer nanoparticles are usually formulated using hydrophobic synthetic polymers or copolymers such as polylactide/polyglycolide (PLA, PLGA), polyacrylates, polycaprolactones or natural polymers such as albumin, gelatin, alginate, collagen, and chitosan…. (Figure 3D). PLA and PLGA have been the most investigated nanoparticles for drug delivery (Langer, 1997). The degradation of these polymers can be altered by changing the block copolymer composition and molecular weight. Hence, the release of an encapsulated therapeutic agent can be adjusted to last from days to months. Polymer nanoparticles are mainly formulated using emulsion/solvent evaporation or solvent-displacement techniques (Jain, 2000). Using these methods, a variety of therapeutic agents including low molecular weight lipophilic or hydrophilic drugs and high molecular weight DNA or antisense oligonucleotides can be encapsulated (Prabha and Labhasetwar, 2004).

2.4.3. Lipid nanocarriers

Solid lipid nanoparticles (SLNs) represent an alternative colloidal matrix carrier system with a solid lipid core inside which the hydrophobic drug is dispersed or dissolved (Figure 3E). The whole is surrounded by a monolayer of phospholipids and polymers (Brioschi *et al.*, 2009). They have a size around 100 nm. High drug loading, good stability and reproducibility characterise SLNs. Moreover, controlled release of the therapeutic agent can be achieved for up to several weeks in the case of specific formulations.

Lipid nanocapsules (LNCs), like SLNs, are built by combining the use of poly(ethylene glycol) (PEG) and lipid monolayer in the shell (Figure 3F) in order to surround and stabilise an oily liquid core. This core can encapsulate lipophilic drugs. LNCs have the same advantages as SLNs: good stability, good protection and control of drug delivery. Moreover, the use of solutol® in their composition inhibits drug efflux pumps which actively remove chemotherapeutic drugs from the brain (Huynh *et al.*, 2009). SLNs and LNCs present some advantages for drug delivery because they are formulated without organic solvents, are well tolerated, are biodegradable (depending on polymer used) and possess a high degree of availability for targeting thanks to their high level stability. SLN/LNC systems can represent an innovative way to administer molecules into the brain as well as intravenously.

3. Nanocarriers in brain tumour therapy

Chemotherapy is usually essential to obtain cancer remission. Nanotechnology constitutes a new strategy to deliver chemotherapy into the brain and consequently to improve treatment. It can also be used for immunotherapy or radiotherapy. Systemic or local delivery to the brain has been used to administer these drug-loaded nanocarriers and various approaches have been evaluated for their selective targeting of brain tumours.

3.1. Local delivery (see examples and references in Table 1)

In order to avoid systemic side effects, local injections of chemotherapeutic agents can be performed using two different methods. The first method is the stereotaxy bolus which generates a simple diffusion of the drugs into the brain (Figure 4A). Several assays with drug-loaded nanocarriers have shown promising results in brain tumour therapy. However, a major problem is the slow movement of nanocarriers within the brain due to limited diffusion coefficients and back-flow of the injection because of the closely-packed arrangement of cells in both the grey and white matter microenvironments (Nicholson et al., 1998).

To overcome these problems, a second stereotatic technique called CED (convection enhanced delivery) has emerged (Figure 4B). This method is based on the convection of a fluid by maintaining a pressure gradient during interstitial infusion, achieving a greater dose and volume of distribution compared to diffusion alone. Passive CED has been the subject of many studies in the field of nanotechnology in combination with a multitude of molecules including ferrocifen, doxorubicin, topotecan, and synthetic retinoid Am80. Radiotherapy by passive targeting has also been tested by CED.

Different approaches of active CED have emerged such as the functionalisation of the drug-loaded nanocarrier surface with ligands or antibodies to specifically target the tumour endothelium and tumour associated antigens (TAAs). Currently, most tests are based on the use of antibodies against the TAA epidermal growth factor receptor (EGFR) or its mutant EGFRvIII which is expressed in 25% of glioblastomas but not in the normal brain. Another approach of active targeting is the use of stem cells as cellular carriers for nanoparticles, knowing the specific tropism of these cells for brain tumours (Roger *et al., in press*). Roger *et al*. (2010) showed that polylactide nanoparticles and LNCs could be efficiently internalised into mesenchymal stem cells without cell viability and differentiation being affected. Furthermore, these nanoparticle-loaded cells were able to migrate towards an experimental human glioma model and their therapeutic effect was evidenced *in vitro* and *in vivo* (unpublished results). All these local strategies showed promising results; however, they do not provide practical solutions to everyday life nor the possibility of adjustment and adaptation for each patient.

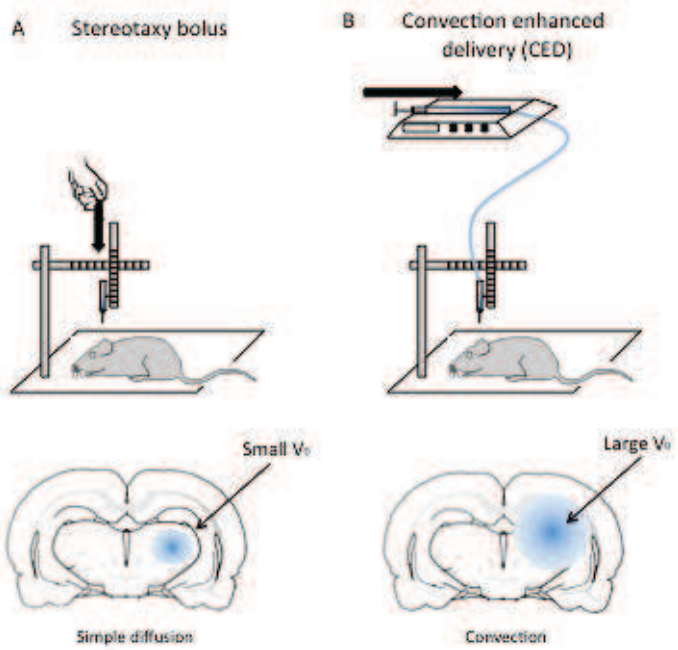

Figure 4: Schematic representation of nanocarrier local delivery approaches. Local injection is performed by: (A) stereotaxy bolus that consists of simple diffusion in the brain parenchyma, and induces a weak volume of distribution (V_D); (B) stereotaxy-convection enhanced delivery (CED) that consists in delivering a large volume of solution by the application of a constant pressure gradient, inducing a large V_D.

nanocarriers	loaded molecule	injection method	targeting	targeting molecule	cell model	result	ref
platinum NPs	/	bolus	passive	/	rat C6	diminution of the tumor size and volume	Lopez et al., 2010
PLA NPs	BCNU (Carmustine)	bolus	active	transferin	rat C6	significantly prolonged survival	Kang et al., 2009
LNCs	ferrocifen	CED	passive	/	rat 9L	significantly prolonged survival	Allard et al., 2009
PEG liposomes	doxorubicine	CED	passive	/	human U87MG + U251	significantly prolonged survival	Kikuchi et al., 2008
liposomes (no PEG)	topotecan	CED	passive	/	human U87MG	significantly prolonged survival	Grahn et al., 2009
polymer micelles	doxorubicin	CED	passive	/	rat 9L	significantly prolonged survival	Inoue et al., 2009
Polymer micelles	synthetic retinoid Am80	CED	passive	/	human U87MG	significantly prolonged survival	Yokosawa et al., 2010
LNCs	ferrocifen + radiotherapy	CED	passive	/	rat 9L	significantly prolonged survival	Allard et al., 2010
LNCs	paclitaxel + radiotherapy	CED	passive	/	rat 9L	significantly prolonged survival	Vinchon-Petit et al., 2010
dendrimers	methotrexate	CED	active	mAb EGFR (cetuximab)	rat F98	significantly prolonged survival	Wu et al., 2006
boronated dendrimers (PAMAM)	/	bolus and CED	active	EGF	rat F98	significantly prolonged survival	Yang et al., 2009
boronated dendrimers	/	CED	active	mAb EGFR and EGFRVIII (cetuximab + L8A4)	rat F98	significantly prolonged survival	Yang et al., 2009
MNPs	/	CED	active	mAb EGFRvIII (L8A4)	human U87MG (mutant EGFR vIII)	speicific targeting	Hadjipanayis et al., 2010

Table 1: Local delivery of nanocarriers in experimental glioma models. NPs: Nanoparticles; PLA: Polylactide; BCNU: 1,3-bis(2-chloroethyl)-1 nitrosourea; LNCs: Lipid nanocapsules; CED: Convection enhanced delivery; PEG: Polyethylene glycol; mAb: Monoclonal antibody; EGF: Epidermal growth factor; EGFR: EGF receptor; PANAM: poly(amidoamine); MNPs: Magnetic NPs.

3.2. Systemic delivery (see examples and references in Table 2)

The greatest advantages of using systemic, drug-loaded nanocarrier delivery are their non-invasive nature and the possibility to allow repeated injections over short periods. The most commonly used method for systemic administration of nanocarriers into the body is the intravenous route. After intravenous injection, the nanocarriers are very quickly eliminated from the bloodstream due to the activation of the immune system by these foreign particles. The phagocytic mechanism of the mononuclear phagocyte system cells is the first cause advanced for this phenomenon. To improve half-life of nanoparticles in blood, stealth nanoparticles (generation 2) have been developed according to different parameters such as size, zeta potential, and surface modification with hydrophilic PEG (Vonarbourg *et al.,* 2006). The improvement of the half-life allows passive targeting of a tumour *via* the phenomenon of EPR (enhanced permeability and retention) (Maeda *et al.*, 2000) (Figure 5A). The occurrence of this phenomenon at the tumour area is due to the organisation, structure and properties of neoangionenesis tumour vessels, these being more permeable than conventional vessels. In addition, cancer cells are constantly growing and therefore more readily accept the entry of molecules or external structures as nanocarriers. Finally, there is a lack of lymphatic drainage in tumoural environment. This causes a "natural" accumulation of nanostructures in tumours.

Liposomes, micelles and nanoparticles were used for passive targeting, which led to significantly prolonged survival of C6 glioma bearing rats. To improve passive targeting, “semi-active” strategies were used. For example, the addition of surfactants such as polysorbate 80 in the formulation of nanoparticles is known to allow receptor-mediated endocytosis by the brain capillary endothelial cells after absorption of apolipoproteins B and E. In a number of rat studies, polysorbate 80-nanocarriers carrying doxorubicine, gemcitabine, or indomethacin crossed the BBB and reached therapeutic areas in the brain, thereby extending survival in glioma models. In another strategy, superparamagnetic nanoparticles, which can be concentrated within the tumour tissue by local application of an external magnetic field, have been also developed and thereby allow non-targeted tissue and organs to remain unaffected.

As with local strategy, active targeting strategies consisting of grafting specific molecules onto the surface of nanoparticles to transport drug-loaded nanocarriers across the BBB and then target brain gliomas have also been explored (Figure 5B). Transferrin (TF) ligand that binds to the TF receptor, which is over-expressed on the brain capillary endothelium and on the surface of proliferating brain tumour cells, has been tested (Figure 6). The functionalisation of nanocarriers with an RGD sequence; peptides containing the Asn-Gly-Arg (NGR) motif, p-aminophenyl-a-D-manno-pyranoside (MAN) or interleukin-13 (IL-13) has also been performed (Figure 6). RGD sequences facilitate interaction between drug delivery nanocarriers and some integrins such as integrin avb3, widely over-expressed on tumoural neovasculature and glioma cells. The motif NGR links to aminopeptidase N (CD13), a membrane-spanning molecule, over-expressed on tumour cells and most tumour endothelial cells. MAN has a specific affinity to the glucose transporter GLUT1, which is mainly expressed in the luminal surface of the brain capillaries and the choroid plexus.

These strategies have shown promising results in experimental glioma models; however, the major difficulty remains in knowing cell surface markers able to specifically target the BBB and tumour cells. At present, no unique glioma-specific antigen has been discovered due to the intra-tumoural heterogeneity and the inter-patient variability. However, despite these difficulties, the intravenous route remains a vital challenge for non-invasive administration and particularly for repeated administration for cancerous diseases in the brain.

nanocarriers	loaded molecule	injection method	targeting	targeting molecule	cell model	result	ref
liposomes	arsenic trioxide	iv	passive	/	rat C6	survival significantly prolonged	Zhao et al., 2008
polymer micelles	SN-38	iv	passive	/	human U87MG	survival significantly prolonged	Kuroda et al., 2010
PLGA NPs	doxorubicin	iv	passive	/	rat 101/8	survival significantly prolonged	Gelperina et al., 2010
CBSA NPs	aclaturin	iv	passive	/	rat C6	survival significantly prolonged	Lu et al., 2007
polysorbate NPs	doxorubicin	iv	semi-active	polysorbate-80	rat 101/8	survival significantly prolonged	Steiniger et al., 2004
polysorbate NPs	doxorubicin	iv	semi-active	polysorbate-80	rat 101/8	survival significantly prolonged and antiangiogenic effect	Hekmatara et al., 2009
PBCA NPs	doxorubicin	iv	semi-active	polysorbate-80	rat 101/8	survival significantly prolonged	Ambruosi et al., 2006
PBCA NPs	gemcitabin	iv	semi-active	polysorbate-80	rat C6	survival significantly prolonged	Wang et al., 2009
nanocapsules	indomethacin	ip	semi-active	polysorbate-80	rat C6	survival significantly prolonged	Bernardi et al., 2009
Superparamagnetic NPs	paclitaxel	iv	semi-active	magnetism	rat C6	survival significantly prolonged	Zhao et al., 2010
Liposomes	epirubucin	iv	active	TF	rat C6	survival significantly prolonged	Tian et al., 2010
PEG-DPSE micelles	paclitaxel	iv	active	NGR	rat C6	inhibition of tumoral growth	Zhao et al., 2010
PEG-DPSE micelles	paclitaxel	iv	active	RGD	human U87MG	survival significantly prolonged	Zhan et al., 2010
liposomes (PEG)	daunorubicin	iv	active	MAN and TF	rat C6	survival significantly prolonged	Ying et al, 2009
liposomes (PEG)	doxorubicin	ip	active	IL-13	human U87MG	survival significantly prolonged compare to doxorubicin liposome without IL-13	Madhankumar et al., 2009

Table 2: Systemic delivery of nanocarriers in experimental glioma models. SN-38: active drug of irinotecan; PLGA: Polylactide-polyglycolide, CBSA: cationic bovine serum albumin; NPs: Nanoparticles; PBCA: Polybutylcyanoacrylate; LNCs: Lipid nanocapsules; TF: Transferrin, PEG: polyethylene glycol; PEG-DSPE: 1,2-distearoyl-*sn*-glycero-3-phosphoethanolamine-N-[amino(polyethylene glycol)-2000]; NGR: Asn-Gly-Arg; RGD: Arg-Gly-Asp; MAN: p--aminophenyl-α-D-manopyroside; IL-13: Interleukin-13.

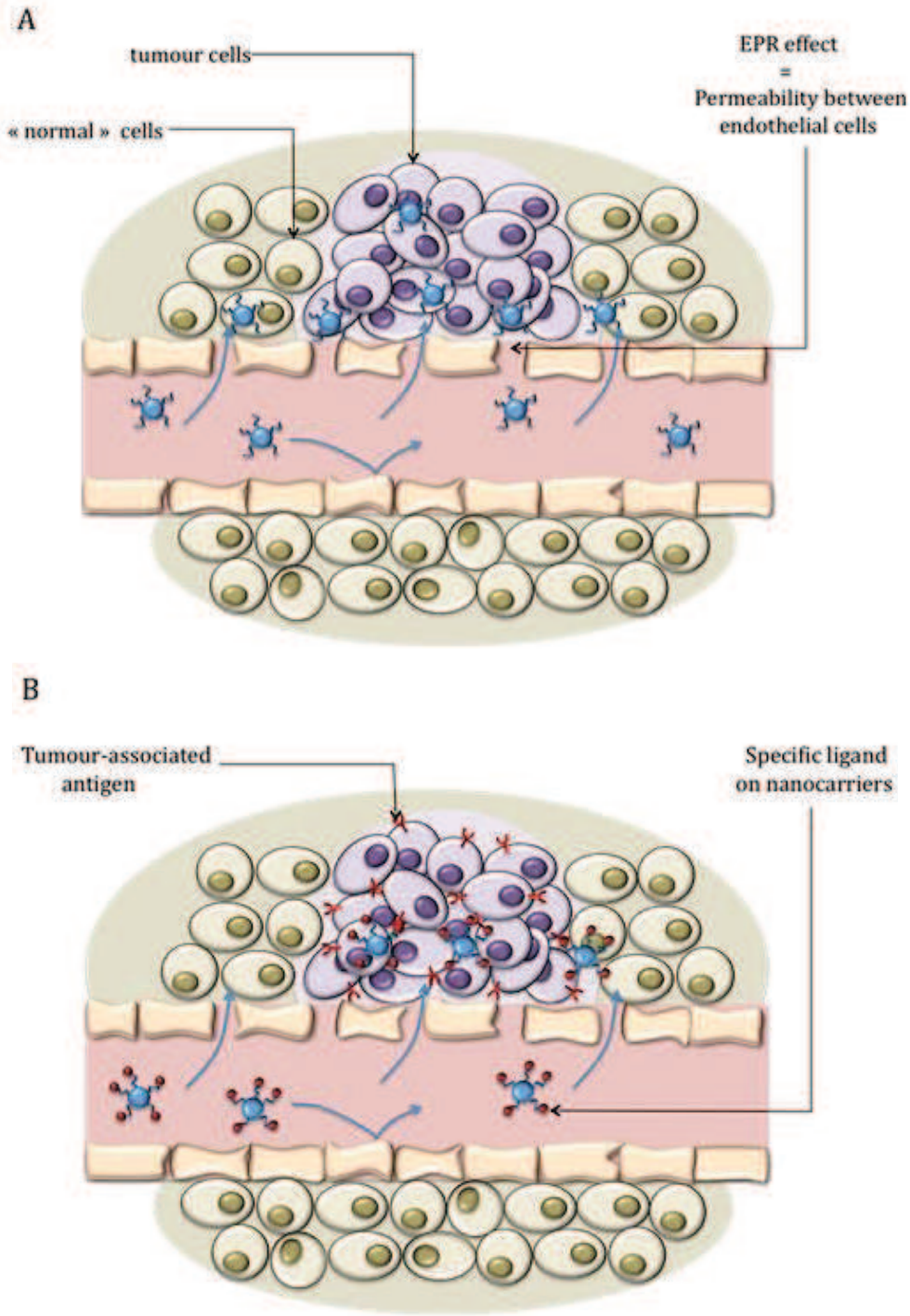

Figure 5: Passive and active targeting of nanocarriers in brain tumour. (A) Passive targeting is based on the longevity of the nanocarrier in the blood and its accumulation in the tumour site *via* the EPR effect. (B) Active targeting is based on the functionalisation of the nanocarrier with ligands that bind to tumour-associated antigens over-expressed on tumour cells.

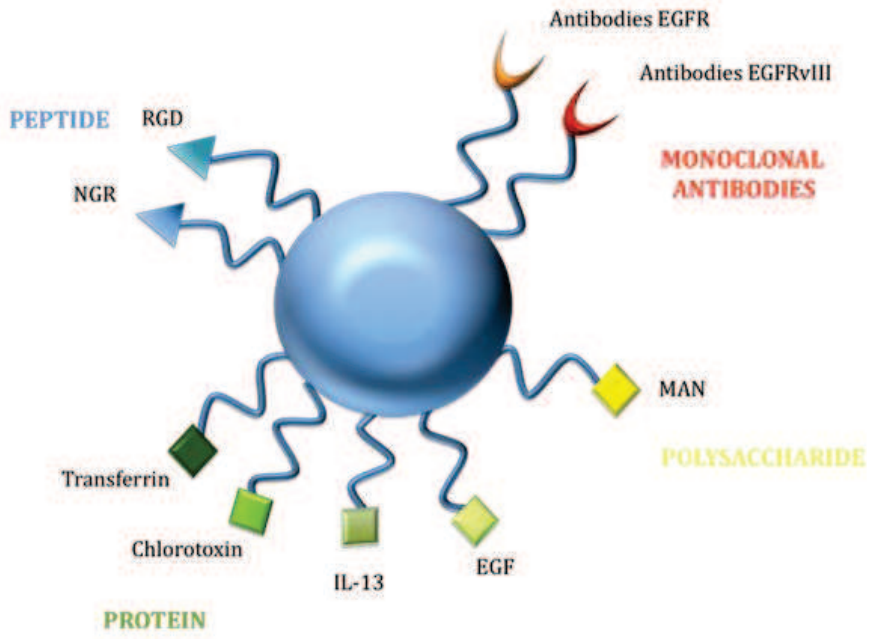

Figure 6: Representation of ligands used to functionalise nanocarriers to target specifically brain tumour cells. Four types of ligands are mainly used in brain tumour therapy: monoclonal antobodies [anti-EGFR (epidermal growth factor receptor) and anti-EGFRvIII (EGFR variant III)], proteins [transferrin, chlorotoxin, EGF and interleukin-13 (IL-13)], peptides [RGD (Arg-Gly-Asp) and NGR (Asn-Gly-Arg)] and polysaccharide [Man (p-aminophenyl-α-D-manopyroside)]

4. Future strategies of treatment (Table 3)

Now, after almost 40 years of research, nanoparticles have become a real platform for chemotherapy. However, chemotherapy may not be sufficient to induce glioma remission. Many studies have been working on combining various treatments (chemotherapy, radiotherapy and/or immunotherapy). For example, Allard *et al*. (2010) recently studied the association of radiotherapy with chemotherapy encapsulated in lipid nanocapsules, showing a synergistic effect on survival.

Over the last decade, gene therapy has undergone considerable expansion with improved knowledge of the genome and also with the discovery of siRNA. Gene therapy involves inserting a fragment of RNA or DNA into the cell that can directly/indirectly modify the expression of a target gene. Strategies consist of increasing the expression of a gene with the insertion of a new copy, or by inhibiting the expression of a gene with the insertion of siRNA. Due to renal filtration, nuclease degradation, and a poor cellular uptake, the encapsulation of these hydrophilic molecules is necessary to consider their use *in vivo*. As most nanoparticles have a predominantly hydrophobic solid or liquid core, the combination of nucleic acids with hydrophobic forms has necessitated the development of appropriate formulations. A possible association within liposomes has been largely developed: indeed, cationic lipids used for liposome formulation can react with the negative charge of nucleic acids and form stable complexes called lipoplexes. In addition, they have a good cellular uptake. Gupta *et al.,* (2007) demonstrated this transfection ability in nude mice that received U87 human glioma cells. An alternative form was developed by Morille *et al*., (2010) and consisted of the encapsulation of lipoplexes within lipid nanocapsules. They showed long-circulating properties and accumulation by EPR effect in sub-cutaneous U87MG glioma model after intravenous injection. Moreover, examples of active targeting were realised by grafting TF or chlorotoxin. This latter agent is commonly used for

labelling property, but in this case, chlorotoxin modified nanoparticles showed an improved cellular uptake and high gene expression.

Several studies worked on diminution of the expression of target gene, using nanocarriers delivering EGFR siRNA and EGFR as well as transforming growth factor beta (TGFb) antisense oligonucleotides, and showed promising results in experimental animal glioma models. In fact, EGFR gene is often over-expressed in cancer cells like glioblastoma, and consequently conducts to high proliferative capacity and aggressive form. TGFb is an anti-inflammatory factor that causes an immunosuppression and promotes tumoural development. In parallel, some studies worked on increasing the expression of target gene by using nanocarriers delivering therapeutic DNA encoding tumor necrosis factor alpha (TNFa) or TNF-related-apoptosis-inducing-ligand (TRAIL). TRAIL is involved in the phenomenon of "extrinsic" apoptosis pathway and can bypass the block of intrinsic apoptosis. TNFa is a pleiotropic inflammatory cytokine that promotes the immune response.

In conclusion, gene therapy for cancer represents a new therapeutic possibility in the context of brain tumours, and is gaining more and more interest due to recent successes achieved in vivo.

nanocarriers	loaded molecule	injection method	targeting	targeting molecule	model	result	ref
liposomes	GFP (ADN)	stereotaxy bolus	active	TAT peptide	human U87MG	good transfection in vivo	Gupta et al., 2007
LNCs	DNA	iv	passive	/	human U87MG	tumoural accumulation in vivo	Morille et al., 2010
MNPs	DNA (GFP)	iv	active	chlorotoxin	rat C6	DNA delivery in tumor and highly expression	Kievit et al., 2010
dendriworms	siRNA (EGFR)	CED	passive	/	human primary GBM	inhibition of EGFR by siRNA	Agrawal et al., 2009
PBCA NPs	antisens oligonucleotid (TGFβ)	ip	passive	/	rat F98	survival significantly prolonged	Schneider et al., 2008
folated PAMAM dendrimers	antisens oligonucleotide (EGFR)	stereotaxy bolus	passive	/	rat C6	survival significantly prolonged	Kang et al., 2010
CBSA-PEG NPs	plasmid pORF-hTRAIL	iv	passive	/	rat C6	inhibition of tumor growth	Lu et al., 2006
polypropylenimine dendrimers	TNFα	iv	active	TF	human T98G et A431	transfection in vivo in A431 and antiproliferative capacity in T98G	Koppu et al., 2010

Table 3: Preclinical studies on gene, siRNA or antisens oligonucleotide delivery with nanocarriers in brain tumour therapy. GFP: Green fluorescence protein; TAT peptide: Transactivator of transcription peptide; LNC: Lipid nanocapsules; PEI: Polyethylene Imine; ODN: Oligodeoxynucleotide; TF: Transferrin; MNPs: Magnetic nanoparticles; EGFR: Epidermal growth factor receptor; CED: Convection enhanced delivery; PBCA: poly(α-butyl-cyanoacrylate); TGFβ: Transforming growth factor β; GBM: Glioblastomas; PANAM: poly(amidoamine); CBSA: Cationic bovine serum, PEG: Polyethylene glycol, TNFa: Tumor necrosis factor α; TRAIL: TNF-related-apoptosis-inducing-ligand.

References

Agrawal A, Min DH, Singh N, Zhu H, Birjiniuk A, von Maltzahn G, Harris TJ, Xing D, Woolfenden SD, Sharp PA, Charest A, Bhatia S. Functional delivery of siRNA in mice using dendriworms. ACS Nano. 2009 Sep 22; 3(9):2495-504.

Allard E, Huynh NT, Vessières A, Pigeon P, Jaouen G, Benoit JP, Passirani C. Dose effect activity of ferrocifen-loaded lipid nanocapsules on a 9L-glioma model. Int J Pharm. 2009 Sep 11; 379(2):317-23.

Allard E, Jarnet D, Vessières A, Vinchon-Petit S, Jaouen G, Benoit JP, Passirani C. Local delivery of ferrociphenol lipid nanocapsules followed by external radiotherapy as a synergistic treatment against intracranial 9L glioma xenograft. Pharm Res. 2010 Jan; 27(1):56-64.

Allard E, Jarnet D, Vessières A, Vinchon-Petit S, Jaouen G, Benoît JP, Passirani C. Local delivery of ferrociphenol lipid nanocapsules followed by external radiotherapy as a synergistic treatment against intracranial 9L gliomas. Pharmaceutical Research 27(1):56-64, 2010

Ambruosi A, Gelperina S, Khalansky A, Tanski S, Theisen A, Kreuter J. Influence of surfactants, polymer and doxorubicin loading on the anti-tumour effect of poly(butyl cyanoacrylate) nanoparticles in a rat glioma model. J Microencapsul. 2006 Aug; 23(5):582-92.

Bernardi A, Braganhol E, Jäger E, Figueiró F, Edelweiss MI, Pohlmann AR, Guterres SS, Battastini AM. Indomethacin-loaded nanocapsules treatment reduces in vivo glioblastoma growth in a rat glioma model. Cancer Lett. 2009 Aug 18; 281(1):53-63.

Brioschi AM, Calderoni S, Zara GP, Priano L, Gasco MR, Mauro A. Chapter 11 - Solid lipid nanoparticles for brain tumors therapy: State of the art and novel challenges. Prog Brain Res. 2009; 180:193-223.

Deeken JF, Löscher W. The blood-brain barrier and cancer: transporters, treatment, and Trojan horses. Clin Cancer Res. 2007 Mar 15; 13(6):1663-74.

Gelperina S, Maksimenko O, Khalansky A, Vanchugova L, Shipulo E, Abbasova K, Berdiev R, Wohlfart S, Chepurnova N, Kreuter J. Drug delivery to the brain using surfactant-coated poly(lactide-co-glycolide) nanoparticles: influence of the formulation parameters. Eur J Pharm Biopharm. 2010 Feb; 74(2):157-63.

Grahn AY, Bankiewicz KS, Dugich-Djordjevic M, Bringas JR, Hadaczek P, Johnson GA, Eastman S, Luz M. Non-PEGylated liposomes for convection-enhanced delivery of topotecan and gadodiamide in malignant glioma: initial experience. J Neurooncol. 2009 Nov; 95(2):185-97.

Gupta B, Levchenko TS, Torchilin VP. TAT peptide-modified liposomes provide enhanced gene delivery to intracranial human brain tumor xenografts in nude mice. Oncol Res. 2007; 16(8):351-9.

Hadjipanayis CG, Machaidze R, Kaluzova M, Wang L, Schuette AJ, Chen H, Wu X, Mao H. EGFRvIII antibody-conjugated iron oxide nanoparticles for magnetic resonance imaging-guided convection-enhanced delivery and targeted therapy of glioblastoma. Cancer Res. 2010 Aug 1; 70(15):6303-12.

Harisinghani M.G, Barentsz J, Hahn P F, Deserno W M, abatabaei S T, vande Kaa C H, de la Rosette J, Weissleder R. Noninvasive detection of clinically occult lymph-node metastases in prostate cancer. New England Journal of Medicine 348 (2003) 2491-U5.

Hekmatara T, Bernreuther C, Khalansky AS, Theisen A, Weissenberger J, Matschke J, Gelperina S, Kreuter J, Glatzel M. Efficient systemic therapy of rat glioblastoma by nanoparticle-bound doxorubicin is due to antiangiogenic effects. Clin Neuropathol. 2009 May-Jun; 28(3):153-64.

Huynh NT, Passirani C, Saulnier P, Benoît JP. Lipid nanocapsules : a new platform for nanomedicine. International Journal of Pharmaceutics 379(2): 201-209, 2009

Inoue T, Yamashita Y, Nishihara M, Sugiyama S, Sonoda Y, Kumabe T, Yokoyama M, Tominaga T. Therapeutic efficacy of a polymeric micellar doxorubicin infused by convection-enhanced delivery against intracranial 9L brain tumor models. Neuro Oncol. 2009 Apr; 11(2):151-7.

Jain RA. The manufacturing techniques of various drug loaded biodegradable poly(lactide-co glycolide) (PLGA) devices. Biomaterials 2000; 21 (23):2475e90.

Kang C, Yuan X, Li F, Pu P, Yu S, Shen C, Zhang Z, Zhang Y. Evaluation of folate-PAMAM for the delivery of antisense oligonucleotides to rat C6 glioma cells in vitro and in vivo. J Biomed Mater Res A. 2010 May; 93(2):585-94.

Kang C, Yuan X, Zhong Y, Pu P, Guo Y, Albadany A, Yu S, Zhang Z, Li Y, Chang J, Sheng J. Growth inhibition against intracranial C6 glioma cells by stereotactic delivery of BCNU by controlled release from poly(D,L-lactic acid) nanoparticles. Technol Cancer Res Treat. 2009 Feb; 8(1):61-70.

Kievit FM, Veiseh O, Fang C, Bhattarai N, Lee D, Ellenbogen RG, Zhang M. Chlorotoxin labeled magnetic nanovectors for targeted gene delivery to glioma. ACS Nano. 2010 Aug 24; 4(8):4587-94.

Kikuchi T, Saito R, Sugiyama S, Yamashita Y, Kumabe T, Krauze M, Bankiewicz K, Tominaga T. Convection-enhanced delivery of polyethylene glycol-coated liposomal doxorubicin: characterization and efficacy in rat intracranial glioma models. J Neurosurg. 2008 Nov; 109(5):867-73.

Koppu S, Oh YJ, Edrada-Ebel R, Blatchford DR, Tetley L, Tate RJ, Dufès C. Tumor regression after systemic administration of a novel tumor-targeted gene delivery system carrying a therapeutic plasmid DNA. J Control Release. 2010 Apr 19; 143(2):215-21.

Kuroda J, Kuratsu J, Yasunaga M, Koga Y, Saito Y, Matsumura Y. Potent antitumor effect of SN-38-incorporating polymeric micelle, NK012, against malignant glioma. Int J Cancer. 2009 Jun 1; 124(11):2505-11.

Langer R. Tissue engineering: a new field and its challenges. Pharm Res 1997; 14(7):840-1.

López T, Figueras F, Manjarrez J, Bustos J, Alvarez M, Silvestre-Albero J, Rodríguez-Reinoso F, Martínez-Ferre A, Martínez E. Catalytic nanomedicine: a new field in antitumor treatment using supported platinum nanoparticles. In vitro DNA degradation and in vivo tests with C6 animal model on Wistar rats. Eur J Med Chem. 2010 May; 45(5):1982-90.

Lu W, Sun Q, Wan J, She Z, Jiang XG. Cationic albumin-conjugated pegylated nanoparticles allow gene delivery into brain tumors via intravenous administration. Cancer Res. 2006 Dec 15; 66(24):11878

Lu W, Wan J, She Z, Jiang X. Brain delivery property and accelerated blood clearance of cationic albumin conjugated pegylated nanoparticle. J Control Release. 2007 Mar 12; 118(1):38-53.

Madhankumar AB, Slagle-Webb B, Wang X, Yang QX, Antonetti DA, Miller PA, Sheehan JM, Connor JR. Efficacy of interleukin-13 receptor-targeted liposomal doxorubicin in the intracranial brain tumor model. Mol Cancer Ther. 2009 Mar; 8(3):648-54.

Maeda H, Wu J, Sawa T, Matsumura Y, Hori K. 2000. Tumor vascular permeability and the EPR effect in macromolecular therapeutics: a review. J Control Release 65:271-284.

Morille M, Montier T, Legras P, Carmoy N, Brodin P, Pitard B, Benoît JP, Passirani C. Long-circulating DNA lipid nanocapsules as new vector for passive tumor targeting. Biomaterials. 2010 Jan; 31(2):321-9.

Morille M, Passirani C, Dufort S, Bastiat G, Pitard B, Coll JL, Benoît JP. In vivo gene expression in tumor after the systemic injection of PEGylated DNA lipid nanocapsules. Biomaterials, under press, 2010

Muldoon LL, Soussain C, Jahnke K, Johanson C, Siegal T, Smith QR, Hall WA, Hynynen K, Senter PD, Peereboom DM, Neuwelt EA. Chemotherapy delivery issues in central nervous system malignancy: a reality check. J Clin Oncol. 2007 Jun 1; 25(16):2295-305.

Nanjwade BK, Bechra HM, Derkar GK, Manvi FV, Nanjwade VK. Dendrimers: emerging polymers for drug-delivery systems. Eur J Pharm Sci. 2009 Oct 8; 38(3):185-96.

Nicholson C, Sykova E. Extracellular space structure revealed by diffusion analysis. Trends Neurosci 1998; 21(5):207e15.

Nishiyama N, Kataoka K. Current state, achievements, and future prospects of polymeric micelles as nanocarriers for drug and gene delivery. Pharmacol Ther. 2006 Dec; 112(3):630-48.

Prabha S, Labhasetwar V. Critical determinants in PLGA/PLA nanoparticle- mediated gene expression. Pharm Res 2004; 21(2):354e64.

Roger M, Clavreul A, Venier-Julienne MC, Passirani C, Montero-Menei C, Menei P. The potential of combinations of drug-loaded nanoparticle systems and adult stem cells for glioma therapy. Biomaterials (in press).

Roger M, Clavreul A, Venier-Julienne MC, Passirani C, Sindji L, Schiller P, Montero-Menei C, Menei P. Mesenchymal stem cells as cellular vehicles for delivery of nanoparticles to brain tumours. Biomaterials 31(32):8393-8401, 2010

Schneider T, Becker A, Ringe K, Reinhold A, Firsching R, Sabel BA. Brain tumor therapy by combined vaccination and antisense oligonucleotide delivery with nanoparticles. J Neuroimmunol. 2008 Mar; 195(1-2):21-7.

Steiniger SC, Kreuter J, Khalansky AS, Skidan IN, Bobruskin AI, Smirnova ZS, Severin SE, Uhl R, Kock M, Geiger KD, Gelperina SE. Chemotherapy of glioblastoma in rats using doxorubicin-loaded nanoparticles. Int J Cancer. 2004 May 1; 109(5):759-67.

Stupp R, Hegi ME, Mason WP, van den Bent MJ, Taphoorn MJ, Janzer RC, Ludwin SK, Allgeier A, Fisher B, Belanger K, Hau P, Brandes AA, Gijtenbeek J, Marosi C, Vecht CJ, Mokhtari K, Wesseling P, Villa S, Eisenhauer E, Gorlia T, Weller M, Lacombe D, Cairncross JG, Mirimanoff RO. Effects of radiotherapy with concomitant and adjuvant temozolomide versus radiotherapy alone on survival in glioblastoma in a randomised phase III study: 5-year analysis of the EORTC-NCIC trial. Lancet Oncol. 2009 May; 10(5):459-66.

Tian W, Ying X, Du J, Guo J, Men Y, Zhang Y, Li RJ, Yao HJ, Lou JN, Zhang LR, Lu WL. Enhanced efficacy of functionalized epirubicin liposomes in treating brain glioma-bearing rats. Eur J Pharm Sci. 2010 Oct 9; 41(2):232-43.

Ulrich AS. Biophysical Aspects of Using Liposomes as Delivery Vehicles. Bioscience Reports, Vol. 22, No. 2, April 2002

Vinchon-Petit S, Jarnet D, Paillard A, Benoit JP, Garcion E, Menei P. In vivo evaluation of intracellular drug-nanocarriers infused into intracranial tumours by convection-enhanced delivery: distribution and radiosensitisation efficacy. J Neurooncol. 2010 Apr; 97(2):195-205.

Vonarbourg, A., Passirani, C., Saulnier, P., Benoit, J.P. Parameters influencing the stealthiness of colloidal drug delivery systems. Biomaterials. 2006, 27, 4356–4373.

Wang CX, Huang LS, Hou LB, Jiang L, Yan ZT, Wang YL, Chen ZL. Antitumor effects of polysorbate-80 coated gemcitabine polybutylcyanoacrylate nanoparticles in vitro and its pharmacodynamics in vivo on C6 glioma cells of a brain tumor model. Brain Res. 2009 Mar 19; 1261:91-9.

Wu G, Barth RF, Yang W, Kawabata S, Zhang L, Green-Church K. Targeted delivery of methotrexate to epidermal growth factor receptor-positive brain tumors by means of cetuximab (IMC-C225) dendrimer bioconjugates. Mol Cancer Ther. 2006 Jan; 5(1):52-9.

Yang W, Barth RF, Wu G, Huo T, Tjarks W, Ciesielski M, Fenstermaker RA, Ross BD, Wikstrand CJ, Riley KJ, Binns PJ. Convection enhanced delivery of boronated EGF as a molecular targeting agent for neutron capture therapy of brain tumors. J Neurooncol. 2009 Dec; 95(3):355-65.

Yang W, Barth RF, Wu G, Tjarks W, Binns P, Riley K. Boron neutron capture therapy of EGFR or EGFRvIII positive gliomas using either boronated monoclonal antibodies or epidermal growth factor as molecular targeting agents. Appl Radiat Isot. 2009 Jul; 67(7-8 Suppl):S328-31.

Ying X, Wen H, Lu WL, Du J, Guo J, Tian W, Men Y, Zhang Y, Li RJ, Yang TY, Shang DW, Lou JN, Zhang LR, Zhang Q. Dual-targeting daunorubicin liposomes improve the therapeutic efficacy of brain glioma in animals. J Control Release. 2010 Jan 25; 141(2):183-92.

Yokosawa M, Sonoda Y, Sugiyama S, Saito R, Yamashita Y, Nishihara M, Satoh T, Kumabe T, Yokoyama M, Tominaga T. Convection-enhanced delivery of a synthetic retinoid Am80, loaded into polymeric micelles, prolongs the survival of rats bearing intracranial glioblastoma xenografts. Tohoku J Exp Med. 2010; 221(4):257-64.

Zhan C, Gu B, Xie C, Li J, Liu Y, Lu W. Cyclic RGD conjugated poly(ethylene glycol)-co-poly(lactic acid) micelle enhances paclitaxel anti-glioblastoma effect. J Control Release. 2010 Apr 2; 143(1):136-42.

Zhao BJ, Ke XY, Huang Y, Chen XM, Zhao X, Zhao BX, Lu WL, Lou JN, Zhang X, Zhang Q. The antiangiogenic efficacy of NGR-modified PEG-DSPE micelles containing paclitaxel (NGR-M-PTX) for the treatment of glioma in rats. J Drug Target. 2010 Aug 2 [Epub ahead of print]

Zhao M, Liang C, Li A, Chang J, Wang H, Yan R, Zhang J, Tai J. Magnetic paclitaxel nanoparticles inhibit glioma growth and improve the survival of rats bearing glioma xenografts. Anticancer Res. 2010 Jun; 30(6):2217-23.

Zhao S, Zhang X, Zhang J, Zhang J, Zou H, Liu Y, Dong X, Sun X. Intravenous administration of arsenic trioxide encapsulated in liposomes inhibits the growth of C6 gliomas in rat brains. J Chemother. 2008 Apr; 20(2):253-62.

PUBLICATION :

EGFR siRNA LIPID NANOCAPSULES EFFICIENTLY TRANSFECT GLIOMA CELLS *IN VITRO*

Contents lists available at ScienceDirect

International Journal of Pharmaceutics

journal homepage: www.elsevier.com/locate/ijpharm

EGFR siRNA lipid nanocapsules efficiently transfect glioma cells *in vitro*

Pauline Resnier[a,b], Stephanie David[c], Nolwenn Lautram[a,b], Gaëtan J.-R. Delcroix[d,e], Anne Clavreul[a,b,f], Jean-Pierre Benoit[a,b], Catherine Passirani[a,b,*]

[a] LUNAM – Université d'Angers, F-49933 Angers, France
[b] INSERM U1066 – Micro et Nanomédecines Biomimétiques, Angers, France
[c] EA 6592 – Nanomédicaments et nanosondes, Université François-Rabelais, Tours, France
[d] University of Miami Tissue Bank, Interdisciplinary Stem Cell Institute, Department of Othopaedics, University of Miami Miller School of Medecine, Miami, FL, USA
[e] Geriatric Research, Education, and Clinical Center and Research Service, Bruce W.Carter Veterans Affairs Medical Center, Miami, FL, USA
[f] Département de Neurochirurgie, Centre Hospitalier Universitaire d'Angers, F-49100 Angers, France

ARTICLE INFO

Article history:
Received 18 February 2013
Received in revised form 22 March 2013
Accepted 2 April 2013
Available online 10 April 2013

Keywords:
Nanomedicine
Brain tumor
Gene therapy
CH50
U87MG

ABSTRACT

Glioma are the most common malignant tumors of the central nervous system and remain associated with poor prognosis, despite the combination of chemotherapy and radiotherapy. EGFR targeting represents an interesting strategy to treat glioma. Indeed, a high level of endothelial growth factor receptors expression (EGFR), involved in the malignancy of the tumor, has been observed in glioma. Our strategy consisted in using EGFR siRNA entrapped into lipid nanocapsules (LNCs) *via* cationic liposomes. *In vitro* analyses on U87MG human glioma cells were performed to evaluate firstly the capacity of LNCs to efficiently deliver the siRNA and secondly the effect of EGFR siRNA targeting on U87MG proliferation. Then, the complement protein consumption was evaluated by CH50 assays to verify the suitability of the siRNA LNCs for systemic administration. The EGFR siRNA LNCs exhibited an adequate size lower than 150 nm as well as a neutral surface charge. The IC50 profile together with the 63% of protein extinction demonstrated the significant action of EGFR siRNA LNCs compared to scrambled LNCs. Dose and time-dependent survival assays showed a decrease of U87MG growth evaluated at 38%. Finally, low complement consumption demonstrated the suitability of EGFR siRNA LNCs for intravenous injection. In conclusion, EGFR siRNA LNCs demonstrated their capacity to efficiently encapsulate and deliver siRNA into U87MG human glioma cells, and will therefore be usable in the future for *in vivo* evaluation.

1. Introduction

Malignant brain tumors are often associated with poor prognosis. The low survival median, of only 15 months in the case of glioblastoma (GBM), despite the use of surgery, chemotherapy with temozolomide (Temodal®) and radiotherapy, has encouraged research for new treatment (Stupp and Roila, 2009). GBM are the most aggressive form of malignant brain tumors, and are characterized by a high infiltration capacity in healthy brain tissue leading to difficult tumor resection. The endothelial growth factor receptor (EGFR) has been described as an oncogene in many types of cancer, including GBM (Yang et al., 2012). The over-expression and/or amplification of EGFR protein, described in half-primary GBM cases, has been associated with abnormal proliferation and a chemo/radioresistance phenomenon (Hatanpaa et al., 2010; Watanabe et al., 1996). To combat this drug resistance, various inhibitors of EGFR, such as antibodies (Cetuximab®) and more recently tyrosine kinase inhibitors (TKI) (Gefitinib®), have been developed and tested in numerous *in vitro* and *in vivo* models. These studies have proved the relevance of EGFR targeting in GBM with anti-proliferative properties. Moreover, its impact on glioma stem cells was also demonstrated recently (Geoerger et al., 2008; Jin et al., 2013). However, despite numerous clinical trials, none of these inhibitors have been approved yet for clinical glioma treatment (Joshi et al., 2012; Taylor et al., 2012; Thiessen et al., 2010). The low efficiency of these candidate drugs could be explained by the specific biological environment in GBM. In fact, a resistance mechanism against antibodies or TKI usually appears in the form of variant protein expression, rendering the therapeutic approach ineffective. To prevent this phenomenon, the RNAi mechanism could represent a new opportunity thanks to the use of specific siRNA tools that do not depend on protein interaction, 3D conformation, or protein variants (Fire et al., 1998). Indeed, the siRNA used in this study was

* Corresponding author at: INSERM U1066, IBS-CHU, 4 rue Larrey, 49933 Angers Cedex 9, France. Tel.: +33 244 688 534; fax: +33 244 688 546.
E-mail address: catherine.passirani@univ-angers.fr (C. Passirani).

0378-5173/$ – see front matter © 2013 Elsevier B.V. All rights reserved.
http://dx.doi.org/10.1016/j.ijpharm.2013.04.001

described as naturally acting through the micro RNA pathway to inhibit proteins like EGFR (Michiue et al., 2009).

Systemic delivery to the brain remains a challenge due to the presence of the blood brain barrier (BBB) that strongly limits the exchanges between blood and neuronal cells. Chemical or therapeutic agents (such as TKI, antibodies, and siRNA) cannot cross, or only partially, this membrane by passive transport (Wang et al., 2012). For this reason, the development of synthetic carriers represents a great opportunity to ameliorate the passage through the BBB, especially for hydrophilic drugs. Thanks to specific targeting, nanomedicines could improve biodistribution into the brain after systemic injection by (i) the passive strategy with enhanced permeability and retention (EPR) effect (Maeda, 2001); (ii) by the active strategy with ligand grafting on the surface of the delivery system, such as transferrin (Beduneau et al., 2008).

Considering the systemic nucleic acid transport, nanocarriers are necessary to protect them from the blood compartment. In fact, nucleases and the immune system can rapidly degrade siRNA. The delivery systems can enhance the half-life of siRNA into blood and favor their accumulation into targeted organs (Morille et al., 2010). Numerous nanomedicines have been developed to encapsulate siRNA, such as liposomes, micelles, and dendrimers. The majority of these systems were made of a mixture of cationic polymers and lipid components entrapping siRNA thanks to electrostatic interactions. Lipid nanocapsules (LNCs) consisting of a lipid liquid core of triglycerides and a rigid shell of lecithin and polyethylene glycol, have been developed in our laboratory (Heurtault et al., 2002). The simple formulation process is based on phase-inversion of an emulsion. These LNCs have recently been modified to encapsulate DNA, complexed with cationic lipids forming lipoplexes, and have shown efficient *in vitro* and *in vivo* effects in different animal models (David et al., 2012a,b; Morille et al., 2011). In our recent work, these delivery systems were adapted to siRNA encapsulation (David et al., 2012c). We tested these siRNA LNCs on glioma cells in order to prove the efficient delivery of siRNA into the cytoplasm and the effect of EGFR inhibition by siRNA on U87MG human glioma cells.

2. Materials and methods

2.1. SiRNA LNC formulation

Lipid nanocapsules (LNCs) were formulated, as described before (Heurtault et al., 2002), by mixing 20%, w/w Labrafac WL 1349 (caprylic-capric acid triglycerides, Gatefossé S.A. Saint-Priest, France), 1.5%, w/w Lipoid S75-3 (Lipoid GmbH, Ludwigshafen, Germany), 17%, w/w Kolliphor® HS 15 (BASF, Ludwigshafen, Germany), 1.8%, w/w NaCl (Prolabo, Fontenay-sous-Bois, France) and 59.8%, w/w water (obtained from a Milli-Q system, Millipore, Paris, France) together under magnetic stirring. Briefly, three temperature cycles between 60 and 95 °C were performed to obtain phase inversions of the emulsion. A subsequent rapid cooling and dilution with ice cooled water (1:1.4) at the phase-inversion temperature (PIT) led to blank LNC formation.

To obtain siRNA LNCs, the water in the last step was replaced by lipoplexes, *i.e.* siRNA as EGFR siRNA (sense sequence: 5′-CACAGUGGAGCGAAUUCCU-3′; Eurogentec, Seraing, Belgium) and control (scrambled) siRNA (sense sequence: 5′-UCUACGAGGCACGAGACUU-3′; Eurogentec, Seraing, Belgium) complexed with cationic liposomes in a defined charge ratio of cationic lipid charge *versus* anionic siRNA charge (± ratio). During this work, liposome LNCs, *i.e.* LNCs with liposome introduction at the last step without siRNA, were also used as control vehicle.

For liposome preparation, a cationic lipid DOTAP (1.2-dioleyl-3-trimethylammoniumpropane) (Avanti® Polar Lipids Inc., Alabaster, AL, USA), solubilized in chloroform, was weighted in the ratio 1/1 (M/M) with the neutral lipid DOPE (1.2-dioleyl-sn-glycero-3-phosphoethanolamine) (Avanti® Polar Lipids Inc., Alabaster, AL, USA) to obtain a final concentration of 30 mM of cationic lipid charge, considering the number of lipid charges per molecule (1 for DOTAP). After chloroform evaporation under vacuum, deionized water was added to hydrate the lipid film over night at 4 °C which was sonicated the day after.

2.2. Characterization

The size and Zeta potential of LNCs were measured by the Dynamic Light Scattering (DLS) method using a Malvern Zetasizer® apparatus (Nano Series ZS, Malvern Instruments S.A., Worcestershire, UK) at 25 °C, in triplicate, after dilution in a ratio of 1:200 with deionized water.

Moreover, a spectrophotometric method, based on work recently described by David et al. (2012c), was used to evaluate the encapsulation efficiency. Briefly, siRNA LNCs were mixed with chloroform and water to separate respectively hydrophilic and lipophilic components, sodium hydroxide to destabilize lipoplexes and absolute ethanol to destroy LNCs. After multiple centrifugations, four compartments were obtained: free siRNA, free lipoplexes (*i.e.* siRNA associated with liposomes), encapsulated siRNA and encapsulated lipoplexes into LNCs. To determine the concentration of siRNA, the optical density (Morille et al.) of each sample were determined at 260 nm by UV spectrophotometer (UV-2600, Shimadzu, Noisiel, France) in triplicate conditions. These physico-chemical parameters (size, charge surface and encapsulation) were characterized after formulation and 1 month later to study their stability.

2.3. Cell culture

Human glioma cell line U87MG and human macrophage/monocyte THP-1 were obtained from ATCC. U87MG cells were grown in Minimum Essential Medium Eagle (Lonza, Verviers, Belgium) supplemented with 10% of fetal bovine serum (Lonza, Verviers, Belgium), 1% of antibiotics (10 units of penicillin, 10 mg of streptomycin, 25 μg of amphotericin B/mL; Sigma–Aldrich, Saint Louis, USA), 1% of non-essential amino acids (Lonza) and 1% of sodium pyruvate (Lonza). THP-1 macrophages were grown in Roswell Park Memorial Institute (RPMI) 1640 medium (Lonza) supplemented with adapted substrates as described in the ATCC protocol. Cell lines were cultured according to the ATCC protocol and maintained at 37 °C in a humidified atmosphere with 5% CO_2. THP-1 cell adherence and differentiation into 24-well plates was allowed by medium supplemented with 100 mM phorbol 12-myristate 13-acetate (PMA, Sigma, Saint-Quentin Fallavier, France) for 48 h.

2.4. Transfection

U87MG cells were seeded onto 24-well plates at the density of 5×10^4 cells/well and precultured overnight. Before transfection, the medium was changed to a fresh one containing no serum. Treatment with different LNCs (blank, liposome, scrambled and EGFR siRNA) were realized at a final dose of 37.5–300 ng siRNA/well and removed 4 h post-transfection. These cells were subsequently cultured for an additional time and the medium was removed every two days.

2.5. Flow cytometry

Immunostaining was performed to evaluate the expression of membranous EGFR protein. For this, 96 h after transfection, cells were seeded in 96-well plate, washed twice with PBS (lonza), and

incubated with primary antibodies (EGFR or isotype) for 1 h at 4 °C. After a second wash with PBS/fetal calf serum/azide 0.02%, secondary antibody coupled with FITC (polyclonal goat antimouse Ig/FITC, goat F(ab2'), Dako, Trappes, France) was incubated for 30 min at 4 °C and washed. Cell suspensions were fixed with PBS/azide 0.02%/formaldehyde 1%, protected from light and conserved at 4 °C. Analyses were performed with a FACScalibur flow cytometer (BD Bioscience, San José, USA) in collaboration with SCCAN platform (Angers).

2.6. Survival assay

Glioma cells and macrophages were seeded onto 24-well plates at a density of 5×10^4 cells/well and pre-cultured overnight or 48 h for THP-1. Dose-dependent transfection was realized as described above to determine the $IC_{50}$and cells were subsequently cultured for two days. Cytotoxicity assays were performed using MTS (3-(4,5-dimethylthiazol-2-yl)-5-(3-carboxymethoxyphenyl)-2-(4-sulfophenyl)-2Htetrazolium) (Promega, Madison, USA). For this, 100 μL of MTS/well were disposed and plates were incubated 2.5–4 h at 37 °C in a humidified atmosphere with 5% CO_2. The OD at 492 nm was evaluated by Mutliskan Ascent (Labsystems, Fisher Scientific, Wilmington, USA).

2.7. Proliferation study

Glioma cells were seeded onto 24-well plates at a density of 5×10^4 cells/well and pre-cultured overnight. A time-dependent transfection with the low dose (10 ng) was realized and cells were subsequently cultured for ten days and the medium was removed every two days. To evaluate the progression of the glioma cells, sphere formation was followed every day. For this, scores were defined: 0 corresponding to the absence of a sphere in a well, 1: irregular apparition of small spheres, 2: regular distribution of small spheres, 3: regular medium spheres, 4: regular large spheres. The cells were photographed at day 10 after treatment. Moreover, every two day, cells were suspended by trypsin (0.5 g porcin trypsin, 0.2 g EDTA; Sigma, Saint Louis, USA), and two washes were realized with PBS. Analyses with trypan blue staining was used to count the number of cells per well.

2.8. Complement test

Complement consumption was assessed in normal human serum (NHS) (provided by the Etablissement Francais du Sang, CHU, Angers, France) by measuring the residual hemolytic capacity of the complement system after contact with LNCs. The final dilution of NHS in the mixture was 1:4 (V/V) corresponding to 100 μL of NHS into 400 μL of reactive media. The technique consisted in determining the amount of serum able to lyse 50% of a fixed number of sensitized sheep erythrocytes with rabbit anti-sheep erythrocyte antibodies (CH50), according to the procedure described by Vonarbourg et al. (2009). Complement activation was first expressed as a function of the surface area in order to compare different formulations. Nanoparticle surface areas were estimated using the equation: $S = 3m/r\rho$, where S is the surface area [cm^2], m is the weight [g] in 1 mL of suspension, r is the average radius [cm] determined by DLS, and ρ is the volumetric mass [g/cm^3] of the nanoparticles estimated at 100 g/cm^3.

2.9. Statistical analyses

Comparisons between the treated cells of all groups were performed either using a classical analysis of variance (one-way ANOVA) followed by a Scheffe's *post hoc* analysis. Statistical significance was ascribed to a threshold p-value of 0.05.

3. Results

3.1. siRNA LNC formulation

3.1.1. Size and Zeta potential

The size and Zeta potential of siRNA LNCs were determined using a Nanosizer apparatus. Measurements were realized 1 day after formulation and 1 month after storage at 4 °C to evaluate the physico-chemical stability of siRNA LNCs (Table 1). Blank LNCs exhibited a stable size, narrow distribution around 60 nm and a negative Zeta potential estimated at −5 mV over a 1 month period. Liposome LNCs showed a decreasing evolution in size and an increasing surface charge after 1 month at 4 °C. The Zeta potential was largely positive due to cationic lipids and their polydispersity index (PdI) that decreased strongly with time from 0.26 to 0.05. Concerning the two different lipoplexe CR used to obtain siRNA LNCs, an influence was observed with an increase of size after formulation with 90 nm and 122 nm respectively for CR of 2.5 and 5 compared to blank LNCs (56 nm). Moreover, this parameter was associated to a high PdI just inferior to 0.3 (limit of monodispersity). As observed with time for liposome LNCs, siRNA LNCs presented a high reduction of size and PdI with a gain of Zeta potential (Table 1).

3.1.2. Encapsulation efficiency

An adapted method based on UV spectroscopy was used to evaluate the encapsulation efficiency of siRNA into LNCs. Briefly; four compartments of siRNA localization (free siRNA, free lipoplexes, encapsulated siRNA and encapsulated lipoplexes) were separated using an easy chloroform extraction as described above. Analyses of EGFR siRNA LNC encapsulation efficiency were performed, in a similar way as for size, one day and 1 month after formulation (Table 1). The encapsulation was estimated at 29% and 40% for respectively CR 2.5 and 5. The stability of encapsulated doses was confirmed for both CR 1 month after formulation. The majority of encapsulated siRNA was associated with liposomes. However, a non-negligible part of siRNA was not associated with liposome but was still encapsulated into LNCs as previously observed. According to their size, Zeta potential and encapsulation stability, one day-old EGFR siRNA LNCs were used in the following experiments.

3.2. Analysis of efficient transfection in vitro

Four days after EGFR siRNA LNC treatment, the EGFR protein level was evaluated by flow cytometry (Fig. 1). No protein extinction was observed with siRNA alone in opposition to what was observed with siRNA associated with a commercial transfection agent (ICAfectin®, Invitrogen, Saint Aubin, France) which resulted in a 55% of inhibition with a low dose of siRNA (37.5 ng) (Fig. 1). Liposome and scrambled LNCs showed no difference of EGFR expression compared to non-treated cells. Moreover, CR 2.5 LNCs had no effect on U87MG EGFR expression until 300 ng, the maximal dose (Fig. 1A). CR 5 LNCs demonstrated a dose-dependent response with a maximal inhibition estimated at 63%, equivalent to the positive control result (Fig. 1B). Consequently, CR 5 LNCs were chosen to perform *in vitro* assays.

3.3. Determination of IC_{50}

The cytotoxicity of EGFR siRNA LNCs was performed on two cell lines: U87MG glioma and THP-1 human cells in differentiated macrophages. EGFR siRNA had only a little impact on U87MG cell

Table 1
Characterization of EGFR siRNA LNCs.

Type of LNCs	Liposome type and CR	Date	Size (nm)	PdI	Zeta (mV)	Encapsulation yield (%)
EGFR siRNA LNCs	DOTAP/DOPE 2.5	1 day	90 ± 1	0.22 ± 0.01	+1 ± 1	29 ± 9
		1 month	56 ± 1	0.09 ± 0.02	+24 ± 5	24 ± 3
	DOTAP/DOPE 5	1 day	122 ± 1	0.26 ± 0.01	+4 ± 1	40 ± 12
		1 month	70 ± 1	0.06 ± 0.01	+26 ± 1	42 ± 7
Liposome LNCs	DOTAP/DOPE 5	1 day	102 ± 10	0.26 ± 0.01	+5 ± 2	/
		1 month	58 ± 2	0.05 ± 0.01	+34 ± 2	/
Blank LNCs	/	1 day	56 ± 1	0.04 ± 0.01	−6 ± 1	/
		1 month	60 ± 2	0.03 ± 0.01	−5 ± 1	/

CR: charge ratio, PdI: polydispersity index (monodispersity: PdI < 0.3).

viability, with a low IC_{50} evaluated at 40 ng (Fig. 2). This effect was considered specific since the survival of differentiated THP-1 cells was not affected by the EGFR siRNA. Toxicity of liposome and scrambled LNCs was observed at 250 and 80 ng on U87MG (Fig. 2A) and 70 and 120 ng on THP-1 cells respectively (Fig. 2B). Following these results, a dose of 10 ng siRNA corresponding to 0.1 mg/mL of LNCs was chosen to study the growth progression for 10 days as it led to cytotoxicity (30%) compared to control conditions.

3.4. Proliferation impact

After 10 days, pictures of U87MG cells were taken (Fig. 3A). The apparition of spheres into wells was recorded as described above in the cell proliferation study. A different organization of U87MG cells was evidenced between non-treated cells (a), cells treated with liposome LNCs (b) and scrambled LNCs (c) compared to cells that received EGFR siRNA LNCs (d) (Fig. 3A). EGFR siRNA LNCs significantly decreased the formation of U87MG spheres from Days 6 to 10 (Fig. 3B). Liposome and scrambled LNCs followed the same

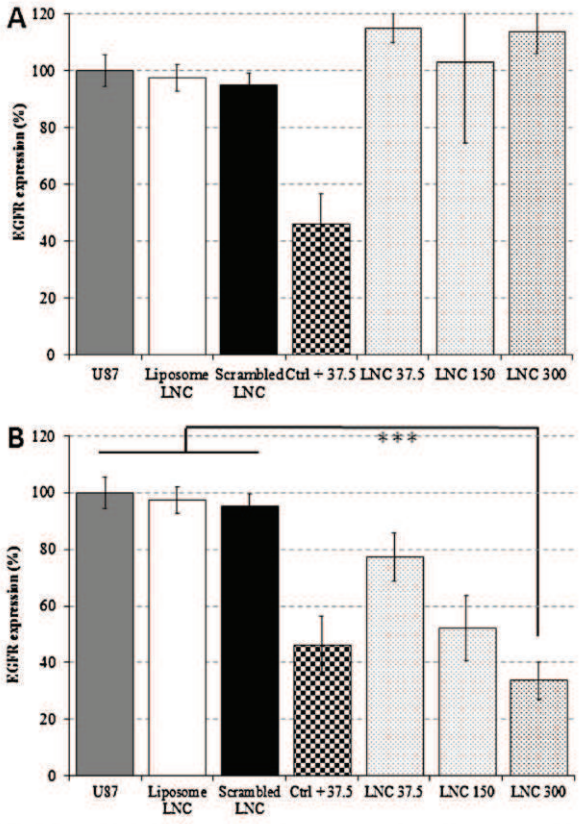

Fig. 1. Expression of EGFR protein by flow cytometry analyses after treatment with two CR of EGFR siRNA LNCs. These analyses by flow cytometry of EGFR levels were realized four days after treatment with increasing doses comprised between 37.5 ng and 300 ng of siRNA per well. The EGFR protein level was expressed in function of non-treated cells. (A) Analyses of DOTAP/DOPE CR 2.5 LNCs. (B) Analyses of DOTAP/DOPE CR 5 LNCs. Statistical analyses ANOVA one way *post hoc* Scheffe, $^{***}p = 0.001$.

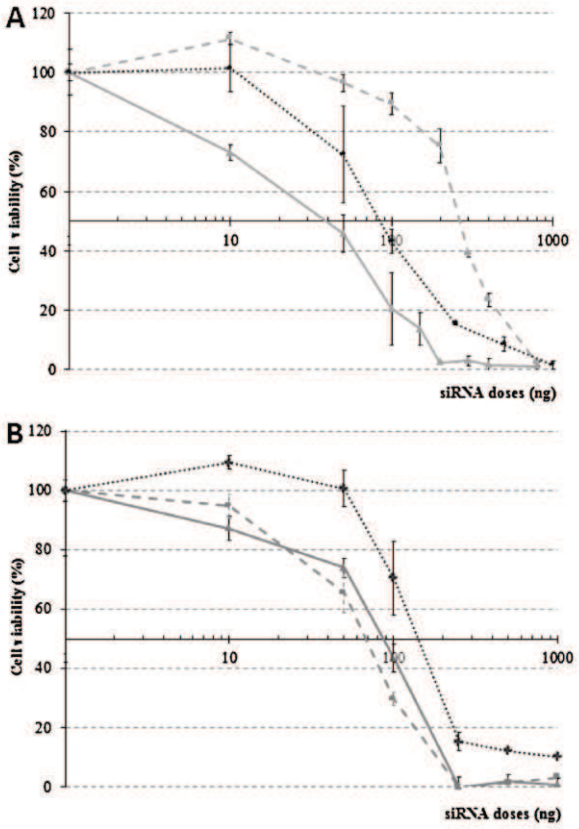

Fig. 2. Determination of IC_{50} values of EGFR siRNA LNCs on human glioma cells (U87MG) (A) and differentiated macrophages (THP-1) (B). (A) EGFR siRNA into LNCs (—▲—) had an impact on U87MG viability with IC_{50} estimated lower than 40 ng of siRNA compared to control conditions with IC50 superior at 80 ng (liposome — ■ - and scrambled siRNA LNCs ···◆···). (B) On macrophages, EGFR siRNA LNCs did not modify the cell viability.

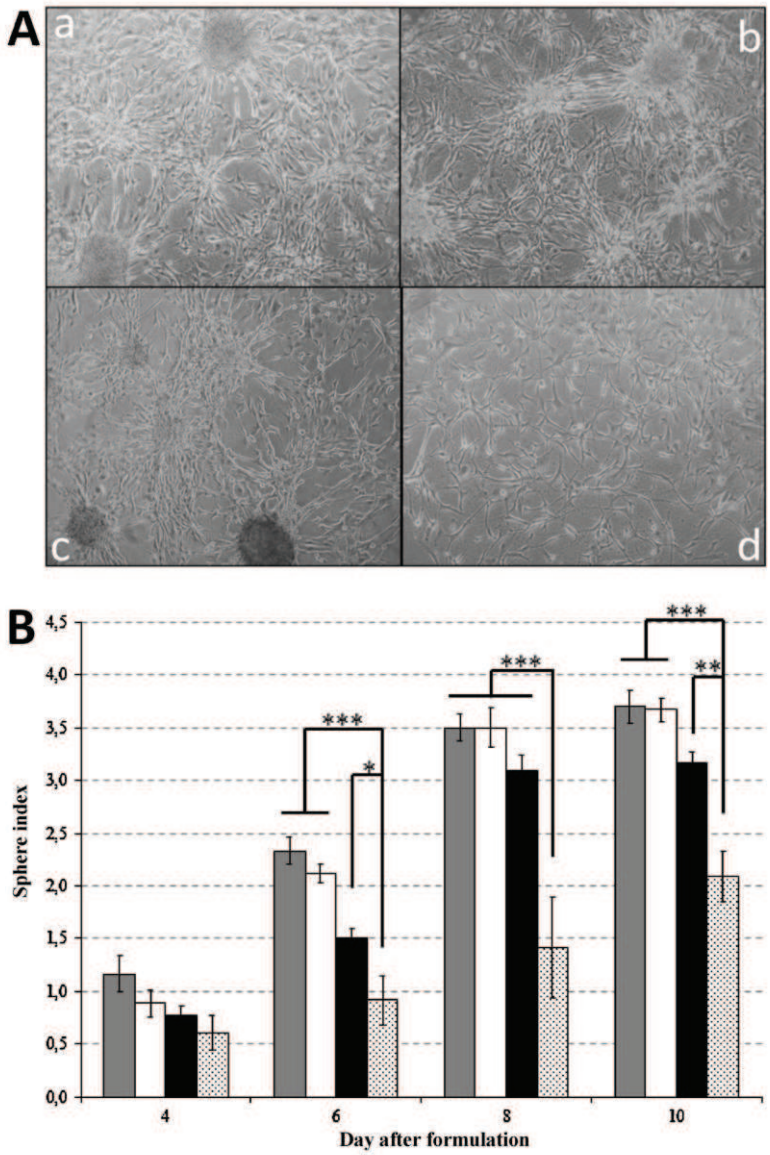

Fig. 3. (A) Pictures of U87MG realized 10 days after treatment with a low dose of LNCs. Large spheres were observed on U87MG culture (a), and after 4 h incubation with liposome LNCs (b), and scrambled LNCs (c) contrary to the treatment with EGFR siRNA LNCs (d). (B) Impact of EGFR siRNA LNCs on U87MG spheroid formation. Spheroid formation was significantly inhibited by EGFR siRNA (■) from Days 6 to 10. Liposome (□) and scrambled (■) LNCs presented the same behavior as non-treated cells (■). Statistical analyses ANOVA one way *post hoc* Scheffe, $^{*}p = 0.05$, $^{**}p = 0.01$ and $^{***}p = 0.001$.

progression as non-treated cells with maximal index obtained at day 10 (Fig. 3B). To confirm this result, a determination of cell numbers was realized in parallel. EGFR LNC treatment presented a significant difference with all controls at day 10 (Fig. 4). On the final day, a difference above 30% was evidenced between EGFR siRNA LNCs and all control LNCs.

3.5. *Complement activation*

The diameter of nanoparticles was controlled by a classical method before performing CH50 assays (Fig. 5). The analysis of complement proteins activation was performed on liposomes, lipoplexes, blank LNCs, liposome LNCs, and EGFR siRNA LNCs to compare their behavior in contact with human serum (Fig. 5). No activation of complement proteins was evidenced with siRNA alone (data not shown). The very low activation profile of blank LNCs was already described due to negative surface charge and a size of around 60 nm (Morille et al., 2010). In opposition to LNCs, positively-charged surface delivery system such as liposome and lipoplexes led to a high consumption of complement proteins with higher profile for lipoplexes. Thanks to the neutral charge of our device, intermediate consumption was evidenced for loaded LNCs

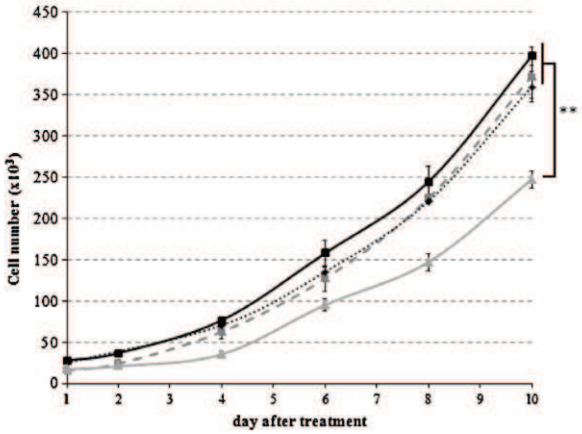

Fig. 4. Evolution of U87MG cellular proliferation after one treatment with 10 ng of EGFR siRNA LNCs. This dose allowed a decrease of cell numbers with EGFR siRNA LNCs (—▲—) compared to other treatments such as liposome LNCs (– ■ –) and scrambled siRNA LNCs (••◆••) from Day 5 to Day 10. A significant difference with non-treated cells (—■—) was evidenced on Day 10. Statistical analyses ANOVA one way *post hoc* Scheffe, $^{**}p = 0.01$.

(liposome and siRNA), which were close to the blank LNC profile until 400–500 cm^2.

4. Discussion

In this study, we developed a specific delivery system targeting EGFR protein by using an RNAi mechanism for glioma therapy. This nanomedicine consists of the association of DOTAP/DOPE siRNA cationic lipoplexes and lipid nanocapsules (LNCs) to combine (i) the efficient electrostatic interaction of lipids and siRNA, (ii) the high transfection capacity of cationic lipids and (iii) the systemic delivery of nanocapsules thanks to their stealth property (Vonarbourg et al., 2009). DOTAP and DOPE lipids have been commonly used as transfection agents and as components in nucleic acid delivery systems (Resnier et al., 2013). In this work, two different charge ratios (2.5 and 5) were studied to follow their impact on siRNA LNC formulation. These two formulations presented a size inferior to 150 nm, a neutral Zeta potential and an encapsulation stability adequate for a long circulating profile. However, measures realized 1 month later highlighted the change of physicochemical properties of siRNA LNCs over time. Size diminution and surface charge increases could signify that LNCs were reorganized in positive smaller particles, possibly due to the large amount of cationic tensio-active molecules (Lecithin, DOTAP and DOPE). This point could also explain the difference of size between siRNA LNCs CR 2.5 and 5. Twice as many lipids were introduced into the CR 5 formulation compared to CR 2.5, which could lead to larger nanoparticles. Despite this phenomenon, the encapsulated part of siRNA was unchanged and the high CR was more interesting because it led to higher encapsulation efficiency, estimated at 40% of initial quantity of siRNA, which corresponds to a concentration of 100 μg of encapsulated siRNA per mL of LNCs (=300 mg of LNCs).

The protein inhibition study confirmed the benefit of using this high charge ratio during our formulation. Indeed, it resulted in an extinction of membranous EGFR evaluated at 63%. This high extinction percentage was most likely due to our nanomedicine composition. Indeed, lipid components of siRNA LNCs, *i.e.*, cationic lipids and lecithin, could promote the passage through cell membranes by their hydrophilic polar heads. The slightly positive surface charge of siRNA LNCs is expected to favor the electrostatic interactions between nanocapsules and cell membrane to facilitate their internalization. In fact, LNCs are known to be well-internalized by cancer cells, especially for the larger ones (100 nm) by multiple, non-receptor-dependent internalization pathways such as clathrin, endocytosis and cavoelae pathways (Paillard et al., 2010). Finally, a major role of these lipids in endosomal escape has already been demonstrated, especially for DOTAP and DOPE lipids involved in two well-known mechanisms: the proton sponge effect and membrane destabilization (Cardarelli et al., 2012; Varkouhi et al., 2011).

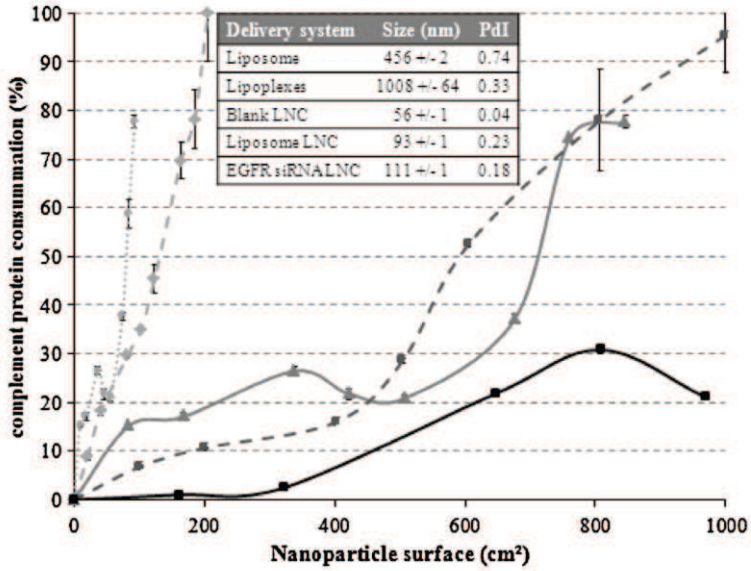

Fig. 5. Evaluation of complement protein consumption by lipoplexes, liposomes and LNCs. Liposomes (– ◆ –) and lipoplexes (·····◆·····) showed a high activation profile compared to LNC formulations. Blank LNCs (—■—) were characterized by a low activation profile and loaded forms (liposome LNCs – ■ – and EGFR siRNA LNCs —▲—) presented an intermediate profile.

Combined with the initial properties of LNCs concerning their endosomal escape capacities, these lipids could favor this phenomenon (Paillard et al., 2010).

In the literature, the inhibition of EGFR in glioma models was assessed by shRNA form, another RNAi strategy. ShRNAs correspond to an intermediate form before mature siRNA is formed, and are characterized by a hairpin loop structure. However, shRNAs are not stable, so their use is generally replaced by a DNA plasmid encoding for these shRNAs. The siRNA LNCs showed a similar extinction of EGFR protein as the shRNA EGFR used in combination with classic transfection agents (Inaba et al., 2011). PAMAM dendrimers, used for shRNA plasmid transfection, showed after 48 h transfection an inhibition of EGFR lower than siRNA LNCs on glioma cells (35% *versus* 63%) (Han et al., 2010). Moreover, cell proliferation was significantly reduced by our siRNA EGFR LNCs after only 10 days of treatment. Electroporation of shRNA plasmid resulted to similar results with a 40% of cell density decrease after 6 days. However this transfection methodology, *i.e.* electroporation, is not translatable to clinical situations.

The benefit of LNCs is their possible use for intravenous injection as we validated their capacity to protect siRNA from complement opsonisation by CH50 assay. In fact, the low activation profile obtained in complement activation experiments confirmed the possible capacity of siRNA LNCs to circulate a long time in blood. This result can be explained by the benefit of the nanocapsule shell that hides the positive charges of the lipids thanks to weak links with negative PEG dipoles (Vonarbourg et al., 2005), thereby conferring stealth property to our LNCs in opposition to lipoplexes. This great enhancement in the behavior of our LNCs is more likely due to the presence of PEG chains at the surface of LNCs, as demonstrated in our previous works on DNA LNCs (David et al., 2012a). To evaluate this, *in vivo* experiments should be realized to define the half-life time and biodistribution of siRNA LNCs in a murine glioma model.

Interestingly, EGFR expression has also been described to be involved in chemo and radioresistance phenomena (Watanabe et al., 1996). For this, the potential of combinatory treatments could be assessed like Chen and co-workers did with doxorubicin and c-myc siRNA (Chen et al., 2010). In the future, the impact of siRNA EGFR inhibition on sensitization of classic chemotherapeutic agent or radiation could be studied *in vitro* and *in vivo*.

5. Conclusion

Our lipid nanocapsules (LNCs) were created 10 years ago by an easy process formulation and have now been fully characterized. Moreover, previous studies have demonstrated the possibility to encapsulate hydrophilic nucleic acids into these systems. Here, our first aim consisted of the study of the impact of CR used and the stability depending on EGFR siRNA LNC physico-chemical parameters. Analyses of protein levels allowed us to conclude on the promising delivery of siRNA into the cytoplasm by LNCs thanks to the high degree of inhibition observed. The potential of EGFR siRNA targeting to combat glioma progression was evidenced on cell growth and U87MG sphere development. Finally, stealth properties evaluated by CH50 assay, confirmed for EGFR siRNA LNCs, the possibility of future treatment to combat glioma cell proliferation alone or as an adjuvant treatment by systemic injection.

Acknowledgments

This work was supported by the foundation "Association de Recherche contre le Cancer" and by "La Ligue contre le cancer 49 et 35". We would like to thank the SFR "Structure Fédérative de Recherche – Interactions cellulaires et applications thérapeutiques" and the active participation of SCCAN platform, especially Dr Catherine Guillet for flow cytometry analyses.

References

Beduneau, A., Hindre, F., Clavreul, A., Leroux, J.C., Saulnier, P., Benoit, J.P., 2008. Brain targeting using novel lipid nanovectors. J. Control. Release 126, 44–49.
Cardarelli, F., Pozzi, D., Bifone, A., Marchini, C., Caracciolo, G., 2012. Cholesterol-dependent macropinocytosis and endosomal escape control the transfection efficiency of lipoplexes in CHO living cells. Mol. Pharm. 9, 334–340.
Chen, Y., Wu, J.J., Huang, L., 2010. Nanoparticles targeted with NGR motif deliver c-myc siRNA and doxorubicin for anticancer therapy. Mol. Ther. 18, 828–834.
David, S., Carmoy, N., Resnier, P., Denis, C., Misery, L., Pitard, B., Benoit, J.P., Passirani, C., Montier, T., 2012a. In vivo imaging of DNA lipid nanocapsules after systemic administration in a melanoma mouse model. Int. J. Pharm. 423, 108–115.
David, S., Montier, T., Carmoy, N., Resnier, P., Clavreul, A., Mevel, M., Pitard, B., Benoit, J.P., Passirani, C., 2012b. Treatment efficacy of DNA lipid nanocapsules and DNA multimodular systems after systemic administration in a human glioma model. J. Gene Med. 14, 769–775.
David, S., Resnier, P., Guillot, A., Pitard, B., Benoit, J.P., Passirani, C., 2012c. siRNA LNCs – a novel platform of lipid nanocapsules for systemic siRNA administration. Eur. J. Pharm. Biopharm. 81, 448–452.
Fire, A., Xu, S., Montgomery, M.K., Kostas, S.A., Driver, S.E., Mello, C.C., 1998. Potent and specific genetic interference by double-stranded RNA in *Caenorhabditis elegans*. Nature 391, 806–811.
Geoerger, B., Gaspar, N., Opolon, P., Morizet, J., Devanz, P., Lecluse, Y., Valent, A., Lacroix, L., Grill, J., Vassal, G., 2008. EGFR tyrosine kinase inhibition radiosensitizes and induces apoptosis in malignant glioma and childhood ependymoma xenografts. Int. J. Cancer 123, 209–216.
Han, L., Zhang, A., Wang, H., Pu, P., Jiang, X., Kang, C., Chang, J., 2010. Tat-BMPs-PAMAM conjugates enhance therapeutic effect of small interference RNA on U251 glioma cells in vitro and in vivo. Hum. Gene Ther. 21, 417–426.
Hatanpaa, K.J., Burma, S., Zhao, D., Habib, A.A., 2010. Epidermal growth factor receptor in glioma: signal transduction, neuropathology, imaging, and radioresistance. Neoplasia 12, 675–684.
Heurtault, B., Saulnier, P., Pech, B., Proust, J.E., Benoit, J.P., 2002. A novel phase inversion-based process for the preparation of lipid nanocarriers. Pharm. Res. 19, 875–880.
Inaba, N., Fujioka, K., Saito, H., Kimura, M., Ikeda, K., Inoue, Y., Ishizawa, S., Manome, Y., 2011. Down-regulation of EGFR prolonged cell growth of glioma but did not increase the sensitivity to temozolomide. Anticancer Res. 31, 3253–3257.
Jin, X., Jin, X., Sohn, Y.W., Yin, J., Kim, S.H., Joshi, K., Nam, D.H., Nakano, I., Kim, H., 2013. Blockade of EGFR signaling promotes glioma stem-like cell invasiveness by abolishing ID3-mediated inhibition of p27(KIP1) and MMP3 expression. Cancer Lett. 328, 235–242.
Joshi, A.D., Loilome, W., Siu, I.M., Tyler, B., Gallia, G.L., Riggins, G.J., 2012. Evaluation of tyrosine kinase inhibitor combinations for glioblastoma therapy. PLoS ONE 7, e44372.
Maeda, H., 2001. The enhanced permeability and retention (EPR) effect in tumor vasculature: the key role of tumor-selective macromolecular drug targeting. Adv. Enzyme Regul. 41, 189–207.
Michiue, H., Eguchi, A., Scadeng, M., Dowdy, S.F., 2009. Induction of in vivo synthetic lethal RNAi responses to treat glioblastoma. Cancer Biol. Ther. 8, 2306–2313.
Morille, M., Montier, T., Legras, P., Carmoy, N., Brodin, P., Pitard, B., Benoit, J.P., Passirani, C., 2010. Long-circulating DNA lipid nanocapsules as new vector for passive tumor targeting. Biomaterials 31, 321–329.
Morille, M., Passirani, C., Dufort, S., Bastiat, G., Pitard, B., Coll, J.L., Benoit, J.P., 2011. Tumor transfection after systemic injection of DNA lipid nanocapsules. Biomaterials 32, 2327–2333.
Paillard, A., Hindre, F., Vignes-Colombeix, C., Benoit, J.P., Garcion, E., 2010. The importance of endo-lysosomal escape with lipid nanocapsules for drug subcellular bioavailability. Biomaterials 31, 7542–7554.
Resnier, P., Montier, T., Mathieu, V., Benoit, J.-P., Passirani, C., 2013. Current status of siRNA delivery systems to combat cancers: from needs and challenges to opportunities and clinical perspectives. Adv. Drug Deliv. Rev..
Stupp, R., Roila, F., 2009. Malignant glioma: ESMO clinical recommendations for diagnosis, treatment and follow-up. Ann. Oncol. 20, 126–128.
Taylor, T.E., Furnari, F.B., Cavenee, W.K., 2012. Targeting EGFR for treatment of glioblastoma: molecular basis to overcome resistance. Curr. Cancer Drug Targets 12, 197–209.
Thiessen, B., Stewart, C., Tsao, M., Kamel-Reid, S., Schaiquevich, P., Mason, W., Easaw, J., Belanger, K., Forsyth, P., McIntosh, L., Eisenhauer, E., 2010. A phase I/II trial of GW572016 (lapatinib) in recurrent glioblastoma multiforme: clinical outcomes, pharmacokinetics and molecular correlation. Cancer Chemother. Pharmacol. 65, 353–361.
Varkouhi, A.K., Scholte, M., Storm, G., Haisma, H.J., 2011. Endosomal escape pathways for delivery of biologicals. J. Control. Release 151, 220–228.
Vonarbourg, A., Passirani, C., Desigaux, L., Allard, E., Saulnier, P., Lambert, O., Benoit, J.P., Pitard, B., 2009. The encapsulation of DNA molecules within biomimetic lipid nanocapsules. Biomaterials 30, 3197–3204.

Vonarbourg, A., Saulnier, P., Passirani, C., Benoit, J.P., 2005. Electrokinetic properties of noncharged lipid nanocapsules: influence of the dipolar distribution at the interface. Electrophoresis 26, 2066–2075.
Wang, T., Agarwal, S., Elmquist, W.F., 2012. Brain distribution of cediranib is limited by active efflux at the blood-brain barrier. J. Pharmacol. Exp. Ther. 341, 386–395.
Watanabe, K., Tachibana, O., Sata, K., Yonekawa, Y., Kleihues, P., Ohgaki, H., 1996. Overexpression of the EGF receptor and p53 mutations are mutually exclusive in the evolution of primary and secondary glioblastomas. Brain. Pathol. 6, 21–223, discussion 23–24.
Yang, W., Xia, Y., Cao, Y., Zheng, Y., Bu, W., Zhang, L., You, M.J., Koh, M.Y., Cote, G., Aldape, K., Li, Y., Verma, I.M., Chiao, P.J., Lu, Z., 2012. EGFR-induced and PKCepsilon monoubiquitylation-dependent NF-kappaB activation upregulates PKM2 expression and promotes tumorigenesis. Mol. Cell 48, 771–784.

CURRICULUM VITAE

Pauline RESNIER

27/04/1988 (26 ans)
20 rue du chanoine Libault
49600 Beaupréau
06 17 17 74 88
pauline.resnier@etud.univ-angers.fr

EXPERIENCES PROFESSIONNELLES

2011-2014 **Doctorat en sciences pharmaceutiques**
INSERM U1066 – Micro et nanomédecines biomimétiques, Angers
(Directeur : Pr. J-P BENOIT)

- Développement et évaluation *in vitro* et *in vivo* de nanocapsules lipidiques chargées en siRNA pour le traitement du mélanome, sous la direction du Pr. Catherine PASSIRANI
- Monitorat et vacations à l'Université Catholique de l'Ouest et à l'IUT Biologie, Angers

2011 (6 mois) **Stage de Master 2**
INSERM U1066 – Micro et nanomédecines biomimétiques, Angers

- Développement et évaluation *in vitro* de nanocapsules lipidiques chargées en siRNA pour le traitement du gliome, sous la direction du Pr. Catherine PASSIRANI

2010 (3 mois) **Stage de Master 1**
INSERM U892 – Equipe 7: Immunité Innée et Immunothérapie, Angers

- Etude sur les mécanismes immunitaires et non immunitaires impliqués dans le rejet tumoral dans un modèle de glioblastome, sous la direction du Pr. Dominique COUEZ

2009 (2 mois) **Stage de Licence (3ème année, stage volontaire)**
UPRES 3860 – Cardioprotection, Remodelage, et Thrombose, Angers

- Comparaison des méthodes de post-conditionnement dans le remodelage du myocarde, sous la direction du Dr. Sophie TAMAREILLE

FORMATION

2011 Diplôme **d'Expérimentation Animale** Niveau 1,
ONIRIS, Ecole vétérinaire de Nantes, Nantes

2009-2011 **Master** Biosignalisation Cellulaire, Moléculaire et physiopathologie,
Mention Bien, Université d'Angers, Angers

2006-2009 **Licence** Biologie Cellulaire et physiologie, *option biologie cellulaire et moléculaire*
Mention Bien, Université Catholique de l'Ouest, Angers

2006 **Baccalauréat** Scientifique, *Mention Assez Bien*, Beaupréau

COMPETENCES

Formulation, caractérisation et analytique

- Formulation de vecteurs synthétiques (liposomes, nanocapsules lipidiques)
- Mesure de la taille des particules par diffusion dynamique de la lumière (DLS)
- Mesure du potentiel zéta
- Spectrophotomètrie UV
- Initiation aux méthodes d'HPLC et UPLC

Etudes *in vitro*

- Culture cellulaire (lignées tumorales issues de mélanome, gliome et macrophage)
- Test de viabilité (MTS, MTT, cy-quant)
- Transfection d'ARN interférent avec des nanocapsules lipidiques et agents commerciaux
- Analyses protéiques : Western blot, cytométrie de flux, immuno-histochimie (TUNEL)
- Analyses ARNm (RT-Q-PCR)
- Réalisation de coupe tissulaire (cryo-coupe)

Etudes *in vivo*

- Manipulation et soins des animaux
- Implantations de cellules tumorales (injection sous-cutanée, ou par stéréotaxie)
- Injections intraveineuses et intrapéritonéales
- Prélèvements sanguins intracardiaques
- Etudes pharmacocinétiques
- Etudes d'efficacité anti-tumorale

Diplôme d'expérimentation animal de niveau I obtenu en 2011

Enseignement et encadrement

- Contrat de moniteur pour les 1ères années de DUT Biologie au sein de l'IUT d'Angers, sous la responsabilité de Sophie FAGOT (64h de TP de biochimie)
- Vacations (2011-2012) pour les 1ères années de Licence de Biologie au sein de l'Institut de Biologie Appliquée et d'Ecologie (IBEA) à l'Université Catholique de l'Ouest (UCO) d'Angers, sous la responsabilité de Amélie CHATEL (20h CM et 40h TP)
- Encadrement de stagiaires (de la licence professionnelle au Master 2)

Compétence générale

- Rédaction de différents appels d'offres (INCA, ARC, CGO, La Ligue contre le Cancer)
- Gestion des budgets et des commandes imputés aux projets

Langues

- Anglais scientifiques (écriture d'articles et présentations orales)
- Espagnol (base scolaire)

REFERENCES

Référence académique Pr. Catherine PASSIRANI, INSERM U1066-MINT
catherine.passirani@univ-angers.fr

CENTRES D'INTERETS

Voyages Séjours réguliers en pays étrangers (Espagne, Pays-Bas, République Tchèque)
Musique Pratique du violon (10 ans) et de la guitare (2 ans)
Sport Pratique de la Zumba, badminton, footing

LISTE DES TRAVAUX

TRAVAUX SCIENTIFIQUES

ARTICLES SCIENTIFIQUES

Resnier P, Galopin N, Sibiril Y, Briganti A, Legras P, Vessières A, Montier T, Jaouen G, Benoit J-P, Passirani C. Efficient ferrocifen anticancer drug and Bcl-2 gene therapy using lipid nanocapsules for in vivo melanoma treatment. *En rédaction*

Resnier P, Emina A.L, Galopin N, Bejaud J, David S, Benvegnu T, Pecorari F, Chourpa I, Benoit J-P, Passirani C. Innovative affitin and PEG modifications onte siRNA lipid nanocapsules influence cell uptake, *in vivo* biodistribution and tumor targeting. Journal of controlled release, *Soumission*

Resnier P, Lequinio P, Lautram N, André E, Gaillard C, Bastiat G, Benoit JP, Passirani C. Efficient *in vitro* gene therapy with PEG siRNA lipid nanocapsules for passive targeting strategy in melanoma. Biotechnol J. 2014 Sep 26. doi: 10.1002/biot.201400162.

Resnier P, David S, Lautram N, Delcroix G, Clavreul A, Benoit JP, Passirani C. EGFR siRNA lipid nanocapsules efficiently transfect glioma cells *in vitro*. Int J Pharm. 2013 Oct 1;454(2):748-55

David S, **Resnier P,** Guillot A, Pitard B, Benoit JP, Passirani C. siRNA LNCs - a novel platform of lipid nanocapsules for systemic siRNA administration. Eur J Pharm Biopharm. 2012 Jun; 81(2):448-52.

David S, Carmoy N, **Resnier P**, Denis C, Misery L, Pitard B, Benoit JP, Passirani C, Montier T. *In vivo* imaging of DNA lipid nanocapsules after systemic administration in a melanoma mouse model. Int J Pharm. 2012 Feb 14; 423(1):108-15.

David S, Montier T, Carmoy N**, Resnier P**, Clavreul A, Mével M, Pitard B, Benoit JP, Passirani C. Treatment efficacy of DNA lipid nanocapsules and DNA multimodular systems after systemic administration in a human glioma model. J Gene Med. 2012 Dec; 14(12):769-75.

REVUES SCIENTIFIQUES

Resnier P, Montier T, Mathieu V, Benoit JP, Passirani C. Current status of siRNA delivery systems to combat cancers: from needs and challenges to opportunities and clinical perspectives. Biomaterials. 2013 Sep;34(27):6429-43

Resnier P, Clavreul A, Passirani C. "Chapter 15: Nanocarriers for the treatment of brain tumors. Book: Nanomedecine and the nervous system". Editors: King's College, London, ISBN: 9781466505117

COMMUNICATIONS

COMMUNICATIONS ORALES

Resnier P, Emina A.L, Galopin N, Bejaud J, David S, Benvegnu T, Pecorari F, Chourpa I, Benoit J-P, Passirani C. Biodistribution, tumor targeting and melanoma anticancer properties of innovative pegylated siRNA lipid nanocapsules. Workshop SFNano "Tools and models for translation of Drug Delivery Systems", 2-4 Octobre 2014, Porto, Portugal

Resnier P, Galopin N, Briganti A, Vessières A, Jaouen G, Benoit J-P, Passirani C. Co-delivery of siRNA and ferrocifen-based drugs by lipid nanocapsules for melanoma treatment. Translational nanomedicines international meeting, 27-29 Aout 2014, Angers, France

Resnier P, Bejaud J, Legras P, Benvegnu T, Pécorari F, Chourpa I, Benoit J-P, Passirani C. Etude de l'impact sur l'internalisation cellulaire et le comportement sanguin de nanocapsules lipidiques de siRNA modifies en surface. 8ème journée du CGO, 19-20 juin 2014, Les sables d'Olonne, France

⇨ **1er prix communication orale**

Resnier P, Bejaud J, Yilmaz N, Lautram N, Legras P, Benvegnu T, Benoit J-P, Passirani C. Development of smart siRNA lipid nanocapsules. 28th GTRV Scientific Meeting, 2-4 Décembre 2013, Orléans, France

Resnier P, David S, Delcroix G, Lautram N, Clavreul A, Benoit J-P, Passirani C. EGFR siRNA lipid nanocapsules showed efficient in vitro transfection and growth inhibition of glioma cells. Colloque Nano-Hybrides X, 12-16 Mai 2013, Porquerolles, France

COMMUNICATIONS POSTERS

Resnier P, Emina A.L., Galopin N, David S, Bejaud J, Benvegnu T, Pécorari F, Chourpa I, Benoit J-P, Passirani C. Nano-vectorisation de siRNA: développement de stratégie de ciblage tumoral et alternative thérapeutique au mélanome. 18èmes Journées Jeunes Chercheurs de l'ARC, 22-23 Octobre 2014, Cité Universitaire Paris, France

Resnier P, Bejaud J, Legras P, Benvegnu T, Pecorari F, Chourpa I, Benoit J-P, Passirani C. Development of pH sensitive and Affitin siRNA LNCs: evaluation of cellular uptake and stealth properties. 9th World Meeting on Pharmaceutics, Biopharmaceutics, Pharmaceutical technology, 31 mars - 03 Avril 2014, Lisbonne, Portugal

Resnier P, LeQuinio P, Lautram N, André E, Gaillard C, Bastiat G, Benoit J-P, Passirani C. Characterization and structure of siRNA lipid nanocapsules for gene therapy. 28th GTRV Scientific Meeting, 2-4 Décembre 2013, Orléans, France

Resnier P, LeQuinio P, Lautram N, Gaillard C, Benoit J-P, Passirani C. Development and characterization of siRNA lipid nanocapsules targeting sodium pump alpha 1 subunit in melanoma model. 27th GTRV Scientific Meeting, 3-5 Décembre 2012, Sanofi Paris, France

Resnier P, David S, Clavreul A, Benoit J-P, Passirani C. Physicochemical characteristics of siRNA loaded lipid nanocapsules: in vitro toxicity and biological effect on glioma cells. 5ème Journée thématique de l'IFR 132, 8 Décembre 2011, Angers, France

Resnier P, David S, Delcroix G, Lautram N, Clavreul A, Benoit J-P, Passirani C. EGFR siRNA loading into Lipid Nanocapsules shown in vitro efficient transfection and growth inhibition of glioma cells. 26th GTRV Scientific Meeting, 5-7 Décembre 2011, Bruxelles, Belgique

RÉSUMÉ

Le mélanome métastatique reste à l'heure actuelle une pathologie dramatique avec une survie moyenne de 13 mois après diagnostic, démontrant l'échec des chimiothérapies. Ces travaux de thèse ont pour but de développer une stratégie alternative utilisant les siRNA (petits ARN interférents) encapsulés au sein de nanocapsules lipidiques (LNC) pour une injection intraveineuse. Les premiers travaux ont porté sur le développement et l'amélioration du procédé de formulation des LNC chargées en siRNA. Les résultats ont permis une encapsulation à hauteur de 35%, une stabilité prolongée supérieure à 3 mois et une efficacité d'extinction du gène cible dans les cellules de mélanome. La deuxième partie de la thèse s'est orientée sur les stratégies de ciblage du mélanome après administration systémique. Différentes modifications de surface des LNC à l'aide de polyéthylène glycol (PEG) et d'Affitins (peptide d'affinité) ont été mises au point. La biodistribution sur des animaux « sains » ou des animaux greffés en sous-cutanés (mélanome humain) a révélé des comportements distincts en fonction des recouvrements utilisés. Les formes pegylées ont montré une accumulation préférentielle au site tumoral en comparaison avec les formes non modifiées ou modifiées avec les Affitins. Dans une troisième partie, des études d'efficacité anti-tumorale ont été réalisées avec un siRNA ciblant la protéine Bcl-2 ou la sous unité alpha 1 de la pompe Na/K ATPase. Une réduction du volume tumoral de 25% est observée avec les LNC siRNA Bcl-2. Par ailleurs, l'association de nouvelles chimiothérapies, les ferrocifènes, et des siRNA Bcl-2, montrent grâce à leur co-encapsulation au sein des LNC, des effets prometteurs. Ces travaux démontrent ainsi la capacité des LNC à délivrer des siRNA par voie intraveineuse dans de nouvelles stratégies de ciblage du mélanome.

mots-clés : nanomédecines, thérapie génique, mélanome, ciblage, PEG

ABSTRACT

Metastatic melanoma represents the most aggressive form of skin cancer with a median survival around 13 months. The low efficacy of actual chemotherapy is explained by important resistance phenomenon. The objective of this work consists in developing a new alternative strategy based on siRNA (small interfering RNA) encapsulated into lipid nanocapsules (LNCs) for intravenous injection. Firstly, the experiments were focused on development and optimization of formulation process for the encapsulation of siRNA into LNCs. The result demonstrated an encapsulation efficiency evaluated at 35% by spectrophotometer analysis, an important stability at 4°C (for at less 3 month) and an efficient gene inhibition in melanoma cells. The second part of this work studied the melanoma targeting potential of surface modified LNCs after systemic injection. In this way, pegylation with different polymers and Affitin grafting (affinity peptide) was performed on siRNA LNCs. The biodistribution on healthy animals and subcutaneous melanoma tumor bearing mice revealed the distinct behavior of various modified LNCs. All pegylated LNCs showed a preferential accumulation in tumor site in comparison with non-modified or Affitins LNCs. In a third part, the anti-cancer efficacy was tested with siRNA targeting Bcl-2, an anti-apoptotic member, or Alpha 1 subunit of Na/K ATPase. A reduction of tumoral volume evaluated at 25% was observed for Bcl-2 siRNA LNC. Moreover, the association with new promising anticancerous drug, ferrocifens, and Bcl-2 siRNA co-encapsulated into LNCs evidenced promising effects. This work demonstrated the capacity of LNC to deliver siRNA into melanoma cells and tumor after systemic administration thank to new targeting strategies in melanoma

keywords : nanomedicines, gene therapy, melanoma, targeting, PEG

Présidence de l'université
40 rue de rennes – BP 73532
49035 Angers cedex
Tél. 02 41 96 23 23 | Fax 02 41 96 23 00

université angers

ENGAGEMENT DE NON PLAGIAT

Je, soussigné(e) Melle Pauline RESNIER déclare être pleinement conscient(e) que le plagiat de documents ou d'une partie d'un document publiée sur toutes formes de support, y compris l'internet, constitue une violation des droits d'auteur ainsi qu'une fraude caractérisée. En conséquence, je m'engage à citer toutes les sources que j'ai utilisées pour écrire ce rapport ou mémoire.

signé par l'étudiant(e) le **15** / **10** / **2014**

Cet engagement de non plagiat doit être signé et joint à tous les rapports, dossiers, mémoires.

Présidence de l'université
40 rue de rennes – BP 73532
49035 Angers cedex
Tél. 02 41 96 23 23 | Fax 02 41 96 23 00

université angers

l'université nantes angers le mans
PÔLE DE RECHERCHE ET D'ENSEIGNEMENT SUPÉRIEUR

université angers

Thèse de Doctorat

Pauline RESNIER

Nano-vectorisation de siRNA via des nanocapsules lipidiques
Contournement de la résistance du mélanome aux chimiothérapies conventionnelles

Lipid nanocapsules for siRNA delivery
Bypass of the endogenous resistance of melanoma to chemotherapeutic agents

Résumé

Le mélanome métastatique reste à l'heure actuelle une pathologie dramatique avec une survie moyenne de 13 mois après diagnostic, démontrant l'échec des chimiothérapies. Ces travaux de thèse ont pour but de développer une stratégie alternative utilisant les siRNA (petits ARN interférents) encapsulés au sein de nanocapsules lipidiques (LNCs) pour une injection intraveineuse. Les premiers travaux ont porté sur le développement et l'amélioration du procédé de formulation des LNCs chargées en siRNA. Les résultats ont permis une encapsulation à hauteur de 35%, une stabilité prolongée supérieure à 3 mois et une efficacité d'extinction du gène cible dans les cellules de mélanome. La deuxième partie de la thèse s'est orientée sur les stratégies de ciblage du mélanome après administration systémique. Différentes modifications de surface des LNCs à l'aide de polyéthylène glycol (PEG) et d'Affitins (peptide d'affinité) ont été mises au point. La biodistribution sur des animaux « sains » ou des animaux greffés en sous-cutanés (mélanome humain) a révélé des comportements distincts en fonction des recouvrements utilisés. Les formes pegylées ont montré une accumulation préférentielle au site tumoral en comparaison avec les formes non modifiées ou modifiées avec les Affitins. Dans une troisième partie, des études d'efficacité anti-tumorale ont été réalisées avec un siRNA ciblant la protéine Bcl-2 ou la sous unité alpha 1 de la pompe Na/K ATPase. Une réduction du volume tumoral de 25% est observée avec les LNC siRNA Bcl-2. Par ailleurs, l'association de nouvelles chimiothérapies, les ferrocifènes, et des siRNA Bcl-2, montrent grâce à leur co-encapsulation au sein des LNCs, des effets prometteurs. Ces travaux démontrent ainsi la capacité des LNCs à délivrer des siRNA par voie intraveineuse dans de nouvelles stratégies de ciblage du mélanome.

Mots clés
Nanomédecines, thérapie génique, mélanome, ciblage, PEG

Abstract

Metastatic melanoma represents the most aggressive form of skin cancer with a median survival around 13 months. The low efficacy of actual chemotherapy is explained by important resistance phenomenon. The objective of this work consists in developing a new alternative strategy based on siRNA (small interfering RNA) encapsulated into lipid nanocapsules (LNCs) for intravenous injection. Firstly, the experiments were focused on development and optimization of formulation process for the encapsulation of siRNA into LNCs. The result demonstrated an encapsulation efficiency evaluated at 35% by spectrophotometer analysis, an important stability at 4°C (for at less 3 month) and an efficient gene inhibition in melanoma cells. The second part of this work studied the melanoma targeting potential of surface modified LNCs after systemic injection. In this way, pegylation with different polymers and Affitin grafting (affinity peptide) was performed on siRNA LNCs. The biodistribution on healthy animals and subcutaneous melanoma tumor bearing mice revealed the distinct behavior of various modified LNCs. All pegylated LNCs showed a preferential accumulation in tumor site in comparison with non-modified or Affitins LNCs. In a third part, the anti-cancer efficacy was tested with siRNA targeting Bcl-2, an anti-apoptotic member, or Alpha 1 subunit of Na/K ATPase. A reduction of tumoral volume evaluated at 25% was observed for Bcl-2 siRNA LNC. Moreover, the association with new promising anticancerous drug, ferrocifens, and Bcl-2 siRNA co-encapsulated into LNCs evidenced promising effects. This work demonstrated the capacity of LNC to deliver siRNA into melanoma cells and tumor after systemic administration thank to new targeting strategies in melanoma.

Key Words
Nanomedicines, gene therapy, melanoma, targeting, PEG